UNIVERSITÀ degli STUDI di CATANIA
Dipartimento di Agricoltura, Alimentazione e Ambiente
Di3A

UNIVERSITÀ DEGLI STUDI DI CATANIA

DOTTORATO DI RICERCA IN AGRICULTURAL, FOOD AND ENVIRONMENTAL SCIENCE (Internazionale)

XXXII CICLO

RNASeq analysis of giant cane reveals the leaf transcriptome dynamics under long-term salt stress

Dott. Angelo Sicilia

Advisor:
Chiar. ma Prof.ssa Angela Roberta Lo Piero

Coordinator:
Chiar. mo Prof. Cherubino Leonardi

Ph. D. attended during 2016/2019

”Le cose sono unite da legami invisibili,
non puoi cogliere un fiore senza turbare una stella”

Galileo Galilei – 1630

Questo lavoro è la conclusione di tre intensi e appaganti anni di apprendimento e maturazione, non solo scientifica, ma anche personale. Vorrei servirmi delle prossime righe per ringraziare le persone senza le quali oggi ne io ne questa tesi saremmo qui.

Ringrazio prima di tutto la Prof.ssa Lo Piero, guida professionale e personale. Il suo sapere, i suoi consigli ed il suo sostegno mi hanno aiutato ad orientarmi con entusiasmo in un mondo mai semplice, spesso duro, ma affascinante e gratificante come quello della ricerca.

Ringrazio Danilo, braccio destro nonché compagno di avventure (e disavventure). La sua curiosità e passione per la ricerca mi hanno spinto a fare sempre meglio. Sempre pronto ad aiutare, il suo contributo è stato fondamentale nel raggiungimento di importanti traguardi professionali.

Ringrazio tutti i tesisti che si sono susseguiti nel laboratorio. Da ognuno di loro ho imparato qualcosa di nuovo ed importante.

Ringrazio i miei genitori e mio fratello, presenza e sostegno costante lungo tutto il percorso universitario. Sempre pronti a gioire dei miei successi e a dare consigli davanti alle scelte più difficili. Se ho visto l'America è grazie a loro.

Ringrazio Giulia, mia irrinunciabile metà. Ha saputo sempre incoraggiarmi e motivarmi anche nei momenti più difficili. Mi ha insegnato a gioire delle vittorie, anche le più piccole. La sua presenza ed il suo sostegno sono stati la spinta costante che mi hanno portato al traguardo. È da quando è iniziato il dottorato che pianifica questo giorno.

Infine, ringrazio me stesso per averci creduto fino alla fine. Ne sono successe di cose negli ultimi anni. Ho trovato la mia più grande passione, l'ho fatta diventare il mio lavoro, ho superato confini geografici, ho abbattuto quelli che pensavo fossero i miei limiti personali e ho raggiunto traguardi importanti. Anni fa ho imparato il significato della parola "resilienza": capacità di un corpo di assorbire un urto senza rompersi. Ne ho fatto il mio motto.

INDEX

1. Abstract 6
2. Sommario 7
3. Introduction 9
   3.1 Bioenergy, biomass and biotechnology 9
      3.1.1 The energy issue 9
      3.1.2 The bioenergy sector 13
      3.1.3 Biomass: new alternative energy sources 16
      3.1.4 Biofuels 18
   3.2 Marginal lands: the energy vs food solution 22
   3.3 Genetic improvement of energy crops 24
   3.4 Salt stress: a threat for plant growth and productivity 26
      3.4.1 Plant and abiotic stress 26
      3.4.2 Physiology of salt stress 30
      3.4.3 Salt toxicity 33
      3.4.4 Mechanisms of salt stress response and tolerance 36
   3.5 Giant reed (Arundo donax L.): a promising energy crop 46
      3.5.1 Reproduction 49
      3.5.2 Lifecycle and agronomy 52
      3.5.3 A. donax L. as feedstock: advantages and disadvantages 55
      3.5.4 A. donax and salinity 60
   3.6 Genetic investigations 62
      3.6.1 Transcriptomics and RNA-seq 62
      3.6.2 SSR as molecular markers 73
      3.6.3 Beyond genetics: epigenetics and cytosine methylation for gene expression regulation 77
4. Aim of the work 84

5. Materials and methods 87
5.1 Plant material and application of salt stress..... 87
5.2 Sample collection and RNA extraction 89
5.3 RNA sequencing..... 90
5.3.1 Library preparation for transcriptome sequencing..... 90
5.3.2 Clustering and next generation sequencing.. 91
5.3.3 De novo transcriptome assembling and gene functional annotation 91
5.3.4 Identification of clusters specifically involved in the salt stress response 92
5.3.5 Quantification of gene expression and differential expression analysis..... 92
5.4 Multiple sequence alignment and phylogenetic analysis 93
5.5 Real-time validation of selected DEG candidates using qRT-PCR..... 93
5.6 SSR analysis and validation 94
5.7 Cytosine methylation analysis..... 95
6. Results..... 97
6.1 Effect of salt stress upon A. donax morpho-biophysiological parameters..... 97
6.2 Transcriptomic analysis..... 99
6.2.1 Transcript assembly and annotation..... 99
6.2.2 Identification of differentially expressed genes 102
6.2.3 Functional classification of DEGs..... 105
6.2.4 Identification of functional genes related to salt stress tolerance 114
6.3 SSR analysis 144
6.3.1 Identification and distribution of SSR markers 144

6.3.2 Validation of SSRs 147
6.4 Epigenetic analysis 147
7. Discussion 149
8. Conclusions 169
Appendices 174
References 205

1. Abstract

Bioenergy can provide a crucial contribution in satisfying the increasing demand of sustainable energy production and the possibility to assign marginal land to bioenergy crop cultivation represents the main strategy to overcome the conflict between land uses for food or for energy production. The bioenergy crop Arundo donax L. is known to be able to grow in marginal land and in adverse environmental conditions. Considering the frequent occurrence of soil salinity and to compensate for the lack of informations about the molecular mechanism involved in A. donax response to salt stress, we de novo sequenced, assembled and analyzed the leaf transcriptome of two A. donax clones (G2 and G34) subjected to two levels of long-term salt stress (namely, S3 severe and S4 extreme). The picture that emerges from the identification of functional genes related to salt stress in G2 is consistent with a dose-dependent response to salt, suggesting a deep re-programming of gene expression in S4 samples. In S4 conditions, a dramatic switch from C3 Calvin cycle to C4 photosynthesis is likely to occur. The severe salt treatment resulted upon G34 in a lower number of DEGs if compared with the same treatment in G2, suggesting a weaker re-programming of the gene expression. Therefore, the comparative analysis of the transcriptomic response of G2 and G34 to salt stress highlights a different behavior of the two clones under the same stress level. Considered the distinct response to salt doses, genes either involved in severe or in extreme salt response could constitute useful markers of the physiological status of A. donax in salinized soil. Finally,

many of the unigenes identified in the present study have the potential to be used for the development of A. donax varieties with improved productivity and stress tolerance. Considered the different behaviour of G2 and G34 ecotype to salinity, an extended analysis of other clones could lead to the identification of new genetic sources for stress tolerance.

2. Sommario

Le bioenergie possono fornire un contributo fondamentale nel soddisfare la crescente richiesta di produzione di energia sostenibile. La possibilità di assegnare terreni marginali alla coltivazione di piante da bioenergia rappresenta la principale strategia utile a superare il conflitto tra uso del suolo per produzione di cibo o di energia. La coltura bioenergetica Arundo donax L. è nota per essere in grado di crescere in terreni marginali e in condizioni ambientali avverse. Considerata la frequente presenza di suoli altamente salinizzati e per compensare la mancanza di informazioni sul meccanismo molecolare coinvolto nella risposta di A. donax allo stress salino, abbiamo sequenziato, assemblato e analizzato de novo il trascrittoma fogliare di due cloni di A. donax (G2 e G34) sottoposti per un lungo periodo a due livelli di stress salino (S3 severo e S4 estremo). Il quadro che emerge dall'identificazione di geni funzionanali legati allo stress salino in G2 è coerente con una risposta dose-dipendente al sale, che suggerisce una

riprogrammazione profonda dell'espressione genica nei campioni S4. In condizioni di sale estremo, è probabile che si verifichi un drammatico passaggio dal ciclo C3 Calvin alla fotosintesi C4. Il trattamento severo ha portato in G34 ad un numero inferiore di DEG se confrontato con lo stesso trattamento in G2, suggerendo una riprogrammazione più debole dell'espressione genica. Pertanto, l'analisi comparativa della risposta trascrittomica di G2 e G34 allo stress salino evidenzia un diverso comportamento dei due cloni sottoposti allo stesso livello di stress. Considerata la differente risposta alle diverse dosi di sale, i geni coinvolti nella risposta al trattamento sia severo che estremo potrebbero costituire utili marcatori dello stato fisiologico di A. donax nei suoli salinizzati. Infine, molti degli unigeni identificati nel presente studio hanno il potenziale per essere utilizzati per lo sviluppo di varietà di A. donax con produttività e tolleranza allo stress migliorate. Considerato il diverso comportamento degli ecotipi G2 e G34 rispetto alla salinità, un'analisi estesa di altri cloni potrebbe portare all'identificazione di nuove fonti genetiche per la tolleranza allo stress.

3. Introduction

3.1 Bioenergy, biomass and biotechnology

3.1.1 The energy issue

The energy issue has become of fundamental importance in the last few decades and extremely complex to deal with due to a combination of different causes. Phenomena such as the demographic explosion recorded in the last century which was followed by a strong urbanization, the improvement of the economic conditions of ever wider group of population with a consequent increase in the demand for goods, as well as the rapid industrialization of various nations led to a significant increase in global energy demand. It is moreover estimated that by 2050, human population may grow to 9.6 billion or about 2.0 people ha−1 of cultivated land, which calls for considerable increases in agricultural production and energy demand (Bruinsma, 2009).

This last requirement was met in the 20th century thanks to the use of fossil fuels of organic origin, such as coal, natural gas, but above all, oil and non-renewable energy sources whose consumption has grown exponentially worldwide.

However, their use is becoming increasingly unsustainable from an environmental, political and economic point of view. The geopolitical instability existing in the main oil-producing countries and in the surrounding areas has repercussions on the security of supplies and on the prices of the raw materials, however destined to grow due to the expected depletion of reserves. Fossil fuels are also responsible for the today most important environmental problems, such as air and water pollution, acidification of rainfall and climate change due to

the accumulation of greenhouse gases in the atmosphere. The global increase in temperatures, the melting of glaciers, and increasingly frequent episodes of drought and flood, represent, in fact, the main challenges that humanity will have to face in the coming years (Brennan and Owende, 2010; Hannon et al. , 2010; Mata et al., 2010; Castelli, 2011; Yusuf et al., 2011; Aguirre et al., 2012; Gupta and Verma, 2015).

For these reasons, many countries in the world, including the United States (US) and the European Union (EU), have begun to develop new energy policies with the aim of using alternative energy sources, sustainable from both an environmental and an economic point of view, as well as introducing more efficient and environmentally friendly technologies (Figure 1).

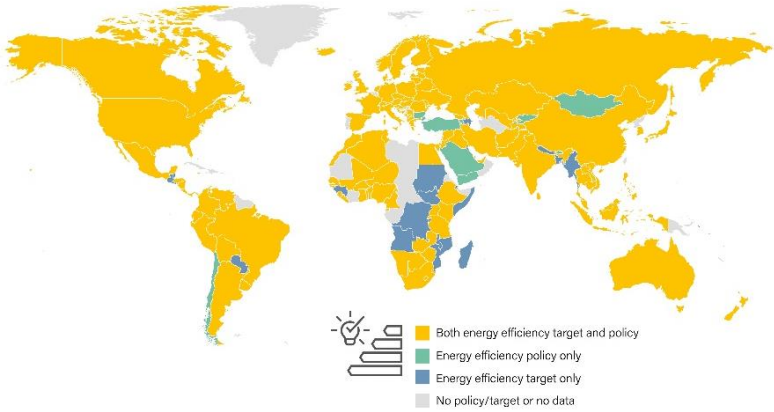

Figure 1. Countries with energy efficiency policies and targets, end-2017. (Source: REN21 Policy Database).

Since the 1980s, the EU has pursued a policy of supporting new technologies in the renewable energy sector. This

commitment has been further accentuated in recent years and since 2008 the EU has adopted a long-term energy policy aiming to make the European economy competitive and sustainable by 2050, with low carbon emissions and environmentally friendly, more efficient from the point of view of energy consumption and safe from the point of view of energy supply (Figure 2).

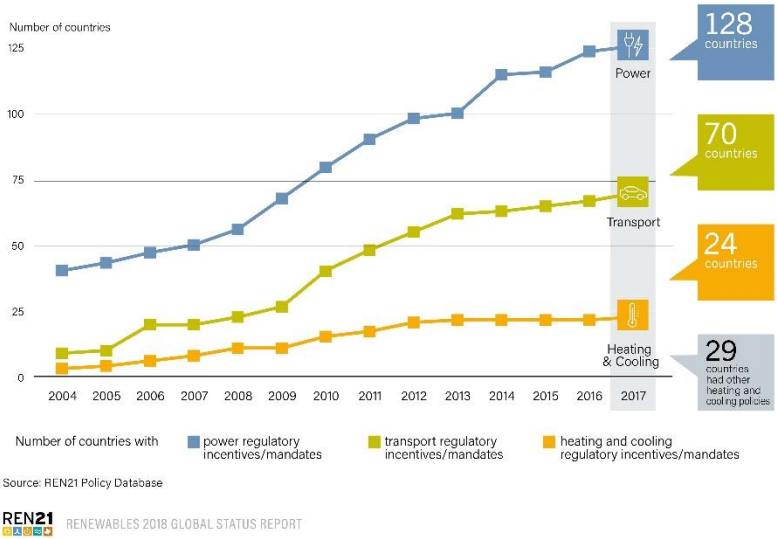

Figure 2. Number of countries with renewable energy regulatory policies, by sector, 2004-2017. (Source: REN21 Policy Database).

In order to reach these goals, the EU has set intermediate targets for climate and energy with a 2020, 2030 and 2050 deadline (European Commission, 2009). The existence of common objectives allows to coordinate the efforts of the various European countries and ensure a stable regulatory framework for the potential investors (European Commission, 2015; Scarlat et al., 2015). Directive

2009/28/EC identifies the essential strategies for achieving energy self-sufficiency and mitigating climate impact in the use of renewable energy and in increasing energy efficiency, with consequent energy savings. It therefore sets minimum targets that must be reached by the member states of the union by 2020:

- reducing greenhouse gas emissions by 20% (compared to 1990 levels);
- achieve an improvement in energy efficiency of 20%;
- satisfy 20% of the total energy requirement through renewable sources; in particular it establishes that in the transport sector at least 10% of the requirement must be met by renewables.

In 2014, due to socio-political changes, and new perspectives on sustainability, the European Commission published an update of the EU directive 2009/28/EC for the period from 2020 to 2030, which sets new targets for 2030:

- reducing greenhouse gas emissions by at least 40% compared to 1990 levels, reduction that must be equal to 60% by 2040;
- bring the share of energy consumption satisfied by renewable sources to at least 27%;
- obtain a minimum improvement of at least 27% of the energy efficiency that can possibly be increased to 30%.

European countries have responded to this energy and environmental challenges by boosting renewable energy and bioenergy production (Gan and Smith, 2011; Lorenzi and Baptista, 2018; Marques et al., 2018). In terms of results, the EU is well advanced in achieving the targets set for 2020. In fact, in 2014, emissions were 23% lower than in 1990.

3.1.2 The bioenergy sector

The aforementioned policies led to a significant growth of the renewable energy sector and its expansion continues more rapidly than expected (REN21, 2016). In fact, the share of renewable energy in the world is expected to increase from 23% in 2015 to 28% in 2021.

2015 marked a very important turning point for renewable energies, as it was the year in which the historic coal overtaking took place. The result of this overcome is that in 2015 renewable energy covered 4% of the global demand in the transport sector (IEA, 2017).

Among the various renewable energy sources (solar, wind, geothermal, hydroelectric, etc.) the production of energy from biomass (bioenergy) is becoming increasingly important. Biomass is in fact one of the most widely available renewable sources on our planet, the technologies for converting it into energy are in many cases simple and well known, and above all, biomass is the only source from which it is possible to obtain liquid biofuels. In 2015 the use of bioenergy in the world increased on average by around 8%, with higher growth rates in China, Japan, Germany and the United Kingdom. The main biofuel producing countries are the United States (46% of global production) and Brazil (24%), followed by the EU (15%).

Bioethanol is the main biofuel (74% of total production), followed by biodiesel (22%). Bioethanol production in 2015 increased by 4% globally, while biodiesel production has decreased at a global level due to restrictions in some Asian countries, although growth has continued in the main producing countries.

About bioenergy consumption, it was estimated that in 2016 the renewable share of total final energy consumption is

around 10% (Figure 3), and the 10-years (2005-2015) growth rate of the renewable energy consumption is around 5%. Bioenergy consumption is large in the heat sector (27% of this sector), although bioenergy for electricity and transport biofuels are growing faster (25% and 3% respectively) (Figure 4) (REN21, 2018).

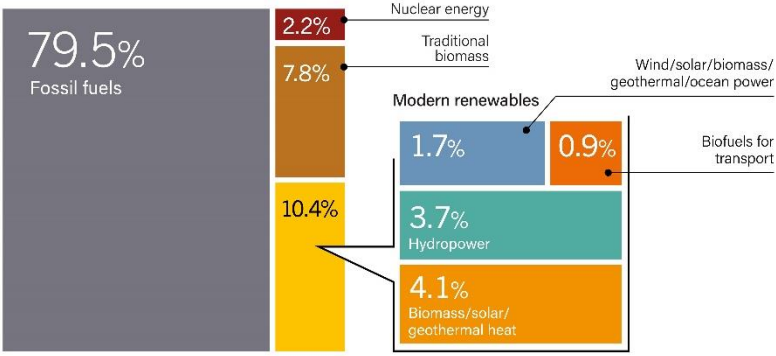

Figure 3. Estimated renewable share of total final energy consumption. (Source: REN21 Policy Database).

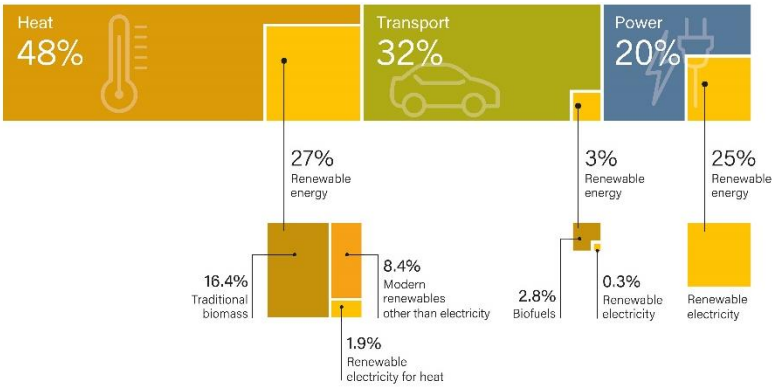

Figure 4. Renewable energy in total final energy consumption, by sector, 2015. (Source: REN21 Policy Database).

Nevertheless, bioenergy production also involves environmental and socio-economic issues. The sustainability of bioenergy production is affected by environmental, economic and social issues (Jin and Sutherland, 2018). Several studies explored different aspects related to the environmental sustainability of biomass use for bioenergy production, including greenhouse gas (GHG) emissions, energy and resource efficiency, land use, water use and biodiversity protection (Pedroli et al., 2013; Mathioudakis et al., 2017; Welfle et al., 2017; Saha and Eckelman, 2018). The economic sustainability of bioenergy involves short and long-term profitability of feedstock, interaction with advances in society, cost of installation and production, cost of feedstock transport and the net balance between costs and benefits (Dale et al., 2013; Zabaniotou, 2018). The social sustainability of bioenergy includes several aspects, such as preserving, livelihoods and safe working conditions, ensuring affordable access to food and guaranteeing the reliability of energy supply.

Despite these issues, Life Cycle Assessment (LCA) has been widely used as tool to evaluate the environmental performance of different renewable energy pathways (Buonocore et al., 2015, 2018a; Fazio and Monti, 2011; González-Garcia et al., 2012; Röder and Thornley, 2018) and several LCA studies showed the benefits associated to bioenergy production in terms of greenhouse gas emissions reduction and energy balance (Muench and Guenther, 2013; Roos and Ahlgren, 2018).

3.1.3 Biomass: new alternative energy sources

In the energy field, the term biomass defines any substance of organic origin, therefore deriving from living organisms, plants or animals, which has not undergone any fossilization process and can be used for energy purposes. It represents a sophisticated form of solar energy storage. Recent technological development is now making possible to exploit its potential in the production of energy and biofuels in new ways (Offermann et al., 2011; Castelli 2011; Yusuf et al., 2011).

The use of biomass is advantageous because, at least at a theoretical level, it does not increase the global quantity of carbon dioxide (CO_2) present in the atmosphere. The amount of CO_2 emitted during the energy production in fact corresponds to the amount which has been fixed by photosynthetic organisms during growth, which is simply returned to the atmosphere faster, and becomes available again for photosynthesis. Furthermore, the use of biomass for energy production has the potential of deliver important benefits, such as improved energy security due to a smaller dependence on fossil fuel supply, reduction of greenhouse gas emission (GHG) and related climate impact such as air pollution, acidification, eutrophication, ozone depletion, and revitalization of rural economies connected to new job opportunities (McBride et al., 2011).

From a practical point of view, in order to evaluate the convenience of using biomass for energy production, it is necessary to take into account the many aspects of its use, which range from the various phases of pre-production, to the industrial energy production phase and finally to its distribution. This type of analysis is called "Life Cycle Assessment (LCA) and allows to understand the impact on

the environment of a specific good or service. As for energy crops, for example, we must not forget that agricultural practices, if not carefully managed, can be a source of pollution for soil, water and air. Furthermore, the expansion of energy crops can have a negative impact on land use, with repercussions on environmental protection and biodiversity, as well as coming into conflict with food security measures. Factors such as fuel consumption for agricultural practices or supply logistics can even lead to an excess of the energy demand for biomass production compared to the amount of energy that can actually be obtained (Hill el al., 2006; Scott et al., 2010; Lam et al., 2012; Kendall and Yuan, 2013; Slade and Bauen, 2013).

Biomass can be used in various ways (Antizar-Ladislao and Turrion-Gomez, 2008; Castelli, 2011; Brennan and Owende, 2010; Ho et al., 2014a; Yue et al., 2014; Behera et al., 2015; Guo et al., 2015; Gupta and Verma, 2015; Sarsekeyeva et al., 2015). The direct combustion of biomass produces thermal and electrical energy. Biomass can be used to produce fuels of various kinds, liquids, solids and gases, which in turn can be used to produce heat or electricity or can be used as biofuels in the transport sector. Finally, biomass can be used to produce chemical compounds.

Currently, biomass and waste are a significant global energy source, accounting for over 70% of all renewable energy production and providing a contribution for final energy consumption comparable to that of coal (IEA,2017).

There are several plant species which have shown potential to be used as bioenergy crops, depending upon their suitability to the available land and climatic conditions (Li et al., 2008). Lignocellulosic crops may provide the entire aboveground biomass, instead grasses like switchgrass and

miscanthus may be preferred for cultivation on marginal lands owing to their potential to grow on poor soils (where food crops cannot yield profitability) because of lower nutrient requirements and better water use efficiencies (Fargione et al., 2010; Heaton et al., 2008; Sang and Zhu, 2011; Stewart et al., 2009).

As the cultivation practices of most energy crop such as miscanthus and giant reed are still little known, significant short-term progresses towards increasing the sustainability of cropping systems are reasonably not a chimera. Generally, the perennial grasses resulted in clearly lower environmental loads compared to annual crops.

The cost of production of biofuels is a major component determining the viability of their commercialization. At present, bioenergy produced from cellulosic feedstocks costs higher than fossil fuels (Carriquiry et al., 2014; Lange, 2007). Giant reed was found to be the most cost-effective among the three crops studied owing to its higher yields (Soldatos, 2015).

3.1.4 Biofuels

Depending on the nature of the biomass used for their production, biofuels can be classified as first, second and third generation biofuels, while the fourth generation, based on the emerging synthetic biology, is still in an embryonic stage (Gressel, 2008; Ho et al., 2014a; Baeyens et al., 2015; Aro, 2016).

The raw materials used to produce first generation biofuels are crops rich in sugar and starch for bioethanol production such as sugar cane, sugar beet, sweet sorghum, or cereals, tubers and roots rich in starch, and oilseeds like rapeseed and soybeans for biodiesel production (Ho et al., 2014a).

The production of first-generation biofuels is in continuous and strong growth, nevertheless it manages to satisfy only a minimum share of the total demand for fuel for transport, in a situation in which the demand for fuels is expected to have a notable increase (Taha et al., 2016). This situation has generated many doubts about their ability to constitute a valid alternative to fossil fuels, also considering that their sustainability has been questioned due to the impact of their production, which has socio-economic and environmental effects (Hill et al ., 2006; Gressell, 2008; Ahmad et al., 2011; Deenanath et al., 2012; Ho et al., 2014a; Aro 2016). The main problem is inherent to the impact that first generation biofuels can have on security of food supply and food prices. If we want to increase the share of biofuels in the transport sector, an increasing part of the global production of cereals and vegetable oils should be used for the production of biofuels, with the consequent removal of land and resources for food production. It is therefore evident that the production of food and the production of first-generation biofuels are in competition for arable land and for agricultural resources such as water and fertilizers.

These problems have led the EU to support the need to develop second and third generation biofuels (Directive 2009/28 / EC).

Second generation biofuels tries to answer the problems highlighted above. They are produced from organic materials not intended for food use, so their production has no impact on the agri-food market. In addition, crops destined for these biofuels production must be capable of growing on soils with low agricultural value, such as marginal, nutrient-poor or polluted land, and with a supply of water and other resources, such as fertilizers, limited or null (Hill et al., 2006). While

second-generation biodiesel is produced using oils that are not edible, second-generation bioethanol is obtained mainly from lignocellulosic materials deriving from agricultural waste produced during harvesting, or from herbaceous or woody plants. Energy crops are crops specifically destined for the production of biofuel. These include perennial herbaceous plants (such as miscanthus) and fast-growing trees (such as willows and poplars). These crops can be grown on poor or marginal soils and are able to provide a constant supply flow, thus avoiding expensive storage of large quantities of biomass between one harvest and another (Ho et al., 2014a). The switchgrass (*Panicum virgatum*), miscanthus (*Mischantus sinensis x giganteus*) and common reed (*Arundo donax* L.) are among the most interesting biomass crops in the United States and the European Union (Ho et al., 2014a). In particular, the common reed adapts to a wide range of environmental conditions and is tolerant to moderate drought and salinity conditions, requires few resources for its cultivation, and has high and constant yields over time. In fact, despite being a plant with C3 photosynthesis, its photosynthetic efficiency is comparable to a C4 (Castiglia et al., 2016; Webster et al., 2016).

The methods presented so far to obtain biofuels have one thing in common: the land availability. Therefore, the concern about their effective capacity to constitute a valid alternative to fossil fuels is also present for second-generation biofuels (Chisti, 2008; Kopetz, 2013). Currently, 0.5%–1.7% of the global agricultural land is being utilized to grow energy crops (Ladanai and Vinterback, 2009). It is estimated that, entire global energy demand may be fulfilled if biomass production may be enhanced by 10% through improved management (Ladanai and Vinterback, 2009). Although

biomass potential is sufficient to ensure the EU-targets by 2020 yet the mobilization of biomass plantation still remains challenging (Scarlat et al., 2013).
Another option is represented by the third-generation biofuels, based on the use of microalgae, photosynthetic organisms that live in water. Algae, especially microalgae, are the subject of considerable interest as a potential raw material for the production of biofuels, constituting a source of biodiesel (Mata et al., 2010; Scott et al., 2010; Behera et al., 2015). Fourth-generation biofuels, currently in an early phase, are a logical evolution of the previous generation, thanks to the genetic improvement operated on microalgae leading to the concept of "cellular factory". The goal is to obtain, through synthetic biology, photosynthetic microorganisms (algae or cyanobacteria) that exploit light to produce, starting from simple raw materials such as water and CO_2, useful substances for humans, such as biofuels or other chemical substances, and may be able to secrete them (Aro, 2016).
So, while the biofuels of previous generations are based on biomass, whose availability can be limited for various reasons, the fourth generation has its foundation directly in photosynthesis reactions and is based on the widely available and unlimited economic source, light.
The factors that still hamper the development of an industry capable of converting biomass into fuels on a large scale are high processing costs, rather than the cost and availability of raw materials. In the context of the transformation, the improvement of microorganisms and enzymes, needed to recover energy from biomass, will be fundamental. Furthermore, the challenge will also concern the sustainable production of new biomass, more easily convertible. New

crops and cropping systems will have to be developed in order to promote food and feed co-production and meet the growing demand for cellulosic biomass and oils. The realization of this objective will be favored by a rigorous evaluation and exploration of alternative production and management practices, with crops and cropping systems responding to local needs.

3.2 Marginal lands: the energy vs food solution

As cellulosic feedstocks cannot be produced on arable lands due to the aforementioned environmental and economic concerns, a recommended strategy is to grow them on "marginal lands". Although the term "marginal land" is a common term yet it is a relative term and should be described according to socioeconomic context of the people and the purpose of utilization (Mehmood et al., 2017). According to Peterson and Galbraith (1932), various kinds of lands which are unsuitable for food production, have poor quality, and less economic benefits may be declared as marginal lands. Generally, the marginal lands are usually described as, unproductive or unsuitable for crop production due to poor soil properties, bad quality underground water, drought, undesired topology, unfavorable climatic conditions, subsequently has no or little potential of profitability for conventional food crops (Tang et al., 2010). Overall, marginal lands include brownfields (Smith et al., 2013), previously contaminated lands, and/or affected by diffused contamination, fallow agricultural land due to unfavorable crop production conditions, degraded land (Tilman et al., 2006), or landfills previously used to dispose-off city waste (Nixon et al., 2001). Recently, to avoid negative competition between fuels and food, marginal lands have received

considerable attention. Use of marginal lands to produce cellulosic feedstocks could potentially avoid many problems associated with biofuel production using cropland (Skevas et al., 2014). According to recent global scenario, balancing between food and energy provision, environmental sustainability, maintenance of biodiversity and ecosystem functions are key challenges to deal with. Additional benefits of cellulosic biomass produced on marginal lands are the less need of fertilizer and pesticides along with mitigation of water pollution and GHG (Hill et al., 2006; Robertson et al., 2008). Therefore, using marginal lands to grow energy crops could be a viable option without causing any further food and environment problems (Qin et al., 2011) subjected to the selection and availability of suitable energy crops (Lord, 2015).

For this purpose, the European project, Optimization of Perennial Grasses for Biomass Production in the Mediterranean Area (OPTIMA) was launched with the aim to establish new strategies for the sustainable use of the marginal land in Mediterranean areas (Monti and Cosentino, 2015). In this project, *Miscanthus giganteus* (miscanthus), *Arundo donax* L. (giant reed), *Panicum virgatum* (switchgrass), and *Cynara cardunculus* L. (cardoon) were included as reference grasses and were studied in sufficient depth, in terms of biomass production potential. It was demonstrated that growing perennial grasses in Mediterranean Area prevented the leaching of heavy metals to contaminate the groundwater and provided potential for climate change mitigation in the region (Fernando et al., 2015; Monti and Cosentino, 2015). Similar studies have been conducted all over the world to evaluate the potential of

marginal lands for selected plant species for biomass–bioenergy production.

It is believed that the global energy demand, in the reference scenario for the year 2030 (as projected by the International Energy Agency) could be provided from the bioenergy crops grown sustainably on non-arable lands (Metzger and Huttermann, 2009; Skevas et al., 2014). There are different estimations of the bioenergy potentials using marginal lands, ranging from ∼30 to 1000 Exa-Joule (EJ; 1 EJ = 1018 J) per year of primary energy (Haberl et al., 2011; Hoogwijk et al., 2003, 2005; Smeets et al., 2007), but taking the sustainability into consideration it is estimated that the global technical primary bio-energy potential by 2050 would be in the range of 130–270 EJ y−1 (Beringer et al., 2011; Haberl et al., 2010).

3.3 Genetic improvement of energy crops

In order to make second generation biofuels a valid alternative to fossil energy sources, genetic improvement programs are of fundamental importance. The primary objective of genetic improvement is to increase oil yields for biodiesel and biomass yields for ethanol production, keeping in mind that these increases must be achieved on marginal land and with the least possible interventions by the farmer. Among the objectives of improvement we therefore find the increase in the number of leaves of the plant and / or their surface, the improvement of the efficiency of photosynthesis, the efficiency of the use of resources (such as water and nitrogen), the obtaining of plants resistant to biotic (diseases and parasites) and abiotic stresses (cold, floods, droughts, salinity) so that plants can be grown in a wide variety of environments and can adapt to the effects of global warming. Given that energy crops are destined to be cultivated in

marginal or degraded soils, so as not to compete with traditional agricultural crops, it was also considered a possible use for the phytoremediation of contaminated land, for example from heavy metals.

Over the last decade, the combination of the most modern molecular biology techniques and the classical genetic improvement of agricultural crops has led to a significant increase of their efficiency (Estrela and Cate, 2016). This is especially important when considering tree cultivations, characterized by very long life cycles (Antizar-Ladislao and Turrion-Gomez, 2008; Allwright and Taylor, 2016).

These tools have gradually become available for other energy crops as well. Such crops include perennials trees including poplar (*Populus*) and willow (*Salix*) and grasses such as Miscanthus (*Miscanthus sinensis*, *Miscanthus sacchariflorus*, *Miscanthus giganteus*), *Arundo donax* and switchgrass (*Panicum virgatum*) grown for their lignocellulosic biomass. For example, the identification of more than 100,000 SNPs in the miscanthus genome allowed to identify markers associated with characters such as cell wall composition and biomass production (Slavov et al., 2014). Moreover, thousands of SNPs have recently been identified in switchgrass (*Panicum virgatum*) thanks to the transcriptome sequencing (Serba et al., 2016).

The development of a simple, rapid and effective transformation method (Lu and Kang, 2008), combined with the availability of abundant genomic and transcriptomic data (Nguyen et al., 2013; Kagale et al., 2014; Abdullah et al., 2016), allow to improve both production levels and the quality of the obtainable oil, but also try to improve the agronomic features. For instance, the recent CRISPR / Cas9 technique, which allows genome editing, has been used to

modify the oil fatty acid composition in both *Arabidopsis* and *Camelina* (Jiang et al., 2016)

In addition to the technological challenges, biotechnologies applied to the production of biofuels will have to deal with any possible obstacles arising on the one hand from the legislative aspect and on the other from the perception of public opinion. In particular, this second factor could play an important role. For example, in the EU, adverse public opinion has played a predominant role in restricting the marketing of genetically modified organisms, even though this has not stopped the adoption of technology in much of the rest of the world. It is however possible that energy crops, which appear as crops not destined for human consumption and with obvious environmental benefits and not only, may face considerably lower levels of opposition (Fesenko and Edwards, 2014). Essential requirements in order to obtain the genetic improvement are deep preliminary genetic, transcriptomic and epigenetic studies, leading to a more complete knowledge of the mechanisms involved in growth and productivity and to a punctual detection of the aspects on which to act.

3.4 Salt stress: a threat for plant growth and productivity

3.4.1 Plant and abiotic stress

Plant growth and productivity is adversely affected by nature's threats in the form of various abiotic and biotic stress factors. The most practical definition of a biological stress is an adverse force or a condition, which inhibits the normal functioning and wellbeing of a biological system such as plants (Jones and Jones, 1989, Mahajan and Tuteja, 2005).

Thus, plants are frequently exposed to a plethora of stress conditions such as low temperature, salt, drought, flooding, heat, oxidative stress and heavy metal toxicity. Various anthropogenic activities have accentuated the existing stress factors. Heavy metals and salinity have begun to accumulate in soil and water and may soon reach toxic levels. Plants also face challenges from pathogens including bacteria, fungi, and viruses as well as from herbivores. All these stress factors are a menace for plants and prevent them from reaching their full genetic potential limiting crop productivity. In fact, abiotic stress is the principal cause of crop failure worldwide, dipping average yields for most major crops by more than 50% (Bray et al., 2000).

In response to these stress factors various genes are differentially regulated, which can mitigate the effect of stress and lead to adjustment of the cellular milieu and plant tolerance. In nature, stress does not generally come in isolation and many stresses act hand in hand with each other. In response to these stress signals that cross talk with each other, nature has developed diverse pathways for combating and tolerating them. These pathways act in cooperation to alleviate stress.

The stress is first perceived by the receptors present on the membrane of the plant cells, the signal is then transduced downstream and this results in the generation of second messengers including calcium, reactive oxygen species (ROS) and inositol phosphates. These second messengers, such as inositol phosphates, further modulate the intracellular calcium level. This perturbation in cytosolic Ca^{2+} level is sensed by calcium binding proteins, also known as Ca^{2+} sensors. These sensors apparently lack of any enzymatic activity and change their conformation in a calcium

dependent manner. These sensory proteins then interact with their respective interacting partners often initiating a phosphorylation cascade and target the major stress responsive genes or the transcription factors controlling these genes (Huang et al., 2011). The products of these stress genes ultimately lead to plant adaptation and help the plant to survive and surpass the unfavorable conditions (Mahajan and Tuteja, 2005) (Figure 5).

Thus, plant responds to stresses as individual cells and synergistically as a whole organism. Stress induced changes in gene expression in turn may participate in the generation of hormones like ABA, salicylic acid and ethylene. These molecules may amplify the initial signal and initiate a second round of signaling that may follow the same pathway or use altogether different components of signaling pathway. The various stress responsive genes can be broadly categorized as early and late induced genes. Early genes are induced within minutes of stress signal perception and often express transiently. Various transcription factors are included in the list of early genes as the induction of these genes does not require synthesis of new proteins and signaling components are already primed. In contrast, most of the other genes, which are activated by stress more slowly, i.e. after hours of stress perception, are included in the late induced category (Figure 6).

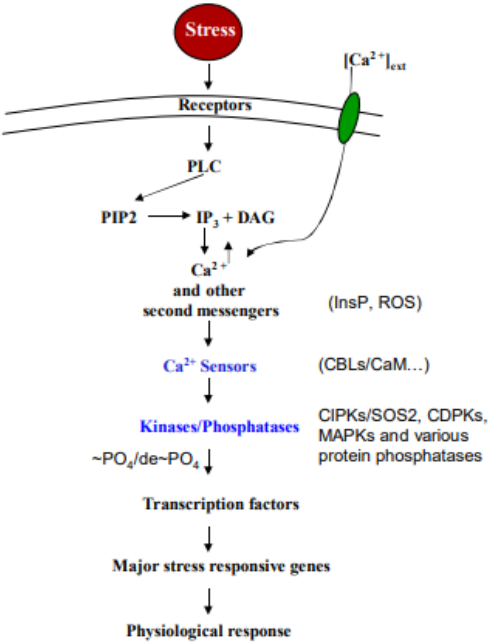

Figure 5. Overview of signaling pathway under stress condition. Stress signal is first perceived by the membrane receptor, which activates PLC and hydrolyses PIP2 to generate IP3 as well as DAG. Following stress, cytoplasmic calcium levels are up-regulated via movements of Ca^{2+} ions from apoplast or from its release from intracellular sources mediated by IP3. This change in cytoplasmic Ca^{2+} level is sensed by calcium sensors which interact with their downstream signaling components which may be kinases and/or phosphatases. These proteins affect the expression of major stress responsive genes leading to physiological responses. (Mahajan and Tuteja, 2005).

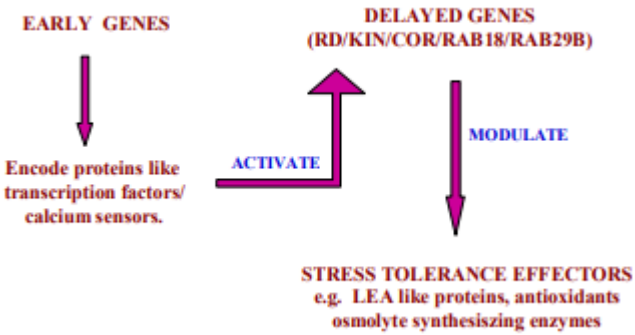

Figure 6. **Early and delayed gene expression in response to abiotic stress signaling.** Various genes are triggered in response to stress and can be grouped under early and late responsive genes. Early genes are induced within minutes of stress perception and often express transiently. In contrast, various stress genes are activated slowly, within hours of stress expression and often exhibit a sustained expression level. Early genes encode for the transcription factors that activate the major stress responsive genes (delayed genes) (Mahajan and Tuteja, 2005)

3.4.2 Physiology of salt stress

Salinity is one of the most brutal environmental stresses that hamper crop productivity worldwide (Flowers, 2004; Munns and Tester, 2008; Gupta and Huang, 2014). Salinity in a given land area depends upon various factors like amount of evaporation (leading to increase in salt concentration), or the amount of precipitation (leading to decrease in salt concentration). Weathering of rocks also affects salt concentration. Inland deserts are marked by high salinity as the rate of evaporation far exceeds the rate of precipitation. Agricultural lands that have been heavily irrigated are highly saline. Since drier areas need intense irrigation, there is extensive water loss through a combination of both evaporation as well as transpiration. This process is known as

evapotranspiration and as a result, the salt delivered along with the irrigation water gets concentrated, year-by-year in the soil. This leads to huge losses in terms of arable land and productivity as most of the economically important crop species are very sensitive to soil salinity.

Salinity impairs plant growth and development via water stress, cytotoxicity due to excessive uptake of ions such as sodium (Na^+) and chloride (Cl^-), and nutritional imbalance (Isayenkov and Maathuis, 2019). Additionally, salinity is typically accompanied by oxidative stress due to generation of reactive oxygen species (ROS) (Tsugane et al., 1999; Hernandez et al., 2001; Isayenkov, 2012). Plant responses to salinity have been divided into two main phases. An ion-independent growth reduction, which takes place within minutes to days, causes stomatal closure and inhibition of cell expansion mainly in the shoot (Munns and Passioura, 1984; Munns and Termaat, 1986; Rajendran et al., 2009). A second phase takes place over days or even weeks and pertains to the build-up of cytotoxic ion levels, which slows down metabolic processes, causes premature senescence, and ultimately cell death (Munns and Tester, 2008; Roy et al., 2014). Ion uptake can occur via the symplastic and the apoplastic pathway (Gao et al., 2007; Negrão et al., 2011; Maathuis et al., 2014). The apoplastic pathway is a direct flow continuum between the outside and the xylem (Yeo et al., 1987; Anil et al., 2005; Krishnamurthy et al., 2009). In most conditions, the contribution of this "bypass" flux is less than 1% of the transpirational volume flow (Hanson et al., 1985; Moon et al., 1986; Yeo et al., 1987). Nevertheless, this can be much greater when transpirational demand is high (Pitman, 1982; Sanderson, 1983). On the other hand, net uptake via the symplastic pathway of Na^+ (Cl^-) into roots is assumed to be

catalyzed by a specific complement of transporters (Figure 1). Nonselective cation channels (NSCCs) are encoded by two gene families: glutamate receptor-like channels (GLRs) and cyclic nucleotide-gated channels (CNGCs) and blocked by Ca^{2+} (Leng et al., 2002; Demidchik et al., 2004, 2018; Demidchik and Maathuis, 2007). The apoplastic Ca^{2+} concentration in root cells is probably in the region of 0.2–0.4 mM (Legué et al., 1997), which is enough to reduce NSCC-mediated flux by 30–50% (Essah et al., 2003). The remaining flux can be further diminished also by organic compounds like cyclic GMP. In monocotyledonous plants, the situation is likely to be different. In contrast to *Arabidopsis*, which contains only the subclass 1, Na^+ selective, AtHKT1 isoform, monocots have multiple HKT isoforms. *Arabidopsis* HKT1 functions in long-distance transport of Na^+ via xylem and phloem (Berthomieu et al., 2003; Sunarpi et al., 2005), but in several cereals HKTs can mediate Na^+ uptake: in rice, OsHKT2;1 catalyzes Na^+ uptake in low K^+, low Na^+ (<2 mM) conditions (Horie et al., 2007). Overexpression of *Hv*HKT2;1 in barley causes increased Na^+ uptake in salt stress conditions (Mian et al., 2011). In contrast to Na^+, Cl^- is an essential nutrient for plants. It has been postulated that Cl^- is transported into the cell by a H^+/Cl^- symport, but its molecular nature is unknown. When plants are exposed to salinity, the external [Cl^-] may be sufficiently high for a fraction of Cl^- to enter passively through anion channels, but the relevant transport mechanism in this case is unknown. Another class of potential Cl^- transporters is the cation chloride cotransporters (CCCs). In *Arabidopsis*, AtCCC has been studied in some detail, showing that it is expressed in root and shoot tissues and most likely involved

in coordinated K^+, Na^+, and Cl^- symport (Colmenero-Flores et al., 2007; Zhang et al., 2010).

3.4.3 Salt toxicity

Salt toxicity directly relates to ion concentrations and can manifest itself in all cell compartments though is usually assumed to be associated with the cytoplast. The presence of high concentrations of Na^+ and Cl^- can disturb water structure via kosmo- and chaotropic effects, inhibit enzymes, and create nutritional imbalance. The higher charge density of Na^+ compared to K^+ means it behaves as a weak "kosmotrope" that organizes and immobilizes water structure around itself. Kosmotropy affects hydrogen bonding between water molecules and polar groups of proteins and nucleic acids, potentially interfering with their biochemical activity. Another potential ion toxicity mechanism that is often referred to in the context of salinity stress is the requirement of many enzymes to bind K^+ which can be disrupted by Na^+ displacing K^+. In some cases, Na^+ can substitute K^+ without significant problems for many biochemical activities. However, in other cases, the requirement for K^+ is more specific; for example, the Kcat for Na^+ activation of pyruvate kinase, a classical example of a K^+ stimulated enzyme (Kachmar and Boyer, 1953), is only about 8% compared to that for K^+. Nevertheless, the approximately 10-fold higher affinity of this enzyme for K^+ (Kachmar and Boyer, 1953) compared to Na^+ ensures that a Na:K ratio of more than 3 would be needed to significantly reduce enzyme activity. In contrast to cytoplasmic concentrations, vacuolar levels of Na^+ and Cl^- readily reach several hundred mM. For example, a recent study on rice cultivars exposed to 50 mM NaCl showed tissue [Na^+] of up to 600 mM (Patishtan et al., 2018).

Consequently, vacuolar Na/K ratios can easily exceed values of 3 or 4. The central vacuole plays a role in ionic homeostasis, pH regulation, and osmotic adjustment. As lytic compartment, the vacuole contains hydrolases, phosphatases, and phosphoesterases (Boller and Kende, 1979) and thus is linked to protein turnover processes like ubiquitination. Despite the extensive information regarding the vacuolar proteome, to our knowledge no vacuole-specific enzymes have been tested for the functional implications of high Na^+ and Cl^- concentrations.

What is the role of potassium in salinity stress? K^+ is the most abundant cation in plant cells and an essential nutrient that is important for many enzymatic reactions, ionic and pH homeostasis and maintaining adequate membrane potential (Maathuis 2009; Ahmad and Maathuis, 2014). Cytosolic K^+ is also an important determinant of plant adaptive responses to a broad range of environmental stresses (e.g. Shabala and Pottosin, 2014). In hydrated form, Na^+ and K^+ are chemically and structurally very similar and, as already mentioned, some biophysical roles of K^+, particularly generating turgor, can be fulfilled by Na^+. Nevertheless, K^+ is uniquely required for many physiological and biochemical processes, whereas Na^+ is not. The transport systems involved in the uptake and distribution of K^+ and Na^+ in combination are key determinants of plant salinity tolerance due to their ability to determine tissue and cytosolic K^+/Na^+ ratios, parameters that are generally believed to impact greatly on salt tolerance (Maathuis and Amtmann, 1999; Shabala and Cuin, 2008). Influx of Na^+ worsens the K/Na ratio, and this is further exacerbated by salt stress-induced K^+ loss, a phenomenon

that is often more pronounced in salt sensitive species (Chen et al., 2007; Wu et al., 2018). GORK (guard cell outward rectifying K^+ channel) type and ROS-activated NSCC-type channels are likely to mediate the main fraction of K^+ efflux (Jayakannan et al., 2013; Wu et al., 2015b). Salinity may increase K^+ circulation via the vascular bundles (Maathuis, 2006; Shabala and Cuin, 2008). Endomembrane channels such as the vacuolar TPKs (two pore K+ channels) are also likely to play an important role. The expression of tobacco TPK1a was increased around twofold by salt stress or osmotic shock (Hamamoto et al., 2008), whereas TPK overexpression in tobacco cells increased their resistance to salt stress. Post-translational modulation of TPK1 also impacts on salt tolerance as was shown for AtTPK1, which becomes phosphorylated by a Ca^{2+}-dependent kinase (CDPK3; Latz et al., 2013) (Figure 2). The ability of plants to retain K^+ in various tissues is an important feature of plant salt tolerance (Wu et al., 2018). Multiple reports suggest that K^+ could play important role in cell signaling during salinity (Shabala 2009, 2017; Anschütz et al., 2014; Shabala and Pottosin, 2014; Wu et al., 2018). In this context, K^+ can cause cell- and tissue-specific metabolic changes and drive a "metabolic switch" to inhibit energy-dependent biosynthetic processes. The ensuing reduction or arrest of plant growth saves energy, which in turn augments the capacity for the synthesis of compounds that help in defence and repair of cellular systems (Demidchik et al., 2014). In all, K^+ homeostasis is intricately linked to salt tolerance.

3.4.4 Mechanisms of salt stress response and tolerance

Plants develop various physiological and biochemical mechanisms in order to survive in soils with high salt concentration. Principle mechanisms include, but are not limited to, ion homeostasis and compartmentalization, ion transport and uptake, biosynthesis of osmoprotectants and compatible solutes, activation of antioxidant enzyme and synthesis of antioxidant compounds, synthesis of polyamines, generation of nitric oxide (NO), and hormone modulation (Gupta and Huang, 2014).

The plant response to salinity is then complex but includes some mechanism to report increasing levels of ions, either in the external medium or within the symplast. Rapid responses such as salt-induced membrane depolarization and Ca^{2+} signals could form early components of salt sensing relays. However, membrane depolarizations do not confer any specificity so are unlikely to be physiologically relevant. Increases in extracellular NaCl cause rapid Ca^{2+} elevation in the cytosol (Knight et al., 1997), but these are often similar to signals induced by equiosmolar levels of osmolytes such as mannitol. However, in some cases, the Ca^{2+} signals are salt specific (e.g. Choi et al., 2014). Reactive oxygen species (ROS) may constitute a potential component upstream of the Ca^{2+} signal: *annexin1* (AtANN1) from *Arabidopsis thaliana* responds to high extracellular NaCl by mediating ROS-activated Ca^{2+} influx through the plasma membrane of plant cells (Laohavisit et al., 2013). Thus, *annexin 1* could be an early key component of root cell adaptation to salinity (Laohavisit et al., 2013). Downstream, Ca^{2+}-dependent signaling can be propagated by calcium-dependent protein kinases (CDPKs) and calcineurin B-like proteins (CBLs)

(Weinl and Kudla, 2008) with CBL-interacting protein kinases (CIPKs) (Boudsocq and Sheen, 2013), which in turn modulate protein activity and gene transcription. Increasing evidence demonstrates the roles of a Salt Overly Sensitive (SOS) stress signalling pathway in ion homeostasis and salt tolerance (Gupta and Huang, 2014; Hasegawa et al., 2000; Sanders, 2000). The SOS signalling pathway consists of three major proteins, SOS1, SOS2, and SOS3 (Figure 7).

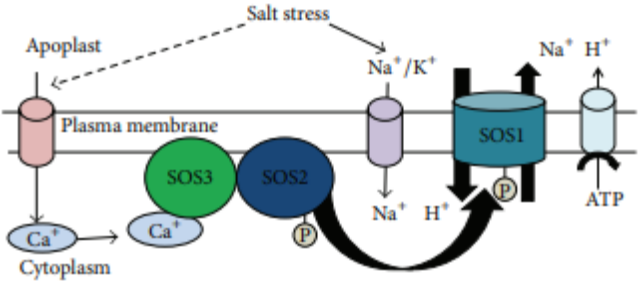

Figure 7. Model of SOS pathway (Gupta and Hang, 2014).

SOS1, which encodes a plasma membrane Na^+/H^+ antiporter, is essential in regulating Na^+ efflux at cellular level. It also facilitates long distance transport of Na^+ from root to shoot. Overexpression of this protein confers salt tolerance in plants (Shi et al., 2000, 2002). SOS2 gene, which encodes a serine/threonine kinase, is activated by salt stress elicited Ca^+ signals. This protein consists of a well-developed N-terminal catalytic domain and a C-terminal regulatory domain (Liu et al., 2000). The third type of protein involved in the SOS stress signalling pathway is the SOS3 protein which is a myristoylated Ca^+ binding protein and contains a myristoylation site at its N-terminus. This site plays an essential role in conferring salt tolerance (Ishitani et al, 2000). C-terminal regulatory domain of SOS2 protein contains a

FISL motif (also known as NAF domain), which is about 21 amino acid long sequence, and serves as a site of interaction for Ca^{2+} binding SOS3 protein. This interaction between SOS2 and SOS3 protein results in the activation of the kinase (Guo et al., 2004). The activated kinase then phosphorylates SOS1 protein thereby increasing its transport activity which was initially identified in yeast (Quintero et al, 2002). SOS1 protein is characterized by a long cytosolic C-terminal tail, about 700 amino acids long, comprising a putative nucleotide binding motif and an autoinhibitory domain. This autoinhibitory domain is the target site for SOS2 phosphorylation. The SOS pathway has additional components such as SOS4 and SOS5 (Shi et al., 2003; Mahajan and Tuteja, 2005), which may be involved in Na^+ and K^+ homeostasis (Mahajan e al., 2008). The *sos4* mutants exhibit higher Na^+/K^+ ratio in comparison with wildtype plants (Mahajan et al., 2008). Due to the outer membrane localization, SOS5 is another potential candidate for (extracellular) Na^+ sensing (Shi et al., 2003; Mahajan et al., 2008). Thus, the SOS pathway is a key regulator of Na^+ homeostasis, for example via SOS1. However, due to interaction with other regulatory proteins, it also participates in regulation of additional mechanisms of ion homeostasis: mutations in AtHKT1, which is responsible for Na^+ translocation to the shoot (Halfter et al., 2000), suppress the *sos3* mutation (Rus et al., 2001). Thus, the SOS2-SOS3 complex is involved in negative regulation of AtHKT1 during salinity stress. SOS2, in addition to modulating SOS1, can interact with vacuolar Na^+/H^+ exchanger (NHX) antiporters and significantly elevate their exchange activity (Zhu, 2002). Intracellular NHX proteins are Na^+, K^+/H^+ antiporters involved in K^+ homeostasis, endosomal pH regulation, and

salt tolerance. Barragan et al. (2012) showed that tonoplast-localized NHX proteins (NHX1 and NHX2: the two major tonoplast-localized NHX isoforms) are essential for active K^+ uptake at the tonoplast, for turgor regulation, and for stomatal function. In fact, more such NHX isoforms have been identified and their roles in ion (Na^+, K^+, H^+) homeostasis established from different plant species (e.g., LeNHX3 and LeNHX4 from tomato) (Galvez et al., 2012). SOS2 may also interact with the N-terminus of CAX1 (a H^+/Ca^{2+} exchanger) (Qiu et al., 2002). It seems likely that SOS1 activity induced by salinity not only relies on the SOS3–SOS2 complex but could be phosphorylated in a phospholipase D (PLD) signaling pathway-dependent manner (Yu et al., 2010): high Na^+ concentrations causes an increase in enzyme activity of PLDα1 that lead to fast accumulation of phosphatidic acid (PA) as a lipid second messenger. PA in turn activates mitogen-activated protein kinase 6 (MPK6), which is capable of directly phosphorylating SOS1 (Yu et al., 2010). Loss of function mutants of PLDα1 and MPK6 exhibit sensitivity to salinity and accumulate more Na^+ accumulation in the shoots. A further SOS1 regulating mechanism originates in nuclear Ca^{2+} signaling in response to high salinity (Guan et al., 2013). Nuclear Ca^{2+} activates the Ca^{2+}-binding protein RSA1, which complexes with RITF1 (RSA1 interacting transcription factor). Subsequently, the activated complex RSA1-RITF1 binds at the SOS1 promoter to augment its transcription (Guan et al., 2013).

Compatible solutes, also known as compatible osmolytes, are a group of chemically diverse organic compounds that are uncharged, polar, and soluble in nature and do not interfere with the cellular metabolism even at high concentration. They mainly include proline (Hoque et al., 2007; Ahmad et al.,

2010; Hossain et al., 2011; Nounjan et al., 2012; Tahir et al., 2012), glycine betaine (Khan et al., 2007; Wang and Nii, 2000), sugar (Kerepesi and Galiba, 2000; Bohnert et al., 1995), and polyols (Ford 1984; Dopp et al., 1985; Ashraf and Foolad, 2007; Saxena et al., 2013). Amino acids such as cysteine, arginine, and methionine, which constitute about 55% of total free amino acids, decrease when exposed to salinity stress, whereas proline concentration rises in response to salinity stress (El-Shintinawy and El-Shourbagy, 2001). Proline accumulation is a well-known measure adopted for alleviation of salinity stress (Saxena et al., 2013; Matysik et al., 2002; Ben Ahmed et al., 2010). Intracellular proline which is accumulated during salinity stress not only provides tolerance towards stress but also serves as an organic nitrogen reserve during stress recovery. Proline is synthesised either from glutamate or ornithine. In osmotically stressed cell glutamate functions as the primary precursor. The biosynthetic pathway comprises two major enzymes, pyrroline carboxylic acid synthetase and pyrroline carboxylic acid reductase. Both these regulatory steps are used to overproduce proline in plants (Sairam and Tyagi, 2004). It functions as an O_2 quencher thereby revealing its antioxidant capability. Glycine betaine is an amphoteric quaternary ammonium compound ubiquitously found in microorganisms, higher plants and animals, and is electrically neutral over a wide range of pH. It is highly soluble in water but also contains nonpolar moiety constituting 3-methyl groups. Because of its unique structural features, it interacts both with hydrophobic and hydrophilic domains of the macromolecules, such as enzymes and protein complexes. Glycine betaine is a nontoxic cellular osmolyte that raises the osmolarity of the cell during stress period; thus, it plays an

important function in stress mitigation. Glycine betaine also protects the cell by osmotic adjustment (Gadallah, 1999), stabilizes proteins (Makela et al., 2000), and protects the photosynthetic apparatus from stress damages (Cha-Um and Kirdmanee, 2010) and reduction of ROS (Ashraf and Foolad, 2007; Saxena et al., 2013). Polyols are compounds with multiple hydroxyl functional groups available for organic reactions. Sugar alcohols are a class of polyols functioning as compatible solutes, as low molecular weight chaperones, and as ROS scavenging compounds (Ashraf and Foolad, 2007). They can be classified into two major types, cyclic (e.g., pinitol) and acyclic (e.g., mannitol). Mannitol synthesis is induced in plants during stressed period via action of NADPH dependent mannose-6-phosphate reductase. These compatible solutes function as a protector or stabilizer of enzymes or membrane structures that are sensitive to dehydration or ionically induced damage. It was found that the transformation with bacterial *mltd* gene that encodes for mannitol-1-phosphate dehydrogenase in both *Arabidopsis* and tobacco (*Nicotiana tabacum*) plants confer salt tolerance, thereby maintaining normal growth and development when subjected to high level of salt stress (Binzel et al., 1988; Thomas et al., 1995). Accumulations of carbohydrates such as sugars (e.g., glucose, fructose, fructans, and trehalose) and starch occurs under salt stress (Parida et al., 2004). The major role played by these carbohydrates in stress mitigation involves osmoprotection, carbon storage, and scavenging of reactive oxygen species. It was observed that salt stress increases the level of reducing sugars (sucrose and fructans) within the cell in a number of plants belonging to different species (Kerepesi and Galiba, 2000). Besides being a carbohydrate reserve, trehalose accumulation protects

organisms against several physical and chemical stresses including salinity stress. They play an osmoprotective role in physiological responses (Ahmad et al., 2013). Sucrose content was found to increase in tomato (*Solanum lycopersicum*) under salinity due to increased activity of sucrose phosphate synthase (Gao et al., 1998). Sugar content, during salinity stress, has been reported to both increase and decrease in various rice genotype (Alamgir and Yousuf Ali, 1999). In rice roots it has been observed that starch content decreased in response to salinity while it remained fairly unchanged in the shoot. Decrease in starch content and increase in reducing and no-reducing sugar content were noted in leaves of *Bruguiera parviflora* (Parida et al., 2004). Other early components in NaCl-induced sensing and signaling may be the previously mentioned ROS and cyclic nucleotides such as cGMP. Both cGMP and ROS show rapid transient increases in cytoplasmic levels after salinity stress onset (Kiegle et al., 2000; Donaldson et al., 2004). The rise of cellular cGMP can be detected within seconds after application of salinity and osmotic stress (Donaldson et al., 2004). Furthermore, cGMP inhibits Na^+ influx in several plant species (Maathuis and Sanders, 2001; Essah et al., 2003; Rubio et al., 2003) while it can regulate transcription of various genes related to salinity stress and promote K^+ uptake (Maathuis, 2006, 2014; Isner and Maathuis, 2016). A rise in ROS is detected within minutes after the onset of salinity stress, and this phenomenon can activate downstream MAPK cascades (Miller et al., 2010; Maathuis, 2014). Recent studies demonstrate participation of ROS in transcriptional regulation. The ROS-sensitive transcription factor ERF1 (ethylene response factor) in rice can bind to multiple promoters, including those of MAPKs, and improves general

performance of plants under salinity stress (Schmidt et al., 2013). ROS are also thought to alter ion fluxes; for example, outward rectifying K^+ channels are directly activated by ROS in *Arabidopsis* roots (Demidchik et al., 2010). The model further postulates that moderate K^+ decrease in the cytosol will generate a low level of ROS designated for signaling, while high levels of salinity generate damaging ROS that activate K^+ efflux channels and accelerate cellular K^+ leak. Thus, fast and significant K^+ loss could lead to acute ROS toxicity and development of programmed cell death (PCD). Antioxidant metabolism, including antioxidant enzymes and non-enzymatic compounds, plays critical parts in detoxifying ROS induced by salinity stress. Salinity tolerance is positively correlated with the activity of antioxidant enzymes, such as superoxide dismutase (SOD), catalase (CAT), glutathione peroxidase (GPX), ascorbate peroxidase (APX), and glutathione reductase (GR) and with the accumulation of non-enzymatic antioxidant compounds (Asada, 1999; Gupta et al., 2005).

Nitric oxide (NO) is a small volatile gaseous molecule, which is involved in the regulation of various plant growth and developmental processes, such as root growth, respiration, stomata closure, flowering, cell death, seed germination and stress responses, as well as a stress signalling molecule (Delledonne et al., 1998; Lamattina et al., 2003; Besson-Bard et al., 2008; Zhao et al., 2009; Crawford, 2006). NO directly or indirectly triggers expression of many redox-regulated genes. NO reacts with lipid radicals thus preventing lipid oxidation, exerting a protective effect by scavenging superoxide radical and formation of peroxynitrite that can be neutralized by other cellular processes. It also helps in the activation of antioxidant enzymes (SOD, CAT, GPX, APX,

and GR) (Bajgu, 2014). Exogenous NO application has been found to play roles in stress mitigation (Sung and Hong, 2010; Hossain et al., 2010; Xiong et al., 2010), but the effects depend on NO concentration.

About hormone regulation of salinity tolerance, ABA is an important phytohormone whose application to plant ameliorates the effect of stress condition(s). It has long been recognized as a hormone that is upregulated due to soil water deficit around the root. Salinity stress causes osmotic stress and water deficit, increasing the production of ABA in shoots and roots (He and Cramer, 1996; Cabot et al., 2009; Cramer and Quarrie, 2002; Kang et al., 2005; Popova et al., 1995). The accumulation of ABA can mitigate the inhibitory effect of salinity on photosynthesis, growth, and translocation of assimilates (Popova et al., 1995; Jeschke, 1997). The positive relationship between ABA accumulation and salinity tolerance has been at least partially attributed to the accumulation of K^+, Ca^{2+} and compatible solutes, such as proline and sugars, in vacuoles of roots, which counteract with the uptake of Na^+ and Cl^- (Chen et al., 2001; Gurmani et al., 2011). ABA is a vital cellular signal that modulates the expression of a number of salt and water deficit-responsive genes. Fukuda and Tanaka (Fukuda and Tanaka, 2006) demonstrated the effects of ABA on the expression of two genes, HVP1 and HVP10, for vacuolar H^+-inorganic pyrophosphatase, and of HvVHA-A, for the catalytic subunit (subunit A) of vacuolar H^+-ATPase in *Hordeum vulgare* under salinity stress. ABA treatment in wheat induced the expression of MAPK4-like, TIP 1, and GLP 1 genes under salinity stress (Keskin et al., 2010). Some other compounds having hormonal properties, such as salicylic acid (SA) and brassinosteroids (BR), also participate in plant abiotic stress

responses (Fragnire et al., 2011; Clause and Sasse, 1998). Under salinity stress, endogenous level of SA increased along with the increase in the activity of salicylic acid biosynthetic enzyme in rice seedling (Sawada et al., 2006). Jayakannan et al. (2013) have recently shown that SA improves salinity tolerance in *Arabidopsis* by restoring membrane potential and preventing salt-induced K^+ loss via a guard cell outward rectifying $K(^+)$ (GORK) channel. *Arabidopsis* seedling pretreated with SA showed upregulation of H^+-ATPase activity, thereby improving K^+ retention during salt stress; SA pretreatment did not prevent accumulation of Na^+ in roots but somehow helped to reduce the concentration of accumulated Na^+ in the shoot (Jayakannan et al. 2013). Application of BR enhanced the activity of antioxidant enzymes (SOD, POX, APX, and GPX) and the accumulation of non-enzymatic antioxidant compounds (tocopherol, ascorbate, and reduced glutathione) (El-Mashad and Mohamed, 2012).

Finally, transcription factors are considered as most important regulators that control gene expressions. Among them, bZIP, WRKY, AP2, NAC, C2H2 zinc finger gene, and DREB families comprise a large number of stress-responsive members. These transcription factor genes are capable of controlling the expression of a broad range of target genes by binding to the specific cis-acting element in the promoters of these genes. Johnson et al. (2002) observed that the expression of bZIP genes were upregulated in salt-sensitive wheat cultivar, when exposed to long-term salinity, but decreased in salt-tolerant variety. Overexpression of a NAC transcription factor in both rice and wheat confers salt tolerance, thereby predicting their role in stress mitigation (Nakashima et al., 2007). In rice transcriptional regulators

that have been demonstrated to play a significant role in abiotic stress responses involve DREB1/CBF, DREB2, and AREB/ABF (Mizoi et al., 2012; Fujita et al., 2011; RoyChoudhury et al., 2008; Ito et al., 2006; Fujita et al., 2013). Transcriptions factors such as OsNAC5 and ZFP179 show an upregulation under salinity stress, which may regulate the synthesis and accumulation of proline, sugar, and LEA proteins that in turn play an integral role in stress tolerance (Song et al., 2011). In *Arabidopsis*, salt stress results in the upregulation of AtWRKY8 which directly binds with the promoter of RD29A, suggesting it to be as one of the target genes of AtWRKY8 (Hu et al., 2013).

Genetic variations and differential responses to salinity stress in plants differing in stress tolerance enabled plant biologists to identify physiological mechanisms, sets of genes, and gene products that are involved in increasing stress tolerance and to incorporate them in suitable species to yield salt tolerant varieties. Considering the mechanisms above mentioned, tolerance to both osmotic and hyperionic stress is thus governed by a multitude of physiological and molecular mechanisms: osmotic tolerance, ionic tolerance, and tissue tolerance (Rajendran et al., 2009; Roy et al., 2014).

3.5 Giant reed (Arundo donax L.): a promising energy crop

Arundo donax L., common name "giant cane" or "giant reed", is a plant that grows spontaneously in different kinds of environments and that it is widespread in temperate and hot zones all over the world (Corno et al., 2014) (Figure 8).

A. donax belongs to the Poaceae family, in the tribe of Arundinaceae along with other species such as *Arundo plinii*

Turra, *Arundo collina* Tenore, *Arundo mediterranea* Danin (Mariani et al., 2010) and other ornamental species.

Figure 8. *Arundo donax* L. (Giant reed).

The plant originally developed in East Asia, getting successively into the Mediterranean area and then spreading around the world through human activity (Hardion et al., 2012; Mariani et al., 2010; Polunin and Huxley, 1987). Human domestication occurred in the Mediterranean region (Zeven and de Wet, 1982). Another hypothesis suggests that *A. donax* and its related species had origins in the Mediterranean area (Zeven and de Wet, 1982); in any case by now the presence of this plant is certified in all inhabited continents and in very different environments. *A. donax* is a hydrophyte plant able to grow in soil rich in water, especially near channels, rivers, lakes, ponds and marshes, where it shows the maximum biomass yields. The phylogenetic origin is not very clear: the chromosome number of *A. donax* is not yet certain because of the high number of chromosomes and

their small size, so that different authors have reported different chromosome numbers. Firstly Hunter (1934) counted 110 chromosomes as did Bucci et al. (2013) and Pizzolongo (1962). However, Christopher and Abraham (1971) reported 108 chromosomes, while Haddadchi et al. (2013) reported 84 chromosomes (2n = 7x = 84). It can be guessed that different ploidy levels of *A. donax* may depend on the different territory in which the plant has grown and of course may depend on its evolutionary history. The variability in chromosome number has been observed in the related species *P. australis*, where both euploid and aneuploid plants have been found (euploid numbers, between 3x and 12x, with x = 12); the more frequently found varieties in Europe are tetraploids while in Asia the more widespread varieties are octoploids with 96 chromosomes (Clevering and Lissner, 1999). Such genetic plasticity in aquatic plants is not surprising, taking into consideration the vegetative reproducing system that increases the probability of accumulating chromosomal mutations (not filtered by the process of meiosis). A simple hypothesis to explain the formation of the 2n = 108 or 110 *A. donax* sterile species, is based on the fusion of reduced (n = 36) and unreduced (n = 72) gametes from fertile progenitors (2n = 72) such as *A. plinii* (Bucci et al., 2013; Hardion et al., 2012). Regarding the genotypic diversity among clonal populations sampled in different regions, again, data are different depending on the country studied and molecular markers used. However, genetic diversity has been very low, as expected for an agamic-reproducing plant, with the exception of data reported by Haddadchi et al. (2013) in Australia and Khudamrongsawat et al. (2004) in USA, although in this last case more probably the result obtained depended on the type

of molecular marker used (RAPD). Despite its low genetic diversity, heritable phenotypic differences among clones of *A. donax* have been reported that could be explored to improve several plant characteristics such as number of culms, culm diameter and height (Cosentino et al., 2006; Pilu et al., 2014). For these reasons the genetic improvement of this plant, aiming to obtain better performance as an energy crop, needs to be mainly based on clonal selection. Micro-projectile bombardment-mediated transformation of *A. donax* has been performed, obtaining transient expression of green fluorescent protein (GFP) and β-glucuronidase (GUS) genes, although high frequency plant regeneration from embryogenic callus is still to be optimized (Dhir et al., 2010). However, the new genome editing techniques such as CRISPR/Cas9 may represent a good tool for the genetic improvement. Genetic improvement of this species would be aimed to improve the traits biomass production, quality and the capacity of plants to propagate efficiently *in vitro* culture or by propagules.

3.5.1 Reproduction

A. donax is a sterile plant (Else, 1996; Wijte et al., 2005) because of the absence of division of the megaspore cell mother (Bhanwra et al., 1982). Hence being unable to produce seeds, sowing cannot be used to propagate the plant for agriculture purposes (Khudamrongsawat et al., 2004). Because of its sterility, *A. donax* has developed asexual vegetative reproduction, allowing its rapid spread throughout the world; new plants can be generated every year directly from rhizomes (Figure 9), the underground structure of the plant: in a temperate climate, during spring and summer, the rhizomes explores the soil laterally and allow the expansion

of the plant with the creation and germination of buds. In addition, rhizome fragments can be obtained from live plants; this requires healthy rhizomes and the right environmental conditions for germination. Beside rhizome propagation, another natural plant reproduction method consists of rooting at the nodes. *A. donax* is able to generate new individuals from stem fragments coming from breakage and/or from lateral canes that bend down, getting in touch with the soil (Figure 9). In the presence of the right conditions (e.g. moisture) these fragments can produce roots from nodes, allowing the development of new shoots (Boland, 2006). Thanks to this ability, the principal means for canes to disperse is via water, i.e. *A. donax* usually grows along water bodies; during floods stem fragments transported by water, in the presence of the right conditions, can generate new canes (Brinke, 2010; Decruyenaere and Holt, 2005; Else, 1996). Some authors report that fragments can produce new plants only if there is an axillary bud present (Boose and Holt, 1999; Else, 1996; Wijte et al., 2005). The natural reproduction of *A. donax* could be explored for agronomic purposes. The cane fragments can be used to produce propagules characterized by the presence of developed below- and above-ground structures that allow a very high percentage of plant establishment (~100%) and the successive development of vigorous plants, right from the first year of plantation. Developed plants can be produced, also, by hydroponic and micropropagation techniques, producing plants with both roots and an active photosynthetic apparatus (Figure 9).

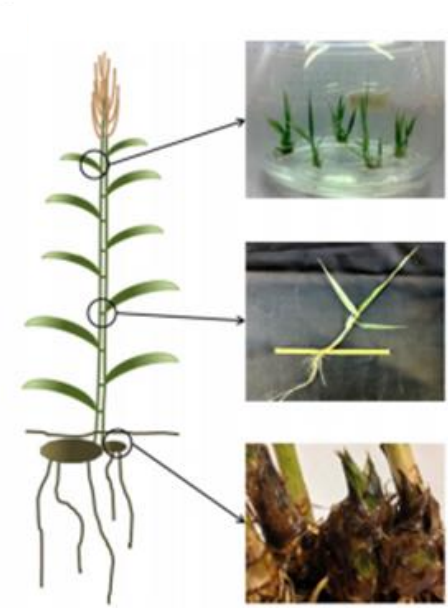

Figure 9. *A. donax* reproduction techniques: micro-propagation (from axillary bud) (top), hydroponic technique (from nodes) (middle) and rhizome propagation (from rhizome buds) (bottom) (Corno et al., 2014).

The hydroponic technique is based on the natural plant ability to develop new plants from nodes. Mature cane fragments can be cut into smaller pieces (about 15 cm) containing at least one node and put into water under particular conditions, so that each node is able to generate one shoot with its own roots (Ceotto and Di Candilo, 2010; Pilu et al., 2014). Micro-propagation refers to *A. donax in vitro* reproduction technique (Takahashi et al., 2010) starting from axillary buds, and inducing tillering, by using media supplemented with 0–1 mg L^{-1} of BA (6-benzyladenine) and 0–0.1 mg L^{-1} of NAA (1-naphthaleneacetic acid). It is possible to promote root formation and root growth by modifying the BA/NAA ratio,

hence the "seedlings" obtained can be transplanted into pots for continued development. It is also possible to induce callus formation using a medium containing 2,4-D (2,4-dichlorophenoxyacetic acid) alone; the callus produced is able to generate shoots useful for propagation after its transfer into a hormone-free medium (Takahashi et al., 2010).

3.5.2 Lifecycle and agronomy

In a temperate climate the *A. donax* lifecycle begins in March with the sprouting of new canes from rhizomes (Figure 10); therefore, rhizomes play a key role in this phenological phase (Nassi o di Nasso et al., 2013). This stage is crucial for plant productivity because it determines future plant yield and growth rapidity.

Figure 10. *A. donax* lifecycle in a temperate climate (Corno et al., 2014).

Generally, the first growing stages are the most important: if the plant suffers early water shortages, biomass height and yield are lower than normal (Abichandani, 2007; Perdue, 1958; Watts, 2009). During springtime plant growth is very fast with an important biomass production that gives to *A. donax* the status of one of the biggest herbaceous plants in the world: its height ranges from 2 to 8 m (Perdue, 1958) but in some areas, such as temperate and subtropical climate zones and according to water availability, the plants can reach over 9 m in height (Giessow et al., 2011). The fast growth and the ability of *A. donax* to accumulate biomass are the most important characteristics distinguishing this plant from other herbaceous plants. The growth velocity is assisted by the fact that *A. donax*, although it is a C3 grass, has the typical development of a C4 plant. Unlike normal C3, *A. donax* shows high photosynthetic yields thanks to the greater saturation level of the photosystem than other C3 plants, allowing high biomass accumulation (Papazoglou et al., 2005, 2007; Rossa et al., 1998). New canes develop during early summer, but they are smaller and thinner than the growth during spring. Plant flowering occurs from August to October, according to the climatic conditions. Plant senescence begins at the end of November and continues during winter months; during this period the plant turns yellow, but it is not dead inside. The stalk tissues, in fact, are still alive inside allowing a faster vegetative restart in the successive season (February). In February, canes restart vegetative activity, developing nodal buds and generating secondary branches; these structures typically appear earlier than new canes coming from the rhizomes. During this phase the rhizome is very important as it releases nutrients (Nassi o di Nasso et al., 2013) allowing rapid growth at the beginning

of the season. Both environmental and climatic conditions may cause prolongation or shortening of the different phenological phases: in warmer places, the winter dormancy is shorter than in other areas or completely absent in the case of subtropical climates. High nitrogen concentrations, also, could lead to no dormancy during the year (Decruyenaere and Holt, 2005).

A. donax cultivation consists in soil preparation, transplantation of the propagules, irrigation, fertilization and harvest. The most important steps are related to the first year when the operations for planting and the plant establishment are required. Soil preparation consists in soil plowing (about 40–45 cm depth for rhizomes and less for propagules) (Fiala, 2009) and fertilization; transplanting of rhizomes can be done between March and April at a depth of 15–20 cm (Fiala, 2009).

On the whole, and referring to a temperate climate, about 5000–10,000 plants ha−1 are required to ensure good production after 1–2 years from the plantation, with low agronomic inputs such as irrigation, fertilization and phytosanitary interventions. Nowadays, new crop approaches suggest the reduction of the plant density, while keeping the same biomass yields. Angelini et al. (2005) suggested that a lower plant density could encourage production of more tillers and stalks and, consequently, more plant productivity than using high-density planting.

A. donax establishment in the field represents the most delicate moment for its cultivation: during this period the plants can suffer from water shortage stress, requiring additional irrigation; in addition, if weeds are dominant among the younger cane shoots, herbicide treatment may be necessary. During the second year the strong development of

A. donax suppresses weeds and normally does not need additional water. After the first year of plantation, *A. donax* does not need organic or inorganic fertilization to complete its lifecycle and to achieve high yields, but the application of fertilizers enhances biomass production. The addition of nutrients (Angelini et al., 2005; Christou et al., 2003; Gilbert et al., 2010), especially nitrogen (Borin et al., 2013; Quinn et al., 2007) promotes a better development of rhizomes and consequently of new sprouts, allowing yield increases.
An *A. donax* plantation produces biomass for about 10–15 years, or even more if it is harvested every year and adequately fertilized. In any case in the last years of cultivation, biomass yields decline (Angelini et al., 2009).

3.5.3 A. donax L. as feedstock: advantages and disadvantages

The adaptability of the plants to different kinds of environments, soils and growing conditions, in combination with the high biomass production and the low input required for its cultivation, confer on *A. donax* many advantages when compared to other energy crops (Table 1).
A. donax produces high amount of biomass per surface unit if compared to traditional energy crops; yield depends on several factors such as the age of the plants, pedo-climatic conditions, plant density and agronomics, so that high variability is reported in the literature. Average biomass production (aboveground part of plant) is around 15.5 kg dry matter (DM) m−2 (Giessow et al., 2011). *A. donax* can grow in different environmental conditions (Lewandowski et al., 2003): salinity does not seem to affect plant growth (Peck, 1998; Perdue, 1958) and it is possible to achieve high biomass yields under high salinity conditions thanks to its

halophyte behavior; for example, it was reported that in Australia *A. donax* could be a good solution for several saline soils (Williams et al., 2008). In California, for example, *A. donax* easily grows along beaches and in estuaries with brackish water conditions (Else, 1996). Water availability is not a limiting factor for plant growth: it was reported that *A. donax* could resist both soils characterized by lack of water and soils which was water-saturated (Lewandowski et al., 2003).

A. donax cultivation is possible in almost all climatic regions, with limitations only due to the cold; recently, researchers have been developing clones resistant to cold stress, allowing its cultivation in colder climates (Pompeiano et al., 2013). The adaptability to all these conditions makes this plant suitable for marginal and abandoned lands (Lewandowski et al., 2003), i.e. soils that are not suitable for traditional agriculture. Nassi o Di Nasso et al. (2013) showed competitive yields of *A. donax* (20 Mg ha−1 DM) on low fertility sandy soil. This specie showed, also, a strong adaptability to soil containing high macro-element content, such as N (Ambrose and Rundel, 2007) and P (Williams et al., 2008). Because of high biomass production, attention must be paid to the impact of *A. donax* cultivation on soil properties. Literature speculates that prolonged nutrient uptake could reduce the availability of the main elements in the soil, especially N (Angelini et al., 2009; Borin et al., 2013). Other authors reported positive effects on soil, i.e. the increase of both organic matter and microbial biomass content (Riffaldi et al., 2012). In particular, because *A. donax* is a no tillage crop, soil can accumulate organic matter more than that obtainable with other cultures such as, for example cropping sequences: legumes and cereal conventionally

cultivated, and natural grassland (with forage removal) (Riffaldi et al., 2012). Other positive effects are reported by Christou et al. (2003) that highlighted the importance of *A. donax* on preserving soil erosion in soil slopes and in limiting nitrate leaching. From an economic point of view, the excellent biomass yields compensate for both plantation and water supply costs (Giessow et al., 2011) and herbicide treatments during the first crop year (Lewandowski et al., 2003). Currently, in Italy, estimated costs to produce *A. donax* are of about 700–1000 € ha−1 year−1 (as the average of 10 years) and 13–20 € Mg−1 DM (as the average of 10 years and 10,000 plant ha−1) in the Po Valley, North Italy. These investment costs are much lower than those reported for other energy crops cultivated in the same pedo-climatic region such as corn, sorghum, rye and triticale. The most expensive aspect of *A. donax* culture is the initial investment to purchase "seedlings" material (rhizome or micro-propagated plants) (e.g. 3000–5000 € Ha−1). These costs are those currently applied in an Italian commercial context during the *A. donax* sales campaign on 2013 and 2014 that involved about 40 different farms. *A. donax* has been used for phytoremediation of soil contaminated by Hg, Cd, Cr, As, Pb, Ni, Mn, Zn and Fe. Moreover *A. donax* has been used for treating urban wastewater (Mandi and Abissy, 2000), aqueous solutions from industrial processes (Zhang et al., 2008) and in general wastewater containing organic compounds (Sudha and Vasudeva, 2009). The capacity of *A. donax* to grow in different environments and to resist the competition of other plant species, has promoted the colonization of different areas (Quinn et al., 2007; Virtue et al., 2010). Because of that experience, some authors indicated that *A. donax* cultivation is not recommended in floodplains

and riparian areas, because of the risks for the natural equilibrium of the ecosystem (Virtue et al., 2010). Nevertheless, only rarely and under specific conditions *A. donax* represents a threat for native plants by altering the ecosystem (Giessow et al., 2011; Herrera and Dudley, 2003; Lowe et al., 2000; Mack, 2008; Spencer et al., 2005; Tracy and DeLoach, 1998), and it does not represent a threat above all when it is used as energy crop in an agricultural area, where its weed potential is limited by the natural sterility of the plant. A list of advantages and disadvantages of *A. donax* as feedstock is reported in Table 1.

When investigating the energy balance of perennial crops under different crop managements in the Mediterranean, giant reed has been found to have a higher energy efficiency than other species (e.g. miscanthus) (Angelini et al., 2009; Mantineo et al., 2009; Monti et al., 2009; Fazio and Barbanti, 2014), thanks to the high biomass and cellulose yield.

A. donax grows spontaneously and abundantly all over Italy, with rapid growth and high yield capacity. In Italy, this species was utilized industrially since 1930, when Snia-Viscosa registered a trademark to obtain cellulose pasta for the production of rayon viscose and paper (Facchini, 1941).

From 1997 to 2000, a European project (FAIR3 CT96 2028): "Giant reed (*A. donax* L.) Network Improvement, productivity and biomass quality" has been carried out to obtain useful information on the possibility to utilize this species on wide scale in Europe (Cosentino et al., 2006).

Within this framework, in the South of Italy research were carried out in order to examine the existing phenotypic and genotypic variability in the extensively diffuse populations of *A. donax* in this area.

Table 1. Advantages and disadvantages of A. donax as feedstock

Aspects	Advantages	Disadvantages
Agronomical	High biomass yields per ha	Not recommended in floodplain
	Adaptation to different kind of environments	High initial investment costs
	Adaptation to different kinds of soils	Potential weed in no-agricultural area
	Use of marginal lands	
	Lower tillage and cost than traditional crops	
	No seeds reproduction	
	Vegetative reproduction by micro-propagation or by rhizome	
Environmental	Phytodepuration properties	
	Strong reduction in using chemicals	
	Promoting biodiversity	
	Promoting soil organic matter accumulation	
Utilization	More biogas production per cultivated area	Lower biogas production per dry matter ton than traditional crops
	More bio-ethanol production per cultivated area	Pretreatment need
	Green Chemistry	
	Different industrial uses	

3.5.4 A. donax and salinity

Different studies have been conducted in the last twenty years trying to understand the adaptability of *A. donax* to marginal lands and adverse environmental conditions. Many authors focused on the utilization of wastewater to grow this crop, but mostly they tested the ability of *A. donax* to grow in high salinity conditions and to maintain a high yield in terms of biomass production. These studies identified *A. donax* as "moderately tolerant" to NaCl. Williams et al., in 2008 presented trial results for *A. donax* growing on saline soil and irrigated with saline winery wastewater for biomass production, nutrient removal, salt tolerance, weed risk and carbon sequestration. In this trial *A. donax* tolerated up to 25 dS/m salinity in the soil water extract for several months giving 45.2 tonnes of oven dry tops per hectare in the first year. This yield is over twice that reported for conventional crops such as forage sorghum, kenaf or lucerne, when grown on arable land with high rainfall or better-quality water. For these reasons they described *A. donax* as a crop having the potential to form the basis of a new biofuel and/or pulp paper industry using the underutilized resources of saline wastewater and saline/marginal lands in Australia.

Later in 2014 Nackley and Kim tested the whole-plant and leaf responses to salinity using rhizomes of *A. donax* collected from a population found growing wild, approx. 5 meters above the high tideline along of the San Francisco Bay, San Rafael, CA, USA. They transplanted the rhizomes and applied eight salt level ranging from 0 to 42 dS m^{-1}. Classic growth analysis showed >80% reduction in overall growth at the highest salinities. Yet, there was zero mortality indicating that *A. donax* is able to tolerate high levels of salt. Declining photosynthesis rates were strongly correlated ($R^2 > 0.97$) with decreasing stomatal conductance, which was in

turn closely related to increasing salinity. Leaf gas exchange revealed that stomata and leaf limitations of carbon dioxide were three times greater at high salinities. Nonetheless, even when salinities were 38–42 dS m^{-1} *A. donax* was able to maintain assimilation rates 7–12 µmol m^{-2} s^{-1}. Further, by maintaining 50% relative growth at salinities ~12 dS m^{-1} *A. donax* can be classified as 'moderately salt tolerant'. *A. donax* leaf gas exchange and whole plant salt tolerance are greater than many important food crops (i.e. maize, rice), the bioenergy feedstock *Miscanthus x giganteus*, as well as some uncultivated plant species (i.e. *Populus* and *Salix*) that are indigenous in regions *A. donax* currently invades.

Another study conducted by Sánchez and collaborator (2015) was carried out in order to clarify the salinity and water stress effects on biomass production in *A. donax*. In this experiment five clones of giant reed were subjected to increasing salt levels (mild and severe) in two locations: University of Catania (Italy) and University of Barcelona (Spain) and other eight clones were subjected to both salinity and water stress in different combinations. Photosynthetic and physiological parameters as well as biomass production were measured in these plants. According to data collected, giant reed seems to be more tolerant to salt than water stress.

More recently, De Stefano et al., (2017), evaluated growth parameters of several *A. donax* clones, collected in different hydrogeological basins in Campania and Lazio regions (Italy), under two salt regimes in hydroponics: mild NaCl stress (50 mM NaCl, 5.6 mS cm^{-1} EC, for 10 days) and a severe NaCl treatment (150 mM, 18.8 mS cm^{-1} EC, for 21 days) enabling the identification of ecotypes maintaining plant growth under high salinity. Among several biometric parameters, 4th leaf width, and shoot and root dry weight consistently highlighted differences between ecotypes. Gas-

exchange parameters also responded to severe NaCl treatment, while the photosystem efficiency was good, regardless of treatment. These results, together with the appearance of NaCl toxicity symptoms only after severe salt treatment, without plant mortality, and by less than 50% inhibition for most growth parameters, confirmed the moderate tolerance of *A. donax* to this kind of stress.

3.6 Genetic investigations

3.6.1 Transcriptomics and RNA-seq

The transcription of a subset of genes into complementary RNA molecules specifies a cell's identity and regulates the biological activities within the cell. Collectively defined as the transcriptome, these RNA molecules are essential for interpreting the functional elements of the genome and understanding development and disease (Kukurba et al., 2015). The transcriptome has a high degree of complexity and encompasses multiple types of coding and noncoding RNA species. Historically, RNA molecules were relegated as a simple intermediate between genes and proteins, as encapsulated in the central dogma of molecular biology. Therefore, messenger RNA (mRNA) molecules were the most frequently studied RNA species because they encoded proteins via the genetic code.

Initial gene expression studies relied on low-throughput methods, such as Northern blots and quantitative polymerase chain reaction (qPCR), that are limited to measuring single transcripts. Over the last two decades, methods have evolved to enable genome-wide quantification of gene expression, or better known as transcriptomics. The first transcriptomics studies were performed using hybridization-based microarray technologies, which provide a high-throughput option at

relatively low cost (Schena et al. 1995). However, these methods have several limitations: the requirement for a priori knowledge of the sequences being interrogated, problematic cross-hybridization artifacts in the analysis of highly similar sequences and limited ability to accurately quantify lowly expressed and very highly expressed genes (Casneuf et al. 2007; Shendure 2008). In contrast to hybridization-based methods, sequence-based approaches have been developed to elucidate the transcriptome by directly determining the transcript sequence. The development of high-throughput next-generation sequencing (NGS) has revolutionized transcriptomics by enabling RNA analysis through the sequencing of complementary DNA (cDNA) (Wang et al. 2009). This method, termed RNA sequencing (RNA-Seq), has distinct advantages over previous approaches and has revolutionized our understanding of the complex and dynamic nature of the transcriptome. RNA-Seq provides a more detailed and quantitative view of gene expression, alternative splicing, and allele-specific expression. Recent advances in the RNA-Seq workflow, from sample preparation to sequencing platforms to bioinformatic data analysis, has enabled deep profiling of the transcriptome and the opportunity to elucidate different physiological and pathological conditions.

A typical RNA-Seq experiment consists of isolating RNA, converting it to complementary DNA (cDNA), preparing the sequencing library, and sequencing it on an NGS platform (Figure 11).

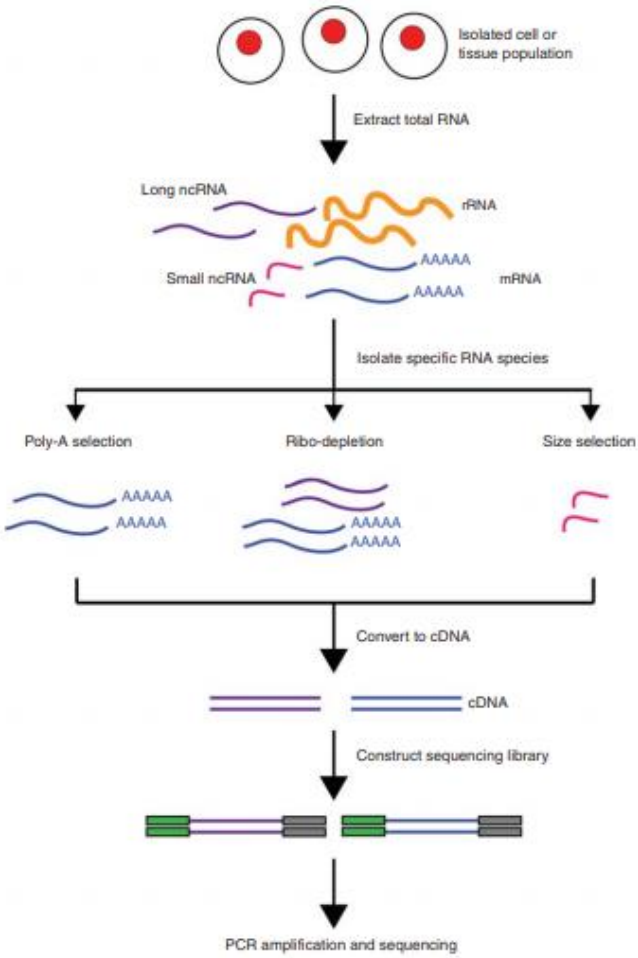

Figure 11. Overview of RNA-Seq experiment. First, RNA is extracted from the biological material of choice (e.g., cells, tissues). Second, subsets of RNA molecules are isolated using a specific protocol, such as the poly-A selection protocol to enrich for polyadenylated transcripts or a ribo-depletion protocol to remove ribosomal RNAs. Next, the RNA is converted to complementary DNA (cDNA) by reverse transcription and sequencing adaptors are ligated to the ends of the cDNA fragments. Following amplification by PCR, the RNA-Seq library is ready for sequencing (Kukurba and Montgomery, 2015).

The first step in transcriptome sequencing is the isolation of RNA from a biological sample. To ensure a successful RNA-Seq experiment, the RNA should be of sufficient quality to produce a library for sequencing. The quality of RNA is typically measured using the RNA Integrity Number (RIN) between 1 and 10 with 10 being the highest quality samples showing the least degradation. The RIN estimates sample integrity using gel electrophoresis and analysis of the ratios of 28S to 18S ribosomal bands. Low-quality RNA (RIN< 6) can substantially affect the sequencing results and lead to erroneous biological conclusions. Following RNA isolation, the next step in transcriptome sequencing is the creation of an RNA-Seq library, which can vary by the selection of RNA species and between NGS platforms. The construction of sequencing libraries principally involves isolating the desired RNA molecules, reverse-transcribing the RNA to cDNA, fragmenting or amplifying randomly primed cDNA molecules, and ligating sequencing adaptors. An appropriate library preparation protocol that will enrich or deplete a "total" RNA sample for particular RNA species must be chosen. In fact, the total RNA pool includes ribosomal RNA (rRNA), precursor messenger RNA (pre-mRNA), mRNA, and various classes of noncoding RNA (ncRNA). In most cell types, the majority of RNA molecules are rRNA, typically accounting for over 95% of the total cellular RNA. If the rRNA transcripts are not removed before library construction, they will consume the bulk of the sequencing reads, reducing the overall depth of sequence coverage and thus limiting the detection of other less-abundant RNAs. Many protocols focus on enriching for mRNA molecules before library construction by selecting for polyadenylated (poly-A) RNAs. In this approach, the 3′ poly-A tail of mRNA

molecules is targeted using poly-T oligos that are covalently attached to a given substrate (e.g., magnetic beads). Universal to all RNA-Seq preparation methods is the conversion of RNA into cDNA because most sequencing technologies require DNA libraries. Finally, sequencing adaptors are ligated to the ends of the cDNA fragments.

However, many experimental details, dependent on a researcher's objectives, should be considered before performing RNA-Seq. These include the use of biological and technical replicates, depth of sequencing, and desired coverage across the transcriptome.

When designing an RNA-Seq experiment, the selection of a sequencing platform is important and dependent on the experimental goals. Currently, several NGS platforms are commercially available and other platforms are under active technological development (Metzker, 2010). The majority of high-throughput sequencing platforms use a sequencing-by-synthesis method to sequence tens of millions of sequence clusters in parallel. In recent years, the sequencing industry has been dominated by Illumina, which applies an ensemble-based sequencing-by-synthesis approach (Bentley et al., 2008). Using fluorescently labeled reversible-terminator nucleotides, DNA molecules are clonally amplified while immobilized on the surface of a glass flowcell. Because molecules are clonally amplified, this approach provides the relative RNA expression levels of genes. To remove potential PCR-amplification biases, PCR controls and specific steps in the downstream computational analysis are required. One major benefit of ensemble-based platforms is low sequencing error rates (<1%) dominated by single mismatches. Currently, the Illumina HiSeq platform is the most commonly applied next-generation sequencing technology for RNA-Seq and has set the standard for NGS sequencing. The platform

has two flow cells, each providing eight separate lanes for sequencing reactions to occur. The sequencing reactions can take between 1.5 and 12 d to complete, depending on the total read length of the library. Another important consideration for choosing a sequencing platform is transcriptome assembly. Transcriptome assembly is necessary to transform a collection of short sequencing reads into a set of full-length transcripts.

Gene expression profiling by RNA-Seq provides an unprecedented high-resolution view of the global transcriptional landscape. Data coming from an RNA sequencing are raw data that need to be further processed and analyzed in order to obtain a clear and complete view of the transcriptome and of the gene expression status. The conventional pipeline for RNA-Seq data includes generating FASTQ-format files contains reads sequenced from an NGS platform, aligning these reads to an annotated reference transcriptome or assembly of a *de novo* transcriptome, quantification of genes expression, quality assessment and differential genes expression. (Figure 12).

Mapping RNA-Seq reads to the genome is considerably more challenging than mapping DNA sequencing reads because many reads map across splice junctions. After RNA-Seq reads are aligned, the mapped reads can be assembled into transcripts. The majority of computational programs infer transcript models from the accumulation of read alignments to the reference genome (Trapnell et al., 2010; Li et al., 2011; Roberts et al., 2011a; Mezlini et al., 2013).

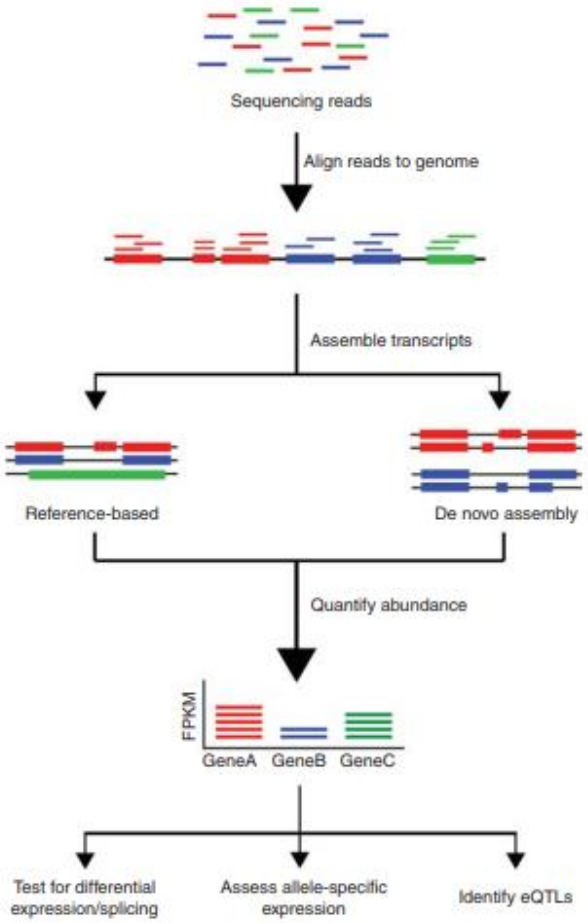

Figure 12. Overview of RNA-Seq data analysis. Following typical RNA-Seq experiments, reads are first aligned to a reference genome. Second, the reads may be assembled into transcripts using reference transcript annotations or de novo assembly approaches. Next, the expression level of each gene is estimated by counting the number of reads that align to each exon or full-length transcript. Downstream analyses with RNA-Seq data include testing for differential expression between samples, detecting allele-specific expression, and identifying expression quantitative trait loci (eQTLs) (Kukurba and Montgomery, 2015).

An alternative approach for transcript assembly is *de novo* reconstruction, in which contiguous transcript sequences are assembled with the use of a reference genome or annotations (Robertson et al., 2010; Grabherr et al., 2011; Schulz et al., 2012). A common downstream feature of transcript reconstruction software is the estimation of gene expression levels. To accurately estimate gene expression, read counts must be normalized to correct for systematic variability, such as library fragment size, sequence composition bias, and read depth (Oshlack and Wakefield, 2009; Roberts et al., 2011b). To account for these sources of variability, the reads per kilobase of transcripts per million mapped reads (RPKM) metric normalizes a transcript's read count by both the gene length and the total number of mapped reads in the sample. For paired end-reads, a metric that normalizes for sources of variances in transcript quantification is the paired fragments per kilobase of transcript per million mapped reads (FPKM) metric, which accounts for the dependency between paired-end reads in the RPKM estimate (Trapnell et al., 2010).

A primary objective of many gene expression experiments is to detect transcripts showing differential expression across various conditions. In this context next-generation high-throughput sequencing techniques have become an increasingly useful tool for exploring whole plant genomes, providing a means for analyzing plant molecular regulatory mechanisms in specific environments such as various abiotic stress conditions, including heavy metal toxicity, herbicide toxicity and salt toxicity (Bahieldin et al., 2009; Zhang et al., 2016b; Gu et al., 2017).

Nevertheless, salt stress response mechanisms in plants remain poorly understood due to the complexity of the response process and the genetic variability among plant species. Moreover, our knowledge of the genetic bases of salt

tolerance is largely based on genetic studies in model or crop species (Hanin et al., 2016).

De novo RNA sequencing (RNA-Seq) assembly might facilitate the study of transcriptomes for non-model plant species such as *A. donax* L. for which the genome sequence is not available and for which transcriptomic data under salt stress conditions are poor. This approach will enable an almost exhaustive survey of its transcriptomes and will allow the discovery of virtually all expressed genes in a plant tissue under abiotic stress such al salt stress. Useful *A. donax* genomic resources were provided by the work of Sablok et al. (2014) which used tissue-specific NGS of four different organs (leaf, culm, bud and root) of one *A. donax* ecotype constituting a comprehensive reference catalog of transcripts aimed at characterizing and improving the spatial and temporal patterns of expression underlying the high productivity of biomass. Transcriptomes of *A. donax* is, from that moment, accessible through a customized BLAST server (http://ecogenomics.fmach.it/arundo/) for mining and exploring the genetic potential of this species. Furthermore, they based on functional annotation and homology comparison to 19 prospective biofuel Poaceae species, to provide the first genomic view of this crop. The analysis of the transcriptome revealed strong differences in the enrichment of the Gene Ontology categories and the relative expression among different organs, and the analysis of transcripts putatively involved in stress in *A. donax,* by using as reference the comprehensive resource provided by the Arabidopsis Stress Responsive Gene Database (ASRGDB), led to the identification of genes related to salt and heavy metal tolerance, particularly interesting considering the tolerance of *A. donax* to these stresses. This study allowed to identify several expressed genes that could be preferential

targets for functional studies, for metabolic engineering or for tailoring growth habit/development of the giant reed to higher bioenergy yield. One year later a shoot transcriptome was obtained from an *A. donax* invasive ecotype in order to establish a molecular dataset allowing following studies of the abiotic stress capabilities of this plant (Barrero et al., 2015). They used an llumina Hi-Seq protocol to sequence the transcriptome of actively growing shoots from an invasive genotype collected along the Rio Grande River and reported the assembly of 27,491 high confidence transcripts with at least 70% coverage of known genes in other Poaceae species. A *de novo* assembly and annotation of the leaf transcriptome of *A. donax*, using a RNA-seq approach, was provided by Evangelistella and collegues in order to have a more complete gene expression catalogue and allow a comprehensive comparison among various assemblies (Evangelistella et al., 2017). The genomic resource was generated using three ecotypes originating from distant geographical locations (Greece, Croatia, Portugal) that, for this reason, could have accumulated heritable phenotypic differences. A global comparison of homology between the transcriptomes of *A. donax* and four other species of the Poaceae family revealed a high level of global sequence similarity within this family. In addition, comparative analyses with several phylogenetically related species with more complete genomic information were performed, allowing the identification of putative genes controlling important agronomic or domestication traits. Particularly, genes encoding for stress-associated proteins (SAPs), for lignin and cellulose biosynthesis, purine and thiamine metabolism, and stomatal development and distribution were analyzed. The highest sequence similarity (the lowest e-value) with the phylogenetically related species was obtained with *S. italica*,

followed by *S. bicolor*, *Zea mays*, and *O. sativa* ssp. Japonica. The biological pathway found to be the more represented by Evangelistella et al. (2017) were purine and thiamine metabolism, phenylpropanoid biosynthesis, starch and sucrose metabolism, cellulose biosynthesis, carbon fixation, stomatal development and distribution pathways, and finally the presence of homologous transcripts encoding for SAPs. Additionally, simple sequence repeats (SSRs) were identifed in the leaf transcriptome, thereby obtaining the first genetic marker catalogue for *A. donax*, which could be used for population genetics studies. That study has broadened the knowledge of the transcriptome profle in *A. donax* vegetative tissue (leaf), grown under natural conditions. Recently, the first characterization of *A. donax* transcriptome in response to drought has been reported by Fu et al. (2016). They obtained by Illumina-based RNA-seq the whole root and shoot transcriptomes of young *A. donax* plants subjected to osmotic/water stress with 10 and 20 % polyethylene glycol (PEG) and identified a total of 3034 differentially expressed genes (DEGs) between conditions in each organ. While the same percentage of DEGs was found in root and shoot, a great share of genes resulted differentially expressed in between control and severe water stress compared to the control versus mild water stress, indicating the successful induction of varying degrees of water stress as a function of PEG concentration. Interestingly, the majority of stress-related genes belonged to categories "salt," "oxidative," "dehydration," and "osmotic." This is expected, as water limitation is known to cause reduced turgor and integrity of membranes, increase of intracellular ionic and nonionic solute concentrations and enhanced production of reactive oxygen species (ROS), that cross-trigger responses to high-salinity, oxidative and osmotic stresses. The higher

responsivity was found in roots compared to shoots at the early stages of water stress. Thus, a qualitatively different responses between root and shoot tissues was underlined. Among the most significantly enriched metabolic pathways identified using a crucial role was played in both shoots and roots by genes involved in the signaling cascade of abscisic acid. They further identified relatively large organ-specific differences in the patterns of drought-related transcription factor AP2-EREBP, AUX/IAA, MYB, bZIP, C2H2, and GRAS families, which may underlie the transcriptional reprogramming differences between organs. This work led to the identification of early-responsive genes to water stress which might constitute a basin of information for the improvement of giant reed productivity under water limitation, but no genomic or transcriptomic resources of *A. donax* subjected to salty soil are available so far and might be useful to understand the response mechanism to this abiotic stress.

3.6.2 SSR as molecular markers

Genome analysis using molecular markers allows to detect diversity due to mutations of homologous DNA regions in different individuals belonging to the same species or to different species. The differences between individuals at the nucleotidic sequence level constitute a set of genetic markers with high discriminating power that represents a very accurate genomic analysis system. A molecular marker can be defined as that genomic locus, detectable with specific probes or primers which, thanks to its presence, distinguishes in a characteristic and unequivocal way the chromosomal tract with which it is identified and the regions that surround it at the 5 'and 3 ' ends. Molecular markers are generally not referable to the activity of specific genes, but are based

directly on the detection of differences (polymorphisms) in the nucleotide sequence of DNA due to insertions, deletions, translocations, duplications, single mutations, etc. Molecular markers present different positive aspects: 1) they are not interfered by the environment; 2) they cover any part of the genome (transcribed or not transcribed regions), allowing to detect differences even between genetically similar and phenotypically indistinguishable individuals; 3) do not have epistatic or pleiotropic effects; 4) in many cases they have codominant expression, thus allowing to distinguish the heterozygotes from homozygotes. Some types of markers are based on the hybridization process (RFLP, VNTR) while others are based on PCR (RAPD, SSR, AFLP).

Among the molecular markers above mentioned, SSRs (*Simple Sequence Repeat*), also known as microsatellites, are multi-allele, co-dominant, highly informative, occur with high relative abundance and good coverage across the genome, and are experimentally reproducible (Powell et al., 1996; Ahmad et al., 2018). SSRs allow to highlight polymorphisms at repeated DNA sequences level. The sequencing of genomes of model plants, such as *Arabidopsis thaliana*, but also of cultivated plants, such as rice and maize, highlighted a prevalent presence of repeated elements. The cultivated plants have very large genomes and a general rule has emerged according to which the proliferation of the number of repeated sequences increases progressively with the increase in the size of the genomes. In fact, there are many repeated sequences dispersed in the plant genome, even very simple from a structural point of view. It has been estimated that in plant genomes there are, on average, 154 SSR regions each Mb, that is one microsatellite every 6.5 Kb.

At a structural level, SSRs are sequence blocks containing DNA motifs of 1 to 6 base pairs repeated between 5–50 times

and flanked by sequences that are generally unique in the genome, but conserved in organisms (Powell et al., 1996; Pan et al., 2007) (Figure 13). SSRs are classified into mono-, di-, tri-, tetra-, penta-, or hexa-SSRs based on the number of repeated base pairs, and into perfect, imperfect, and compound SSRs, which display perfect repetitions, interruption with novel nucleotides, and two or more tandem motifs (Selkoe and Toonen, 2006).

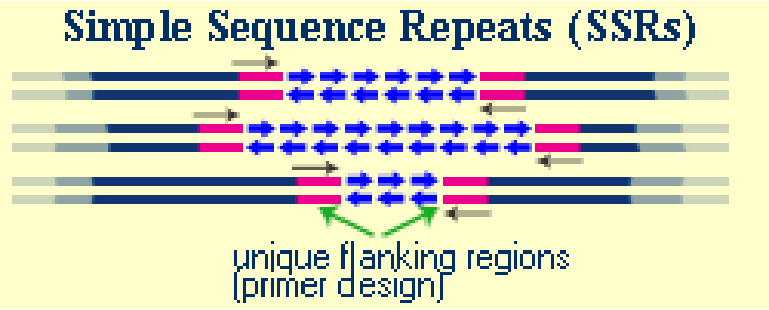

Figure 13. Structure of SSRs. Blue arrows indicate repeated motifs.

The detection of SSR markers requires preliminary information regarding the sequences flanking the microsatellite in 5 'and in 3' ends in order to design the specific primers upstream and downstream the microsatellite itself. In fact, the polymorphisms of the nucleotide sequences under examination are highlighted using PCR with the pair of primers specific for the regions flanking the repeated sequences. The primers thus designed allow to amplify single microsatellite loci that may differ between individuals not for the basic motif, but for the number of times this motif is repeated. The amplification products are normally subjected to electrophoresis in polyacrylamide gel, since only this matrix allows to highlight polymorphism of a few (2-5) nucleotides, but in the last years, thanks to the Next-

generation sequencing (NGS) technologies, the amplification products can be easily sequenced and motif's number of repetitions analyzed.

Ultimately, SSRs are a class of molecular markers capable of highlighting very high genetic diversity. This characteristic makes microsatellites particularly suitable for genotyping and varietal identification, as well as for evolutionary studies. Because of the asexual vegetative reproduction and the low genotypic diversity among clonal populations of *A. donax*, the development of genetic markers become of fundamental importance, in order to obtain genetic tools commonly used for assessing genetic diversity, the development of genetic maps, marker-assisted selection (MAS) breeding, comparative genomics and allowing clones identification and traceability. SSRs are an ideal choice for developing markers for *A. donax* because of their abundance, high polymorphism, codominance, reproducibility, and cross-species transferability. No genetic markers were reported for *A. donax* until 2017, when Evangelistella and collaborators exploited transcriptome data for the development and characterization of gene-based SSR markers. They provided the first SSR marker catalogue and a set of PolySSRs for *A. donax*. The distribution of the SSR classes within leaf unitranscripts with respect to the untranslated (5′-UTR and 3′-UTR) and the coding sequence (CDS) regions in the identifed ORFs was also investigated. A total of 8364 SSRs were obtained from 7491 unitranscript sequences, so 775 sequences contained more than one SSR. Out of the total 8364 SSRs, 5592 were located in the UTR and CDS regions, of which 611 (10.93%), 2059 (36.82%), and 2922 (52.25%) SSRs were located in the 5′ UTR, CDS, and 3′ UTR, respectively. In order to find gene-related markers and to reveal homology with known proteins, they conducted

functional categorization of unitranscripts containing SSRs. Functional annotation revealed that unitranscripts containing PolySSRs belonged to key genes involved in the hydrolysis of ABA glucose ester (ABA-GE) to free ABA (i.e., β-glucosidase 10), in the positive regulation of ABA signaling pathway (i.e., 3-ketoacyl-CoA thiolase) and to several transcription factors (TFs) involved in enhancing drought tolerance in plants, such as myeloblastosis (MYB) TFs (i.e., MYB1R1) and heat stress TFs (i.e., HSFA3).

In contrast to genomic SSRs, genic SSRs are located in the coding region of the genome and are highly transferable to related taxa (Zhao et al., 2013). Therefore, they can directly influence phenotype and also be in close proximity to genetic variation in coding or regulatory regions corresponding to traits of interest. SSRs located in coding and untranslated regions can be efficient functional markers (Li et al., 2004). Considering these advantages, a deep analysis of SSR markers obtained from transcriptomic data of plants subjected to abiotic stress will be very useful.

3.6.3 Beyond genetics: epigenetics and cytosine methylation for gene expression regulation

Epigenetics refers to heritable changes in gene expression that occur without modification of the underlying DNA sequence. It involves histone Post-Translational Modifications (PTMs), such as methylation, acetylation, phosphorylation, and ubiquitination (Allis and Jenuwein, 2016; Gallusci et al., 2016; Rodrigues and Zilberman, 2015), and DNA methylation. Epigenetic changes influence chromatin structure and, in turn, the accessibility of genetic information making this mechanism important to many biological processes. DNA methylation at the 5′ position of cytosine contributes to the epigenetic regulation of nuclear

gene expression and to genome stability. This consists in a modification resulting from the covalent addition of a methyl group to the fifth position of the aromatic ring in cytosine. 5-methyl-cytosine (5mC); it is widely studied in numerous systems and plays an important regulatory role in fruit biology (Giovannoni et al., 2017). In plants, 5mC occurs in symmetrical (CG/CHG) or asymmetrical (CHH) contexts (where H = A, C, or T). Such changes are transmitted through DNA replication and cell propagation, thereby determining and maintaining cell-type specific gene expression patterns (Vermaak et al., 2003; Chan et al., 2005; Reyes, 2006; Li et al., 2007; Eichten et al., 2014; Pikaard and Mittelsten, 2014). The mechanisms underlying the generation of specific DNA methylation patterns are best understood in the model plant *Arabidopsis thaliana*, in which mutations in components of the DNA methylation and demethylation machineries and regulatory factors are generally not lethal.

A specific DNA methylation state reflects the outcome of the dynamic regulation of establishment, maintenance and active-removal activities. These activities are catalyzed by various enzymes that are targeted to specific genomic regions by distinct pathways.

De novo DNA methylation is mediated through the RNA-directed DNA methylation (RdDM) pathway, which involves small interfering RNAs (siRNAs) and scaffold RNAs in addition to an array of proteins (Zhang et al., 2018). In particular, DOMAINS REARRANGED METHYLASE 2 (DRM2) catalyzes de novo DNA methylation in a sequence-independent manner. This reaction may be assisted by RNA-DIRECTED DNA METHYLATION 1 (RDM1), which associates with both AGO4 and DRM2 and may bind single-stranded methylated DNA. On the other hand maintenance of plant DNA methylation depends on the cytosine sequence

context and is catalyzed by DNA methyltransferases that are regulated by different mechanisms: CG cytosine methylation is maintained by METHYLTRANSFERASE 1 (MET1) (He et al., 2011; Kankel et al., 2003), maintenance of CHG methylation in *A. thaliana* is catalyzed by the DNA methyltransferase CHROMOMETHYLASE 3 (CMT3) and by a much lesser extent by CMT2 (Lindroth et al., 2001; Stroud et al., 2014) and finally CHH methylation is maintained by DOMAINS REARRANGED METHYLASE 2 (DRM2) or CMT2, depending on the genomic region (Liu et al., 2014; Huettel et al., 2006; Zemach et al., 2013). The lack of DNA methyltransferase activity or shortage of a methyl donor following DNA replication results in failure to maintain methylation, which is known as passive DNA demethylation (Rocha et al., 2005; Groth et al., 2016). DNA methylation can also be erased enzymatically, which is referred to as active DNA demethylation. In contrast to the DNA methylation reaction, which is catalyzed by a single DNA methyltransferase enzyme, active DNA demethylation requires a team of enzymes, with the enzyme initiating the process referred to as a DNA demethylase. In plants, a family of bifunctional 5-mC DNA glycosylases–apurinic/apyrimidinic lyases initiates active DNA demethylation through a base excision repair pathway (Gong et al., 2002; Gehring et., 2006; Ortega-Galisteo et al., 2008).
Changes in DNA methylation are associated with a wide range of molecular mechanisms such as gene expression and transposon silencing, resulting in an active regulation of important biological processes such as ripening, flowering and stress response (Seymour et al., 2008). An evidence of the correlation between methylation and fruit ripening has been found by Giovannoni and collaborators, which revealed that epigenome modification, particularly DNA

demethylation, plays a critical role as an important ripening regulatory component in tomato (Giovannoni et al., 2017).
Generally, the excessive methylation of plant genomes will inhibit the expression of genes, which leads to silence of genes; meanwhile hypomethylation is required for gene expression (Richard, 1997; Lukens and Zhan, 2007). Promoter DNA methylation directly represses transcription by inhibiting the binding of transcription activators or promoting the binding of transcription repressors or indirectly represses transcription by promoting repressive histone modifications (Zhu et al., 2016). Instead, in some cases, promoter methylation induces gene transcription, such as in the ROS1 gene in *A. thaliana* and in hundreds of genes that inhibit fruit ripening in tomato (Lang et al., 2017; Zhang and Zhu, 2012; Zhang et al., 2006), but this mechanism is less understood. Presumably, DNA methylation may enhance the binding of some transcription activators or may inhibit the binding of some transcription repressors. In the case of genes activated by promoter DNA methylation, active demethylation causes transcriptional silencing of the genes (Lang et al., 2017).
Furthermore, flowering, heterosis and a broad spectrum of biotic and abiotic stress responses influence epigenome architecture (Dowen et al., 2012; King, 2015; Schnable and Springer, 2013). The connection between plant epigenetics and stress was hypothesized in *Arabidopsis* and experimentally supported in rice, in which at least some stress-induced phenotypes depend upon altered DNA methylation (Boyko and Kovalchuk, 2008; Wang et al., 2011). Many evidences about the link between stress exposure and sequence-specific changes in DNA methylation have been collected in the last years. For example, it was demonstrated that prolong exposure to cold triggers a stable

transcriptional silencing of *FLC* leading to flowering inhibition in *Arabidopsis* (Henderson and Dean, 2004). Moreover, flowering time directly correlates with the level of DNA methylation in *MET1* antisense knockouts (Finnegan et al., 1998a). The met1 mutants do not require cold treatment to initiate the flowering, which proves that the developmental switch was epigenetically controlled.

Exposure to cold of root tissues of maize seedlings resulted in DNA demethylation of the nucleosome core regions (Steward et al., 2000). In fact, the DNA replication was strongly reduced in chilled tissues, thus allowing speculations that genome hypomethylation was the result of active rather than passive demethylation. The cold induced demethylation of a nucleosome core and relaxation of chromatin structure could serve as a stress-induced transcriptional switch for many stress-regulated genes (Steward et al., 2002).

Several other papers suggest that changes in DNA methylation are required for stress protection. Dyachenko et al. (2006) demonstrated a two-fold increase in CpNpG methylation level in nuclear genome of *M. crystallinum* plants exposed to high salinity conditions. The increase in methylation was associated with switching from C3-photosynthesis to CAM metabolism.

Methylation contributes greatly to the plants ability to respond to stress (Boyko and Kovalchuk, 2008). Hypomethylation found in tobacco met1 results in specific expression of 31 genes, many of which being related to stress response (Wada et al., 2004). Wang and collaborators (2011) demonstrated that drought could induce genome-wide changes in DNA methylation/demethylation, accounting for 12.1% of total site-specific methylation differences in the rice genome. This drought-induced DNA methylation pattern was genotype- specific, as reflected by large differences in the

detected DNA methylation/demethylation sites between a drought tolerant genotype and a drought sensitive genotype. Furthermore, the drought-induced DNA methylation/demethylation alteration showed a significant level of developmental and tissue specificity with the overall DNA methylation level induced by drought.

A variety of techniques have been used to detect site-specific levels of DNA methylation (Tollefsbol, 2004). The bisulfite genomic sequencing method is unmatched in its ability to determine methylation at all CpG dinucleotides within a small region of DNA providing the highest level of resolution and information. However, this method is not appropriate for the investigation of large numbers of loci because of the costs and time requirements involved. An alternative technique that can be used to rapidly profile the DNA methylation status of numerous loci without the use of sodium bisulfite is based on a methyl-sensitive amplification polymorphism (MSAP) technique, in which methylated or unmethylated regions are detected using a methylation–dependent endonuclease, that cleaves methylated DNA. This technique has three basic steps: (1) the digestion of a DNA sample of interest with a methylation-dependent restriction enzyme (MDRE); (2) the designing of primers to specific genomic regions; (3) a real-time PCR amplification reaction to monitor the formation of the PCR product. Using the real-time PCR, the methylation can then be indirectly evaluated by measuring the level of digestion and can then be readily screened across the genome (Reyna-Lopez et al., 1997). With the MSAP technique, single sites or small regions of DNA can be analyzed without the use of bisulfite conversion while using relatively small amounts of source DNA. Primers can be designed to analyze virtually any restriction site(s) found in non-repetitive sequences.

With the added convenience of being able to use the same templates to assay many different regions, this assay provides quality results requiring a modest investment of material and time (Oakes et al., 2006). All these characteristics make the MSAP method a rapid, quantitative method for the analysis of DNA methylation at single sites or within small regions of DNA.

4. Aim of the work

The demographic explosion which was followed by a strong urbanization and an increase in the demand for goods led to a significant increase in global energy demand. Thus, sustainable energy production is one of the main challenges that humanity will face in the coming years. As reported by many authors, the necessity to meet the increased global energy demand and at the same time cope with the ongoing climate change are the main factors supporting the policies of many countries in favor of the growth of renewable energy as alternative sources to fossil resources. In this context, bioenergy crops, can provide a crucial contribution in satisfying the demand for energy resources of our planet. But the global increase in temperatures, the melting of glaciers, and increasingly frequent episodes of droughts and floods, represent an important limiting factor for crops cultivation and growth. Considering the frequent occurrence of soil salinity in the Mediterranean area due to the climate change and the potential use of marginal soil for energy crop cultivation, a deep knowledge of the global physiological and transcriptomic response of bioenergy crops to salt is needed.
Among the bioenergy crops, *Arundo donax* L. is known to be able to grow in unfavorable environments, in particular in salty soils.
Since no information are still available about the *A. donax* genetic and transcriptomic response to this kind of stress, we aimed to analyze the effect of two levels (severe and extreme) of prolonged period of salt stress upon the *A. donax* whole leaf transcriptome by using a RNA-seq approach in order to

elucidating the biological processes underlying the salt tolerance in a non- model plant.
Thus, the work aims to:

- evaluate the different response to two level of long-term salt stress in terms of plant phenotype and physiology of different *A. donax* clones, despite the low genetic diversity;
- understand and describe the molecular mechanism controlling and regulating the response of the *A. donax* to salt stress conditions;
- find out the principal genes and molecular pathways influenced by stress application and salt concentration and potentially involved in the stress tolerance;
- analyze the osmotic and salt stress related biological pathways and their different regulation in different clones;
- understand whether the epigenetic regulation participates to the differential gene expression caused by stress;
- look for molecular markers capable to genetically discriminates the different clones or associated to specific phenotypes.

Two *A. donax* clones, showing contrasting behavior when the severe and extreme stress were applied, where subjected to a *de novo* transcriptome assembly using the RNA-seq approach, and differentially expressed genes (DEGs) were analyzed. A functional classification of DEGs was conducted in order to highlight the principal genetic functions influenced by the stress.
The RNA-Seq datasets were analyzed in the different salt concentrations focusing on genes and pathways known to be related to soil salinity, in order to investigate the effect of salt

dose. Furthermore, clusters related to salt sensory and signaling, transcription factors, hormone regulation, Reactive Oxygen Species (ROS) scavenging, osmolyte biosynthesis and biomass production were analyzed.

In order to find out a putative correlation between gene expression and DNA methylation, we also performed a methylation status analysis of differentially expressed genes, as resulted from the transcriptomic analysis. All the selected genes have a salt stress related function and they were chosen since they are reported to be differentially methylated in other plant species.

Finally, we exploited transcriptome data looking for SSRs located in coding sequences or associated to specific phenotype potentially useful as genetic marker for genetic analysis such as clone's traceability or marker assisted selection (MAS).

5. Materials and methods

5.1 Plant material and application of salt stress

The experiment was conducted at the Department of Agriculture, Food and Environment (Di3A) of the University of Catania, initially using four different giant reed clones, namely G2 , G18, G20 and G34 ecotypes, originated from Caltagirone (Italy), (latitude 37°14', longitude 14°31'), Biancavilla (Italy) (latitude 37°38', longitude 14°52'), Capo D' Orlando (Italy) (latitude 38°08', longitude 14°43') and Birgi (Italy) (latitude 38°01', longitude 12°32') respectively and collected for the Giant reed Network project (Figure 14) (Cosentino et al., 2006).

Figure 14. Geografical origins of analyzed clones.

The trial started on July 7th, 2017, by transplanting *A. donax* rhizomes into 25 l pots (40 cm diameter and 30 cm height) containing a sandy soil as substrate. Before transplantation, the rhizomes were weighed using a laboratory scale and the number of buds was counted. For each ecotype, samples showing homogeneous rhizome weight and same bud number were used for transplanting. The individual rhizomes were then placed at 15 cm depth, one for each pot. The pots were arranged according to a randomized block factor scheme, performing three biological replicates for treatments. During the experiment, the irrigation was carried out on a weekly basis, and until the first sprouts have been released, tap water (5 l per pot) has been used. The first irrigation with saline water was carried out on August 3rd, 2017. Salt stress was imposed by adding different concentrations of NaCl to the irrigation water. In particular, S0 samples (no salt added), S3 (severe salt stress, 256.67 mM NaCl corresponding to 32 dS m-1 electric conducibility, EC), S4 (extreme salt stress, 419.23 mM NaCl corresponding to 50 dS m-1 electric conducibility, EC), this last concentration being very close to the seawater NaCl concentration (3%), where Na^+ molarity is about 460 mM and Cl^- is around 540 mM (Mahajan and Tuteja, 2005). Before leaf harvest, the following morpho-biometric and physiological parameters were measured: number of culms, height of the main culm, number of green and senescent leaves, net photosynthesis by infrared gas analyzer (IRGA) (LICOR 6400, LI-COR bioscience) and chlorophyll content measured in SPAD units (SPAD 502, Konica Minolta). Net photosynthesis was measured during the maximum light irradiation (12:00 PM). Moreover, the measurement of the yielded biomass was also carried out, by measuring dry matter (DM) weight after the storage of fresh biomass in an oven at 65°C for one week (Cosentino et al.,

2006). The collected data were submitted to ANOVA analysis, using CoStat 6.003 software. The averages were separated by the Student Newman Keuls (SNK) test when P ≤0.05. On the basis of the aforementioned parameters suggesting contrasting behavior under salinity stress (S3 and S4 salt levels) among the clones under investigation, G2 and G34 were selected to perform the global transcriptomic analysis. Unfortunately, because of an unexpected fire happened before sample harvest, G34 plants subjected to S4 salt level were lost and the following analysis of G34 clone were carried out only with S0 and S3 salt level.

5.2 Sample collection and RNA extraction

In November 17th, 2017, fully expanded, no senescing G2 and G34 leaves (the 3rd leaf from the top) were harvested and immediately frozen with liquid nitrogen. Then, plant material, kept frozen by continuously liquid nitrogen adding, was ground using precooled mortar and pestle followed by RNA isolation using the Spectrum Plant Total RNA Extraction Kit (Sigma-Aldrich, St. Louis, MO, USA) according to the manufacturer's instructions. RNA degradation and contamination were monitored on 1% agarose gels. RNA purity and concentration were assayed using the NanoDrop spectrophotometer (ThermoFisher Scientific, Waltham, MA, USA). RNA integrity was assessed using the Agilent Bioanalyzer 2100 system (Agilent Technologies, Santa Clara, CA, USA). Before to be sequenced, the RNA samples were subjected to quality parameter evaluation. The average RNA Integrity Number (RIN) was of 7.8 and there was very slight genomic DNA contamination confirming that all the samples have such high-quality level to be processed (Table 2 in Results).

5.3 RNA sequencing

5.3.1 Library preparation for transcriptome sequencing

A total amount of 1.5 µg RNA per sample was used as input material for the RNA sample preparations. Sequencing libraries were generated using NEBNext® Ultra™ RNA Library Prep Kit for Illumina® (New England Biolabs, Ipswich, MA, USA) following manufacturer's recommendations. Briefly, mRNA was purified from total RNA using poly-T oligo-attached magnetic beads. Fragmentation was carried out using divalent cations under elevated temperature in NEBNext First Strand Synthesis Reaction Buffer (5X). First strand cDNA was synthesized using random hexamer primer and M-MuLV Reverse Transcriptase (RNase H-). Second strand cDNA synthesis was subsequently performed using DNA Polymerase I and RNase H. Remaining overhangs were converted into blunt ends via exonuclease/polymerase activities. After adenylation of 3' ends of DNA fragments, NEBNext Adaptor with hairpin loop structure were ligated to prepare for hybridization. In order to select cDNA fragments of preferentially 150~200 bp in length, the library fragments were purified with AMPure XP system (Beckman Coulter, Beverly, MA, USA). Then 3 µl USER Enzyme by NEB was used with size-selected, adaptor-ligated cDNA at 37°C for 15 min followed by 5 min at 95 °C before PCR. Then PCR was performed with Phusion High-Fidelity DNA polymerase, Universal PCR primers and Index (X) Primer. At last, PCR products were purified (AMPure XP system) and library quality was assessed on the Agilent Bioanalyzer 2100 system.

5.3.2 Clustering and next generation sequencing

Cluster generation and sequencing were performed by Novogene Bioinformatics Technology Co., Ltd. (Beijing, China). The clustering of the index-coded samples was performed on a cBot Cluster Generation System using a PE Cluster kit cBot-HS (Illumina). After cluster generation, the library preparations were sequenced on Illumina HiSeq2000 platform to generate pair-end reads. Raw data (raw reads) of fastq format were firstly processed through in-house perl scripts. In this step, clean data were obtained by removing reads containing adapter, reads containing poly-N and low-quality reads. At the same time, Q20, Q30, GC-content and sequence duplication level of the clean data were calculated. All the downstream analyses were based on clean data with high quality (Figure 16 in Results section).

5.3.3 De novo transcriptome assembling and gene functional annotation

De novo transcriptome assembly was accomplished using Trinity (r20140413p1 version) with min_kmer_cov:5 parameters (k=25). Trinity is the software chosen to complete the transcriptome reconstruction process in the absence of a reference genome. Then Hierarchical Clustering was performed by Corset (v1.05 version) to remove redundancy (parameter -m 10). Corset works by clustering contigs based on shared reads and separates contigs when different expression patterns between samples are observed. Corset also uses the read information to filter out contigs with a low number of mapped read (less than 10 reads by default). Afterwards the longest transcripts of each cluster were selected as Unigenes. Gene function was annotated based on the following databases: National Center for Biotechnology Information (NCBI) non-redundant protein sequences (Nr),

NCBI non-redundant nucleotide sequences (Nt), Protein family (Pfam), Clusters of Orthologous Groups of proteins (KOG/COG), Swiss-Prot, Kyoto Encyclopedia of Genes and Genomes (KEGG), Ortholog database (KO) and Gene Ontology (GO) (Figure 16 in Results).

5.3.4 Identification of clusters specifically involved in the salt stress response

In order to discriminate among clusters specifically regulated by salt treatment from those also involved in the response to other abiotic stress (oxidative, water deprivation stress, cold, heavy metals), the GO term lists relative to each comparison (G2_S3 vs G2_CK, G2_S4 vs G2_CK, G34_S3 vs G34_CK and G34-S3 vs G2-S3) were filtered and exclusively salt-regulated clusters were extrapolated. For the identification of transcription factors responsive to salt stress in *A. donax*, we mined the available salt stress-responsive transcription factor database of rice (SRTFDB) (Yoo et al., 2010) by Blastn searches with an e value cutoff of 1e−5.

5.3.5 Quantification of gene expression and differential expression analysis

Gene expression levels were estimated by RSEM (v1.2.26 version) with bowtie2 mismatch 0 parameters in order to map to Corset filtered transcriptome. For each sample, clean data were mapped back onto the assembled transcriptome and readcount for each gene was then obtained from the mapping results. Differential expression analysis between control and salt stressed samples was performed using the DESeq R package (1.12.0 version, padj<0.05). The resulting p-values were adjusted using the Benjamini and Hochberg's approach for controlling the false discovery rate. The genes with an adjusted p-value <0.05 found by DESeq were assigned as

differentially expressed. The GO enrichment analysis of the differentially expressed genes (DEGs) was implemented by the GOseq R packages (1.10.0, 2.10.0 version, corrected p-value<0.05 based) Wallenius non-central hyper-geometric distribution [85]. Furthermore, to analyze the *Arundo donax* transcriptome all of the unigenes were submitted to the KEGG pathway database for the systematic analysis of gene functions. KOBAS software (v2.0.12 version, corrected p-value<0.05) was used to test the statistical enrichment of differential expression genes in KEGG pathways.

5.4 Multiple sequence alignment and phylogenetic analysis

Multiple alignment analysis of fifteen amino acid sequences of selected proteins (CIPK1-SOS2 like, cation transporter HKT9, NHX1, NHX2, SOS2 and ETHE 1) was carried out by MUSCLE by executing MEGA X 10.0.5 (https://www.megasoftware.net/). The phylogenetic tree was created using MEGA X 10.0.5 by the ML (maximum likelihood) method following the Jones, Taylor and Thornton (JTT) substitution model and 1000 bootstrap replicate with other default parameters.

5.5 Real-time validation of selected DEG candidates using qRT-PCR

Total RNA (2.5 μg) extracted from sample leaves as described above, was reversed transcribed using the SuperScript™ Vilo™ cDNA synthesis kit by ThermoFisher Scientific, according to the manufacturer's instructions. Real-time qRT-PCR was performed for a total of ten DEGs with PowerUp SYBR Green Master mix by ThermoFisher Scientific and carried out in the Bio-Rad iQ5 Thermal Cycler detection system. All the genes were normalized with *A.*

donax 26 S proteasome non-ATPase regulatory subunit 11 gene (RPN6) that was reported to be a suitable housekeeping gene in abiotic stress conditions (Poli et al., 2017). All reactions were performed in triplicate and fold change measurements calculated with the 2−ΔΔCT method. Sequences of primers used for real-time PCR are provided in Appendix III - Table S2.

5.6 SSR analysis and validation

MISA (v1.0, default parameters; Minimum number of repeats of each unit size is: 1-10; 2-6; 3-5; 4-5; 5-5; 6-5) is used for the SSR detection of unigenes.

These markers include repetitions of one, two, three, four, five or six bases with 10, 6, 5.5 and 5 uninterrupted repetitions. TransDecoder v3.0.0 was used in order to have the best 5'-UTR, CDS and 3'-UTR regions. Afterwards, the positions of transcribed domains were combined with the SSRs positions, in order to assign the microsatellites within the ORFs (Open Reading frames).

SSRs validation was conducted by amplifying and sequencing five microsatellite regions chosen randomly in 5'-UTR, CDS and 3'-UTR (EST-SSR) coding sequences. The five primer sets were designed using the primer-BLAST software (https://www.ncbi.nlm.nih.gov/tools/primer-blast/) and their sequences and amplicons are listed in Appendix IX - Table S9. The PCR on DNA extracted from both G2 and G34 clones was performed on a 50 µl total volume, according BIOTAQ™ DNA Polymerase (BIOLINE, Singapore) protocol and the following amplification conditions:

Pre-denaturation	95°C for 2 min.	1 cycle
Denaturation	95°C for 1 min.	
Annealing	57/60°C, for 1 min.	40 cycles
Extension	72°C for 30 sec.	
Final extension	72°C for 1 min.	1 cycle

PCR products were then subjected to a 3% agarose gel electrophoresis, running at a voltage of 90 volt for 3 hours. Bands showing the expected size were excised and purified using the PureLink™ Quick Gel Extraction & PCR Purification Combo Kit (Invitrogen by Thermo Fisher Scientific, Lituania) according the producer's instructions. The obtained DNA was sequenced by Eurofins Genomics (Milano) and sequences were analyzed looking for repeated motifs.

5.7 Cytosine methylation analysis

Once the DNA was extracted, digestion was performed using the methylation-sensitive endonuclease McrBC (New England Biolab Inc., Ipswich, US). McrBC recognizes two half-sites of 5'-G/AmC-3' (Stewart et al., 2000). The recognition sequence is a non-palindrome, thus, along with 5'-GmCG-3' and 5'-AmCG-3', McrBC will also recognize the sequences 5'-mCGC-3' and 5'-mCGT-3' (complementary to the recognition sequence). Optimal separation of the two half-sites is 55–103 bp and the enzyme cleaves the DNA in between the two sites approximately 30 bp from either site (Stewart et al., 2000). Digestion was performed according the following conditions: NEBuffer 2 (1X), BSA (200 µg/ml), GTP (3 mM), McrBC (15 U), 500 ng DNA, ddH2O up to 25 µl. Digestion was carried out at 37°C for 8 hours and 65°C for 20 minutes. As McrBC requires GTP for cleavage (Irizarry et al., 2008), for each sample a 'Test reaction' in

which GTP is included in the digestion cocktail and a 'Reference reaction' in which GTP is not included in the digestion cocktail were prepared.
Real-time PCR was performed using the PowerUp™ SYBR® Green Master Mix (Applied Biosystems, Foster City, US) according the manufacturer's instructions: 40 ng of digested DNA was mixed with Master Mix 1X, 400 nM of each primer in a total volume of 20 µl. The program for qRT-PCR in Bio-Rad iQTM5 cycler was set as follows:

UDG activation	50°C for 2 min.	1 cycle
Pre-denaturation	95°C for 2 min.	1 cycle
Denaturation	95°C for 15 sec.	
Annealing	56/59°C, for 15 sec.	38 cycles
Extension	72°C for 1 min.	

Primers were designed using the primer-BLAST software (https://www.ncbi.nlm.nih.gov/tools/primer-blast/) on genes resulted differentially expressed from the transcriptomic analysis and having a salt stress related function, and reported to be differentially methylated from the literature. Primers sequences are listed in Appendix X - Table S10.
A 'Test reaction' tube and a 'Reference reaction' tube where prepared adding DNA from 'Test reaction' and 'Reference reaction' of the digestion step respectively. Each sample was screened in double technical replicates. The mean Ct values obtained were used to calculate ΔCt and methylation percentage using the following equations:

$$\Delta Ct = [Ct(test) - Ct(reference)] \quad (1)$$

$$Methylation\% = 100 - (100 \times 2^{-\Delta Ct}) \quad (2)$$

6. Results

6.1 Effect of salt stress upon A. donax morpho-biophysiological parameters

As described in the Methods section, *A. donax* G2, G18, G20 and G34 morpho-biometric and physiological parameters were measured at sampling date after being subjected to two levels of prolonged salt stress imposition (S3, severe and S4, extreme), being both doses much higher than that used to define a soil area as "salinized" (EC 4 dS m-1). Data from the S4 treatment of G34 genotype could not be obtained because of a fire occurred in the field that destroyed those plants. Considering the average values of the four clones, we observed that both the leaf number per pot, the stem number and the main stem height per pot, were significantly reduced by salt stress, and this effect was more pronounced in correspondence of the S4 treated samples (Appendix I - Figure S1a, S1b and S1c). Similarly, physiological parameters such as SPAD, leaf chlorophyll content, net photosynthesis and biomass yield per pot decreased especially under extreme salt stress conditions (S4) compared with untreated S0 samples (Appendix I – Figure S1d, S1e and S1f). The ecotypes under investigation exhibited different phenotypes in response to salt treatments, although they reproduce asexually and, for this reason, they should have low levels of genetic diversity. In particular, the whole data analysis revealed that G20 clone did not growth under extreme salt stress conditions, suggesting that it is highly sensitive to high salt concentration (Appendix I - Figure S1). Although both G2 and G18 clone grew under severe (S3) and extreme (S4) salt stress conditions, G2 clone showed higher

stem and leaf number per pot, and higher physiological parameters than those recorded in G18 clone in S4 conditions. Indeed, G2 clone produced considerable higher biomass yield than that reported in G18 clone in extreme salt stress conditions, in an environment in which likely none crops could have survived (Zörb et al., 2018) (Appendix I - Figure S1f). G34 clone showed a higher leaf number per pot and stem number per pot compared to the other clones, despite its lower main stem height in both S0 and S3 conditions (Appendix I - Figure S1a, S1b, S1c). However, G34 resulted to be the clone with the lower relative decrease in the first two parameters when comparing S0 and S3 treatments. Therefore, further transcriptomic analysis was conducted upon G2 and G34 clones subjected to salt stress. The picture of giant reed phenotype under salt stress is shown in Figure 15.

Figure 15. Picture of giant reed phenotype under salt stress

6.2 Transcriptomic analysis

6.2.1 Transcript assembly and annotation

In this study, we carried out a comprehensive identification of transcriptional responses of *A. donax* G2 and G34 clones to two different levels of prolonged salt stress by RNA-Seq (see experimental design in Methods section). In figure 16, a flow chart describing the *de novo* transcriptome assembly is reported (see details in Fig.16 caption). Raw reads were filtered to remove reads containing adapters or reads of low quality, so that the downstream analyses are based on a total of 1074 million clean reads with an average of ~ 71.6 million reads (~10.7 G) per sample, the average percentage of Q30 and GC being 94.5 % and 53.7 %, respectively (Table 2). *De novo* assembly of clean reads resulted in 312,694 transcripts and 228,266 unigenes with N50 length of 1,944 and 1,931, respectively (Table 2), in line with previous N50 reports (Sablok et al., 2014; Fu et al., 2016), indicating that a good coverage of the transcriptome has been achieved. To evaluate the assembly consistency, the filtered unique reads were mapped back to the final assembled leaf transcriptome and the average read mapping rate using the alignment software Bowtie2 was 66.50%. (Table 2). Both transcript and Unigene length distribution is reported in Appendix II - Figure S2. These data showed that the throughput and sequencing quality were high enough to warrant further analysis. To achieve comprehensive gene functional annotation, all assembled unigenes were blasted against public databases, including National Center for Biotechnology Information (NCBI), Protein family (Pfam), Clusters of Orthologous Groups of proteins (KOG/COG), Swiss-Prot, Ortholog database (KO) and Gene Ontology (GO) (Table 3). A total of 148,190 unigenes were annotated in at least one searched database, accounting for 64.92 % of the obtained total

unigenes. Among them, 128,536 (56.31%) and 116,575 (51.07%) assembled unigenes showed identity with sequences in the Nr and Nt databases, respectively. The percentage of assembled unigenes homologous to sequences in KO, Swiss-Prot, Pfam, GO and KOG databases were 19.94, 37.85, 40.1, 42.17 and 15.97%, respectively (Table 3).

Table 2. Summary statistics of the RNA quality and sequencing results

Average RIN	7,8
Clean reads	1074 million
N° of transcripts	312,694
N° of Unigenes	228,266
Average of read mapped rate	66.5%
Transcripts N50 (bp)	1,944
Unigenes N50 (bp)	1,931
Q30 (%)	94.5
GC content (%)	53.7

Table 3. Number and percentage of successful annotated genes.

Database	N° of Unigenes	%
Annotated in Nr	128,536	56.31
Annotated in Nt	116,575	51.07
Annotated in KO	45,516	19.94
Annotated in SwissProt	86,398	37.85
Annotated in Pfam	91,534	40.1
Annotated in GO	96,260	42.17
Annotated in KOG	36,454	15.97
Annotated in at least one database	148,190	64.92

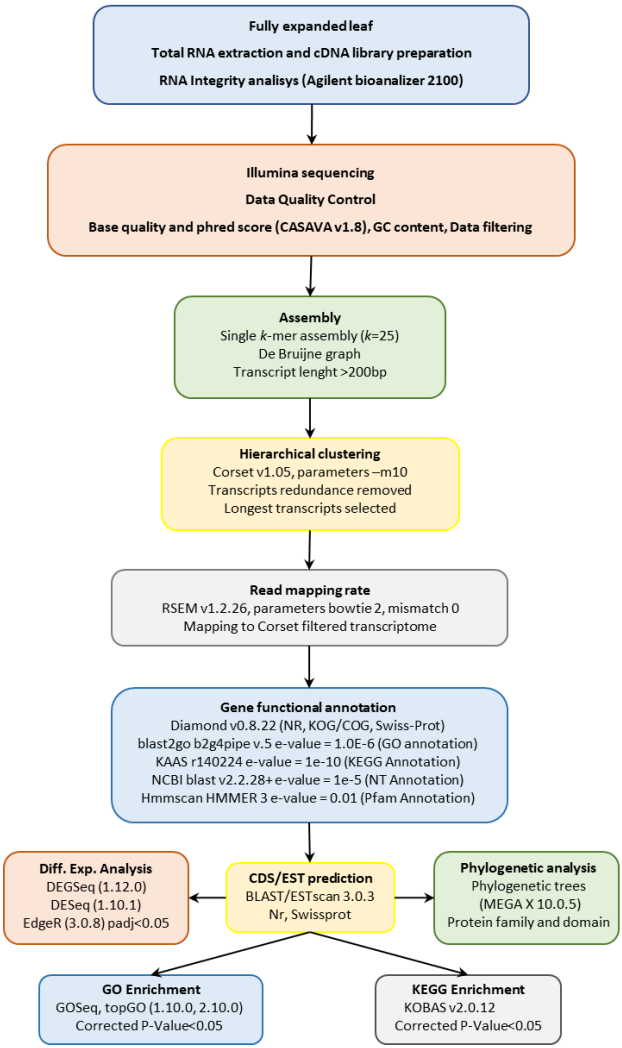

Figure 16. Flowchart of de novo assembly and analysis of Arundo donax leaf transcriptome. After the fully expanded leaf sampling, total RNA extraction and cDNA library preparation was carried out. The RNA integrity and quality analysis were performed (blue) before the Illumina sequencing. The sequencing output data were subjected to quality control of both reads and bases and data filtering (orange) in order to remove

containing adapter reads or reads of low quality. Clean data were used for the de novo assembly of transcripts choosing the single k-mer approach (k=25) (green), and the pre-assembled transcriptome obtained was further processed with Corset for hierarchical clustering by removing transcripts redundancy and by selecting the longest transcripts as unigenes (yellow). The quality of the assembly was assessed by mapping back the reads onto the filtered transcriptome (grey). Finally, gene functional annotation, CDS/EST prediction, differential expression analysis, phylogenetic analysis and GO and KEGG enrichment were carried out.

6.2.2 Identification of differentially expressed genes

The characterization of *A. donax* transcriptional response to salt stress was carried out by the identification of the unigenes whose expression level changed upon NaCl treatments (Table 4). According to the experimental design, a total of 42,484 differentially expressed genes (DEGs) were identified from all the comparisons. In details, 2,086 up-regulated genes and 1,766 down-regulated genes were detected in the G2-S3 vs G2-CK (severe salt stress samples versus control samples), whereas in the G2-S4 vs G2-CK set (extreme salt samples versus control samples) 13,835 up-regulated genes and 11,205 down-regulated genes were found, thus suggesting that G2 clone re-adjusts the network of transcriptional machinery in order to deeply modify gene expression under salt extreme stress conditions (S4) with respect to severe salt conditions (S3) (Table 4). A different response to salt in terms of transcriptomic changes was observed in G34 clone, where only 977 genes resulted up-regulated and 801 genes down-regulated in G34-S3 vs G34-CK comparison (Table 4). Finally, by comparing G34-S3 vs G2-S3, 2,147 gene resulted differentially expressed (836 up-regulated and 1311 down-regulated) (Table 4).

Table 4. DEG number of different comparisons under salt treatments

Comparison	Up-regulated	Down-regulated	Total DEGs
G2-S3 vs G2-CK	2,086	1,766	3,852
G2-S4 vs G2-CK	13,835	11,205	25,040
G2-S4 vs G2-S3	5,765	3,902	9,667
G34-S3 vs G34-CK	977	801	1,778
G34-S3 vs G2-S3	836	1311	2,147
Total DEGs	23,499	18,985	42,484

Venn diagram analysis on G2 clone showed that 2,702 common DEGs are in both G2-S3 vs G2-CK and in G2-S4 vs G2-CK comparisons thus suggesting that their specific involvement in the response to salt stress is not dependent by salt doses (Figure 17a). A total of 1,150 genes are exclusively regulated under severe salt stress condition (G2-S3 vs G2-CK data set), whereas a total of 22,338 genes are specifically regulated during extreme salt stress condition (G2-S4 vs G2-CK data set). Among a total of 9,667 observed DEGs, 1,554 genes were identified as specifically regulated in the G2-S4 vs G2-S3 (extreme salt samples versus severe salt samples) comparison (Fig. 17a). When comparing the same stress condition on the two clones (G2-S3 vs G2-CK and G34-S3 vs G34-CK), only 309 genes are in common on a total of 5,999 DEGs, suggesting a different transcriptomic response of the two clones to the severe stress condition (Figure 17b). Interestingly, a different transcriptomic pattern of the two clones resulted also in control conditions, as a total of 9847 DEGs have been found by comparing G2-CK and G34-CK (data not shown).

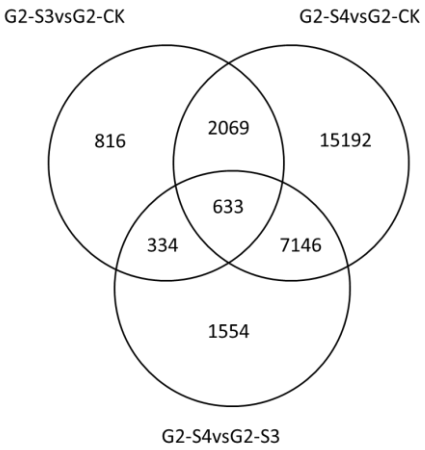

a

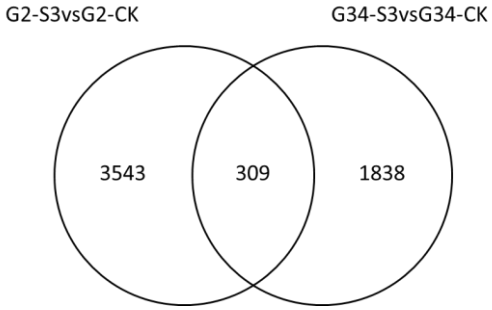

b

Figure 17. Venn diagram of differently regulated genes. a. Comparison among G2-S3 vs G2-CK, G2-S4 vs G2-CK, G2-S4 vs G2-S3 sample sets; **b.** Comparison among G2-S3 vs G2-CK and G34-S3 vs G34-CK.

Validation of expression levels for ten selected DEG candidates was carried out by quantitative real-time PCR (qRT-PCR) (Appendix III - Table S1). The results show high congruence between RNA-Seq results and qRT-PCR (coefficient of determination R2 = 0.91) indicating the

reliability of RNA-Seq quantification of gene expression (Figure 18). Moreover, the selected genes could also constitute useful markers of salt stress in *A. donax*.

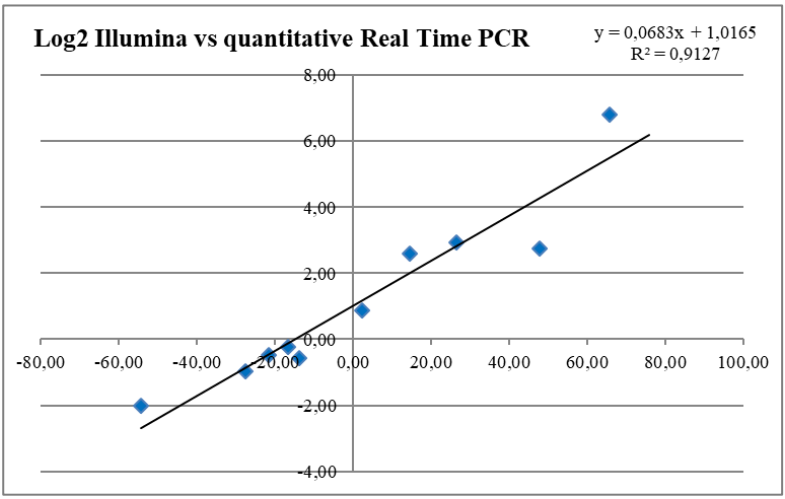

Figure 18. Validation of A. donax DEGs by Real Time qRT-PCR.

6.2.3 Functional classification of DEGs

Gene Ontology (GO) terms, Clusters of Orthologous Groups of proteins (KOG) classification and Kyoto Encyclopedia of Genes and Genomes (KEGG) pathway functional enrichment were performed to identify possible biological processes or pathways involved in salt stress response. Considering the G2-S3 vs G2-CK sample set (Figure 19a), "oxidation-reduction process" (222 up- and 119 down-regulated genes), "transmembrane transport" (125 up- and 97 down-regulated genes) and "carbohydrate metabolic process" (152 up- and 54 down-regulated genes) are the three most enriched GO terms in the Biological Process (BP) ontology. "Oxidoreductase activity" (216 up- and 122 down-regulated genes) is the most enriched GO terms in the Molecular Function (MF) category

ontology indicating that genes acting in this process may play crucial roles in the response to salt treatment (Figure 19a). Among the DEGs belonging to G2-S4 vs G2-CK data set, "metabolic process" (5,934 up- and 4,493 down-regulated genes), "single organism process" (4,834 up- and 3,404 down-regulated genes), "single organism metabolic process" (2,988 up- and 2,090 down-regulated genes) and "oxidation-reduction process" (1,355 up- and 831 down-regulated genes) are the most represented in the category of BP. "Catalytic activity" is the main category in the MF group (5,380 up- and 3,836 down-regulated genes) but also "oxidoreductase activity" and "transporter activity" are highly represented in this group (Figure 19b). Interestingly, the same categories are represented in the G2-S4 vs G2-S3 sample set (Figure 19c), although in this last comparison lower numbers of genes are involved (Figure 19c).

Considering the G34-S3 vs G34-CK dataset (Figure 19d), "oxidation-reduction process" (100 up- and 42 down-regulated genes), "transmembrane transport" (59 up- and 31 down- regulated genes) and "carbohydrate metabolic process" (33 up- and 20 down- regulated genes) are the three most enriched GO terms in the Biological Process (BP) ontology (Figure 19d), the same terms found in G2-S3 vs G2-CK comparison but with lower gene number involved. The "oxidoreductase activity" (78 up- e 19 down- regulated genes) is the main enriched GO term of the MF group, thus indicating the importance of this process in the salt stress response.

Finally, considering the G34-S3 vs G2-S3 dataset (Figure 19e), "metabolic process" (56 up- ad 46 down-regulated), "oxidation-reduction process" (52 up- and 20 down-regulated genes) and "single-organism metabolic process" (45 up- and 48 down- regulated genes) are the three most

enriched GO terms in the Biological Process (BP) ontology (Figure 19e). About the MF group, the “oxidoreductase activity” (53 up- and 19 down- regulated genes), “catalytic activity” (51 up- and 50 down-regulated) and “transporter activity” (36 up- and 17 down-regulated) are the main enriched GO term, thus indicating the importance of this process in the salt stress response (Figure 19e).

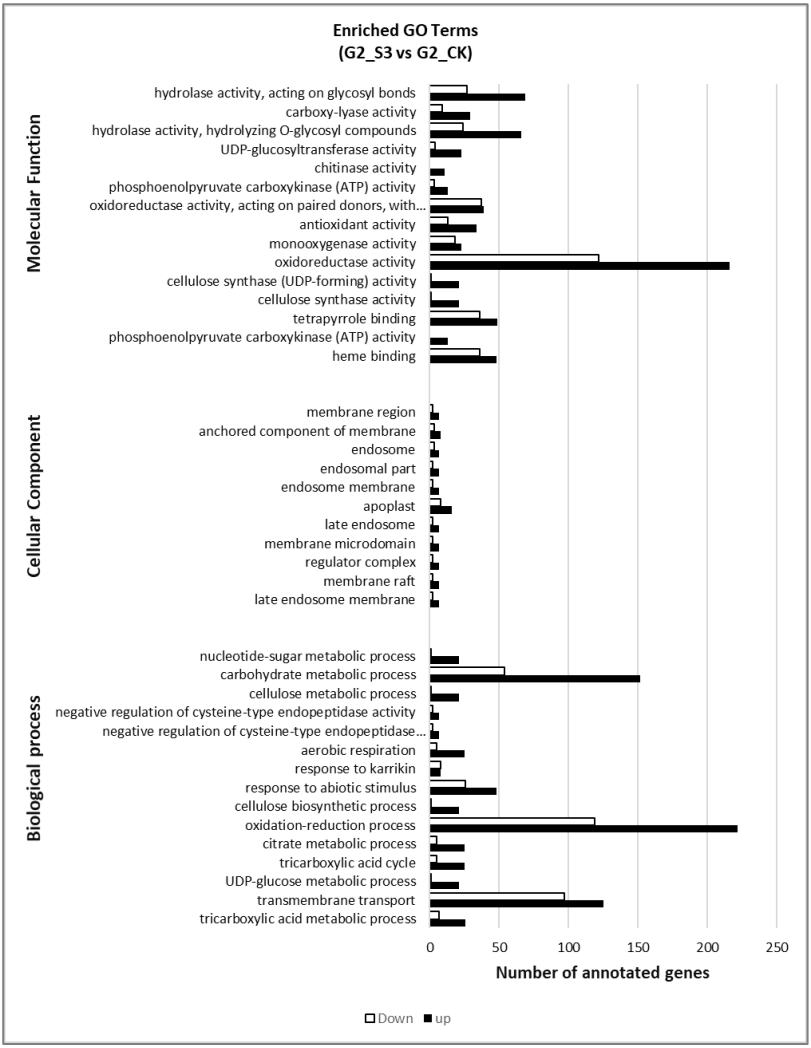

Figure 19a. GO enrichment analysis for the DEGs in *A. donax*. G2-S3 vs G2-CK. The Y-axis indicates the subcategories, and the X-axis indicates the numbers related to the total number of GO terms. BP, biological processes; CC, cellular components; MF, molecular functions.

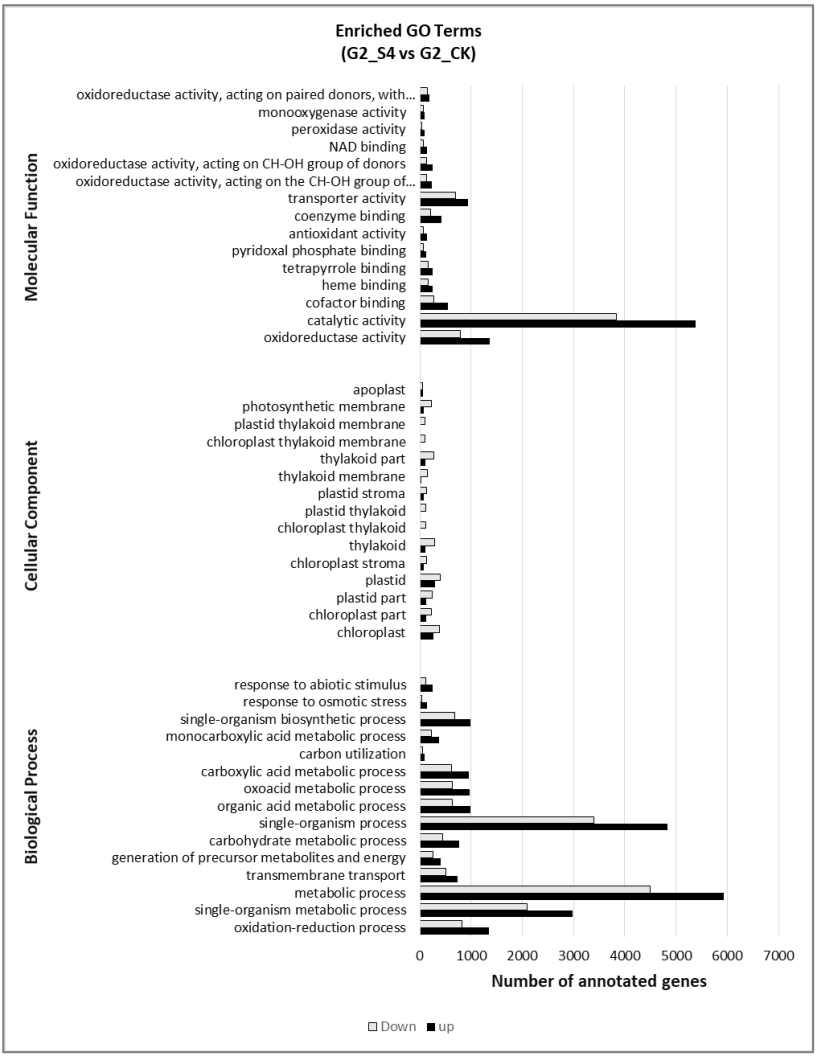

Figure 19b. GO enrichment analysis for the DEGs in *A. donax*. G2-S4 vs G2-CK. The Y-axis indicates the subcategories, and the X-axis indicates the numbers related to the total number of GO terms. BP, biological processes; CC, cellular components; MF, molecular functions.

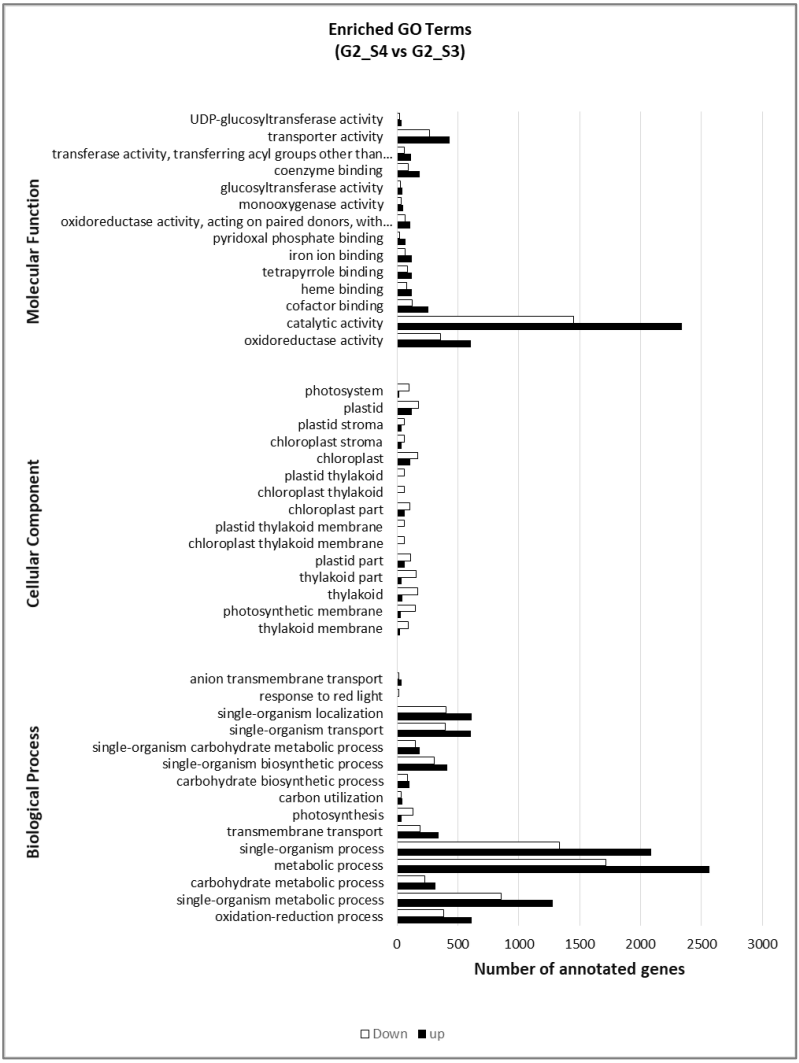

Figure 19c. GO enrichment analysis for the DEGs in *A. donax*. G2-S4 vs G2-S3. The Y-axis indicates the subcategories, and the X-axis indicates the numbers related to the total number of GO terms. BP, biological processes; CC, cellular components; MF, molecular functions.

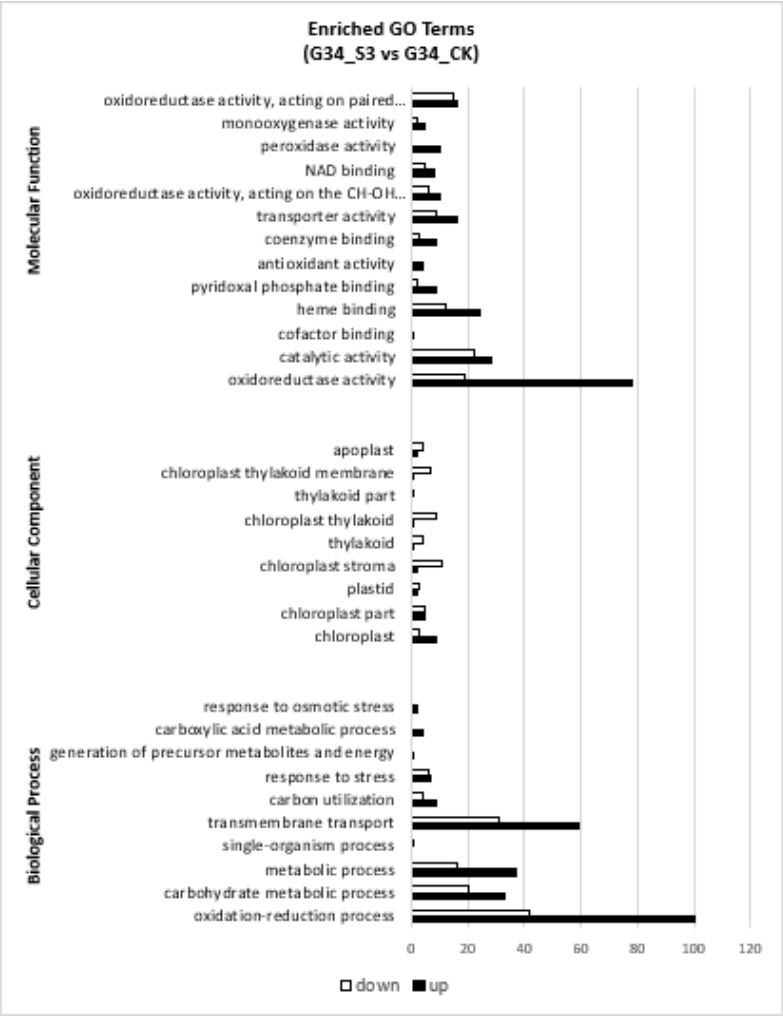

Figure 19d. GO enrichment analysis for the DEGs in *A. donax*. G34-S3 vs G34-CK. The Y-axis indicates the subcategories, and the X-axis indicates the numbers related to the total number of GO terms. BP, biological processes; CC, cellular components; MF, molecular functions.

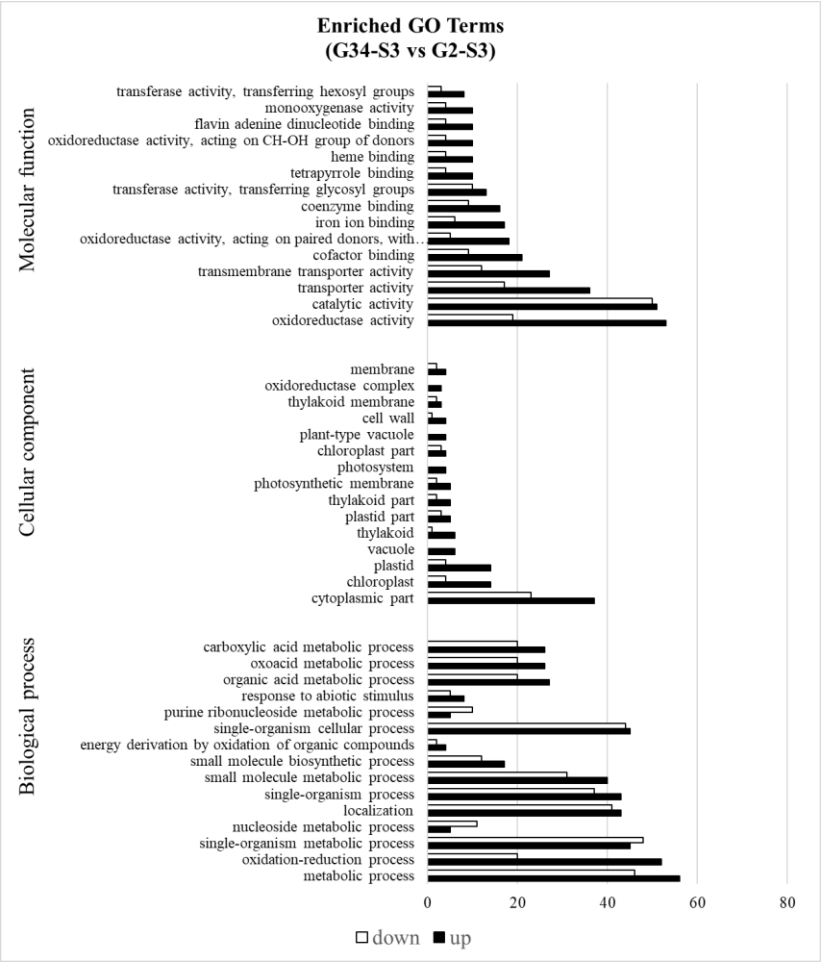

Figure 19e. GO enrichment analysis for the DEGs in *A. donax*. G34-S3 vs G2-S3. The Y-axis indicates the subcategories, and the X-axis indicates the numbers related to the total number of GO terms. BP, biological processes; CC, cellular components; MF, molecular functions.

To predict and classify possible functions, all unigenes (228,266) were aligned to the KOG database and were assigned to the KOG categories (Appendix IV Figure S3).

Among the KOG categories, the cluster for "general function" (16%) represented the largest group, followed by "posttranslational modification, protein turnover, chaperones" (13.4%) and "signal transduction mechanisms" (9.3%). "Translation, ribosomal structure and biogenesis" (8%), "RNA processing and modification" (6.4%) and "transcription" (5.6%) were the largest next categories, whereas, only a few unigenes were assigned to "nuclear structure" and "extracellular structure". In addition, a discrete number of unigenes were assigned to "intracellular trafficking, secretion, and vesicular transport" (Appendix IV – Figure S3). The sets of DEGs originated from the above-described four comparisons were also mapped onto KEGG pathways. Table S3 in Appendix V shows the main fifty KEGG pathway terms sorted by a decreasing order of the gene number involved in the pathways in relation to all the comparison under investigation (G2-S3 vs G2-CK, G2-S4 vs G2-CK, G2-S4 vs G2-S3, G34-S3 vs G34-CK and G34-S3 vs G2-S3). Overall, the results show that the maximum number of DEGs were observed in the "carbon metabolism" pathway, followed by the "biosynthesis of amino acids" and "carbon fixation in photosynthetic organisms" indicating that a deep reprogramming of these metabolisms under salt treatments occurred. The reprogramming activity of the metabolic pathways is supported by the involvement of other important pathways such as "ribosome", "RNA transport", "mRNA surveillance pathway" and "aminoacyl-tRNA biosynthesis" that gives support to an increased re-modulation of protein biosynthesis. "Plant hormone signal transduction', which comprises the transcripts of several hormone-responsive proteins involved in regulation and signal transduction and two other important pathways, including 'phenylalanine metabolism' and 'plant-pathogen interaction' were also

found to be regulated by salt in our study (Appendix V - Table S3). Other examples of relevant pathways, which are known to be involved in responses to abiotic stresses, in general are 'starch and sucrose metabolism', 'arginine and proline metabolism' and "AMPK signaling pathway' (Appendix V - Table S3).

6.2.4 Identification of functional genes related to salt stress tolerance

To unravel the *A. donax* G2 and G34 salt stress response and to investigate the effect of salt dose, we analyzed the RNA-Seq datasets from each of the aforementioned comparisons, focusing on genes and pathways known to be related to soil salinity. In this further analysis, those clusters showing a threshold of +/- 10.000 $\log_2$fold change have been considered as DEGs (up- or down-regulated) in the *A. donax* transcriptome (Table 5-9). For each cluster, the alignment of *A. donax* sequence has been performed and the score of these alignments was reported (% identity and e value) thus providing valuable indications of the cluster similarity with the reported genes (Table 5-9). Congruously, tables report clusters whose % of identity was higher than 50 and the e value < 0.05.

Table 5. List of DEGs related to salt stress response identified in G2-S3 vs G2-CK comparison

Cluster ID	Database description	Percent identity	E value	log_2 fold change
Salt sensory and signaling mechanisms				
14027.182899	*Oryza sativa* subsp. j*aponica* Group CBL-interacting protein kinase 1 (CIPK1-SOS2 like), (XM_015766590.1)	93.33%	4e-23	+ 39.581
14027.54233	*Setaria italica* probable cation transporter HKT9, (XM_004967183.2)	86.32%	1e-132	+ 18.352
14027.155903	*Phragmites australis* pcnhx1 mRNA for putative Na+/H+ antiporter (NHX1), (Nt ID: AB211145.1)	93.40%	3e-54	-21.136
14027.181583	*Arabidopsis thaliana* Sodium/hydrogen exchanger 2 (NHX2), (Swissprot ID: Q56XP4)	77.78%	8e-79	-19.411
Transcription factors				
14027.152638	*Setaria italica* protein TIFY 10B-like, (Nr ID: XP_004958300.1)	84.77%	2e-131	-25.354
14027.159286	*Setaria italica* trihelix transcription factor GTL1, (Nt ID: XM_012842882.1)	88.89%	2e-101	+ 14.963
14027.107730	*Panicum miliaceum* ABSCISIC ACID-INSENSITIVE 5-like protein 7, (Nr ID: RLM78209.1)	78.41%	4e-93	+ 15.107
Hormone regulation of salt stress response				
14027.74861	*Triticum urartu* Abscisic acid 8'-hydroxylase 1, (Nr ID: EMS68885.1)	85.54%	4e-112	+ 47.347
14027.144393	*Setaria italica* abscisic acid receptor PYL8, (Nt ID: XM_004951229.2).	77.85%	4e-80	+ 11.825

14027.137264	*Setaria italica* abscisic acid receptor PYR1-like, (Nr ID: XP_004983564.1)	85.34%	1e-104	+ 12.624
14027.173535	*Oryza sativa* serine/threonine-protein kinase SnRK (SnRK), (Swissprot ID: Q75H77)	79.69%	8e-32	+ 14.238
14027.235757	*Setaria italica* probable protein phosphatase 2C 30, (Nt ID: XM_004984868.2)	87.80%	6e-170	+27.333
14027.228612	*Setaria italica* cytochrome P450 734A1, (Nr ID: XP_004962129.1)	89.90%	2e-58	+ 16.547
14027.99729	*Saccharum arundinaceum* 1-aminocyclopropane-1-carboxylate oxidase (ACC oxidase), (Nr ID: ABM74187.1)	91.46%	1e-122	+15.804
14027.265476	*Setaria italica* indole-3-pyruvate monooxygenase YUCCA2-like, (Nr ID: XP_004967465.1)	75.33%	1e-107	-40.837
ROS scavenging regulatory mechanisms				
14027.179813	*Setaria italica* L-ascorbate peroxidase, (Nt ID: XM_004984762.3)	92.70%	2e-67	+17.074
14027.36507	*Zea mays* glutathione transferase 23 (GST), (Swissprot ID: Q9FQA3)	86.94%	1e-142	+14.004
14027.206288	*Setaria italica* NADP-dependent malic enzyme, chloroplastic, (Nr ID: XP_004960887.1)	99.50%	4e-152	+ 15.008
14027.147540	*Setaria italica* malate dehydrogenase, mitochondrial (MDH), (Nt ID: XM_004961089.3)	84.14%	2e-167	+ 12.416
Osmolyte biosynthesis				
14027.146844	*Setaria italica* delta-1-pyrroline-5-carboxylate synthase (P5CS), (Nt ID: XM_004961829.3)	91.92%	6e-168	+ 40.924
14027.163839	*Setaria italica* proline dehydrogenase (PDH), (Nt ID: XM_004983669.2)	89.55%	3e-114	-28.271

14027.196396	*Oryza sativa Japonica Group* Arginine decarboxylase 1 (ADC), (Nr ID: XP_015643038.1)	92.73%	1e-142	+46.553
Photosynthesis and photorespiration				
14027.153819	*Pisum sativum* RuBisCO large subunit-binding protein subunit alpha, chloroplastic, (Swissprot ID: P08926)	74.89%	4e-110	- 35.119
14027.193818	*Setaria italica* peroxisomal (S)-2-hydroxy-acid oxidase, (Nt ID: XM_004958250.2)	92.51%	5e-156	+ 22.634
Biomass digestibility and biofuel production				
14027.274380	*Setaria italica* cinnamoyl-CoA reductase 2-like, (Nt ID: XP_004956337.1)	67.31%	3e-149	+39.522
14027.178971	*Zea mays* caffeoyl CoA 3-O-methyltransferase, (Nr ID: AAP33129.1)	91.10%	6e-163	+ 13.644
14027.116333	*Setaria italica* sucrose synthase (Nr ID: XP_004984440.1)	70.19%	2e-136	+ 11.104
14027.238308	*Setaria italica* triacylglycerol lipase SDP1-like, (Nr ID: XP_004970049.1)	78.83%	6e-112	+ 10.393
14027.166055	*Setaria italica* diacylglycerol kinase 1, (Nr ID: XP_004983987.1)	86.87%	2e-146	-15.699

Table 6. List of DEGs related to salt stress response identified in G2-S4 vs G2-CK comparison

Cluster ID	Database description	Percent identity	E value	log_2 fold change
Salt sensory and signaling mechanisms				
14027.85357	*Setaria italica* CBL-interacting protein kinase 1 (CIPK1-SOS2-like), (Nt ID: XM_004967556.3)	92.31%	8e-73	Inf*
14027.198243	*Oryza sativa subsp. japonica* CBL-interacting protein kinase 24 (*SOS2*), (Swissprot ID: Q69Q47)	87.88%	8e-126	+11.098
14027.54233	*Setaria italica* probable cation transporter HKT9, (Nr ID: XP_004967240.1)	86.32%	1e-132	+35.667
14027.155893	*Arabidopsis thaliana* Sodium/hydrogen exchanger 1 (NHX1), (Swissprot ID: Q68KI4)	68.46%	6e-177	+ 14.324
Transcription factors				
14027.159287	*Setaria italica* trihelix transcription factor GTL1, (Nt ID: XM_012842882.1)	81.72%	6e-45	+ 29.044
14027.82197	*Setaria italica* bZIP ABSCISIC ACID-INSENSITIVE 5-like protein 7, (Swissprot ID: Q9M7Q2)	79.96%	9e-82	+ 17.106
Hormone regulation of salt stress response				
14027.234361	*Setaria italica* abscisic acid 8'-hydroxylase 3, (Nr ID: XP_004957014.1)	83.43%	0.0	+ 41.107
14027.144393	*Setaria italica* abscisic acid receptor PYL8, (Nt ID: XM_004951229.2)	77.85%	4e-80	+ 12.599

14027.36786	*Setaria italica* brassinosteroid-6-oxidase 2 cytochrome P450 85A1, (KO ID: K12640)	93.36%	4e-141	+ 19.415
14027.99735	*Oryza brachyantha* 1-amino cyclopropane-1-carboxylate oxidase (ACC oxidase), (Nt ID: XM_006647913.2)	72.38%	2e-149	+22.325
14027.89434	*Oryza sativa Japonica Group* ethylene receptor-like protein 1 (ETR1), (Nr ID: AAL29304.2)	51.05%	3e-48	-18.141
14027.182197	*Arabidopsis thaliana* serine/threonine-protein kinase CTR1, (Swissprot ID: Q05609)	87.50%	3e-145	+ 11.918
14027.226694	*Setaria italica* ETHYLENE INSENSITIVE 3-like 3 protein (EIN3), (Nr ID: XP_004973869.1)	61.43%	1e-113	+ 14.849
14027.190058	*Zea mays* Indole-3-acetaldehyde oxidase (AAO), (Swissprot ID: O23887)	67.55%	4e-175	+13.436
14027.58358	*Setaria italica* probable indole-3-acetic acid-amido synthetase GH3.8, (Nr ID: XP_004958192.1)	69.87%	2e-133	Inf*
14027.189947	*Oryza sativa subsp. japonica* Jasmonic acid-amido synthetase JAR1, (Swissprot ID: Q6I581)	60.65%	2e-167	-28.213
ROS scavenging regulatory mechanisms				
14027.42850	*Flaveria pringlei* NADP-dependent malic enzyme, chloroplastic, (Swissprot ID: P36444)	55.29%	6e-111	Inf*
14027.184286	*Setaria italica* ubiquinol oxidase 2, mitochondrial-like (AOX), (Nr ID: XP_004976683.1)	93.02%	1e-64	+20.525
14027.154629	*Setaria italica* superoxide dismutase [Cu-Zn], (Nt ID: XM_004958551.3)	89.43%	2e-74	+ 36.275

14027.237926	*Setaria italica* superoxide dismutase [Fe] 2, chloroplastic-like, (Nt ID: XM_004964461.2)	98.26%	2e-68	-11.661
Osmolyte biosynthesis				
14027.146844	*Setaria italica* delta-1-pyrroline-5-carboxylate synthase (P5CS), (Nt ID: XM_004961829.3)	91.92%	6e-168	+68.438
14027.197137	*Brachypodium distachyon* delta-1-pyrroline-5-carboxylate dehydrogenase 12A1, mitochondrial (P5CSDH), (Nr ID: XP_010231104.1)	92.46%	5e-138	+17.285
14027.163909	*Oryza sativa* subsp. *indica* Betaine aldehyde dehydrogenase (BADH), (Swissprot ID: B3VMC0)	92.96%	1e-41	+ 15.021
5159.0	*Zea mays* ornithine decarboxylase-like (ODC), (Nr ID: XP_008653000.1)	52.96%	1e-112	+51.866
14027.196396	*Oryza sativa Japonica Group* Arginine decarboxylase 1 (ADC), (Nr ID: XP_015643038.1)	92.73%	1e-142	+65.072
14027.211822	*Setaria italica* spermine synthase-like (SPMS), (Nr ID: XP_004951294.1)	89.78%	2e-175	+ 10.003
Photosynthesis and photorespiration				
14027.158740	*Oryza sativa*, subsp. j*aponica* Group Ribulose bisphosphate carboxylase small chain A, (Swissprot ID: P18566)	88.96%	3e-100	-24.091
14027.70509	*Arundo donax* ribulose-bisphosphate carboxylase large subunit (rbcL), (Nt ID: KJ880079.1)	100.00%	1e-104	-17.789
14027.158959	*Setaria italica* ruBisCO large subunit-binding protein subunit beta, (Nr ID: XP_004975721.1)	95.45%	2e-19	-14.938

14027.168331	*Setaria italica* ribulose bisphosphate carboxylase/oxygenase activase, (Nt ID: XM_004960085.2)	84.71%	1e-46	-15.647
14027.198015	*Oryza brachyantha* phosphoenolpyruvate carboxylase (PEPC), (Nr ID: XP_006644735)	93,85%	1e-174	+11.496
14027.153211	*Oryza sativa* chloroplastic pyruvate phosphate dikinase 1 (PPDK1) (Swissprot ID: Q6AVA8)	88.41%	1e-163	+ 29.711
14027.158029	*Setaria italica* phosphoenolpyruvate carboxylase kinase (PEPC kinase), (Nr ID: XP_004976235.1)	84.05%	2e-127	-40.627
Biomass digestibility and biofuel production				
14027.150588	*Setaria italica* putative cinnamyl alcohol dehydrogenase, (Nt ID: XM_004972526.2)	79.53%	6e-116	+ 14.463

*it means that the read count value of CK samples is zero

Table 7. List of DEGs related to salt stress response identified in G2-S4 vs G2-S3 comparison.

Cluster ID	Database description	Percent identity	E value	log_2 fold change
Salt sensory and signaling mechanisms				
14027.81324	*Setaria italica* probable cation transporter HKT9, (Nr ID: XP_004967240.1)	65.10%	5e-142	+ 25.926
Transcription factors				
14027.184776	*Setaria italica* trihelix transcription factor GTL1, (Nt ID: XM_012842882.1)	80.41%	2e-69	+ 29.515
Hormone regulation of salt stress response				
14027.238560	*Zea mays* 9-cis-epoxycarotenoid dioxygenase 1, chloroplastic, (Swissprot ID: O24592)	85.48%	6e-177	-18.703
14027.234358	*Setaria italica* abscisic acid 8'-hydroxylase 3, (Nr ID: XP_004957014.1)	70.33%	4e-163	+ 23.595
14027.36785	*Setaria italica* brassinosteroid-6-oxidase 2 cytochrome P450 85A1, (KO ID: K12640)	93.12%	2e-105	+24.019
ROS scavenging regulatory mechanisms				
14027.104252	*Flaveria pringlei* NADP-dependent malic enzyme, chloroplastic, (Swissprot ID: P36444)	70.49%	5e-135	Inf*
14027.141579	*Setaria italica* ubiquinol oxidase 2, mitochondrial-like (AOX), (Nr ID: XP_004953576.1)	80.65%	4e-87	+13.511
14027.159513	*Zea Mays* superoxide dismutase [Cu-Zn], (Swissprot ID: P23345)	89.67%	2e-164	+ 11.777

14027.172733	*Setaria italica* superoxide dismutase [Fe] 1, chloroplastic-like, (Nt ID: XM_004981985.2)	72.96%	1e-165	-11.799
Osmolyte biosynthesis				
14027.166473	*Setaria italica* delta-1-pyrroline-5-carboxylate synthase (P5CS), (Nt ID: XM_004970516.2)	95.94%	8e-175	+ 44.106
14027.197137	*Brachypodium distachyon* delta-1-pyrroline-5-carboxylate dehydrogenase 12A1, mitochondrial (P5CSDH), (Nr ID: XP_010231104.1)	92.46%	5e-138	+ 17.324
14027.116788	*Oryza sativa* subsp. *japonica* Betaine aldehyde dehydrogenase 1 (BADH), (Swissprot ID: O24174)	85.80%	2e-94	+ 16.655
14027.196396	*Oryza sativa Japonica Group* Arginine decarboxylase 1 (ADC), (Nr ID: XP_015643038.1)	92.73%	1e-142	+ 18.455
Photosynthesis and photorespiration				
14027.157747	*Oryza sativa* subsp. j*aponica* Group Ribulose bisphosphate carboxylase small chain A, (Swissprot ID: Q0INY7)	94.59%	3e-20	-13.548
14027.70510	*Adiantum capillus-veneris* ribulose-bisphosphate carboxylase large subunit (rbcL), (Swissprot ID: P36476)	94.33%	9e-180	-13.342
14027.168328	*Setaria italica* ribulose bisphosphate carboxylase/oxygenase activase, (Nt ID: XM_004960085.2)	80.30%	4e-66	-10.404
14027.153211	*Oryza sativa* subsp. *japonica* chloroplastic pyruvate phosphate dikinase 1 (PPDK1), (Swissprot ID: Q6AVA8)	88.41%	1e-163	+28.312
14027.170986	*Setaria italica* phosphoenolpyruvate carboxylase kinase (PEPC kinase), (Nt ID: XM_004953094.3)	83.33%	7e-05	-17.751

Biomass digestibility and biofuel production				
14027.76193	*Setaria italica* cinnamyl alcohol dehydrogenase, (Nt ID: XM_004951572.2)	82.35%	2e-132	-11.287
14027.238308	*Setaria italica* triacylglycerol lipase SDP1-like, (Nr ID: XP_004970049.1)	75.07%	4e-168	+ 10.139

*it means that the read count value of CK samples is zero

Table 8. List of DEGs related to salt stress response identified in G34-S3 vs G34-CK comparison.

Cluster ID	Database description	Percent identity	E value	log_2 fold change
Salt sensory and signaling mechanisms				
14027.182899	*Oryza sativa* subsp. j*aponica* Group CBL-interacting protein kinase 1 (CIPK1-SOS2 like), (XM_015766590.1)	93.33%	4e-23	Inf*
14027.155903	*Phragmites australis* pcnhx1 mRNA for putative Na+/H+ antiporter (NHX1), (Nt ID: AB211145.1)	93.40%	3e-54	-12.753
14027.181583	*Arabidopsis thaliana* Sodium/hydrogen exchanger 2 (NHX2), (Swissprot ID: Q56XP4)	77.78%	8e-79	-11.093
Hormone regulation of salt stress response				
14027.99729	*Saccharum arundinaceum* 1-aminocyclopropane-1-carboxylate oxidase (ACC oxidase), (Nr ID: ABM74187.1)	91.46%	1e-122	+18.071
14027.223665	*Arabidopsis thaliana* serine/threonine-protein kinase CTR1, (Swissprot ID: Q05609)	89.36%	1e-02	Inf*
14027.213147	*Setaria italica* probable indole-3-acetic acid-amido synthetase GH3.8, (Nr ID: XP_004958192.1)	81.97%	1e-03	+23.948
ROS scavenging regulatory mechanisms				
14027.54848	*Setaria italica* glutathione transferase GST 23-like, (Nr ID: XP_004966104.1)	79.46%	2e-57	+ 16.425
14027.169726	*Setaria italica* NADP-dependent malic enzyme, chloroplastic, (Nr ID: XP_004960887.1)	96.14%	0.0	+ 15.508

14027.156319	*Setaria italica* superoxide dismutase [Fe] 2, chloroplastic-like, (Nt ID: XM_004964461.2)	93.24%	3e-86	- 10.398
Osmolyte biosynthesis				
14027.146844	*Setaria italica* delta-1-pyrroline-5-carboxylate synthase (P5CS), (Nt ID: XM_004961829.3)	91.92%	6e-168	+28.543
14027.160267	*Setaria italica* polyamine oxidase 2, (Nt ID: XM_004960065.2)	95.00%	5e-137	+20.021
Photosynthesis and photorespiration				
14027.153819	*Pisum sativum* RuBisCO large subunit-binding protein subunit alpha, chloroplastic, (Swissprot ID: P08926)	74.89%	4e-110	- 39.871
14027.193818	*Setaria italica* peroxisomal (S)-2-hydroxy-acid oxidase, (Nt ID: XM_004958250.2)	92.51%	5e-156	+ 14.194
14027.158029	*Setaria italica* phosphoenolpyruvate carboxylase kinase (PEPC kinase), (Nr ID: XP_004976235.1)	84.05%	2e-127	- 32.125
14027.157747	*Oryza sativa* subsp. j*aponica* Group Ribulose bisphosphate carboxylase small chain A, (Swissprot ID: Q0INY7)	94.59%	3e-20	-10.522

*it means that the read count value of CK samples is zero

Table 9. List of DEGs related to salt stress response identified in G34-S3 vs G2-S3 comparison

Cluster ID	Database description	Identity score	E value	log_2 fold change
Salt sensory and signaling mechanisms				
14027.182901	*Oryza sativa* CBL-interacting protein kinase 1 (CIPK1-SOS2-like) (Swissprot ID: Q9LGV5)	96.47%	2e-47	Inf*
Transcription factors				
14027.107730	*Setaria italica* bZIP ABSCISIC ACID-INSENSITIVE 5-like protein 7 (Swissprot ID: Q9M7Q2)	78.41%	4e-93	+ 22.418
Hormone regulation of salt stress response				
14027.225650	*Setaria italica* abscisic acid 8'-hydroxylase 3 (Nr ID: XP_004953596.1)	71.04%	7e-113	- 25.954
14027.162595	*Oryza sativa* serine/threonine-protein kinase SnRK (SnRK), (Swissprot ID: Q75H77)	80.00%	9e-18	+ 16.634
14027.146956	*Arabidopsis thaliana* serine/threonine-protein kinase CTR1, (Swissprot ID: Q05609)	87.05%	1e-140	+ 20.962
14027.21965	*Setaria italica* ETHYLENE INSENSITIVE 3-like 3 protein (EIN3) (Nr ID: XP_004973869.1)	69.64%	1e-158	- 22.436
14027.117700	*Setaria italica* probable indole-3-acetic acid-amido synthetase GH3.8 (Nr ID: XP_012702975.1)	75.23%	7e-87	- 31.598
ROS scavenging regulatory mechanisms				
14027.155781	*Setaria italica* L-ascorbate peroxidase (Nt ID: XM_004958747.1)	97.37%	4e-48	- 16.537

Osmolyte biosynthesis				
14027.231620	*Zea mays* delta-1-pyrroline-5-carboxylate synthase (P5CS) (Nt ID: XM_004970516.2)	93.43%	4e-169	- 20.415
Photosynthesis and photorespiration				
14027.158006	*Oryza sativa* ribulose bisphosphate carboxylase/oxygenase activase (Nt ID: CT830274.1)	66.67%	0.032	+ 17.919
Biomass digestibility and biofuel production				
14027.175228	*Zea mays* putative cinnamyl alcohol dehydrogenase (Nt ID: XM_008659830.1)	91.52%	6e-141	- 23.232
14027.199707	*Zea mays* diacylglycerol kinase 1 (Nr ID: XM_004983930.1)	93.00%	6e-131	- Inf**

*it means that the read count value of G2 samples is zero

**it means that the read count value of G34 samples is zero

6.2.4.1 Salt sensory an signaling mechanism

The analysis of different expressed genes between G2-S3 and G2-CK revealed that homologous to *Oryza sativa* (CBL-interacting protein kinases 1) CIPK1-SOS2-like protein and homologous to *Setaria italica* HKT9 gene are up-regulated in the salt treated samples, whereas genes homologous to the *Arabidopsis* NHX1 and NHX2 (Na^+/H^+ antiporters) are down regulated in response to severe S3 salt stress (Table 5). CIPK1-SOS2-like protein is a serine/threonine protein kinase involved in the activation of plasma membrane Na^+/H^+ antiporter (SOS1) which mediates the exclusion of Na^+ excess out of the cells, whereas HKT9 gene encodes a probable cation transporter. Consequently, the data suggest that the plant response to the S3 salt dose is likely either to increase the activation upon the existing Na^+/H^+ antiporter (SOS1) by the CIPK1-SOS2 like activity, or to adjust the K^+ homeostasis by inducing the expression of HKT9. The down regulation of NHXs indicates that the vacuolar sequestration of Na^+ excess seems to be impaired in the *A. donax* subjected to severe salt stress condition. Considering the G2-S4 vs G2-CK data set, a distinct response to extreme salt stress has been detected (Table 6). Along with the up regulation of CIPK1-SOS2 like and HKT9, the induction of CBL-interacting protein kinase 24 SOS2 (homologs of *Oryza sativa* subsp. Japonica protein) is also specifically up regulated under extreme salt stress conditions (S4). Morevover, the up regulation of NHX1 expression (*Arabidopsis thaliana* sodium/hydrogen exchanger 1) encoding the vacuolar Na^+/H^+ antiporter is observed (Table 6). In G34 clone, the severe stress level leads to the up-regulation of CIPK1-SOS2-like protein and the down regulation of NHX1 and NHX2 (Na^+/H^+ antiporters) proteins (Table 8), suggesting that the same response is achieved in the two G2 and G34 ecotypes to

severe salt treatment.However, the analysis of the G34-S3 vs G2-S3 comparison reveals that CIPK1-SOS2-like is deeply induced indicating that in the G34 ecotype this component takes on a major role in coping the salt stress condition (Table 9).

6.2.4.2 Transcription factors

In our study, DEGs encoding transcription factors (TFs) were identified and divided in 16 subfamilies, as showed in Figure 20, which reports the transcription factor subfamilies sorted by the G2-S4 vs G2-CK DEG number. The results showed that under S3 severe stress condition, an average of 12 TFs for each family are differently regulated. In particular, 23 DEGs belong to auxin/indole acetic acid (AUX/IAA), 21 to bHLH and 19 to NAC families, respectively, indicating that these are the most represented subfamilies and they probably play a key role in regulating the changes of transcriptional regulation in response to salt (Figure 20). It worthwhile to mention that among the downregulated genes belonging to G2-S3 vs G2-CK DEGs, a homolog of *Setaria italica* protein TIFY 10B-like (LOC101761171) known to be a repressor of jasmonate (JA) responses, has been found (Table 5). Moreover, a homolog of *Setaria italica* trihelix transcription factor GTL1 (LOC101762434) that acts as negative regulator of water use efficiency (Yoo et al., 2010; Weng et al., 2012) has been found up-regulated in G2-S3 vs G2-CK data set (Table 5). Finally, homologs of *Setaria italica* bZIP ABSCISIC ACID-INSENSITIVE 5-like protein 7 functioning as transcriptional activator in the ABA-inducible expression of rd29B have been also found among the up-regulated clusters. The role of these differently regulated clusters will be discussed below.

In the G2-S4 vs G2-CK comparison, a deeper modification of the transcription regulation is detected since an average of 53 TFs for each family resulted differently regulated in comparison with untreated samples, being the bHLH (94 DEGs), AUX/IAA (109 DEGs), MYB (88 DEGs) and NAC (91 DEGs) subfamilies the most represented (Figure 20).
The different situation in terms of number of DEGs belonging to TFs subfamilies is observed in G34-S3 vs G34-CK comparison, where the average number of TFs for each family decreases drastically to 7. The most represented subfamilies are bHLH (21 DEGs), WRKY (19 DEGs), AUX/IAA (16 DEGs) and NAC (15 DEGs), probably indicating a lower need to reprogram the regulation of gene expression machinery (Figure 20).

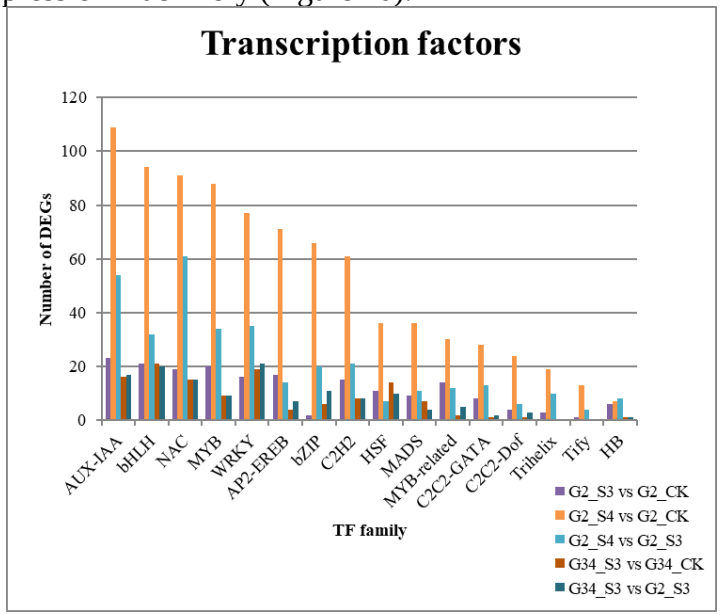

Figure 20. Distribution of transcription factors responsive to salt stress. Data are sorted by number of G2-S4 vs G2 CK DEGs.

Interestingly, homologs of Setaria italica bZIP ABSCISIC ACID-INSENSITIVE 5-like protein 7 have been also found among the up-regulated clusters specifically in the G34-S3 vs G2-S3 comparison which account for a main role of this TF in G34 ecotype (Table 9). A comparative analysis performed using the available database of rice transcription factors under salt stress led to the identification of 449 *A. donax* unigenes, corresponding to high confidence rice TF homologs previously identified as salt or salt/drought genes (Priya and Jain, 2013). Probably because of the altered water potential under salt stress, the majority of these genes (434) are also responsive to drought. A total of 15 genes are specifically responding to salt (Appendix VI - Table S4), and among them, 9 (six up regulated and three downregulated) belong to the AP2-EREBP family (Chen et al., 2016). Interestingly, all the 15 gene are differentially regulated in G2 clone (14 out of the 15 specific salt-related transcription factors in G2-S4 vs G2-CK, the other one in G2-S3 vs G2-CK) but not in G34 (Appendix VI – Table S4), confirming that a different response to salt occurred in G34 ecotype.

6.2.4.3 Hormone regulation of salt stress response

We focused our attention on the main plant hormones involved in salt stress response, such as abscisic acid, brassinosteroid, ethylene, auxin/IAA and jasmonic acid (Golldack et al., 2014; Gupta and Huang, 2014). The analysis of G2-S3 vs G2-CK data set revealed that the genes involved in abscisic acid biosynthesis (NCED, zeathaxin oxidase and aldehyde oxidase) are not differently regulated by long term salt stress, otherwise homolog of *Triticum urartu* (Nr ID: EMS68885.1) abscisic acid 8'-hydroxylase 1 (LOC101782596), involved in ABA catabolism, has been found among the up-regulated genes (Table 5). Based on

these differential expressions, it seems that circulating ABA is channeled in a degradation pathway and the plant responds to prolonged severe stress by lowering ABA levels. Among the up-regulated genes, homologs of *Setaria italica* abscisic acid receptor PYL8 (LOC101768693), of *Setaria italica* ABSCISIC ACID-INSENSITIVE 5-like protein 7 (LOC101778442), *Setaria italica* abscisic acid receptor PYR1-like (LOC101776342), *Oryza sativa* serine/threonine-protein kinase SnRK (SnRK) and to *Setaria italica* probable protein phosphatase 2C 30 (LOC101766228) were discovered. According to these results, although ABA levels seems to be lowered, as the up regulation of abscisic acid 8'-hydroxylase homolog suggests, ABA signal is probably persisting since ABA nucleoplasmatic receptors are up-regulated as well as the SnRK2 which active many downstream ABA-responsive processes (Golldack et al., 2014). As regards G2-S4 vs G2-CK and G2-S4 vs G2-S3 sample data, *Setaria italica* abscisic acid 8'-hydroxylase 3 (LOC101760218) and *Setaria italica* abscisic acid receptor PYL8 (LOC101768693) are up-regulated (Tables 6 and 7). Moreover, the downregulation of homolog to *Oryza sativa* 9-cis-epoxycarotenoid dioxygenase (NCED) in the G2-S4 vs G2-S3 comparison, which is not detected in the G2-S3 vs G2-CK, is observed and it might more clearly indicate that ABA synthesis is not induced in samples subjected to long-term extreme salt stress. As regards brassinosteroids, in the G2-S3 vs G2-CK data set, homolog of *Setaria italica* cytochrome P450 734A6-like BAS1 (LOC101760518), a brassinosteroid inactivator, is up-regulated indicating that brassinosteroid signaling is likely interrupted in response to S3 severe salt treatment (Table 5). Conversely, by the analysis of the G2-S4 vs G2-CK data set (Table 6), confirmed by the G2-S4 vs G2-S3 comparison (Table 7), we discovered that homolog of

Setaria italica cytochrome P450 85A1 (LOC101770408) encoding brassinosteroid-6-oxidase 2, that is implicated in brassinosteroid biosynthesis, is up- regulated under extreme salt stress (Table 6). Transcripts encoding ACC oxidase, namely the ethylene-forming enzyme, have been found up-regulated both under severe (homolog of *Saccharum arundinaceum* 1-aminocyclopropane-1-carboxylate oxidase) and extreme salt stress (homolog of *Oryza brachyantha* 1-aminocyclopropane-1-carboxylate oxidase (LOC102702913). However, in G2-S3 vs G2-CK sample data, none of the ethylene downstream acting genes has been found, neither among the up-regulated nor among the down-regulated clusters (Table 5). Conversely, the analysis of the G2-S4 vs G2-CK revealed that homolog of *Arabidopsis thaliana* receptor ethylene response 1 (ETR 1) is downregulated, whereas clusters related to CTR1 (*Zea mays* serine/threonine-protein kinase CTR1-like) and EIN3 (*Setaria italica* ETHYLENE INSENSITIVE 3-like 3 protein), both implicated in quenching the ethylene signal, are up-regulated (Table 6). Sharp differences between the responses of *A. donax* to salt dose have been detected once we considered the role of auxin/IAA as signal molecule. In this respect, the genes encoding the main biosynthetic enzyme, such as indole-3-pyruvate monooxygenase YUCCA2-like (LOC101757189) (Woodward and Bartel, 2005), is downregulated in G2-S3 vs G2-CK comparison indicating that severe salt stress seems not to implicate an increase in IAA levels. Analyzing the response to extreme salt stress upon *A. donax* leaves, we found a strong induction of different clusters relative to YUCCA-like indole-3-pyruvate monooxygenases, which have been described as a high redundant gene family (Woodward and Bartel, 2005). Unfortunely, several clusters are also found among the

downregulated genes thus rendering difficult to make general conclusions (data not shown). However, a homolog of *Zea mays* indole-3-acetaldehyde oxidase (AAO), involved in the biosynthesis of auxin, is upregulated in S4 samples and also in the G2-S4 vs G2-S3 comparison suggesting that IAA might be synthesized in S4 extreme conditions (Table 7). Moreover, exclusively under extreme stress condition a homolog of auxin responsive GH3 gene family, regulating levels of biologically active auxin, is also up-regulated (Table 6). Finally, homolog of *Oryza sativa* subsp. japonica jasmonic acid-amido synthetase JAR1 is down regulated in G2-S4 vs G2-CK comparison (Table 6) but not in the G2-S3 vs G2-CK samples indicating that under extreme salt stress conditions jasmonic acid biosynthesis might be impaired.

Regarding the hormone regulation in G34 clone (G34-S3 vs G34-CK) we found up-regulated genes involved in ethylene biosynthesis and regulation such as transcripts encoding ACC oxidase (homolog of *Saccharum arundinaceum* 1-aminocyclopropane-1-carboxylate oxidase) and homolog of CTR1 (*Arabidopsis thaliana* serine/threonine-protein kinase CTR1 (Table 8). According to these results, it seems that G34 ecotype subjected to severe S3 salt stress responds similarly to G2 ecotype under extreme S4 salt treatment, this being an important finding of the global analysis. An interesting picture can be deduced once the G34-S3 vs G2-S3 data set is considered, specifically regarding the role of ethylene signaling (Table 9). The analysis revealed that clusters related to CTR1 (*Arabidopsis thaliana* serine/threonine-protein kinase CTR1-like) and EIN3 (*Setaria italica* ETHYLENE INSENSITIVE 3-like 3 protein), both implicated in quenching the ethylene signal, are up-regulated and down regulated in G34-S3 vs G2-S3 samples, respectively (Table 9). Moreover, the down regulation of abscisic acid 8'-

hydrolase is also reported which suggests that abscisic acid signal transduction might be more active in G34 under S3 condition than in G2-S3. A gene involved in auxin biosynthesis (*Setaria italica* indole-3-acetic acid-amido synthetase GH3.8) results down regulated in this comparison (Table 9).

6.2.4.4 ROS scavenging regulatory mechanisms

The analysis of G2-S3 vs G2-CK revealed that, among the antioxidant enzymes, ascorbate peroxidase (APX) expression is up-regulated suggesting that H_2O_2 could be the main ROS the *A. donax* cells have to cope with under severe salt stress (Table 5). Many GSTs are also up-regulated concordantly with their role in salt stress relief (Puglisi et al., 2013; Lo Cicero et al., 2015). Also the plastid NADP-malic dehydrogenase, reducing oxalacetate to malate, thus regenerating the $NADP^+$, is among the up-regulated genes of the G2-S3 vs G2-CK data set, this result being consistent with the electron drainage from an over-reduced photosynthetic chain to other cellular compartments, in particular towards the mitochondria. Indeed, homologs of the mitochondrial malate dehydrogenase (MHD) are also induced by salinity (Table 5). As concerns either the G2-S4 vs G2-CK or G2-S4 vs G2-S3 comparisons (Tables 6 and 7), the plastid NADP-malic dehydrogenase and alternative oxidase (AOX), that transfers electrons towards the respiratory electron chain for energy dissipation, are unequivocally up regulated under extreme salt stress conditions. Similarly to G2-S3 vs G2-CK, G34 clone shows an up-regulation of GST and NADP-dependent malic enzyme, and a down-regulation of superoxide dismutase $[Fe]^2$ (Table 8), this last result being achieved also by the G2 clone but under extreme salt condition. Accordlying, the analysis of the G34-S3 vs G2-S3

comparison highlights that cluster related to *Setaria italica* ascorbate peroxidase (APX) is down regulated indicating that this pathway removing H_2O_2 is specifically induced in G2 ecotype subjected to S3 condition (Tables 5 and 9).

6.2.4.5 Osmolyte biosynthesis

The accumulation of compatible osmolytes, such as proline, glycine betaine, polyamines and sugar alcohols play a key role in maintaining the low intracellular osmotic potential of plants and in preventing the harmful effects of salinity stress (Deinlein et al., 2014; Gupta and Huang, 2014; Hoque et al., 2008). In our study, 1-delta-pyrroline-5-carboxylate synthase (P5CS), the key enzyme of proline biosynthesis, was found up regulated in all comparisons exept G34-S3 vs G2-S3 (G2-S3 vs G2-CK, G2-S4 vs G2-CK, G2-S4 vs G2-S3 and G34-S3 vs G34-CK) (Tables 5-8) suggesting that proline accumulation might represent a pivotal mechanism to overcome the hypersaline conditions and adjust the osmotic status in *A. donax*. The down regulation observed in the G34-S3 vs G2-S3 could account for a lower induction of this gene in the G34-S3 samples than that observable in G2 under S3 conditions (Table 9). Consistent with its catabolic role, proline dehydrogenase (PDH) expression is down regulated in G2-S3 vs G2-CK data set suggesting that the mitochondrial degradation of proline is prevented (Table 5). Conversely, PDH and 1-delta-pyrroline-5-carboxylate dehydrogenase (P5CSDH), both involved in proline catabolism, resulted up regulated in both G2-S4 vs G2-CK and G2-S4 vs G2-S3 data sets (Tables 6 and 7). Biosynthesis pathway of betaine comprises a two steps oxidation of choline in which betaine aldehyde dehydrogenase (BADH) synthesizes betaine from betaine aldehyde. BADH expression is up regulated in G2-S4 vs G2-CK and G2-S4 vs G2-S3 comparisons indicating that

betaine might play a crucial role under S4 extreme stress conditions (Tables 6 and 7). Due to their cationic nature, polyamines can interact with proteins, nucleic acids, membrane phospholipids and cell wall constituents, either activating or stabilizing these molecules. Considering all the comparison data set involving G2 ecotype, clusters encoding arginine decarboxylase (ADC, polyamine biosynthetic enzyme) are up-regulated suggesting that polyamines biosynthesis is induced during long term salt stress, having most likely a role in the salt tolerance mechanism, both under severe and extreme stress condition (Tables 5-7). In addition, clusters homolog to ornithine decarboxylase (ODC) and to spermine synthase (SPMS) are exclusively up-regulated in G2-S4 vs G2-CK comparison, indicating that a stronger activation of the polyamine biosynthesis occurs under extreme salt stress, also involving the polyamine biosynthetic pathway starting from ornithine by the action of ODC (Table 6). The above-mentioned genes and related pathways are not among the DEGs belonging to the G34 ecotypes (listed in Tables 8 and 9), indicating that their involvement in G34 salt stress response is not occurred.

Sugar alcohols are compatible solutes classified into two major types cyclic (e.g., pinitol) and acyclic (e.g., mannitol) (Gupta and Huang, 2014). In our study, neither mannitol-1-phosphate dehydrogenase (mldh) nor inositol methyl transferase (imt) transcripts, respectively involved in mannitol and pinitol biosynthesis, were in the all the comparisons under investigation, indicating that the synthesis of these compounds might be not crucial for salt stress overcoming in *A. donax*.

6.2.4.6 Photosynthesis and photorespiration

The analysis of G2-S3 vs G2-CK DEGs reveals that homologs of both small and large subunits of ribulose-1,5-bisphoshate carboxylase/oxygenase (Rubisco) are not represented neither in the up-regulated or in the down regulated clusters (Table 5). However, homologs of *Pisum sativum* Rubisco large subunit-binding protein subunit alpha, required for the correct assembly of Rubisco, have been discovered among the down-regulated genes, indicating that the process of Rubisco assembly could be strongly affected under S3 salt stress (Table 5). Moreover, clusters encoding glycolate oxidase (*Setaria italica* peroxisomal (S)-2-hydroxy-acid oxidase, LOC101764130), which is a key enzyme of the glycolate recovery pathway induced by photorespiration, is up-regulated in G2-S3 vs G2-CK comparison suggesting that CO_2 assimilation via the C3 Calvin cycle might be impaired in favor of oxygen fixation through the photorespiration pathway (Table 5). The same pattern was found in G34-S3 vs G34-CK suggesting that the mechanism described above is commonly related to the severe salt stress (Table 8). This result is consistent with the decrease of net photosynthesis showed in Appendix I - Figure S1. Conversely, a surprising scenario takes place in the case of *A. donax* G2 samples subjected to extreme salt stress conditions (Table 6). Mainly, clusters encoding both the small and the large Rubisco subunits (homologs of *Oryza sativa* ribulose bisphosphate carboxylase small chain), clusters encoding *Arundo donax* Rubisco large subunit-binding proteins (involved in Rubisco assembly) and *Setaria italica* ribulose bisphosphate carboxylase/oxygenase activase, are among the down-regulated genes. Rubisco activase plays an important role adjusting the conformation of the active center of Rubisco by removing tightly bound

inhibitors thus contributing to the enzyme rapid carboxylation (Carmo-Silva and Salvucci, 2013). These findings indicate that extreme salt treatment induces a strong slowdown if not even a dramatic stop of the C3 Calvin cycle (Tables 6 and 7). However, specifically under S4 extreme salt stress, among the up-regulated DEGs, homologs of *Flaveria trinervia* phosphoenolpyruvate carboxylase (PEPC) and of *Oryza sativa* chloroplastic pyruvate phosphate dikinase 1 (PPDK1) have been identified, both involved in C4 photosynthesis, in which the spatial separation of the initial fixation of atmospheric CO_2 from the Calvin cycle occurs. Concordantly, homologs of *Setaria italica* phosphoenolpyruvate carboxylase kinase 2-like (LOC101779241), the PEPC inactivating enzyme by decreasing of maximal reaction rate, were found down-regulated, suggesting that G2 giant reed response to extreme salt stress tends to maximize the catalytic efficiency of PEPC (Tables 6 and 7). The same PEPC kinase was found down-regulated also in G34 clone under severe S3 condition, but no PEPC and PPDK1 homologues were found activated (Table 8), thus indicating that the C3 to C4 switching might be achieved exclusively under S4 extreme condition. Unfortunately, this could not be evaluated in G34 samples because of the fire occurred in our experimental field. The G34-S3 vs G2-S3 comparison shows that a stronger activation of the Rubisco activase is in G34 ecotype with respect to G2 both under severe salt stress (Table 9).

6.2.4.7 Biomass digestibility and biofuel production

Considering the economical relevance that bioenergy crops assume as source of bioethanol, we analyzed the regulation of several genes involved in the improvement of lignocellulosic biomass. In the *A. donax* transcriptome

subjected to both severe and extreme salt stress, several homologs of phenylpropanoid biosynthetic genes were highly expressed (Table 5-7). In particular, homologs of *Setaria italica* cinnamoyl-CoA reductase 2-like and *Zea mays* caffeoyl CoA 3-O-methyltransferase are among the up-regulated clusters in G2-S3 vs G2-CK samples, being both specifically involved in lignin biosynthesis (Tables 6 and 7) (Xie et al., 2018). Similarly, homolog of *Setaria italica* cinnamyl alcohol dehydrogenase was observed among the up-regulated clusters in the G2-S4 vs G2- CK but also in G2-S4 vs G2-S3 sample indicating that lignin biosynthesis is induced under extreme salt stress condition. Besides the homologs of the phenylpropanoid pathway discussed above, we identified transcripts homologous to sucrose synthase (*Setaria italica* sucrose synthase) in the G2-S3 vs G2-CK comparison, a key enzyme in cellulose biosynthesis. Considered that also lipids can participate to biomass yield, we focused our attention on genes encoding key enzymes such as triacylglycerol lipase and diacylglycerol kinase that were found to be up regulated under severe salt stress (Table 5). No genes linked with lignin and cellulose biosynthesis were found differentially regulated in G34 clone under severe salt stress compared with untreated plants (Table 8). Moreover, clusters related to biomass digestibility and biofuel production, such as cinnamyl alchohol dehydrogenase and diacylglycerol kinase 1, were strongly down regulated in the G34-S3 vs G2-S3 comparison thus suggesting a minor role of these pathways in the G34 under S3 salt stress.

6.2.4.8 *Retrieval and analysis of genes targeted as "salt stress responsive"*

The GO terms were further analyzed in order to retrieve clusters specifically involved in the salt stress response, thus excluding all transcripts also regulated by different abiotic stress, such as water deprivation, cold, heavy metals and oxidative stresses (geneontology.org/). All the retrieved clusters are also found to be involved in salt-induced osmotic stress according to the finding that levels of NaCl higher than 100–150 mM cause osmotic stress, that normally arises up at salinity levels ranging between 50 and 100 mM NaCl (Shavrukov, 2012). The results shown in Appendix VII - Table S5 reveal that among 9 clusters specifically regulated by salt, 7 are up regulated and 2 are down regulated in the G2-S3 vs G2-CK comparison. Among the up regulated genes, the CBL-interacting protein kinase 1 (CIPK1-SOS2 like) has been found (Appendix VII - Table S5) thus suggesting that it induces specific signal transduction pathways under severe salt stress conditions. Instead, clusters related to plasma membrane Na^+/K^+ transporter are down regulated by severe salt stress treatment (Appendix VII - Table S5), both results being already highlighted in Table 5. Only 2 genes resulted specifically regulated by salt in G34-S3 vs G34-CK comparison, 1 up- and 1 down-regulated. Similarly to G2 ecotype, CBL-interacting protein kinase 1 (CIPK1-SOS2 like) has been found up-regulated, and a cation transporter HKT6 has been found down-regulated (Appendix VII – Table S6). A higher number of up and down regulated genes have been found among the G2-S4 vs G2-CK data set, they being 29 and 7, respectively, for a total of 36 clusters (Appendix VII – Table S7). Similarly to G2-S3 vs G2-CK comparison, clusters encoding the CBL-interacting protein kinase 1 (CIPK1-SOS2 like) have been found up regulated under

extreme salt stress S4 (Appendix VII - Table S7, Table 6). Moreover, CBL-interacting protein kinase 24 SOS2 (homolog of *Oryza sativa* subsp. Japonica protein, Table 6) is specifically up regulated under extreme salt stress conditions (S4). Interestingly, clusters encoding homologs of the mitochondrial persulfide dioxygenase ETHE1 (ETHYLMALONIC ENCEPHALOPATHY PROTEIN1), that catalyzes the oxidation of persulfides derived from either cysteine or hydrogen sulfide to thiosulfate and sulfate (Höfler et al., 2016) have been found up regulated in G2-S4 conditions. Finally, clusters mainly related to a probable *Oryza sativa* subsp. Japonica cation transporter HKT6 are down regulated under extreme salt conditions (Appendix VII - Table S7). In order to support the relationship among the main specific salt responsive genes (CIPK1-SOS2 like, cation transporter HKT9, NHX1, NHX2, SOS2 and ETHE 1, Table 6 and Appendix VII – Table S7) and their orthologues, each *A.donax* cluster was aligned with fifteen orthologues from different plant sources and phylogenetic trees were constructed (Appendix VIII - Figure S4a-f). The sequence alignments allowed to classify the proteins within the respective protein family and, in the case of CIPK1-SOS2 like, of persulfide dioxygenase ETHE1 and CBL-interacting protein kinase 24 (SOS2) sequence alignment revealed the presence of specific protein functional domains (Appendix VIII - Table S8). The findings of the phylogenetic trees depicted that all the genes from different plant sources can be subcategorized into subgroups (Appendix VIII - Fig. S4a-f) and that, all the giant reed genes were clustered into one of these subgroups.

6.3 SSR analysis

6.3.1 Identification and distribution of SSR markers

The 228,266 unigenes, were screened for repeat motifs to explore the SSR profile in the *A. donax* leaf transcriptome. The motifs distribution was screened both in untraslated regions (5'-UTR e 3'-UTR) and coding regions (CDS), since many of the sequenced mRNA transcripts contained untranslated regions (UTRs) and occasional remaining introns. A total of 45,529 SSRs were obtained from 39,710 unigenes sequences (17.39%) so 4,993 sequences contained more than one SSR. In addition, 1,573 sequences revealed compound SSR formation (Table 10). A strong enrichment of mono-, di-, and trinucleotide repeat motifs was further detected among each of the SSR classes, whereas longer repeat motifs were clearly under-represented (Table 11, Figure 21).

Table 10. Summary statistics of SSRs analysis

Total number of sequences examined	311960
Total size of examined sequences (bp)	378804057
Total number of identified SSRs	45529
Number of SSR containing sequences	39710
Number of sequences containing more than 1 SSR	4993
Number of SSRs present in compound formation	1573

Table 11. Number of repetition of SSR motifs

Unit size	**Number of SSRs**
1	17466
2	10763
3	16620
4	563
5	93
6	24

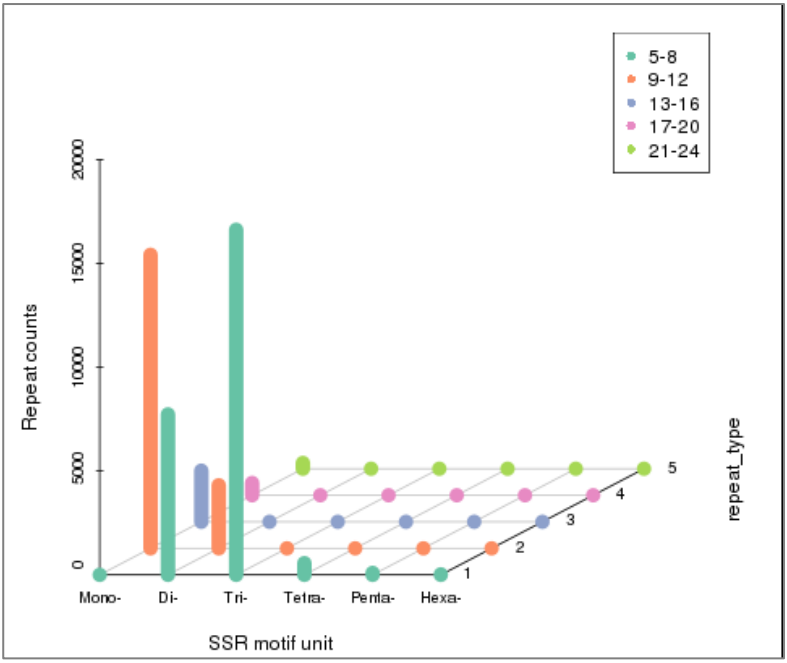

Figure 21. Distribution of SSR motifs

We further investigated the distribution of SSR classes in the unigenes (CDS, 5′ UTR, and 3′ UTR). Out of the total SSRs, 16,221 were located in the UTR and CDS regions, of which 8,650 (53.32%), 2,764 (17.04%), and 4,807 (29.63%) SSRs were located in the 5′ UTR, CDS, and 3′ UTR, respectively. The remaining SSRs (27,736 SSRs; 60.91%) were not ascertained a position because it was not possible to delimit the UTR and CDS regions for the transcripts containing them. In Table 12 is reported the frequency in percentage of each motif. Most of repeated motifs (17,466 SSRs) are mono-base repetitions (38,36 %), followed by tri-base (16,620 SSRs; 36,50 %) and di-base motifs (10,763 SSRs; 23,64 %). As regard the SSRs located in CDS region, most of them (2,410

SSRs) are mono-base repetition (87,20 %), followed by di-base repetitions (334 SSRs; 12,10 %). The same for 5'-UTR and 3'-UTR regions: 7,776 SSRs (89,91 %) and 4,233 SSR (88,06 %) mono-base for 5'-UTR and 3'-UTR respectively, followed by di-base repetitions, 786 SSRs (9,09 %) and (487 SSRs (10,13 %) for 5'-UTR and 3'-UTR respectively. The most abundant nucleotidic patterns found in the analysis are the following: A/T (10,524 SSRs; 23,11 %) and C/G (6,942 SSRs; 15,28 %) for mono-nucleotides, AG/CT (6,559 SSRs; 14,40 %) for di-nucleotides and CCG/CGG (7,777 SSRs; 17,01 %) for tri-nucleotides (Table 12).

Table 12. Nucleotidic patterns

Nucleotide motif	Number of SSRs	Frequency (%)
A/T	10524	23.115
C/G	6942	15.247
AC/GT	1999	4.391
AG/CT	6559	14.406
AT/AT	1510	3.317
CG/CG	695	1.526
AAC/GTT	898	1.972
AAG/CTT	977	2.146
AAT/ATT	234	0.514
ACC/GGT	1082	2.377
ACG/CGT	633	1.390
ACT/AGT	196	0.430
AGC/CTG	2134	4.687
AGG/CCT	2225	4.887
ATC/ATG	464	1.019
CCG/CGG	7777	17.081
AAAT/ATTT	40	0.088
AAGG/CCTT	49	0.108
ATCC/ATGG	55	0.121

6.3.2 Validation of SSRs

As described in methods section SSR validation was conducted by amplifying and sequencing five microsatellite regions chosen randomly in 5'-UTR, CDS and 3'-UTR coding sequences (Appendix IX – Table S9). The repeated motifs are included in sequences belonging to genes homologous to: *Setaria italica* serine/arginine repetitive matrix protein 2 (SRRM2), *Setaria italica* high mobility group nucleosome-binding domain-containing protein 5 (HMGN5), *Setaria italica* protein SHORT-ROOT 1 (SHR1), *Setaria italica* myb-related protein MYBAS1-like (myba), *Setaria italica* squamosa promoter-binding-like protein 2 (SPL1). For all the microsatellites analyzed, the repeated motifs and the number of repetitions were confirmed in both the clones (G2 and G34) by sequence analysis. In fact, five repetitions of AGC motif were detected in SRRM2 and HMGN5 (Appendix IX - Figure S5a and b), six repetitions of AGC motif were detected in SHR1(Appendix IX - Figure S5c), four repetitions of AGC motif were detected in myba (Appendix IX – Figure S5d) and five repetitions of GCA motif were detected in SPL1(Appendix IX - Figure S5e), showing a perfect congruence with the RNA-seq experiment and allowing its validation.

6.4 Epigenetic analysis

The methylation status analysis was carried out on differentially expressed genes having a salt stress related function or on genes reported to be differentially methylated when subjected to salt stress (Kumar et al., 2017). HKT type-II transporter protein (HKT2) and probable cation transporter HKT6 (HKT6) belong to the family of High-affinity Potassium Transporters (HKTs), involved in the homeostasis of sodium and potassium ions in plants under salt stress. In

MSAP analysis, HKT2 and HKT6, both down-regulated in G2-S3 vs G2-CK and G34-S3 vs G34-CK comparisons, resulted hypomethylated in their coding region under salt stress condition (Figure 22). The percentage of methylation of HKT2 decrease from 69% to 33%, and from 58 % to 28% in HKT6 coding region. In G34, both HKT2 and HKT6 methylation percentage does not significantly change when the stress is applied (Figure 22).

A homologous of *Setaria italica* myb-related protein 306-like, involved in response to hormones such as ethylene and auxin, was also analyzed with the MSAP approach. The gene, which is down-regulated in both G2-S3 vs G2-CK and G34-S3 vs G34-CK comparisons, resulted with no methylated cytosines in the coding region in G2 clone, in both G2-CK and G2-S3 samples (from 0% to 1%), and 17% methylated in G34-CK with a decrease to 0% in G34-S3 (Figure 22), indicating that there is not involvement of cytosine methylation in the regulation of this gene in G2.

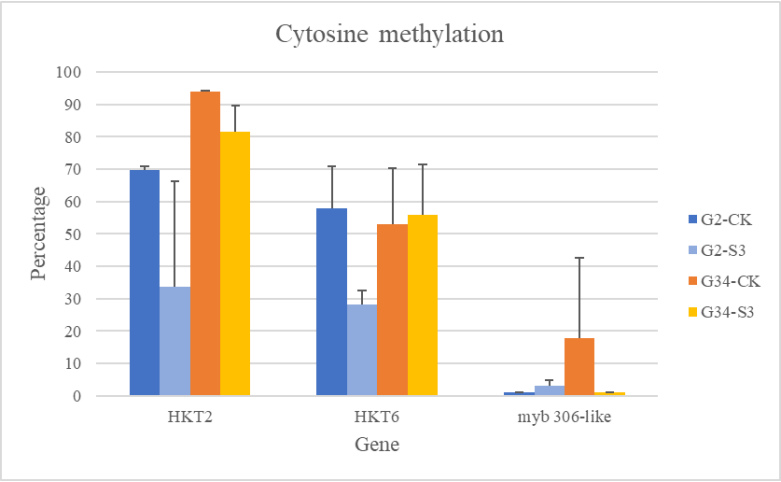

Figure 23. Percentage of cytosine methylation in HKT2, HKT6 and myb 306-like coding region.

7. Discussion

Plants generate high yields if the growth demands are properly supplied as well as light and temperature fit to their optimum requirements. Yield-associated traits are inversely related to abiotic stress conditions such as salt during plant development. Under conditions of moderate salinity (EC 4-8 dS m^{-1}), all important glycophytic crops reduce average yields by 50–80% (Panta et al., 2014). Plants have developed the ability to sense both the hyperosmotic component and the toxic ionic Na^+ component of salt stress (Deinlein et al., 2104). To date the molecular identities of plant hyperosmotic sensors and Na^+ sensors present at the plasma membrane have remained unknown. Recently, Choi et al. (2014) suggested that Ca^{2+}-dependent signaling plays a role in the systemic transmission of signaling as a Ca^{2+} wave propagates preferentially through cortical and endodermal cells from roots to distal shoots. In salt tolerant plants, the cytosolic calcium perturbation actives the Salt Overly Sensitive (SOS) pathway (Liu and Zhu, 1998; MartìnezAtienza et al., 2007). The components of this pathway are the Ca^{2+} sensor (SOS3) which accordingly changes its conformation in a Ca^{2+}-dependent manner and interacts with SOS2, a serine/threonine protein kinase, forming the active SOS2-SOS3 complex. This interaction results in the activation through its phosphorylation of SOS1 (plasma membrane Na^+/H^+ antiporter) which mediates the exclusion of Na^+ excess out of the cells. In addition, the SOS2-SOS3 complex activates NHX, the vacuolar Na^+/H^+ exchanger resulting in the vacuolar sequestration of Na^+ excess thus further

contributing to the restore of ion homeostasis (Zhu, 2002; Barragan et al., 2012).

Focusing on G2 ecotype, the data of this thesis suggest that the SOS pathway is only partially activated under severe salt stress (up-regulation of CIPK1-SOS2-like protein and HKT9) and the down regulation of NHX indicates that the vacuolar sequestration of Na^+ excess seems to be impaired (Table 5 and 7). A specific response to extreme salt stress has been detected (Table 6), since the up regulation of CIPK1-SOS2 like and HKT9 (*Setaria italica* probable cation transporter HKT9) was accompanied by the up-regulation of NHX1 (*Arabidopsis thaliana* sodium/hydrogen exchanger 1) encoding the vacuolar Na^+/H^+ antiporter. Moreover, CBL-interacting protein kinase 24 (homologs of *Oryza sativa* subsp. Japonica protein, Table 6), involved in the regulatory pathway for the control of intracellular Na^+ and K^+ homeostasis and salt tolerance, is specifically up regulated under extreme salt stress conditions (S4). It activates the vacuolar H^+/Ca^{2+} antiporter and operates in synergy with CBL4/SOS3 to activate the plasma membrane Na^+/H^+ antiporter SOS1 (Cheng et al., 2004). As expected, the components of the SOS response are among the salt induced specific genes, indicating their key role in salt detoxification. In addition to that, several transcripts homologous to *Arabidopsis* NHX5 and NHX6 encoding endosomal Na^+/H^+ antiporters are also up-regulated (data not shown). Although the relative log_2fold changes of these clusters are below the +10.000 threshold we established at the beginning of the analysis, these results anyway suggest that the cellular components devoted to Na^+ excess expulsion, located in the tonoplast and in the endosomal membranes all together might participate in reducing the Na^+ cytoplasmic concentrations. The importance of these genes in salt stress relief is supported

by the finding that *Arabidopsis nhx5 nhx6* double knockout showed reduced growth and increased sensitivity to salinity (Bassi et al., 2011).

Downstream of aforementioned activation of Ca^{2+} alteration induced by salinity, kinases become activated and may transduce the hyperosmotic signal to induce protein activities and gene transcription. The activation of transcription factors can occur by the direct binding with calmodulin-binding transcriptional activators (CAMTAs), GT-element binding proteins and MYBs (Mahajan and Tuteja, 2005; Deinlein et al., 2014). Transcription factors (TFs) are considered as the most important regulators controlling the expression of a broad range of target genes ultimately influencing the level of salt tolerance in plants. It is well documented that TFs belonging to the DREB, NAC, MYB, MYC, C2H2 zinc finger, bZIP, AP2/ERF (Ethylene Responsive Factor) and WRKY families are relevant in salt stress response (Golldack et al., 2014). In most cases, the overexpression of these transcription factors successfully enhanced salinity tolerance in many crops (Hanin et al., 2016). By comparing our results with those obtained in *A. donax* subjected to water deficit (Fu et al., 2016), slight differences can be observed in terms of TF subfamilies involved in salt and water stresses, but a greater number of all TFs for each family resulted differently regulated under both severe and extreme salt stress. Interestingly, a major involvement of AUX/IAA TFs is detected under salt stress with respect to *A. donax* plants subjected to drought thus indicating that a different regulation network is induced. Moreover, a total of 449 *A. donax* unigenes correspond to high confidence rice homologs previously identified as salt or salt/drought responsive genes (Priya and Jain, 2013). Most of them (434) resulted also responsive to drought, indicating that the plant responses to

these stresses probably overlap each other and that the downstream metabolic pathways can crosstalk. Significantly, few genes (15) specifically respond to salt treatments and they have been found especially (14 out of 15) among the G2-S4 vs G2-CK DEGs (Appendix VI - Table S4), suggesting they might have a crucial role in the response to extreme salt conditions. Among these clusters, 9 (six up regulated and three downregulated) belong to the AP2-EREBP family (Chen et al., 2016). They have been implicated in various hormones-related signal transduction pathway including abscisic acid (ABA), ethylene and jasmonates (JAs) (Chen et al., 2016), which seem to be strongly involved in *A. donax* extreme salt stress response.

In our study, among the downregulated genes belonging to G2-S3 vs G2-CK DEGs , a homolog of *Setaria italica* protein TIFY 10B-like (LOC101761171) known to be a repressor of jasmonate (JA) responses, has been found (Table 5). As detailed below, an important attribute of JA is its ability to act both as a potent inhibitor of vegetative growth and as a positive regulator of reproductive and defensive processes (Pauwels et al., 2008). These antagonistic JA activities suggest that, in *A. donax* G2 ecotype subjected to severe salt stress, the dilemma of plant "to grow or defend itself" seems to be resolved trying to growth in an unfavorable environment. A homolog of *Setaria italica* trihelix transcription factor GTL1 (LOC101762434) that acts as negative regulator of water use efficiency via the promotion of stomatal density and distribution (Yoo et al., 2010; Weng et al., 2012) has been found up-regulated in G2-S3 vs G2-CK DEGs (Table 5). It has been reported that GTL1 is expressed when *Arabidopsis* plants have sufficient available water but is downregulated by water deficit. *Arabidopsis* thaliana GTL1 loss-of-function mutations result in increased water

deficit tolerance and higher integrated water use efficiency by reducing daytime transpiration without a demonstrable reduction in biomass accumulation. Moreover, GTL1 does not regulate ABA responsiveness, and the lower transpiration rates of *gtl1* defective plants are not caused by differences in stomatal aperture or ABA-induced stomatal closure (Yoo et al., 2010). The observed up-regulation of GTL1 under S3 severe salt stress of G2 reveals the susceptibility of this *A. donax* clone plants to salt-induced water deficit and that it might be a target for gene knockout in order to genetically improve the *A. donax* performance in salty soil. Finally, homologs of *Setaria italica* bZIP ABSCISIC ACID-INSENSITIVE 5-like protein 7 functioning as transcriptional activator in the ABA-inducible expression of rd29B have been also found among the up-regulated clusters. Although their role is still unknown, rd29B proteins has potential to confer abiotic stress resistance in crop species grown in arid and semi-arid regions (Msanne et al., 2011).

The synthesis, sequestration, transportation, and turnover of hormones generate a net of signals that correlates plant growth in dependence on internal and external cues. Among these hormones, abscisic acid regulates important abiotic stress responses, in particular water balance and osmotic stress tolerance under drought and salt stress (Kuromori et al., 2018). ABA levels depend on the equilibrium between synthesis and degradation pathways. Several ABA biosynthetic genes have been isolated from different sources including zeathanxin epoxidase (ABA1), 9-cis-epoxycarotenoid dioxygenase (NCED), ABA aldehyde oxidase (AOX) and ABA3/LOS5 (Xiong et al., 2001). The hydroxylation at the 8'-position of ABA is known as the key step of ABA catabolism, and this reaction is catalyzed by ABA 8'-hydroxylase, a cytochrome P450 (Saito et al., 2004).

ABA signals are perceived by different cellular receptors operating in distinct cellular compartments (Figure 23a). The PYR/PYL/RCARs receptors bind ABA and inhibit type 2C protein phosphatases (PP2C) (Golldack et al., 2014). The PP2C inactivation leads to the accumulation of the active form of SNF1-RELATED PROTEIN KINASE (SnRK2) which in turn positively regulates ABA-responsive transcription factor as well the downstream ABA-responsive metabolic pathways. In this context, the analysis of G2-S3 vs G2-CK means to propose that plant responds to prolonged severe stress by lowering ABA levels (Table 5). However, ABA signal is probably persisting since ABA nucleoplasmatic receptors are up-regulated as well as the PP2C and SnRK2 which, as detailed before, active many downstream ABA-responsive processes (Golldack et al., 2014) (Figure 23a). Recently, the increase of leaf tissue ABA concentrations at two hours after plants were exposed to 50 mM of the ions was observed in maize indicating that ABA synthesis and accumulation are part of the early response to salt (Geilfus et al., 2018). Interestingly, the putative ortholog of AT1G78390, nine-cis-epoxycarotenoid dioxygenase 9 (NCED), is strongly upregulated in both *Arundo* shoots and roots during the early responses to water stress (Fu et al., 2016), this finding being in line with our suggestion that ABA might be not strictly involved in the response to a prolonged salt stress treatment. Brassinosteroids are growth-promoting plant hormones that act to enhance cell expansion and increase tolerance to stresses, including salinity, by mediating the synthesis of enzymatic or non-enzymatic antioxidant systems, proline, or lectins (Bajguz and Hayat, 2009). The specific induction in G2 clone under extreme salt stress (S4) but not in severe (S3) conditions of cytochrome P450 85A1 (LOC101770408) encoding brassinosteroid-6-oxidase 2,

involved in active brassinosteroid biosynthesis might suggest a key role of these hormones in the case extreme environmental conditions are reached. Ethylene is biosynthesized by the plant in response to life-cycle events or environmental cues including among other diseases, mechanical stress, drought or flood. The phenotypes that can be observed with respect to ethylene signaling typically relate to the inhibition of plant growth and seasonal changes in a plant's life cycle. Ethylene is efficiently biosynthesized from 1-aminocyclopropane-1-carboxylic acid (ACC) (Zhou et al., 2002). The mechanism of ethylene action, from perception to function, has been referred to as the "cleave and shuttle model" (Li et al., 2015) (Figure 23b). The most studied of the receptors is ethylene response 1 (ETR1) and downstream of ETR1 in *A. thaliana* is the kinase constitutive triple response 1 protein (CTR1) (Light et al., 2016). In absence of ethylene, this protein directly interacts with the ethylene receptors and it is required to be localized to the endoplasmic reticulum and be kinase active to be signaling active. CTR1 phosphorylates the putative metal transporter ethylene insensitive 2 (EIN2) that triggers its degradation by the Ub/26S proteasome (Light et al., 2016). In the presence of ethylene, CTR1 is inactivated by the interaction with ETR1 and the EIN2 dephosphorylated form is proteolytically cleaved to generate a C-terminal fragment called CEND EIN2. The CEND fragment localizes to the nucleus and initiates transcriptional regulation involving ethylene insensitive 3 (EIN3) and EIN3 like proteins (EIL1) (Figure 23b). Interestingly, transcripts encoding ACC oxidase have been found up-regulated both under severe and extreme salt stress in G2 ecotype whereas homolog of *Arabidopsis thaliana* ETR is downregulated and clusters related to CTR1 and EIN3 are exclusively up-regulated in G2-S4 vs G2-CK samples (Table 6). In our

opinion, this condition might describe a situation in which a low perception of emitted ethylene is attempted under extreme salt stress (down regulation of ETR1 expression), concomitantly to an increased expression of CTR1, of EIN2 and EIN3 with the aim to minimize the negative effect of ethylene upon plant growth.

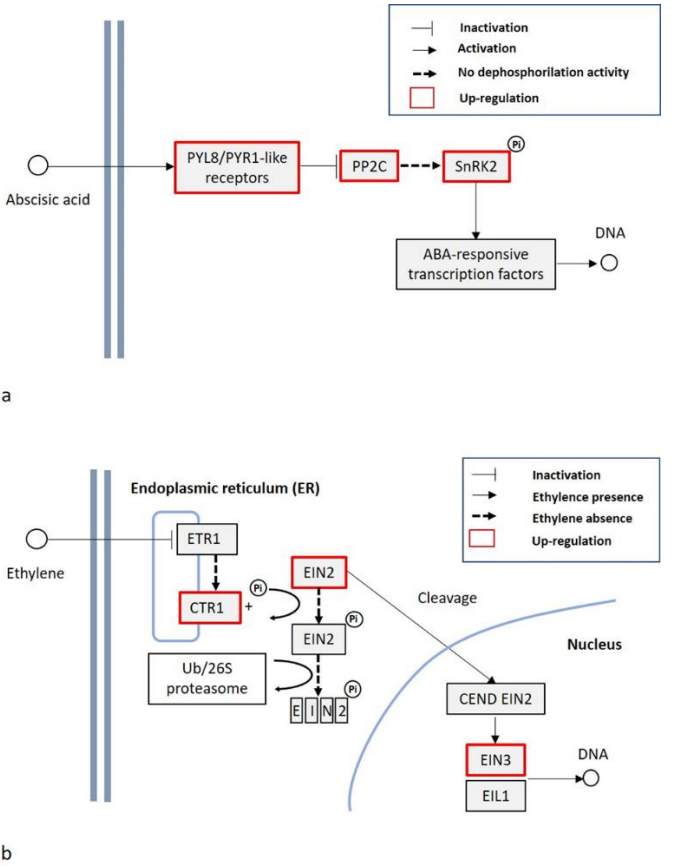

Figure 23. Abscisic acid and ethylene signal pathways. a abscisic acid receptor (PYL8), abscisic acid receptor (PYR1-like), serine/threonine-protein kinase (SnRK); protein phosphatase 2C (PP2C). The

PYR/PYL/RCARs receptors bind ABA and inhibit type 2C protein phosphatases (PP2C). The active form of SnRK2 accumulates and positively regulates ABA-responsive metabolic pathways. **b** ethylene response 1 (ETR1), kinase constitutive triple response 1 protein (CTR1), putative metal transporter ethylene insensitive 2 (EIN2), EIN2 C-terminal fragment (CEND EIN2), ethylene insensitive 3 (EIN3) and EIN3 like proteins (EIL1). In absence of ethylene, CTR1 directly interacts with ETR1 and phosphorylates EIN2 that is in turn degraded. In the presence of ethylene, CTR1 is inactivated and the EIN2 dephosphorylated form is proteolytically cleaved to generate the CEND EIN2, initiating transcriptional regulation involving ethylene insensitive 3 (EIN3) and EIN3 like proteins (EIL1). See the text for details.

Salt also alters the expression of auxin responsive genes and auxin/IAA pathways in different plants conferring higher tolerance to NaCl treatment (Bianco and Defez, 2009). Auxin is assumed to activate the proton pump of the plasma membrane pumping protons from the cytosol into the apoplast, resulting in wall loosening and an increase in wall extensibility (Bianco and Defez 2009). In this respect, a homolog of *Zea mays* indole-3-acetaldehyde oxidase (AAO), involved in the biosynthesis of auxin, is upregulated in S4 samples andalso in the G2-S4 vs G2-S3 comparison suggesting that IAA is synthesized in S4 extreme conditions (Table 6). Moreover, exclusively under extreme stress condition (Table 6) a homolog of auxin responsive GH3 gene family is also up-regulated. All the results, considering the role of GH3 genes in regulating levels of biologically active auxin through amino acid conjugation, thereby targeting them for degradation (Khan and Stone, 2007), indicate that auxin level might be finely tuned in G2 ecotype under S4 extreme stress condition. Globally, the high number of AUX/IAA transcription factors differently regulated in extreme salt environment accounts for a key role of auxins during long-term salt treatment (Figure 20). Finally, jasmonic

acid-amido synthetase JAR1 is exclusively down regulated under extreme salt stress in G2 ecotype (Table 6), indicating that jasmonic acid signaling is likely impaired. The relationship between the salt stress response and the JA pathway is not well understood at molecular and cellular levels. However, large-scale transcriptomic studies have shown JA signaling pathway is activated by salt stress leading to root growth inhibition in Arabidopsis (Valenzuela et al., 2016). The observed down regulation of JAR1 in G2 (Table 6) indicates that the pathway involved in the inhibition of root elongation might be not activated in *A. donax*, likely to address the plant demand to explore soil in the attempt of avoiding stress.

A consequence of high salt in the soil is the generation of a low water potential zone around the roots area making extremely difficult for the plants to obtain water and nutrients. Stomatal closure occurs in order to low water loss by transpiration, but it is at the same time responsible of sharp decrease in CO_2 availability for Calvin cycle and a depletion of oxidized $NADP^+$. The overproduced electrons are transferred to O2 to generate O2●- and a series of dangerous oxygen reactive species (ROSs) causing unrestricted oxidation of various cellular components such as membrane lipids, proteins, and nucleic acid (Scandalios, 2005). Therefore, salinity tolerance is positively correlated with the induction of ROS scavenging enzymes such as superoxide dismutase (SOD), catalase (CAT), glutathione peroxidase (GPX), ascorbate peroxidase (APX), monodehydroascorbate reductase (MDHAR), dehydroascorbate reductase (DHAR) and glutathione transferases (GSTs) (Gupta and Huang, 2014). Moreover, under stress conditions, the activation of malate-oxalacetate (OAA) shuttle permits the transfer of reducing equivalents among compartments. In particular, the

plastid NADP-malate dehydrogenase reduces oxalacetate to malate, thus regenerating the $NADP^+$. Malate is then translocated into the cytoplasm where is converted back in oxaloacetate, generating NADH by the cytosolic malate dehydrogenase. This called malate-valve appears to play a primary role under salinity constituting an important mechanism in salt acclimation (Gawronska et al., 2013). Drainage of electron flow towards the AOX oxidase pathway increases under salt stress (Zhang et al., 2016) and prevents over-reduction of ubiquinone thus lowering excessive ROS generations. The malate-valve seems to be activated under S3 severe salt stress conditions (up-regulation of plastid NADP-malic dehydrogenase encoding gene), this result being consistent with a putative electron drainage from the over-reduced photosynthetic chain to other cellular compartments, in particular towards the mitochondria as homolog of the mitochondrial malate dehydrogenase (MHD) are also induced by salinity (Table 5). Under extreme salt stress, the unequivocal up regulation of the NADP-malic dehydrogenase and AOX oxidase is probably aimed to move the excess of reducing power from plastids to the cytosol and to avoid over-reduction of the mitochondrial respiratory chain. However, most of the other considered clusters related with the cellular antioxidant machinery have been found between both the down and up-regulated clusters. In our opinion, this is because under extreme stress conditions, which is certainly an emergency condition, a discerning regulation is needed both among and inside the cell compartments. To support our hypothesis, the SOD plastid pool comprising Cu/Zn SOD and Fe/SOD results differently regulated, with Cu/Zn SOD up regulated and Fe/SOD down regulated (Tables 6 and 7). As multifunctional amino acid, proline seems to have diverse roles under stress conditions,

such as stabilization of proteins, membranes, and subcellular structures, and protecting cellular functions by scavenging ROSs. Biosynthesis of proline occurs in the chloroplast or cytosol via glutamate pathway in which 1-delta-pyrroline-5-carboxylate synthase (P5CS) catalyzes the key regulatory and rate limiting reaction (Kaur and Asthir, 2015). During proline synthesis, 2 mol of NADPH per mole are consumed thus draining electrons from chloroplasts and contributing to the stabilization of redox balance and maintenance of cellular homeostasis when electron transport chain is saturated because of adverse conditions. Proline catabolism occurs predominantly in the mitochondria involving proline dehydrogenase (PDH) or proline oxidase (POX) and 1-delta-pyrroline-5-carboxylate dehydrogenase (P5CSDH). The PDH and P5CSDH use NAD and FAD as electron acceptor, respectively, that deliver electrons to the respiratory chain to gain energy and resume growth after stress (Kaur and Asthir, 2015). The up-regulation of P5CS found in all the G2 ecotype comparisons suggests that that proline biosynthesis represents a pivotal mechanism to overcome the hypersaline conditions and adjust the osmotic status in *A. donax*. However, since PDH and P5CSDH resulted up regulated in extreme salt stress conditions (Tables 6 and 7), we propose that S4 salt dose triggers a specific response that is not related to the mere proline synthesis to cope with osmotic stress. Regarding this aspect, it has been shown that proline catabolism is enhanced during stress recovery attempts. During this phase, it might function as signaling molecule proposed to regulate the expression of stress recovery genes (Szabados and Savoure, 2010). Therefore, under extreme salt stress, proline levels might be accurately regulated in order to accommodate the whole cell demand in terms of both osmotic potential and redox homeostasis adjustments. Polyamines

play a crucial role in abiotic stress tolerance including salinity and increases in the level of polyamines are correlated with stress tolerance in plants (Yang et al., 2007; Zapata et al., 2008). The comparison of all data sets indicates that polyamines biosynthesis is induced during long-term salt stress in *A.donax* having most likely a role in salt tolerance mechanism, especially under extreme stress condition (Tables 5-8). Photosynthesis is the primary processes to be affected by salinity (Munns and Tester, 2008; Wang and Nii, 2000). Stomata close in response to leaf turgor declines, therefore supply of CO_2 to Rubisco (EC 4.1.1.39) is impaired thus inducing sharp alterations of photosynthetic metabolism. In *A. donax* under severe salt stress condition, CO_2 assimilation via the C3 Calvin cycle seems to be impaired in favor of oxygen fixation through the photorespiration pathway. Moreover, the findings indicate that extreme salt treatment induces a down regulation of all C3 Calvin cycle enzymes and a concomitant switch on of C4 photosynthesis. The induction of PEPC activity and its expression following salt stress is documented in the facultative CAM plant *Mesembryanthemum crystallinum* and it is involved in the change from C3 to CAM photosynthesis (Cushman and Bohnert, 1992). In *A. donax* leaves, the activation of C4 pathway associated to a down-regulation of Rubisco biosynthesis, assembly and activation could be construed as an ultimate rescue attempt to overcome the long-term extreme conditions.

As concern metabolic pathways related to bioenergy production, it has been shown that lignin content in cell wall is inversely related to yield and conversion efficiency of polysaccharides into ethanol (Xie et al., 2018). Unfortunately, in the *A. donax* transcriptome subjected to both severe and extreme salt stress, several clusters involved

in lignin biosynthesis are induced and this unwanted consequence of soil salinization might negatively affect biomass digestibility. This unfavorable circumstance could be compensated by the fact that, after biomass saccharification, lignin residue can be used to produce biodegradable plastic and chemicals (Ragauskas, 2016). Furthermore, the induction of transcripts homologous to sucrose synthase (*Setaria italica* sucrose synthase) in the G2-S3 vs G2-CK comparison accounts for a probable increase in cellulose content that it has been shown to be without negative effects on growth (Coleman et al., 2009). Recently, the lipid fraction has been proposed as pivotal component of green biomass since it stores twice as much energy than cellulose per unit of weight (Ohlrogge, 2009). The up-regulation of key enzymes, such as triacylglycerol lipase and diacylglycerol kinase under severe salt stress supports the hypothesis that *A. donax* G2 response is trying to cope stress by inducing gene expression of pathways involved in biomass yield.

Focusing on G34 ecotype, of which only transcriptomic data under severe salt treatment are available, a fewer number of DEGs have been detected compared with the severe treatment in G2. The SOS pathway is partially activated also in this ecotype (up-regulation of CIPK1-SOS2-like protein) and the vacuolar sequestration of Na^+ excess might be impaired (down regulation of NHX) (Table 8). Interestingly, by comparing G34-S3 vs G2-S3, resulted that CIPK1-SOS2-like is deeply induced in G34-S3, indicating that in the G34 ecotype this SOS component takes on a major role in coping the salt stress condition and allow responding promptly to stress at lower salt concentration (Table 9).

As regards the regulation of transcription, the most differentially regulated TF subfamilies are bHLH, WRKY

and AUX/IAA, indicating that a different regulation network is induced (Figure 20). Furthermore, salt specific transcription factors were not differentially expressed in stressed plants, probably due to a less specific salt stress response. Moreover, the absence of TIFY 10B-like among the differentially regulated transcription factors in G34 ecotype might justify the reduced growth of plants, since no repression of JA signaling occured (Table 8). Finally, homologs of *Setaria italica* bZIP ABSCISIC ACID-INSENSITIVE 5-like protein 7 is the only TF differentially regulated in the G34-S3 vs G2-S3 comparison which account for a main role of this TF in G34 ecotype (Table 9).

The expression of GTL1 transcription factor is neither up-regulated nor down regulated in G34-S3 plants indicating a lower susceptibility to salt stress (Table 8). As regards the ethylene biosynthesis and signaling, ACC oxidase and CTR1 are up regulated in G34 ecotype subjected to severe salt stress (Table 8). Based on this gene expression pattern, it seems that ethylene is produced but the plants try to limit the ethylene sensivity by phosphorilating EIN2 and channeling it towards proteolytic degradation (Figure 23). This mechanism is confirmed when comparing G34-S3 vs G2-S3 (Table 9). Moreover, in this last cited comparison, EIN3 is down-regulated (Table 9), and this repression account for the minimization of ethylene sensivity (Figure 23). As previously described, the same behavior was found in G2 ecotype subjected to extreme salt treatment indicating that in G34 the negative effect of ethylene on plant growth might be blocked in presence of a lower salt concentration (S3 instead of S4), resulting in a lower susceptibility to salt stress. Moreover, the down regulation of abscisic acid 8'-hydrolase is reported in the G34-S3 vs G2-S3 comparison which suggests that

abscisic acid signal transduction might be more active in G34 under S3 condition than in G2-S3 (Table 9).
Considering the induction of ROS scavenging enzymes, G34 clone shows the up-regulation of GST and NADP-dependent malic enzyme, and a down-regulation of superoxide dismutase $[Fe]^2$ (Table 8), this last result being achieved also by the G2 clone but under extreme salt condition.
The importance of proline in the salt stress response is confirmed by the up-regulation of P5CS also in G34 ecotype, thus confirming that proline biosynthesis represents a pivotal mechanism to overcome the hypersaline conditions and adjust the osmotic status in *A. donax* (Table 8). On the other hand, the down regulation observed in the G34-S3 vs G2-S3 could account for a lower induction of this gene in the G34-S3 samples than that observable in G2 under S3 conditions (Table 9).
As regards the genes involved in photosynthesis, PEPC kinase was found down-regulated also in G34 clone under severe S3 condition, but no PEPC and PPDK1 homologues were found activated (Table 8), thus suggesting that the C3 to C4 switching might be achieved exclusively under S4 extreme condition.
Finally, genes linked with lignin and cellulose biosynthesis were not found differentially regulated in G34 clone under severe salt stress compared with untreated plants (Table 8). Moreover, clusters related to biomass digestibility and biofuel production, such as cinnamyl alchohol dehydrogenase and diacylglycerol kinase 1, were strongly down regulated in the G34-S3 vs G2-S3 comparison thus suggesting a minor role of these pathways in the G34 under S3 salt stress.
The comparative analysis between the G2 and G34 transcriptomes suggests a minor susceptibility of G34 to the

severe salt stress conditions as indicated by a lower biochemical rearrangement.

The further analysis performed to identify genes which are regulated uniquely under salt stress conditions highlighted that a very small subset of clusters are up or down regulated by salt and not by other abiotic stress thus suggesting that the response pathways to different environmental cues often cross-talk and overlap each other in plants. As expected, the main salt-specific pathways are related to the SOS response (Liu and Zhu, 1998; MartìnezAtienza et al., 2007) and to the activation of ETHE1 (Krüßel et al., 2014) (Appendix VII – Table S5-S7). In *Arabidopsis* leaves, ETHE1 sulfur dioxygenase has a key function in the degradation of sulfur-containing amino acids and strongly affects the oxidation of branched-chain aminoacids as alternative respiratory substrates in situations of carbohydrate starvation (Krüßel et al., 2014). Therefore, ETHE1 could be relevant for stress tolerance against soil salinity in giant reed.

As already explained, searching and developing of genetic markers is of fundamental importance especially in plants characterized by asexual vegetative reproduction and low genotypic diversity among clonal populations such as *A. donax*. The aim is to obtain genetic tools commonly used for assessing genetic diversity, the development of genetic maps, marker-assisted selection (MAS) breeding, comparative genomics and allowing clones identification and traceability. In particular, genic SSRs can directly influence phenotype and also be in close proximity to genetic variation in coding or regulatory regions corresponding to traits of interest and can be efficient functional markers (Li et al., 2004). Our analysis resulted in a consistent number of repeated motifs (45,529) distributed among clones and untranslated and coding regions. The most abundant motifs were mono- di and

tri-nucleotides repetitions, in line with the previous marker catalogue (Evangelistella et al., 2017). Five SSRs were successfully validated showing a perfect congruence with the RNA-seq experiment and resulting highly conserved in both the clones (Appendix IX – Figure S5a-e), probably due to the fact that natural genetic variation in *A. donax* was reported to be low for the Mediterranean basin (Mariani et al., 2010). Anyway, a higher number of SSRs need to be screened in a larger genetic pool, in order to find clone-specific polymorphic regions or markers associated with agronomic traits.

Changes in DNA methylation are associated with a wide range of molecular mechanisms such as gene expression, resulting in an active regulation of important biological processes such as stress response (Seymour et al., 2008). Furthermore, abiotic stress responses influence epigenome architecture (Dowen et al., 2012; King, 2015; Schnable and Springer, 2013). For these reasons a methylation analysis based on a MSAP approach, is important in order to clarify the role of this cytosine methylation in the regulation of gene expression and in the plant response and adaptation to salt stress.

Kumar et al. (2017) analyzed the methylation status in the coding region of HKT2 in two wheat (*Triticum aestivum* L.) genotypes (Kharchia-65, salt tolerant and HD-2329, salt sensitive) subjected to salt stress. They reported an increase in methylation level in the second quarter of the coding region of HKT2 in both the genotypes, whereas in the first quarter of the gene the hypermethylation was observed only in the salt sensitive genotype. No differences in methylation where detected in salt tolerant genotype. HKT 2 was also reported to be up-regulated in HD-2329 and down-regulated in Kharchia-65. They concluded that the expression of this gene

was not regulated through the modulation of 5-mC; however, it might be controlled through other molecular or epigenetic mechanisms. Anyway, because of the different methylation status in salt sensitive and salt tolerant genotypes, they suppose an epigenetic mechanism behind the stress adaptation.

The three genes subjected to this analysis (HKT2, HKT6 and myb-related protein 306-like) showed different changes in the methylation patterns of their coding region in response to the stress application: HKT2 (down-regulated in severe salt stress conditions in both the clones) resulted hypomethylated when salt stress was applied in both the clones, suggesting an involvement of cytosine methylation in gene regulation of expression. Differently, HKT6 (also down-regulated in stress conditions in both the clones) is not differentially methylated in stressed G2 and G34 compared with the controls (Figure 23), whereas myb-related protein 306-like (down-regulated in both the stressed clones) showed no differences in methylation percentage in G2 and an hypomethylation in G34-S3 compared with the control (Figure 22). The differences found between the methylation status of HKT2 and HKT6 in *A. donax* and the methylation status of the same genes in *Triticum aestivum* by Kumar and collaborators, suggests that epigenetic and in particular cytosine methylation interferes in different ways with regulation of gene expression, depending also on the species. As regards *A. donax,* differences were observed among the two clones, resulting in a probable involvement of cytosine methylation in HKT2 gene expression in both the clones. With respect to the situation reported in wheat, in *A. donax* both gene expression and methylation decrease, suggesting a different epigenetic mechanism in the plant stress adaptation. A slight difference is observed in the cytosine methylation dynamic

between the two clones, probably due to the different stress response highlighted by the transcriptomic analysis.

8. Conclusions

The possibility to assign marginal land to bioenergy crop cultivation for sustainable energy production represents the main strategy to overcome the forthcoming conflict between land demand for feeding the world population and the request of new energy sources to sustain it. Salt affected soils are a widespread agricultural problem limiting crop production due to ionic, osmotic and oxidative stresses with negative impact on plant growth. In this work, the bioenergy crop *A. donax*, known to be able to growth in unfavorable environments, was subjected to long-term salt stress at doses being much higher than that used to define a soil area as "salinized". To cultivate bioenergy crops in such soils might represent the unique possibility of their utilization, releasing suitable soil for crop cultivation. To fill the lack of information about the molecular mechanism involved in *A.donax* response to salt stress, we *de novo* sequenced, assembled and analyzed the leaf transcriptome of two clones of *A. donax*, namely G2 and G34. Unfortunately, due to a fire occurred in the experimental field, we missed the informations about the extreme salt treatment of G34.

The response to salt and other environmental constrains such as drought shares similar attributes. However, we found that most of the *A. donax* annotated DEGs are homologs of genes belonging also to other species (*Setaria italica*, *Zea mays* and *Oryza sativa*) thus suggesting that long term salt stress regulates a specific set of genes providing a general overview of the prolonged salt stress transcriptional responses in *A. donax* (Tables 5-9).

As regards G2 clone, the picture that emerges from the identification of functional genes related to salt stress is consistent with a dose-dependent response to salt. The number of DEGs under extreme salt stress is much higher than that observed in severe salt stress suggesting that a deep re-programming of the gene expression must occur in S4 samples, which, during the experiment, certainly grew in an "emergency" state. For example, as concerns the salt sensory mechanism, the data of this thesis suggests that the SOS pathway is only partially activated under severe salt stress, wherease under extreme salt stress the plant activates also the mechanism of ionic vacuolar sequestration by the over-expression of the vacuolar ionic channels. Also the hormone regulation changes depending on the level of salt treatment: the response to S3 severe salt stress seems not to be dependent by ABA levels as gene involved in its biosynthesis are not differently regulated, whereas, once *A. donax* plants were subjected to S4 extreme salt stress a clear down regulation of ABA biosynthetic genes is registered suggesting that ABA synthesis might have a key role during the onset of stressful conditions as demonstrated in other species (Geilfus et al., 2018) and in the case of water stress (Fu et al., 2016) but not in the case of long term stress. Another distinct trait of the *A. donax* response to S4 extreme salt stress is the induction of clusters involved in brassinosteroid and IAA/AUX biosynthesis which probably have a key role in those more unfavorable conditions. Similarly, the down-regulation of gene involved in jasmonic acid biosynthesis suggests that JA signaling, leading to root growth inhibition, is repressed likely in the attempt to let the roots explore the surrounding soil more efficiently. The analysis of clusters related to ethylene biosynthesis and signaling indicates that, exclusively under S4 extreme salt

stress, the gene transcription is modulated towards the minimization of ethylene negative effects upon plant growth. The *A. donax* leaves subjected to S3 severe salt stress responds to salt-induced oxidative stress by the induction of genes involved in ROS scavenging (APX) and in redistributing the reducing power excess among cell compartments (malate valve). Along with the clusters implicated in the malate valve, under S4 extreme salt stress, also gene encoding the alternative oxidase (AOX) have been found up regulated, highlighting once more that the induction of some pathways occurs in the case of more stringent environmental conditions. A clear involvement of proline and polyamines in coping the salt-induced osmotic stress can be suggested whereas sugars seem not to be involved as osmolytes protecting cell homeostasis. Certainly, the photosynthesis and photorespiration processes are strongly affected since under S3 severe salt treatment, genes involved in Rubisco assembly are down-regulated, and the fact that *A. donax* leaf are impeded to operate CO_2 fixation via C3 Calvin cycle is also supported by the up-regulation of genes involved in photorespiration (glycolate oxidase). Conversely, in S4 extreme salt treated samples, a dramatic change from C3 Calvin cycle to C4 photosynthesis is likely to occur as all gene regulation is addressed to repress Rubisco synthesis and assembly, and to activate the primary CO_2 fixation to PEP in mesophyll cells (C4 pathway), this probably being the main finding of our work. Finally, the up-regulation of key enzymes of lypids biosynthesis, such as triacylglycerol lipase and diacylglycerol kinase under severe salt stress supports the hypothesis that *A. donax* G2 response is trying to cope stress by inducing gene expression of pathways involved in biomass yield.

Considered the distinct response to salt dose, either genes involved in S3 severe or in S4 extreme salt response could constitute useful markers of the physiological status of *A. donax* in salinized soil. Moreover, many of the unigenes identified in the present study have the potential to be used for the development of novel *A. donax* varieties with improved productivity and stress tolerance, in particular the knock out of the GTL1 gene acting as negative regulator of water use efficiency has been proposed as good target for genome editing experiments.

The G34 clone shows a different transcriptomic response to the salt stress application compared with G2. The severe salt treatment resulted upon G34 clone in a lower number of DEGs if compared with the same treatment in G2, suggesting that a weaker re-programming of the gene expression is needed. In our opinion, based on analysis of gene expression, it seems that G34 clone limits salt stress perception, probably due to the strong induction of the SOS pathway component, allowing to respond promptly to stress at lower salt concentration. Moreover, in severe salt stress G34 modulates the transcription of genes related to the ethylene signaling towards the minimization of ethylene negative effects upon plant growth, a situation that in G2 clone is reached exclusively under S4 extreme salt stress. The expression of GTL1 transcription factor is neither up-regulated nor down regulated in G34-S3 plants indicating a lower susceptibility to salt stress. The importance of proline in the salt stress response is confirmed by the up-regulation of P5CS also in G34 clone, thus confirming that proline biosynthesis represents a pivotal mechanism to overcome the hypersaline conditions and adjust the osmotic status in *A. donax.* As regards the genes involved in photosynthesis, G34 subjected to severe stress condition seems to suffer a reduction of

photosynthesis but not a switching from C3 to C4 cycle, thus indicating that this mechanism might be achieved exclusively under S4 extreme condition.

Thus, the comparative analysis of the transcriptomic response of G2 and G34 to salt stress highlights the different behaviour of these clones under the same stress level. Interestingly, a different transcriptomic pattern of the two clones resulted also when comparing them in control conditions, as a consistent number DEGs was found despite the low genetic diversity of *A. donax*. This finding could explain the different response of G2 and G34 clones to salt stress.

The SSR analysis resulted in line with the previous marker catalogue (Evangelistella et al., 2017) in terms of number of repeated motifs and distribution among untranslated and coding regions. Furthermore, five SSRs were successfully validated showing a perfect congruence with the experiment and resulting highly conserved in both the clones, probably due to the low natural genetic variation in *A. donax*. Thus, the SSR catalogue of this experiment consist in a precious source for developing genetic markers for genetic diversity, development of genetic maps, marker-assisted selection (MAS) breeding, comparative genomics and allowing clones identification and traceability.

Finally, the epigenetic analysis of genes involved in stress response, resulted in a different involvement of cytosine methylation in the regulation of gene expression. Two genes resulted down-regulated in stressed plants showed a demethylation in G2, not in G34. On the other hand, a third gene, also down-regulated by the salt stress, did not show any changes in the methylation status in both the clones. Thus, the epigenome is dynamic and clone-dependent.

Appendices

Appendix I

Figure S1. Effect of salt stress upon G2, G18, G20 and G34 ecotype morpho-biometric and physiological parameters. **a** Leaf number per pot. **b** Stem number per pot. **c** Main stem height. **d** SPAD. **e** Net photosynthesis. **f** Dry biomass.

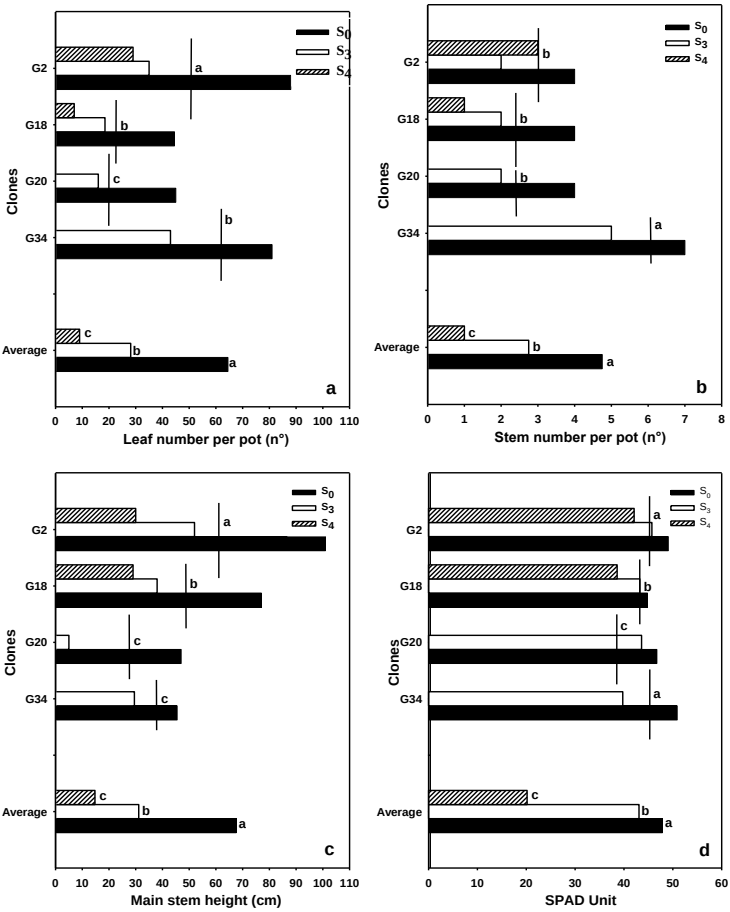

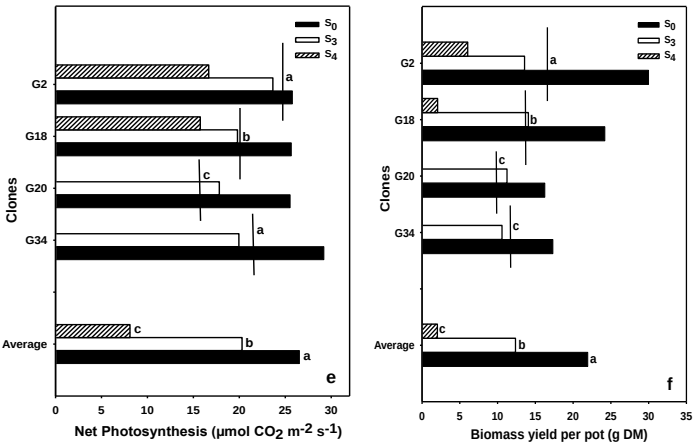
S0
S3
S4
G2
G18
G20
G34
Average
Clones
a
b
c
a
c
b
a
e
0
5
10
15
20
25
30
Net Photosynthesis (µmol CO2 m-2 s-1)
S0
S3
S4
G2
G18
G20
G34
Average
Clones
a
b
c
c
c
b
a
f
0
5
10
15
20
25
30
35
Biomass yield per pot (g DM)

Appendix II

Figure S2. Length distribution of transcripts and Unigenes

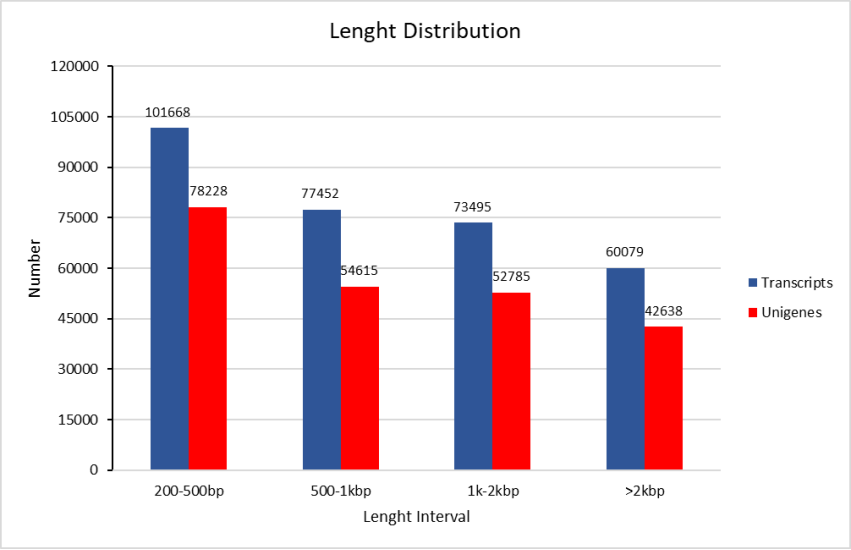

Appendix III

Table S1. Validation of *A. donax* DEGs by Real Time qRT-PCR.

Pattern	Cluster ID	Annotation	log2FC Illumina	log2FC rt-PCR
G2_S4vsG2_CK / Up	14027.257437	methyltransferase PMT26	47,70	2,75
G2_S3vsG2_CK / Up	14027.6881	anthocyanidin 3-O-glucosyltransferase	26,35	2,93
G2_S4vsG2_CK / Up	14027.62961	senescence-associated protein DH	14,488	2,59
G2_S4vsG2_CK / Up	14027.99727	ACC oxidase	2,28	0,87
G2_S4vsG2_CK / Up	14027.51601	uncharacterized protein	65,81	6,82
G2_S4vsG2_CK / Down	14027.163842	proline dehydrogenase 2	-16,64	-0,23
G2_S4vsG2_S3 / Down	14027.231635	palmitoyltransferase	-13,73	-0,56
G2_S4vsG2_S3 / Down	14027.159114	Ribulose bisphosphate carboxylase	-27,5	-0,98
G2_S3vsG2_CK / Down	14027.226133	probable WRKY transcription factor 4	-54,44	-2
G2_S3vsG2_CK / Down	14027.24929	NAC domain-containing protein 77	-21,56	-0,47
All	14027.113435	26 S proteasome non-ATPase regulatory subunit 11		

Table S2. Sequences of primer used for Real Time qRT-PCR validation

Cluster ID	Primer F 5'→3'	Primer R 5'→3'
14027.257437	GCCTCGACAATGAGAAGGCT	GCTTGGTGTGAGGCACATTG
14027.6881	GTGAAGGGCGACCAGTACCT	CCGCGAATATCCTCTGCACG
14027.62961	CGATCACCACCAACTCGACG	GCAGCCGATGGAGTAGACGA
14027.99727	CAACGGCAGGTACAAGAGCG	TCCTCGAACACGAACCTGGG
14027.51601	CCTCTCAGATCCAAGCTCCTCA	TCGGAATCACCTTGTGCCG
14027.163842	GCGTGTTCGTCTCTTGTGTCC	AACTCGAGCACCTTCCTCTCG
14027.231635	AGGTTCGTTTCTGCACAGGC	GGGTCACTGGGAACGAACAC
14027.159114	CAGCAACGGTGGAAGGATCA	TTCTCACGGAAGACGAAGCC
14027.226133	CCAGTGTCAGTCTCCTCCTG	GTCGTCAGATAGCCCGTAGG
14027.24929	CATGCACGAGTATCGCCTCG	GAAGTTTGGCGTTTCGGCAG
14027.113435	CACACGACTAGCAGCTTTCAAG	TTCAAACGTCGGGAAGGTTG

Appendix IV

Figure S3. Clusters of orthologous groups (KOG) classification. All unigenes were aligned to KOG database to predict and classify possible functions. Out of 255809 unigenes, 49848 sequences were assigned to 25 KOG classifications. (A) RNA processing and modification; (B) chromatin structure and dynamics; (C) energy production and conversion; (D) cell cycle control, cell division, chromosome partitioning; (E) amino acid transport and metabolism; (F) nucleotide transport and metabolism; (G) carbohydrate transport and metabolism; (H) coenzyme transport and metabolism; (I) lipid transport and metabolism; (J) transition, ribosomal structure and biogenesis; (K) transcription; (L) replication, recombination and repair; (M) cell wall/membrane/envelope biogenesis; (N) cell motility; (O) posttranslational modification, protein turnover, chaperones; (P) inorganic ion transport and metabolism; (Q) secondary metabolites biosynthesis, transport and catabolism; (R) general function prediction only; (S) function unknown; (T) signal transduction mechanisms; (U) intracellular trafficking, secretion, and vesicular transport; (V) defense mechanisms; (W) extracellular structures; (X) unnamed protein; (Y) nuclear structure; (Z) cytoskeleton.

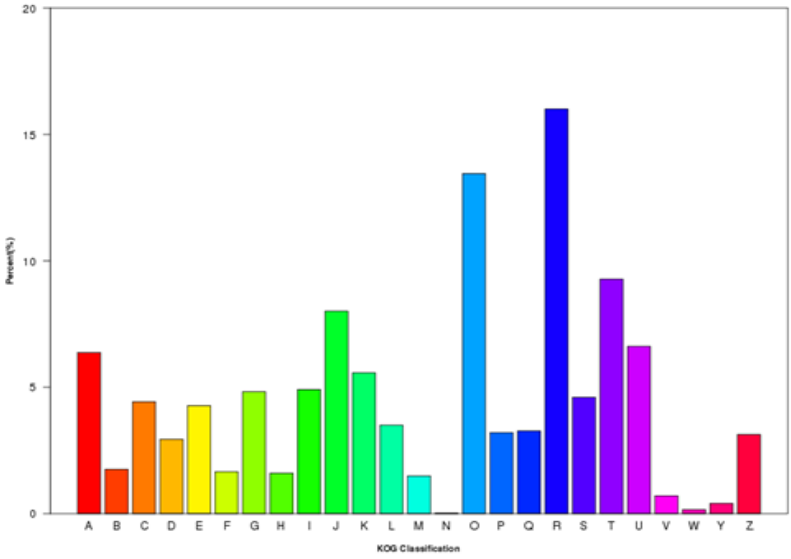
20
15
10
5
0
Percent(%)
A B C D E F G H I J K L M N O P Q R S T U V W Y Z
KOG Classification

Appendix V

Table S3. Distribution of KEGG pathways for DEGs in the three sample sets. Data are sorted by number of G2-S4 vs G2-CK DEGs mapping to KEGG pathways.

Enriched Pathway terms	G2-S3 vs G2-CK	G2-S4 vs G2-CK	G2-S4 vs G2-S3	G34-S3 vs G34-CK	G34-S3 vs G2-S3	Total
Carbon metabolism	55	548	273	25	7	908
Biosynthesis of amino acids	44	463	203	15	10	735
Carbon fixation in photosynthetic organisms	37	259	149	13	4	462
Starch and sucrose metabolism	41	249	102	20	9	421
Ribosome	7	252	148	8	3	418
Plant hormone signal transduction	52	252	89	7	16	416
Phenylpropanoid biosynthesis	61	208	103	5	6	383
Oxidative phosphorylation	20	257	85	9	-	371
Glycolysis / Gluconeogenesis	26	237	83	12	5	363
Glyoxylate and dicarboxylate metabolism	18	189	129	8	-	344
Pyruvate metabolism	30	204	101	9	-	344
Arginine and proline metabolism	31	186	99	7	3	325
Cysteine and methionine metabolism	15	182	86	11	2	296
Phenylalanine metabolism	41	161	77	4	1	284
Glycerophospholipid metabolism	22	154	78	9	7	270
Peroxisome	16	158	79	8	1	262

Protein processing in endoplasmic reticulum	19	178	46	13	3	259
Alanine, aspartate and glutamate metabolism	19	143	77	2	3	244
Citrate cycle (TCA cycle)	23	137	67	14	-	241
Purine metabolism	20	156	49	3	10	238
Glutathione metabolism	11	155	59	7	4	236
Glycine, serine and threonine metabolism	17	132	70	3	-	222
Cyanoamino acid metabolism	19	115	75	6	5	220
Amino sugar and nucleotide sugar metabolism	20	135	48	8	1	212
Plant-pathogen interaction	14	135	43	8	3	203
Lysosome	23	112	54	6	5	200
2-Oxocarboxylic acid metabolism	12	128	52	5	-	197
AMPK signaling pathway	20	119	54	1	1	195
Tyrosine metabolism	7	114	59	3	3	186
Methane metabolism	9	120	48	-	4	181
Pentose phosphate pathway	5	114	53	1	7	180
RNA degradation	10	105	30	7	-	171
Phagosome	21	107	33	7	-	168
Endocytosis	12	111	38	2	2	165
Fatty acid metabolism	7	105	49	2	2	165
RNA transport	9	109	40	2	4	164
Photosynthesis	-	113	93	3	1	160
Fructose and mannose metabolism	5	102	48	2	5	161
Ubiquinone and other terpenoid-quinone biosynthesis	9	97	43	7	1	157
Phenylalanine, tyrosine and tryptophan biosynthesis	9	98	44	3	1	155

Fatty acid degradation	3	88	49	-	1	141
Galactose metabolism	13	92	28	2	3	138
Spliceosome	11	79	22	1	2	115
alpha-Linolenic acid metabolism	3	63	43	4	2	115
Carotenoid biosynthesis	14	58	31	4	8	115
Drug metabolism - cytochrome P450	8	62	29	3	2	104
mRNA surveillance pathway	5	70	26	1	-	102
Aminoacyl-tRNA biosynthesis	3	78	14	5	2	102
Porphyrin and chlorophyll metabolism	2	61	22	3	-	88
Pantothenate and CoA biosynthesis	7	35	19	-	-	61

Appendix VI

Table S4. Transcription factors responsive to salt in *A. donax*, resulted by a comparative analysis with the available database of rice transcription factors.

***A. donax* ID**	**Rice ID**	**% identity**	**E value**	**Family**	**G2-S4 vs G2-CK**	**G2-S3 vs G2-CK**	**G2-S4 vs G2-S3**	**Regulation**	**Diff. Expr.**
14027.146299	Os09g20350	91.67	1,00E-38	AP2-EREBP	1	0	0	Up	Salinity
14027.156597	Os09g20350	81.82	5,00E-08	AP2-EREBP	1	0	0	Down	Salinity
14027.157270	Os09g20350	95.77	3,00E-25	AP2-EREBP	1	0	0	Up	Salinity
14027.171527	Os04g55560	92.73	2,00E-36	AP2-EREBP	1	0	0	Up	Salinity
14027.180316	Os04g55560	85.48	3,00E-33	AP2-EREBP	1	0	0	Up	Salinity
14027.186619	Os02g57790	85.71	4,00E-31	C2H2	1	0	0	Up	Salinity
14027.192028	Os07g39480	85.49	1,00E-131	WRKY	1	0	0	Up	Salinity
14027.248285	Os06g40330	88.71	1,00E-70	MYB	1	0	0	Up	Salinity
14027.250058	Os06g44750	91.49	7,00E-27	AP2-EREBP	1	0	0	Up	Salinity

A. donax ID	Rice ID	% identity	E value	Family	G2-S4 vs G2-CK	G2-S3 vs G2-CK	G2-S4 vs G2-S3	Regulation	Diff. Expr.
14027.250059	Os06g44750	91.49	4,00E-27	AP2-EREBP	1	0	1	Down	Salinity
14027.4111	Os07g22770	89.39	2,00E-35	AP2-EREBP	1	1	0	Down	Salinity
14027.61430	Os03g54170	94.37	1,00E-22	MADS	1	0	0	Down	Salinity
14027.64311	Os01g13030	84.55	6,00E-43	AUX-IAA	1	0	0	Down	Salinity
14027.84501	Os11g45950	89.06	1,00E-11	NAC	1	0	0	Down	Salinity
9227.0	Os06g44750	93.55	4,00E-31	AP2-EREBP	1	0	0	Up	Salinity

Appendix VII

Table S5. Salt stress related genes in G2-S3 vs G2-CK (GO:0009651 Response to salt stress).

Gene_ID	log2FoldChange	Swissprot Description
14027.266446	Inf*	CBL-interacting protein kinase 21 (*Oryza sativa* subsp. japonica)
14027.182899	39.581	CBL-interacting protein kinase 1 (*Oryza sativa* subsp. japonica)
14027.196826	35.123	CBL-interacting protein kinase 1 (*Oryza sativa* subsp. japonica)
14027.182901	33.766	CBL-interacting protein kinase 1 (*Oryza sativa* subsp. japonica)
14027.190185	25.043	CBL-interacting protein kinase 1 (*Oryza sativa* subsp. japonica)
14027.194848	0,93616	Ankyrin repeat-containing protein NPR4 (*Oryza sativa* subsp. Japonica)
14027.149173	0,78963	V-type proton ATPase catalytic subunit A (*Daucus carota*)
14027.230649	-22.658	Probable cation transporter HKT6 (*Oryza sativa* subsp. japonica)
14027.230650	-26.106	Probable cation transporter HKT6 (*Oryza sativa* subsp. japonica)

*it means that the read count value of CK samples is zero

Table S6. Salt stress related genes in G34-S3 vs G34-CK (GO:0009651 Response to salt stress).

Gene ID	log2FoldChange	Swissprot Description
14027.182899	Inf	CBL-interacting protein kinase 1 (*Oryza sativa* subsp. japonica)
14027.230649	-15,51	Probable cation transporter HKT6 (*Oryza sativa* subsp. japonica)

*it means that the read count value of CK samples is zero

Table S7. Salt stress related genes in G2-S4 vs G2-CK (GO:0009651 Response to salt stress).

Gene_ID	log2FoldChange	Swissprot Description
14027.231692	54.475	NAD-dependent malic enzyme 62 kDa isoform (*Solanum tuberosum*)
14027.231386	49.507	Persulfide dioxygenase ETHE1 homolog (*Arabidopsis thaliana*)
14027.196826	42.577	CBL-interacting protein kinase 1 (*Oryza sativa* subsp. Japonica)
14027.190185	34.055	CBL-interacting protein kinase 1 (*Oryza sativa* subsp. Japonica)
14027.130203	25.169	Persulfide dioxygenase ETHE1 homolog (*Arabidopsis thaliana*)
14027.209414	24.094	Calcium-dependent protein kinase 1 (*Oryza sativa* subsp. Japonica)
14027.189242	16.044	Persulfide dioxygenase ETHE1 homolog (*Arabidopsis thaliana*)
14027.90003	14.432	Ankyrin repeat-containing protein NPR4 (*Oryza sativa* subsp. Japonica)
14027.190184	13.951	CBL-interacting protein kinase 1 (*Oryza sativa* subsp. Japonica)
14027.149173	13.206	V-type proton ATPase catalytic subunit A (*Daucus carota*)
14027.146671	12.089	NAD-dependent malic enzyme 62 kDa isoform (*Solanum tuberosum*)
14027.198243	11.098	CBL-interacting protein kinase 24 (*Oryza sativa* subsp. Japonica)
14027.190190	3.837	CBL-interacting protein kinase 1 (Oryza sativa subsp. Japonica)
14027.211592	1,94	COBRA-like protein 1 (Oryza sativa subsp. Japonica)
14027.158801	0,93	V-type proton ATPase catalytic subunit A (*Daucus carota*)
14027.176822	0,92	CBL-interacting protein kinase 24 (*Oryza sativa* subsp. Japonica)
14027.129089	0,82	3-isopropylmalate dehydratase small subunit 3 (*Arabidopsis thaliana*)

14027.163583	0,81	--
14027.176826	0,77	CBL-interacting protein kinase 1 (*Oryza sativa* subsp. Japonica)
14027.169731	0,76	Gamma carbonic anhydrase 2 (*Arabidopsis thaliana*)
14027.181983	0,74	Mitochondrial-processing peptidase subunit alpha (*Solanum tuberosum*)
14027.180575	0,71	CBL-interacting protein kinase 24 (*Oryza sativa* subsp. Japonica)
14027.195126	0,68	3-isopropylmalate dehydratase small subunit 3 (*Arabidopsis thaliana*)
14027.110430	0,67	ATP synthase subunit d (*Arabidopsis thaliana*)
14027.135632	0,63	ATP synthase subunit d (*Arabidopsis thaliana*)
14027.189399	0,59	Mitochondrial-processing peptidase subunit alpha (*Solanum tuberosum*)
14027.219001	0,55	Nascent polypeptide-associated complex subunit alpha-like protein 1 (*Arabidopsis thaliana*)
14027.173498	0,53	Kynurenine formamidase (*Bacillus weihenstephanensis*) (strain KBAB4)
14027.139505	0,52	NADH dehydrogenase [ubiquinone] 1 alpha subcomplex subunit 9 (*Arabidopsis thaliana*)
14027.172033	-0,74	Interferon-related developmental regulator 2 (*Homo sapiens*)
14027.230649	-4.392	Probable cation transporter HKT6 (*Oryza sativa* subsp. Japonica)
14027.162962	-11.339	Interferon-related developmental regulator 2 (*Homo sapiens*)
14027.225205	-25.336	Interferon-related developmental regulator 1 (*Sus scrofa*)
14027.142581	-28.631	--
14027.230647	-43.229	Probable cation transporter HKT6 (*Oryza sativa* subsp. Japonica)

14027.180958	-45.185	CBL-interacting protein kinase 1 (*Oryza sativa* subsp. Japonica)
14027.230650	-55.502	Probable cation transporter HKT6 (*Oryza sativa* subsp. Japonica)

Appendix VIII

Table S8. Protein family and domain description

Cluster ID	Cluster description	Family Name - Descritpion	Domain Name- Descritpion
14027.182899	*Oryza sativa* subsp. japonica Group CBL-interacting protein kinase 1 (CIPK1-SOS2 like)	PKc_like superfamily - Protein kinase family	STKc_SnRK3 - Catalytic domain of the Serine/Threonine Kinases, Sucrose nonfermenting 1-related protein
14027.54233	*Setaria italica* probable cation transporter HKT9	2a38euk superfamily - Potassium uptake protein, Trk family	-
14027.181583	*Arabidopsis thaliana* Sodium/hydrogen exchanger 2 (NHX2)	b_cpa1 superfamily; PRK05326 - Sodium/hydrogen exchanger family; potassium/proton antiporter	-
14027.231386	*Arabidopsis thaliana* Persulfide dioxygenase ETHE1	Glyoxylase or a related metal-dependent hydrolase, beta-lactamase superfamily II	POD-like_MBL-fold - ETHE1 (PDO type I), persulfide dioxygenase A
14027.198243	*Oryza sativa* subsp. Japonica CBL-interacting protein kinase 24 (SOS2)	AMPKA_C_like_superfamily - C-terminal regulatory domain of 5'-AMP-activated protein kinase (AMPK) alpha subunit and similar domains family	CIPK_C - C-terminal regulatory domain of Calcineurin B-Like (CBL)-interacting protein kinases

Cluster ID	Cluster description	Family Name - Descritpion	Domain Name- Descritpion
14027.155903	*Phragmites australis* pcnhx1 mRNA for putative Na+/H+ antiporter (NHX1)	b_cpa1 superfamily; PRK05326 - Sodium/hydrogen exchanger family; potassium/proton antiporter	-

Figure S4. Phylogenetic trees of specific salt responsive genes and their orthologues. **a** cluster 14027-155903 homolog of *Phramites australis* Na^+/H^+ antiporter (NHX1). **b** cluster 14027-181583 homolog of *Arabidopsis thaliana* Na^+/H^+ exchanger 2 (NHX2). **c** cluster 14027-182899 homolog of *Oryza sativa* CBL-interacting protein kinase 1 (CIPK1-SOS2-like). **d** cluster 14027-182899 homolog of *Oryza sativa* CBL-interacting protein kinase 24 (SOS2). **e** cluster 14027-54233 homolog of *Setaria italica* cation transporter (HKT9). **f** cluster 14027-231386 homolog of *Arabidopsis thaliana* persulfide dioxygenase (ETHE1).

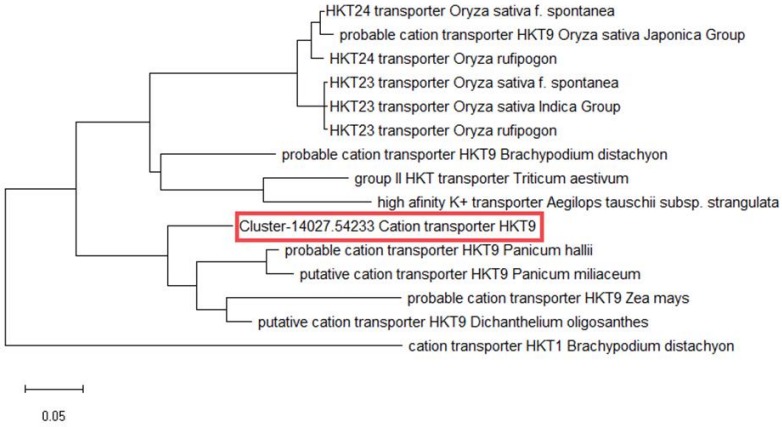

a

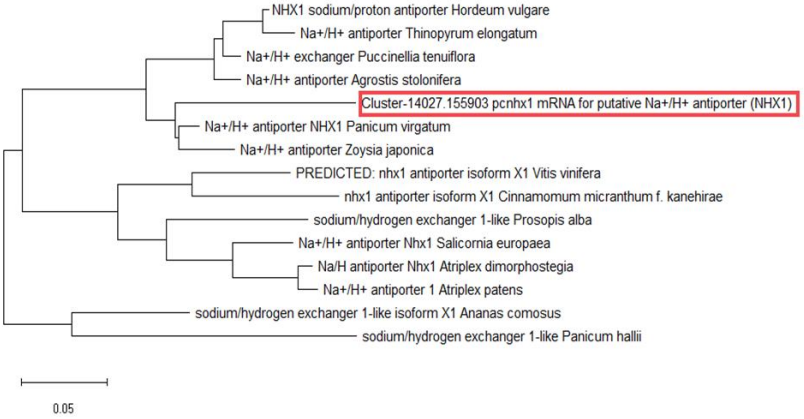
NHX1 sodium/proton antiporter Hordeum vulgare
Na+/H+ antiporter Thinopyrum elongatum
Na+/H+ exchanger Puccinellia tenuiflora
Na+/H+ antiporter Agrostis stolonifera
Cluster-14027.155903 pcnhx1 mRNA for putative Na+/H+ antiporter (NHX1)
Na+/H+ antiporter NHX1 Panicum virgatum
Na+/H+ antiporter Zoysia japonica
PREDICTED: nhx1 antiporter isoform X1 Vitis vinifera
nhx1 antiporter isoform X1 Cinnamomum micranthum f. kanehirae
sodium/hydrogen exchanger 1-like Prosopis alba
Na+/H+ antiporter Nhx1 Salicornia europaea
Na/H antiporter Nhx1 Atriplex dimorphostegia
Na+/H+ antiporter 1 Atriplex patens
sodium/hydrogen exchanger 1-like isoform X1 Ananas comosus
sodium/hydrogen exchanger 1-like Panicum hallii
0.05

b

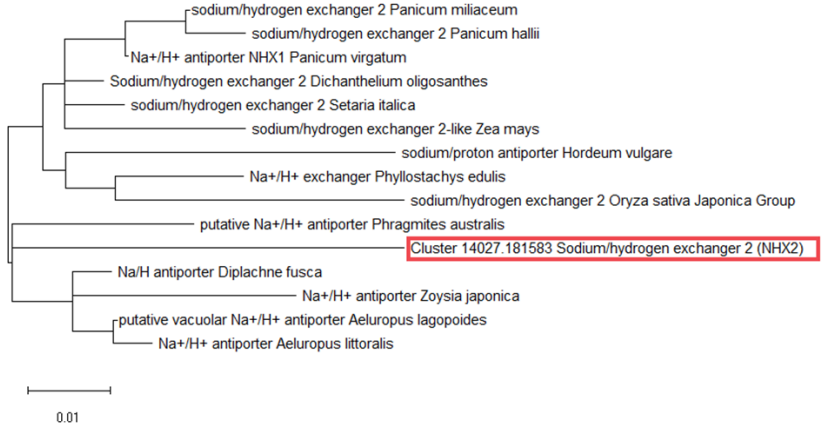
sodium/hydrogen exchanger 2 Panicum miliaceum
sodium/hydrogen exchanger 2 Panicum hallii
Na+/H+ antiporter NHX1 Panicum virgatum
Sodium/hydrogen exchanger 2 Dichanthelium oligosanthes
sodium/hydrogen exchanger 2 Setaria italica
sodium/hydrogen exchanger 2-like Zea mays
sodium/proton antiporter Hordeum vulgare
Na+/H+ exchanger Phyllostachys edulis
sodium/hydrogen exchanger 2 Oryza sativa Japonica Group
putative Na+/H+ antiporter Phragmites australis
Cluster 14027.181583 Sodium/hydrogen exchanger 2 (NHX2)
Na/H antiporter Diplachne fusca
Na+/H+ antiporter Zoysia japonica
putative vacuolar Na+/H+ antiporter Aeluropus lagopoides
Na+/H+ antiporter Aeluropus littoralis
0.01

c

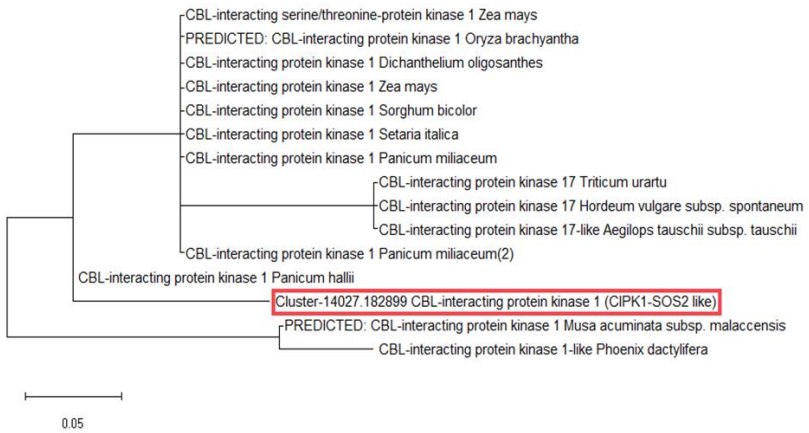
CBL-interacting serine/threonine-protein kinase 1 Zea mays
PREDICTED: CBL-interacting protein kinase 1 Oryza brachyantha
CBL-interacting protein kinase 1 Dichanthelium oligosanthes
CBL-interacting protein kinase 1 Zea mays
CBL-interacting protein kinase 1 Sorghum bicolor
CBL-interacting protein kinase 1 Setaria italica
CBL-interacting protein kinase 1 Panicum miliaceum
CBL-interacting protein kinase 17 Triticum urartu
CBL-interacting protein kinase 17 Hordeum vulgare subsp. spontaneum
CBL-interacting protein kinase 17-like Aegilops tauschii subsp. tauschii
CBL-interacting protein kinase 1 Panicum miliaceum(2)
CBL-interacting protein kinase 1 Panicum hallii
Cluster-14027.182899 CBL-interacting protein kinase 1 (CIPK1-SOS2 like)
PREDICTED: CBL-interacting protein kinase 1 Musa acuminata subsp. malaccensis
CBL-interacting protein kinase 1-like Phoenix dactylifera
0.05

d

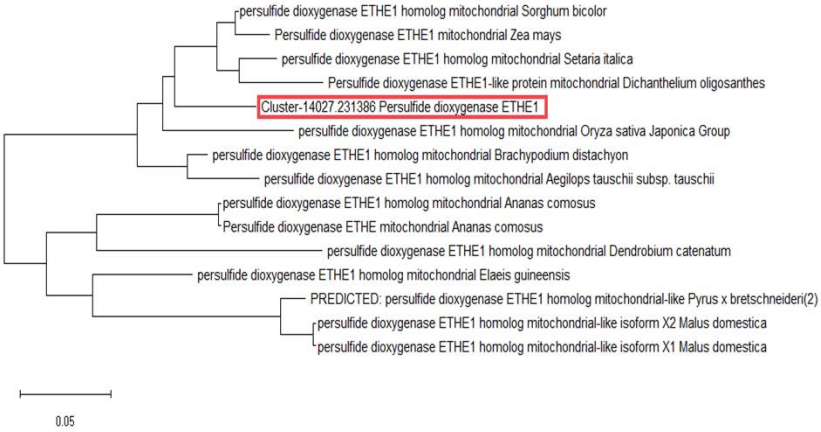
persulfide dioxygenase ETHE1 homolog mitochondrial Sorghum bicolor
Persulfide dioxygenase ETHE1 mitochondrial Zea mays
persulfide dioxygenase ETHE1 homolog mitochondrial Setaria italica
Persulfide dioxygenase ETHE1-like protein mitochondrial Dichanthelium oligosanthes
Cluster-14027.231386 Persulfide dioxygenase ETHE1
persulfide dioxygenase ETHE1 homolog mitochondrial Oryza sativa Japonica Group
persulfide dioxygenase ETHE1 homolog mitochondrial Brachypodium distachyon
persulfide dioxygenase ETHE1 homolog mitochondrial Aegilops tauschii subsp. tauschii
persulfide dioxygenase ETHE1 homolog mitochondrial Ananas comosus
Persulfide dioxygenase ETHE mitochondrial Ananas comosus
persulfide dioxygenase ETHE1 homolog mitochondrial Dendrobium catenatum
persulfide dioxygenase ETHE1 homolog mitochondrial Elaeis guineensis
PREDICTED: persulfide dioxygenase ETHE1 homolog mitochondrial-like Pyrus x bretschneideri(2)
persulfide dioxygenase ETHE1 homolog mitochondrial-like isoform X2 Malus domestica
persulfide dioxygenase ETHE1 homolog mitochondrial-like isoform X1 Malus domestica
0.05

e

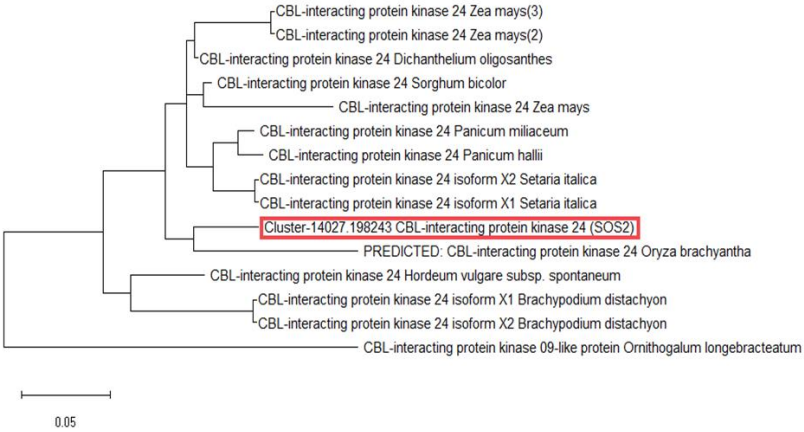
CBL-interacting protein kinase 24 Zea mays(3)
CBL-interacting protein kinase 24 Zea mays(2)
CBL-interacting protein kinase 24 Dichanthelium oligosanthes
CBL-interacting protein kinase 24 Sorghum bicolor
CBL-interacting protein kinase 24 Zea mays
CBL-interacting protein kinase 24 Panicum miliaceum
CBL-interacting protein kinase 24 Panicum hallii
CBL-interacting protein kinase 24 isoform X2 Setaria italica
CBL-interacting protein kinase 24 isoform X1 Setaria italica
Cluster-14027.198243 CBL-interacting protein kinase 24 (SOS2)
PREDICTED: CBL-interacting protein kinase 24 Oryza brachyantha
CBL-interacting protein kinase 24 Hordeum vulgare subsp. spontaneum
CBL-interacting protein kinase 24 isoform X1 Brachypodium distachyon
CBL-interacting protein kinase 24 isoform X2 Brachypodium distachyon
CBL-interacting protein kinase 09-like protein Ornithogalum longebracteatum
0.05

f

Appendix IX

Table S9. Primers for SSRs validation

Cluster ID	SSR	Repetitions	Position	Primer name	Primer sequence
14027.192887	AGC	5	5'-UTR	Ad_SRRM2 For	5'-CGCAAACGCTCCAAGAAACA-3'
				Ad_SRRM2 Rev	5'-GCCCCTCCCTTTTCTCTTCC-3'
14027.42287	AGC	5	CDS	Ad_HMGN5 For	5'-CATTCGAGGTCGTGGGCAG-3'
				Ad_HMGN5 Rev	5'-TCTCCTTCTCCTTCCGCTCA-3'
14027.58603	AGC	6	5'-UTR	Ad_SHR1 For	5'-GAGCATGCACACGCCTTATG-3'
				Ad_SHR1 Rev	5'-TCTTGGTACGGCTCCAGGTA-3'
14027.124297	AGC	4	5'-UTR	Ad_myba For	5'-AAGATCTGAAGAGCAGGCGG-3'
				Ad_myba Rev	5'-TAAGAAATCCCAGCGGCGTT-3'
14027.96747	GCA	5	CDS	Ad_SPL1 For	5'-TCTGTCAGACAACCAGACGC-3'
				Ad_SPL1 Rev	5'-ACCATGGTATTGCTGCAGCT-3'

Figure S5. Sequence of regions analyzed for SSRs validation and electropherograms of Sanger sequencing. In yellow are highlighted the primer sequences, in green SSRs sequences. **a** Cluster-14027.192887. **b** Cluster-14027.42287. **c** Cluster-14027.58603. **d** Cluster-14027.124297. **e** Cluster-14027.96747.

a. Cluster-14027.192887; Ad_SRRM2
GGTTCGCCCCCGTCTCTCTTCTGCTGTCCTCCTCCAGGTGCCG
CCGGACGGACCCCGATGAAGATCAAAGCCGCCGTCGATGAGG
ATGAGGCCGAGCCCAAGAAGATCCGGTCCTCACGCACCAAGC
GCCGCCGTGGCTGCCGCAGCTGCTCCTCCTCCGGTTCTGAATC
TCCACCCCGCAAACGCTCCAAGAAACACAGTAAAAGGATTCC
TGACAAGAAGACCAAAAGGAGCAAGGTTAGCAGCAGCAGCA
GCCGTCGTCGCCGCCGCCGCCGTAGTCTTAGCCCTGACCGTAG
CCTCAGTAGCAGTAGCCCTTCCTCGGTGTCCAGGAGCTTCTCC
CGCCGCAGTAGCTCGACGTCCCACAGCAGCAGCAGTGCCTCT
GAGAGGTCAGTCAGTCCGCCGCCCAGGAGCCGGTCCAGAGAT
GTCAGGAAGAGAAAAGGGAGGGGCAGGGACAGAGACAGAG
ACAGAGACGGAGACAAGGATCGCAAGAGGAGAAAGGCACGG
AGATACTCCAGCAGTACAGCAAGTAGCGGTAGTAGCAGGAGT
AGGAGTAGGAGCACGAAGCGGAGGGATGATGCTACTAGAGA
TAAGGTTCAACAGGATTATGACAATCGGCGCACTTCCT
GGTCT[…]

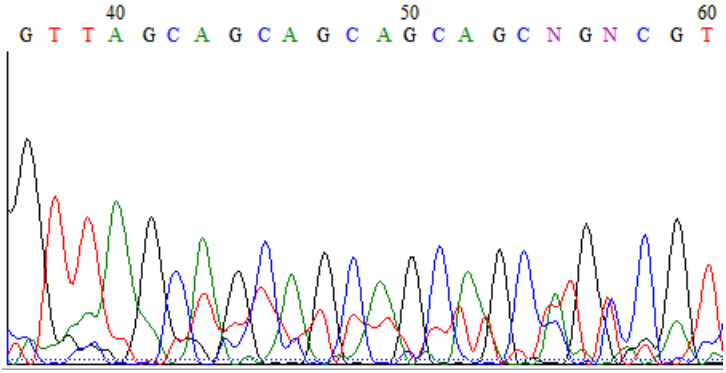

G2

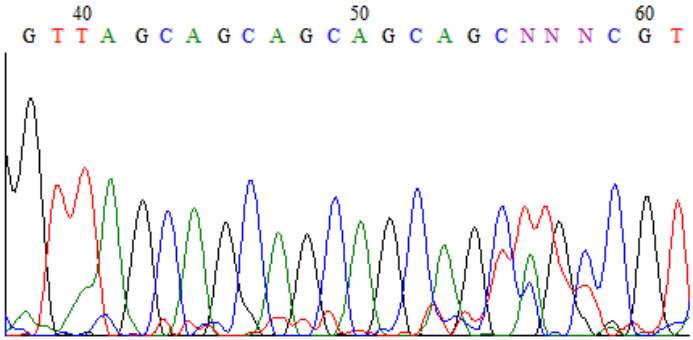

G34

b. Cluster-14027.42287; Ad_HMGN5

[…]CCTGGAGCCCGAAGCCGGCGGCGGCGGAGGAAGCAAGGT
GGTGACCCTCTCCGTTGACTCCCCGACGGCCAACCTCGGTCGA
GGCGACCTGGGCCATGGCAGCCCCTCCAGGGACCGCACCGTT
TCGCGCCGCCACGTGTCCCTCCGCCTCCTCCTCGCCGACGGCG
GCGGGGACCCCGGGGTCGCATTCGAGGTCGTGGGCAGGAACC
CCGTGGTCGTCCGCCGCTCCTCGAATGGCGGAGGAGGAAGCA
GCAGCAGCAGCAGGGTCTTCCGCCGCGGGGAGAAGGGCGAG
CTCGGGGCCGGGGACGCGCTGTCGCTGTCGCTGAGGGCGCCG
TCGTTCTGGGCGGTGCGGAGGAGGGAGGGGGAGGTGGATGC
CTCGGTGCTGGACGCGGTGGCGAGGCGGGAGAGGAGAACGC
GTGAGCGGAAGGAGAAGGAGATGCGAGCGGCGAAGGAGGAG
GCCATGGAGGTCACCGAAGAGGGAGAGGAGGTGGAGGCCGG
CACTGAAATGGAGGGTTTGGAGATCGATTTGACAAGTGTCGA
TCCGGTCCAAGGTGATGTCTTGTTCTCCTTTTTTGCATTGCAG
GGAAGGCGAAATGTTTTCCCTCCACATTTCATTTCAGCACAAA
TTTGA

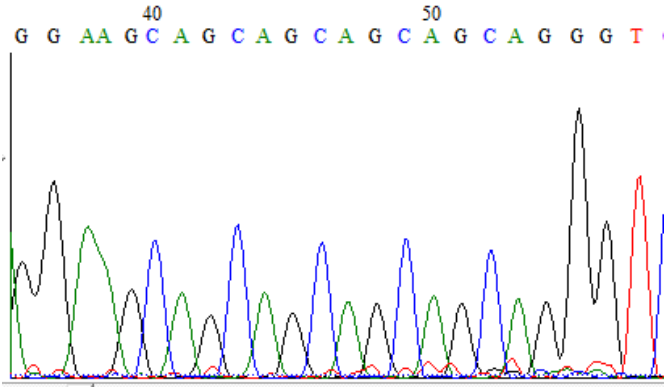
40
50
G G AA GC A G C A G C A G C A G C A G G G T

G2

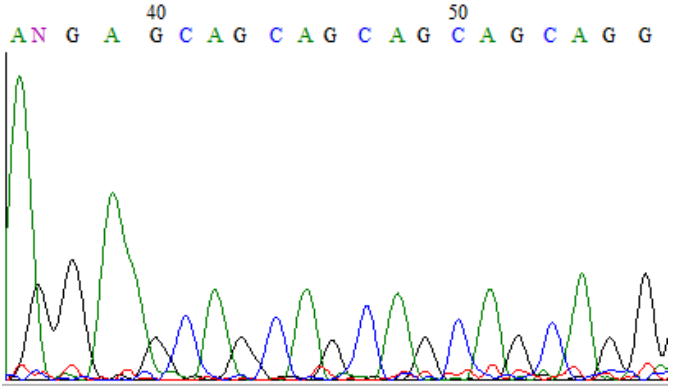
40
50
AN G A G C A G C A G C A G C A G C A G G

G34

c. Cluster-14027.58603; Ad_SHR1
CTAGCTAGCCTTGTCCTCCTCCTACCCTCAGATTCTCACTGCG
CTGCCATTAAAATCCCCCTTGCTTGTTACCACGGCGACCTTGA
GCATGCACACGCCTTATGTTGCCTCCTGGCCGTCGTGGTAGCT
TACATGGATACTTTGTTTAGGTTGGTTAGCCTCCAAGCCTCCG
AGCAGCAGCAGCAGCAGCAGTCCGCGTCGTACAACTCGAGGA
GCACCACGTCGAGCGGCTCGAGGTCGTCGTCGCACCAGACCA
ACGCCTCCTACAACTACTACTACCACAGCAACAGCAGCGGCG
GCGGCGGGCAGTACTACTACGGCCAGCACCACCAGCAGCAGT
ACTACCTGGAGCCGTACCAAGAAGAATGCGGCAACGCCCACC
ACCTTTACATGGATGAAGACTTCTCCTCCTCGTCTTCGTCGAG
GCAGCATTTCCACTCGCACGGCGCGACGGTGCAGCCGCCAAC
GTCGTCCGCGCACACGCCGACGGCGCCGACGCCCCCGCTGTC
CACGGCGTCCACGGCCGCGGGGGCGGCGCACGCGCTGTTCGA
GGCGGCCGACCTGTCGTTCCCGCCGG[…]

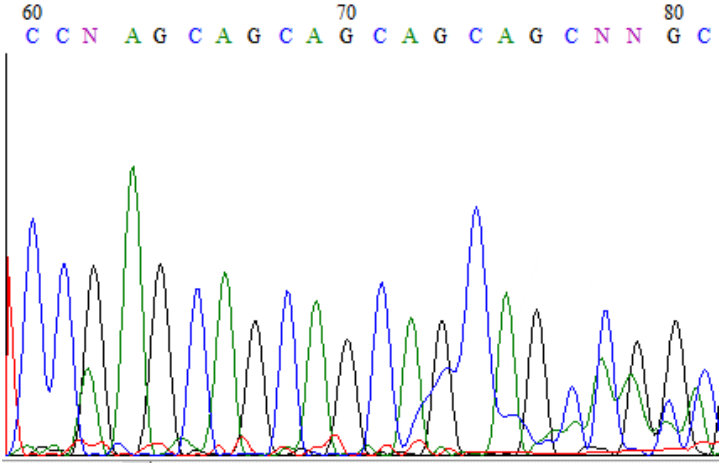

G2

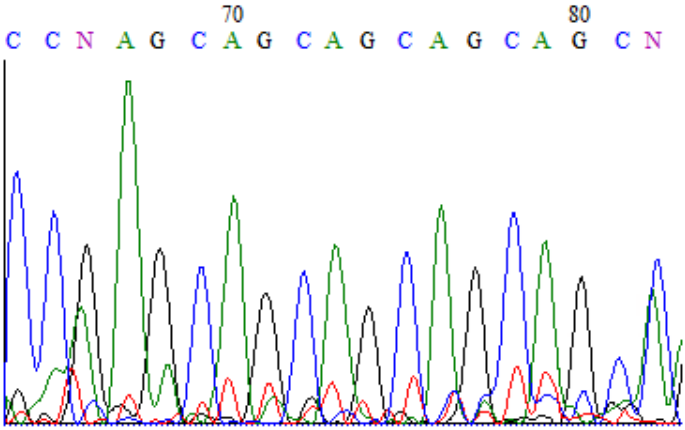

G34

d. Cluster-14027.124297; Ad_myba

AGGGAGCAAGATCTGAAGAGCAGGCGGGAGGAGACCGCCAG
CAGCAGCAGCAGCAGGAGATCAATCGCGGATGCGATCATGTC
CATGCATATGTGTAGCAAGAAGAAGAAGGATCACGAGCAGC
AGGGAGGCGGCAGTACGACGACGACGACCATGCCGATGACG
ACGGCGATGAGGAAGGGGGCGTGGACGGAGGAGGAAGACGC
GCAGCTGGTACGGTTCGTGCGCTTGTTCGGTGAACGCCGCTG
GGATTTCTTAGCAAAGGTCTCAGGTTTGCGCGGTGGCGGGTG
CTCGATCCATCCCCATGCATGCATGCATCATCCATGCCTCCGA
TCCATGGTGATGTTTCTGATCGAGGTGGCGTGCATGCATGAG
GATCGATCGCAGTCCACGGACGGTGGCATGCGCGGTGTTAAT
TAA

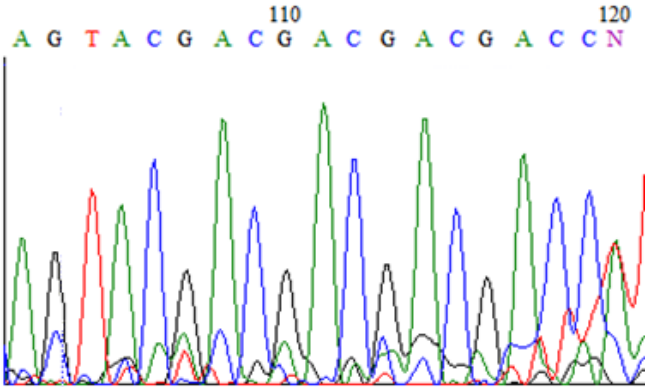

G2

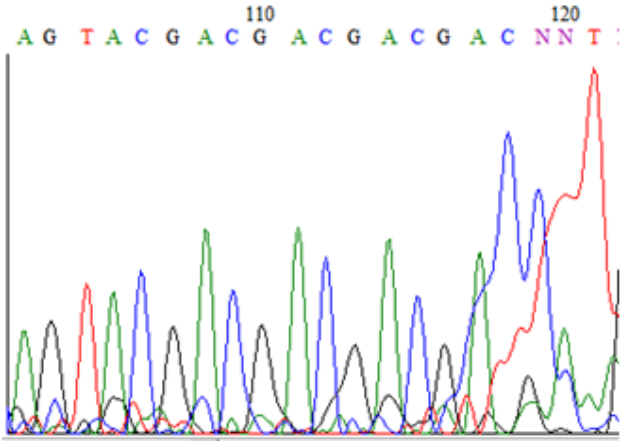

G34

e. Cluster-14027.96747; Ad_SPL1

[…]TCTACCCCGGCAAGGAAAAGAAGCACTTCCCGTTCTTGAC
CGACCACGGCGGGAGCGACGCCGCGGCCTTCGGCTGCCAGCC
GTTCGCCATCACCCCTTCCTTAGAGAGCAGCAGTAAGCAGAG
CAATGGCAACTGTGCTCTCTCTCTTCTGTCAGACAACCAGACG
CCGGCACAGATGTTGATCCCCACCGCGCAGCCCCTCGGCGCG
GCGCTGCAGTACGGCAATGTGGCACGGCTCACCGACGACGGC
GACGTCTCGCTCACCGGGATGTCTTACGTCAGGGCGGGAGAC

AAGCAGACATCCATTCTGGCCACATCTGTTGGTCACACTGCA
GCAGCAGCAGCAGCTGCTTCTCCTGCTCCTGCAAGTGCAGCA
GCAGCACAGCTGCAGCAATACCATGGTTACTACCATGTGAGT
GGCGTCGATCATCAGGGCAACCCAGACGGTGCCGCCATTCAG
GCCCTTCCCTTCTCATCGTGGTAG

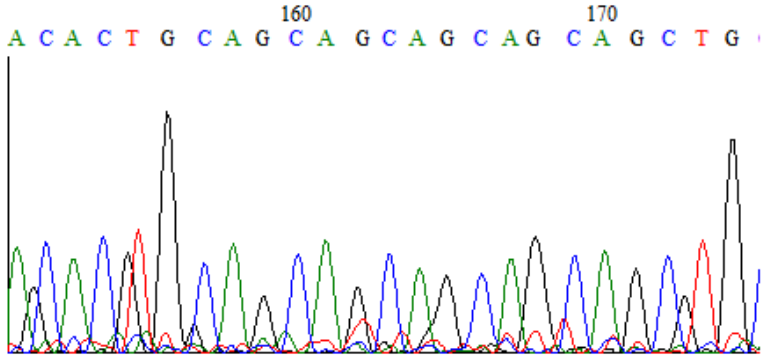

G2

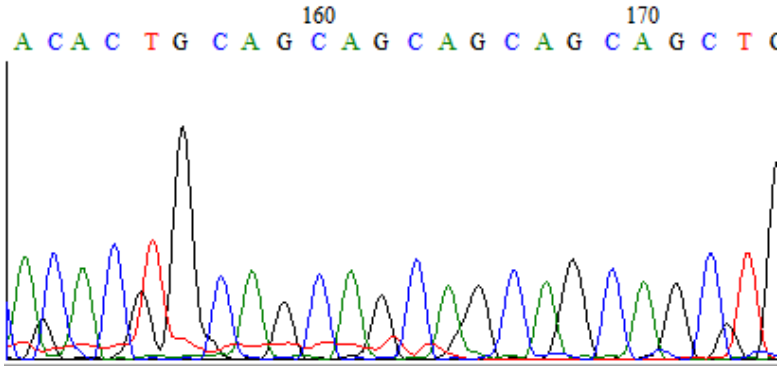

G34

Appendix X

Table S10. Primer sequences for MSAP analysis

Cluster ID	Description	Primer name	Primer sequence 5'→3'
14027.148405	*Aeluropus lagopoides* HKT type-II transporter protein (HKT2;1)	Ad_HKT2 F	GAGCTCGACACCATAGAGCC
		Ad_HKT2 R	TGCAGTTGGCACACTGGTTA
14027.230649	Probable cation transporter HKT6 (*Oryza sativa* subsp. japonica)	Ad_HKT6 F	AGCAATGAAGACAGATCCACTC
		Ad_HKT6 R	TTCCAAGCTCTTCCTCCCTTC
14027.210735	Setaria italica phosphate transporter PHO1-1-like	Ad_myb-related 306 F	GCTGCAGCTTCCATCGTTTG
		Ad_myb-related 306 R	AGCAGACATCCCCATGAGTC

References

Abdullah, H. M., Akbar, P., Paulose, B., Schnell, D., Qi, W., Park, Y., Pareek, A., Dhankher, O. P. (2016). Transcriptome profiling of *Camelina sativa* to identify genes involved in triacylglycerol biosynthesis and accumulation in the developing seeds. Biotechnol. Biofuels, 9, 136.

Abichandani, S. (2007). The potential impact of the invasive species *Arundo donax* on water resources along the Santa Clara River: seasonal and diurnal transpiration. University of California; [Master Thesis].

Aguirre, A. M., Bassi, A., Saxena, P. (2012). Engineering challanges in biodiesel production from microalgae. Critical Rev. Biotech., 8551, 1-16.

Ahmad, A., Wang, J. D., Pan, Y. B., Sharif, R. and Gao, S. J. (2018). Development and use of single sequence repeats (SSRs) markers for sugarcane breeding and genetic studies. Agronomy, 8, 260.

Ahmad, A. L., Yasin, N. H. M., Derek, C. J. C., Lim, J. K. (2011). Microalgae as sustainable energy source for biodies production: a review. Renew. Sust. Energy. Rev., 5, 584-593.

Ahmad, I., and Maathuis, F. J. M. (2014). Cellular and tissue distribution of potassium: physiological relevance, mechanisms and regulation. J. Plant Physiol., 171, 708–714.

Ahmad, P. (2010). Growth and antioxidant responses in mustard (Brassica juncea L.) plants subjected to combined effect of gibberellic acid and salinity. Archives of Agronomy and Soil Science, 56, (5), 575–588.

Ahmad, P., Jaleel, C. A., Salem, M. A., Nabi, G. and Sharma, S. (2010). Roles of enzymatic and nonenzymatic antioxidants in plants during abiotic stress. Critical Reviews in Biotechnology, 30(3), 161–175.

and Umar, S. (2011). Oxidative stress: role of antioxidants in plants, Studium Press, New Delhi, India.

Ahmad, R., Lim, C. J. and Kwon, S. -Y. (2013). Glycine betaine: a versatile compound with great potential for gene pyramiding to improve crop plant performance against environmental stresses. Plant Biotechnology Reports, 7, 49-57.

Alamgir, A. N. M. and Yousuf Ali, M. (1999). Effect of salinity on leaf pigments, sugar and protein concentrations and chloroplast ATPase activity of rice (*Oryza sativa* L.). Bangladesh Journal of Botany, 28(2), 145–149.

Allis, D., Jenuwein, T. (2016). The hallmarks of epigenetic control. Nat. Rev. Genet., 17, 487–500.

Allwright, M. R. and Taylor, G. (2016). Molecular breeding for improved second generation bioenergy crops. Trend Plant Sci., 21, 43-54.

Ambrose, R. F., Rundel, P. W. (2007). Influence of nutrient loading on the invasion of an alien plant species, giant reed (*Arundo donax*), in Southern California riparian ecosystems. UC Water Resources Center technical completion report proj. no. W-960.

Angelini, L. G., Ceccarini, L., Bonari, E. (2005). Biomass yield and energy balance of giant reed (*Arundo donax* L.) cropped in central Italy as related to different management practices. Eur. J. Agron., 22, 375–89.

Angelini, L. G., Ceccarini, L., Nassi o di Nasso, N., Bonari, E. (2009). Comparison of *Arundo donax* L. and *Miscanthus* × *giganteus* in a long-term field experiment in Central Italy: analysis of productive characteristics and energy balance. Biomass Bioenergy, 33, 635–43.

Anil, V. S., Krishnamurthy, P., Kuruvilla, S., Sucharitha, K., Thomas, G., and Mathew, M. (2005). Regulation of the uptake and distribution of Na^+ in shoots of rice (*Oryza sativa*) variety Pokkali: role of Ca^{2+} in salt tolerance response. Physiol. Plant, 124, 451–464.

Anschütz, U., Becker, D., and Shabala, S. (2014). Going beyond nutrition: regulation of potassium homoeostasis as a common denominator of plant adaptive responses to environment. J. Plant Physiol., 171, 670–687.

Antizar-Ladislao, B., Turrion-Gomez, J. L., (2008). Second-generation biofuels and local bioenergy systems. Biofuels. Bioprod. Bioref., 2, 455-469.

Aro, E. M. (2016). From first generation biofuels to advanced solar biofuels. Ambio, 45, 24-31.

Asada, K. (1999). The water-water cycle in chloroplasts: scavenging of active oxygens and dissipation of excess photons. Annual Review of Plant Biology, 50, 601–639.

Ashraf, M. and Foolad, M. R. (2007). Roles of glycine betaine and proline in improving plant abiotic stress resistance. Environmental and Experimental Botany, 59(2), 206–216.

Baeyens, J., Kang, Q., Appels, L., Dewil, R., Yongqin, L. V., Tan, T. (2015). Challenges and opportunities in

improving the production of bio-ethanol. Prog. Energy Comb. Sci., 47, 60-88.

Bahieldin, A., Atef, A., Sabir, J. S., Gadalla, N. O., Edris, S., Alzohairy, A. M., Radhwan, N. A., Baeshen, M. N., Bajguz, A., Hayat, S. (2009). Effects of brassinosteroids on the plant responses to environmental stresses. Plant Physiol. Biochem., 47(1), 1-8.

Bajguz, A. (2014). Nitric oxide: role in plants under abiotic stress. In Physiological Mechanisms and Adaptation Strategies in Plants Under Changing Environment, 137–159, Springer.

Bajguz, A., Hayat, S. (2009). Effects of brassinosteroids on the plant responses to environmental stresses. Plant Physiol Biochem., 47(1), 1-8.

Barcaccia, G., Falcinelli, M. Genetica e genomica. Vol. III. Genomica e biotecnologie. Editor: Liguori, 2006, vol.3, chapter 17 (Marcatori molecolari ed analisi genomica).

Barragan, V., Leidi, E. O., Andrés, Z. et al. (2012). Ion exchangers NHX1 and NHX2 mediate active potassium uptake into vacuoles to regulate cell turgor and stomatal function in *Arabidopsis*. Plant Cell, 24(3), 1127–1142.

Barrero, R. A., Guerrero, F. D., Moolhuijzen, P., Goolsby, J. A., Tidwell, J., Bellgard, S. E., Bellgard, M. I. (2015). Shoot transcriptome of the giant reed, *Arundo donax*. Data Brief., 3, 1–6.

Bassi, E., Ohto, M. A., Esumi, T., Tajima, H., Zhu, Z., Cagnac, O., Belmonte, M., Peleg, Z., Yamaguchi, T., Blumwald, E. (2011). The *Arabidopsis* intracellular Na^+/H^+ antiporters NHX5 and NHX6 are endosome associated and

necessary for plant growth and development. Plant Cell., 23(1), 224-39.

Behera, S., Singh, R., Arora, R., Sharma, N. K., Shukla, M., Kumar, S. (2015). Scope of algae as third generation biofuels. Front. Bioener. Biotech., 2, 90.

Ben Ahmed, C., Ben Rouina, B., Sensoy, S., Boukhriss, M. and Ben Abdullah, F. (2010). Exogenous proline effects on photosynthetic performance and antioxidant defense system of young olive tree. Journal of Agricultural and Food Chemistry, 58(7), 4216–4222.

Bentley, D. R., Balasubramanian, S., Swerdlow, H. P., Smith, G. P., Milton, J., Brown, C. G., Hall, K. P., Evers, D. J., Barnes, C. L., Bignell, H. R., et al. (2008). Accurate whole human genome sequencing using reversible terminator chemistry. Nature, 456, 53–59.

Beringer, T., Lucht, W., Schaphoff, S. (2011). Bioenergy production potential of global biomass plantations under environmental and agricultural constraints. GCB Bioenergy, 3, 299–312.

Berthomieu, P., Conéjéro, G., Nublat, A., Brackenbury, W. J., Lambert, C., Savio, C., et al. (2003). Functional analysis of AtHKT1 in *Arabidopsis* shows that Na(+) recirculation by the phloem is crucial for salt tolerance. EMBO J., 22, 2004–2014.

Besson-Bard, A., Pugin, A. and Wendehenne, D. (2008). New insights into nitric oxide signaling in plants. Annual Review of Plant Biology, 59, 21–39.

Bhanwra, R, Choda, S. P., Kumar, S. (1982). Comparative embryology of some grasses. Proc. Indian Acad. Sci. B., 48, 152–62.

Bianco, C., Defez, R. (2009). *Medicago truncatula* improves salt tolerance when modulated by an indole-3-acetic acid overproducing *Sinorhizobium meliloti* strain. J Exp Bot., 60, 3097-3107.

Binzel, M. L., Hess, F. D., Bressan, R. A. and Hasegawa, P. M. (1988). Intracellular compartmentation of ions in salt adapted tobacco cells. Plant Physiology, 86, 607–614.

Bohnert, H. J., Nelson, D. E. and Jensen, R. G. (1995). Adaptations to environmental stresses. Plant Cell, 7(7), 1099–1111.

Boland, J. M. (2006). The importance of layering in the rapid spread of *Arundo donax* (giant reed). Madroño, 53, 303–12.

Boller, T., and Kende, H. (1979). Hydrolytic enzymes in the central vacuole of plant cells. Plant Physiol., 63, 1123–1132.

Boose, A., Holt, J. (1999). Environmental effects on asexual reproduction in *Arundo donax*. Weed Res., 39, 117–27.

Borin, M., Barbera, A. C., Milani, M., Molari, G., Zimbone, S. M., Toscano, A. (2013). Biomass production and N balance of giant reed (*Arundo donax* L.) under high water and N input in Mediterranean environments. Eur. J. Agron., 51, 117–9.

Boudsocq, M., and Sheen, J. (2013). CDPKs in immune and stress signaling. Trends Plant Sci., 18, 30–40.

Boyko, A., Kovalchuk, I. (2008). Epigenetic control of plant stress response. Environ Mol Mutagen., 49, 61–72.

Bray, E. A., Bailey-Serres, J., Weretilnyk, E. (2000). Responses to abiotic stresses, in: Gruissem, W., Buchannan, B., Jones, R. (Eds.), Biochemistry and Molecular Biology of Plants, American Society of Plant Biologists, Rockville, MD, pp. 158–1249.

Brennan, L., Owende, O. (2010). Biofuels from microalgae. A review of technologies for production, processing, and extraction of biofuels and co-products. Renew. Sust. Energy Rev., 14, 557-577.

Brinke, J. (2010). Effects of the invasive species *Arundo donax* on bank stability in the Santa Clara River, Ventura, CA. California Invasive Plant Council symposium.

Bruinsma, J. (2009). The resource outlook to 2050. By how much do land, water use and crop yields need to increase by2050? Session2: The resource base to 2050: Will there be enough land, water and genetic potential to meet future food and biofuel demands? In: FAO Expert Meeting on How to Feed the World in 2050, Rome, 32pp.

Bucci, A., Cassani, E., Landoni, M., Cantaluppi, E., Pilu, R. (2013). Analysis of chromosome number and speculations on the origin of *Arundo donax* L. (giant reed). Cytol. Genet., 47, 237–41.

Buonocore, E., Mellino, S., De Angelis, G., Liu, G., Ulgiati, S. (2018a). Life cycle assessment indicators of urban wastewater and sewage sludge treatment. Ecol. Indicat., 94, 13-23.

Buonocore, E., Vanoli, L., Carotenuto, A., Ulgiati, S. (2015). Integrating life cycle assessment and emergy synthesis for the evaluation of a dry steam geothermal power plant in Italy. Energy, 86, 476-487.

Cabot, C., Sibole, J. V., Barcelo, J. and Poschenrieder, C. (2009). Abscisic acid decreases leaf Na^+ exclusion in salt-treated *Phaseolus vulgaris* L. Journal of Plant Growth Regulation, 28(2), 187–192.

Carmo-Silva, A. E., Salvucci, M. E. (2013). The regulatory properties of Rubisco activase differ among species and affect photosynthetic induction during light transitions. Plant Physiol., 161, 1645–1655.

Carriquiry, M.A., Du, X., Timilsina, G.R., 2014. Production Costs of Biofuels. In: Timilsina, G. R., Zilberman, D. (Eds.), The Impacts of Biofuels on the Economy, Environment, and Poverty. Springer, New York, pp. 33–46.

Casneuf, T., Van de Peer, Y., Huber, W. (2007). In situ analysis of cross-hybridisation on microarrays and the inference of expression correlation. BMC Bioinformatics. 8, 461.

Castelli, S. (a cura di) (2011). Biomasse ed energia. Produzione, gestione e processi di trasformazione. Edited by Maggioli Editore, Santarcangelo di Romagna, Italia.

Castiglia, D., Sannino, L., Marcolongo, L., Ionata, E., Tamburino, R., De Stradis, A., Cobucci-Ponzano, B., Moracci, M., La Cara, F., Scotti, N. (2016). High-level expression of thermostable cellulolytic enzymes in tobacco transplastomic plants and their use in hydrolysis of an industrially pretreated *Arundo donax* L. biomass. Biotech. Biofuels., 9, 154.

Ceotto, E., Di Candilo. (2010). Shoot cutting propagation of giant reed (*Arundo donax* L.) in water and moist soil: the path forward? Biomass Bioenergy, 11, 1614–23.

Cha-Um, S. and Kirdmanee, C. (2010). Effect of glycinebetaine on proline, water use, and photosynthetic efficiencies, and growth of rice seedlings under salt stress. Turkish Journal of Agriculture and Forestry, 34(6), 517–527.

Chan, S. W. L., Henderson, I. R. and Jacobsen, S. E. (2005). Gardening the genome: DNA methylation in *Arabidopsis thaliana*. Nat. Rev. Genet., 6, 351–360.

Chen, L., Han, J., Deng, X., Tan, S., Li, L., Li, L., Zhou. J., Peng, H., Yang, G., He, G., Zhang, W. (2016). Expansion and stress responses of AP2/EREBP superfamily in Brachypodium Distachyon. Scientific Reports, 6, 21623.

Chen, S., Li, J., Wang, S., Huttermann, A. and Altman, A. (2001). Salt, nutrient uptake and transport, and ABA of *Populus euphratica*; a hybrid in response to increasing soil NaCl. Trees Structure and Function, 15(3), 186–194.

Chen, Z., Pottosin, I. I., Cuin, T. A., Fuglsang, A. T., Tester, M., Jha, D., et al. (2007). Root plasma membrane transporters controlling K^+/Na^+ homeostasis in salt-stressed barley. Plant Physiol., 145, 1714–1725.

Cheng, N. H., Pittman, J. K., Zhu, J. K., Hirschi, K. D. (2004). The protein kinase SOS2 activates the *Arabidopsis* H^+/Ca^{2+} antiporter CAX1 to integrate calcium transport and salt tolerance. J Biol Chem., 279, 2922-2926.

Chisti, Y. (2008). Biodiesel from microalgae beats bioethanol. Trends Biotech., 26, 126-131.

Choi, W. G., Toyota, M., Kim, S. H., Hilleary, R., and Gilroy, S. (2014). Salt stress-induced Ca^{2+} waves are associated with rapid, long-distance root-toshoot signaling in plants. Proc. Natl. Acad. Sci. USA, 111, 6497–6502.

Christopher, I., Abraham, A. (1971). Studies on the cytology and phylogeny of South Indian Bambusoideae, Oryzoideae, Arundinoideae and Festucoideae. Cytologia,36, 579–94.

Christou, M., Mardikis, M., Alexopoulou, E., Cosentino, S. L., Copani, V., Sanzone, E. (2003). Environmental studies on *Arundo donax*. Proceedings of the 8th international conference on environmental science and technology, London, p. 102–10.

Clause, S. D. and Sasse, J. M. (1998). Brassinosteroids: essential regulators of plant growth and development. Annual Review of Plant Biology, 49, 427–451.

Clevering, O. A., Lissner, J. (1999). Taxonomy, chromosome numbers, clonal diversity and population dynamics of *Phragmites australis*. Aquat. Bot., 64, 185–208.

Coleman, H. D., Yan, J., Mansfield, S. D. (2009). Sucrose synthase affects carbon partitioning to increase cellulose production and altered cell wall ultrastructure. Proc. Natl Acad. Sci. USA, 106, 13118–13123.

Colmenero-Flores, J. M., Martinez, G., Gamba, G., Vázquez, N., Iglesias, D. J., Brumós, J., et al. (2007). Identification and functional characterization of cation chloride cotransporters in plants. Plant J., 50, 278–292.

Corno, L., Pilu, R., Adani, F. (2014). *Arundo donax* L.: a non-food crop for bioenergy and bio-compound production. Biotechnology Advances, 32, 1535–1549.

Cosentino, S. L., Copani, V., D'Agosta, G. M., Sanzone, E., Mantineo, M. (2006). First results on evaluation of *Arundo donax* L. clones collected in Southern Italy. Ind. Crop. Prod., 23, 212–22.

Cramer, G. R. and Quarrie, S. A. (2002). Abscisic acid is correlated with the leaf growth inhibition of four genotypes of maize differing in their response to salinity. Functional Plant Biology, 29(1), 111–115.

Crawford, N. M. (2006). Mechanisms for nitric oxide synthesis in plants. Journal of Experimental Botany, 57(3), 471–478.

Cushman, J. C., Bohnert, H. J. (1992). Salt stress induction of crassulacean acid metabolism in a facultative CAM plant. Photosynth Res., 34, 103–1103.

Dale, V. H., Kline, K. L., Perla, D., Lucifer, A. (2013). Communicating about bioenergy sustainability. Environ. Manag., 51, 279-290.

De Stefano, R., Cappetta, E., Guida, G., Mistretta, C., Caruso, G., Giorio, P., Albrizio, R. and Tucci, M. (2018). Screening of giant reed (Arundo donax L.) ecotypes for biomass production under salt stress, Plant Biosystems - An International Journal Dealing with all Aspects of Plant Biology, 152(5), 911-917.

Decruyenaere, J., Holt, J. (2005). Ramet demography of a clonal invader, *Arundo donax* (Poaceae), in Southern California. Plant Soil, 277, 41–52.

Deenanath, E. D., Iyuke, S., Rumbold, K. (2012). The bioethanol industry in sub-Saharan Africa: history, challenges, and prospects. J. Biomed. Biotech.

Deinlein, U., Stephan, A. B., Horie, T., Luo, W., Xu, G., Schroeder, J. I. (2014). Plant salt-tolerance mechanisms. Trends Plant Sci., 19, 371–379.

Delledonne, M., Xia, Y., Dixon, R. A. and Lamb, C. (1998). Nitric oxide functions as a signal in plant disease resistance. Nature, 394(6693), 585–588.

Demidchik, V., Cuin, T. A., and Svistunenko, D. (2010). *Arabidopsis* root K^+ efflux conductance activated by hydroxyl radicals: single-channel properties, genetic basis and involvement in stress-induced cell death. J. Cell Sci., 123, 1468–1479.

Demidchik, V., Essah, P. A., and Tester, M. (2004). Glutamate activates cation currents in the plasma membrane of *Arabidopsis* root cells. Planta, 219, 167–175.

Demidchik, V., and Maathuis, F. J. M. (2007). Physiological roles of nonselective cation channels in plants: from salt stress to signaling and development. New Phytol., 175, 387–404.

Demidchik, V., Shabala, S., Isayenkov, S., Cuin, T. A., and Pottosin, I. (2018). Calcium transport across plant membranes: mechanisms and functions. New Phytol., 220, 49–69.

Demidchik, V., Straltsova, D., Medvedev, S. S., Pozhvanov, G. A., Sokolik, A., and Yurin, V. (2014). Stress-induced electrolyte leakage: the role of K^+-permeable channels and involvement in programmed cell death and metabolic adjustment. J. Exp. Bot., 65, 1259–1270.

Dhir, S., Knowles, K., Livia Pagan, C., Mann, J., Dhir, S. (2010). Optimization and transformation of *Arundo donax* L. using particle bombardment. Afr. J. Biotechnol., 9, 6460–9.

Donaldson, L., Ludidi, N., Knight, M. R., Gehring, C., and Denby, K. (2004). Salt and osmotic stress cause rapid

increases in *Arabidopsis thaliana* cGMP levels. FEBS Lett., 569, 317–320.

Dopp, M., Larher, F. and Weigel, P. (1985). Osmotic adaption in Australian mangroves. Vegetatio, 61, 1–3, 247–253.

Dowen, R. H., Pelizzola, M., Schmitz, R. J., Lister, R., Dowen, J. M., Nery, J. R., Dixon, J. E., Ecker, J. R. (2012). Widespread dynamic DNA methylation in response to biotic stress. PNAS, 109, E2183–91.

Dyachenko, O. V., Zakharchenko, N. S., Shevchuk, T. V., Bohnert, H. J., Cushman, J. C., Buryanov, Y. I. (2006). Effect of hypermethylation of CCWGG sequences in DNA of *Mesembryanthemum crystallinum* plants on their adaptation to salt stress. Biochemistry, 71, 461–465.

Eichten, S. R., Schmitz, R. J. and Springer, N. M. (2014). Epigenetics: beyond chromatin modifications and complex genetic regulation. Plant Physiol., 165, 933–947.

El-Mashad, A. A. A. and Mohamed, H. I. (2012). Brassinolide alleviates salt stress and increases antioxidant activity of cowpea plants (*Vigna sinensis*). Protoplasma, 249(3), 625–635.

El-Shintinawy, F. and El-Shourbagy, M. N. (2001). Alleviation of changes in protein metabolism in NaCl-stressed wheat seedlings by thiamine. Biologia Plantarum, 44(4), 541–545.

Else, J. A. (1996) Post-flood establishment of native woody species and an exotic, *Arundo donax*, in a Southern California riparian system. San Diego University, [Master Thesis].

Essah, P. A., Davenport, R., and Tester, M. (2003). Sodium influx and accumulation in *Arabidopsis*. Plant Physiol., 133, 307–318.

Estrela, R. and Cate, J. H. D. (2016). Energy biotchnology in the CRISPR-Cas9 era. Curr. Opi. Biotech., 38, 79-84.

European Commission (2009). Directive 2009/28/EC of the European Parliament and of the Council on the promotion of the use of energy from renewable sources and amending and subsequently repealing Directives 2001/77/EC and 2003/30/EC. J. Eur. Union, 160, 16-62.

European Commission (2015). Climate action progress report 2015, 1-64.

Evangelistella, C., Valentini, A., Ludovisi, R., Firrincieli, A., Fabbrini, F., Scalabrin, S., Cattonaro, F., Morgante, M., Scarascia Mugnozza, G., Keurentjes, J. J. B., Harfouche, A. (2017). De novo assembly, functional annotation, and analysis of the giant reed (*Arundo donax* L.) leaf transcriptome provide tools for the development of a biofuel feedstock. Biotechnol. Biofuels., 10, 138.

Facchini, P. (1941). La Canna gentile per la produzione della cellulosa nobile l'impresa agricolo-industriale di Torviscosa. SNIA VISCOSA, Milano.

Fargione, J. E., Plevin, R. J., Hill, J. D. (2010). The ecological impact of biofuels. Annu. Rev. Ecol. Evol. Syst., 41, 351–377.

Fesenko, E, Edwards, R. (2014). Plant synthetic biology: A new platform for industrial biotechnology. Journal of Experimental Botany, 65 (8), 1927-1937.

Fazio, S., Barbanti, L. (2014). Energy and economic assessments of bio-energy systems based on annual and perennial crops for temperate and tropical areas. Renew. Energ., 69, 233–241.

Fazio, S., Monti, A. (2011). Life cycle assessment of different bioenergy production systems including perennial and annual crops. Biomass Bioenergy, 35, 4868-4878.

Fernando, A. L., Boleo, S., Barbosa, B., Costa, J., Duarte, M. P., Monti, A. (2015). Perennial grass production opportunities on marginal Mediterranean land. BioEnergy Res., 8, 1523–1537.

Fiala, M. (2009). Biomasse erbacee poliennali adatte alla combustione. Inf. Agrar., 30, 50–3.

Finnegan, E. J., Genger, R. K., Kovac, K., Peacock, W. J., Dennis, E. S. (1998a). DNA methylation and the promotion of flowering by vernalization. Proc. Natl. Acad. Sci. USA, 95, 5824–5829.

Flowers, T. J. (2004). Improving crop salt tolerance. Journal of Experimental Botany, 55 (396), 307–319.

Ford, C. W. (1984). Accumulation of low molecular weight solutes in water-stressed tropical legumes. Phytochemistry, 23(5), 1007–1015.

Fragnire, C., Serrano, M., Abou-Mansour, E., Metraux, J. -P. and L'Haridon, F. (2011). Salicylic acid and its location in response to biotic and abiotic stress. FEBS Letters, 585(12), 1847–1852.

Fu, Y., Poli, M., Sablok, G., Wang, B., Liang, Y., La Porta, N., Velikova, V., Loreto, F., Li, M., Varotto, C. (2016). Dissection of early transcriptional responses to water stress

in *Arundo donax* L. by unigene-based RNA-seq. Biotechnol. Biofuels., 9, 54.

Fujita, Y., Fujita, M., Shinozaki, K. and Yamaguchi-Shinozaki, K. (2011). ABA-mediated transcriptional regulation in response to osmotic stress in plants. Journal of Plant Research, 124(4), 509–525.

Fujita, Y., Yoshida, T. and Yamaguchi-Shinozaki, K. (2013). Pivotal role of the AREB/ABF-SnRK2 pathway in ABRE-mediated transcription in response to osmotic stress in plants. Physiologia Plantarum, 147(1), 15–27.

Fukuda, A. and Tanaka, Y. (2006). Effects of ABA, auxin, and gibberellin on the expression of genes for vacuolar H^+- inorganic pyrophosphatase, H^+-ATPase subunit A, and Na^+/H^+ antiporter in barley. Plant Physiology and Biochemistry, 44(5-6), 351–358.

Gadallah, M. A. A. (1999). Effects of proline and glycinebetaine on *Vicia faba* responses to salt stress. Biologia Plantarum, 42(2), 249–257.

Gallusci, P., Hodgman, C., Teyssier, E., Seymour, G.B. (2016). DNA methylation and chromatin regulation during fleshy fruit development and ripening. Front. Plant Sci., 7, 807.

Galvez, F. J., Baghour, M., Hao, G., Cagnac, O., Rodriguez-Rosales, M. P. and Venema, K. (2012). Expression of LeNHX isoforms in response to salt stress in salt sensitive and salt tolerant tomato species. Plant Physiology and Biochemistry, 51, 109–115.

Gan, J., Smith, C. T. (2011). Drivers for renewable energy: a comparison among OECD countries. Biomass Bioenergy, 35, 4497-4503.

Gao, J. P., Chao, D. Y., and Lin, H. X. (2007). Understanding abiotic stress tolerance mechanisms: recent studies on stress response in rice. J. Integ. Plant Biol., 49, 742–750.

Gao, Z., Sagi, M. and Lips, S. H. (1998). Carbohydrate metabolism in leaves and assimilate partitioning in fruits of tomato (*Lycopersicon esculentum* L.) as affected by salinity. Plant Science, 135(2), 149–159.

Gawronska, K., Romanowska, E., Miszalski, Z., Niewiadomska, E. (2013). Limitation of C3-CAM shift in the common iceplant under high irradiance. J Plant Physiol., 170, 129–135.

Gehring, M. et al. (2006). DEMETER DNA glycosylase establishes MEDEA polycomb gene self-imprinting by allele-specific demethylation. Cell, 124, 495–506.

Geilfus, C. M., Ludwig-Müller, J., Bárdos, G., Zörb, C. (2018). Early response to salt ions in maize (*Zea mays* L.). J Plant Physiol., 220, 173-180.

Giessow, J., Casanova, J., Lecler, R., MacArthur, R., Fleming, G. (2011). *Arundo donax* — distribution and impact report. California Invasive Plant Council.

Gilbert, R., Ferrel, J., Helsen, Z. (2010). Production of giant reed for biofuel. University of Florida; [SS-AGR-318 [online]. Available at https://edis.ifas.ufl.edu/ag327.

Giovannoni, J., Nguyen, C., Ampofo, B., Zhong, S. and Fei, Z. (2017). The epigenome and transcriptional dynamics of fruit ripening. Annu. Rev. Plant Biol., 68, 61–84.

Golldack, D., Li, C., Mohanand, H., Probst, N. (2014). Tolerance to drought and salt stress in plants: unraveling the signaling networks. Front Plant Sci., 5, 151.

Gong, Z. et al. (2002). ROS1, a repressor of transcriptional gene silencing in *Arabidopsis*, encodes a DNA glycosylase/lyase. Cell, 111, 803–814.

González-García, S., Iribarren, D., Susmozas, A., Dufour, J., Murphy, R. J. (2012). Life cycle assessment of two alternative bioenergy systems involving *Salix* spp. biomass: bioethanol production and power generation. Appl. Energy, 95, 111-122.

Grabherr, M. G., Haas, B. J., Yassour, M., Levin, J. Z., Thompson, D. A., Amit, I., Adiconis, X., Fan, L., Raychowdhury, R., Zeng, Q., et al. (2011). Full-length transcriptome assembly from RNA-Seq data without a reference genome. Nat. Biotechnol., 29, 644–652.

Gressel, J. (2008). Transgenics are imperative for biofuel crops. Plant. Sci., 174, 246-263.

Groth, M., Moissiard, G., Wirtz, M., Wang, H., Garcia-Salinas, C., Ramos-Parra, P. A., Bischof, S., Feng, S., Cokus, S. J., John, A., Smith, D. C., Zhai, J., Hale, C. J., Long, J. A., Hell, R., Díaz de la Garza, R. I., Jacobsen, S. E. (2016). MTHFD1 controls DNA methylation in *Arabidopsis*. Nat. Commun., 7, 11640.

Gu, C., Liu, L., Deng, Y., Zhang, Y., Wang, Z., Yuan, H., Huang, S. (2017). De novo characterization of the Iris lactea var. chinensis transcriptome and an analysis of genes under cadmium or lead exposure. Ecotoxicol. Environ. Saf., 144, 507–513.

Guan, Q., Wu, J., Yue, X., Zhang, Y., and Zhu, J. (2013). A nuclear calcium sensing pathway is critical for gene regulation and salt stress tolerance in *Arabidopsis*. PLoS Genet., 9:e1003755. doi: 10.1371/journal.pgen.1003755.

Guo, Y., Qiu, Q. -S., Quintero, F. J. et al. (2004). Transgenic evaluation of activated mutant alleles of SOS2 reveals a critical requirement for its kinase activity and C-terminal regulatory domain for salt tolerance in *Arabidopsis thaliana*. Plant Cell, 16(2), 435–449.

Guo, M., Song, W., Buhain, J. (2015). Bioenergy and biofuels: history, status and perspective. Renew. Sustain. Ener. Rev., 42, 712-725.

Gupta, A., Verma, J. P. (2015). Sustainable bio-ethanol production from ago-residues: a review. Renew. Sustain. Ener. Rev., 41, 550-567.

Gupta, B. and Huang, B. (2014). Mechanism of salinity tolerance in plants: physiological, biochemical, and molecular characterization. International Journal of Genomics, Volume 2014, Article ID 701596, 18 pages http://dx.doi.org/10.1155/2014/701596.

Gupta, K. J., Stoimenova, M. and Kaiser, W. M. (2005). In higher plants, only root mitochondria, but not leaf mitochondria reduce nitrite to NO, in vitro and in situ. Journal of Experimental Botany, 56(420), 2601–2609.

Gurmani, A. R., Bano, A., Khan, S. U., Din, J. and Zhang, J. L. (2011). Alleviation of salt stress by seed treatment with abscisic acid (ABA), 6-benzylaminopurine (BA) and chlormequat chloride (CCC) optimizes ion and organic matter accumulation and increases yield of rice (*Oryza sativa* L.). Australian Journal of Crop Science, 5(10), 1278–1285.

Haberl, H., Beringer, T., Bhattacharya, S.C., Erb, K. -H., Hoogwijk, M. (2010). The global technical potential of bio-energy in 2050 considering sustainability constraints. Curr. Opin. Environ. Sustain., 2, 394–403.

Haberl, H., et al. (2011). Global bioenergy potentials from agricultural land in 2050: Sensitivity to climate change, diets and yields. Biomass Bioenergy, 35, 4753–4769.

Haddadchi, A., Gross, C. L., Fatemi, M. (2013). The expansion of sterile *Arundo donax* (Poaceae) in southeastern Australia is accompanied by genotypic variation. Aquat. Bot., 104, 153–61.

Halfter, U., Ishitani, M., and Zhu, J. K. (2000). The *Arabidopsis* SOS2 protein kinase physically interacts with and is activated by the calcium-binding protein SOS3. Proc. Natl. Acad. Sci. USA, 97, 3735–3740.

Hamamoto, S., Marui, J., Matsuoka, K., Higashi, K., Igarashi, K., Nakagawa, T., et al. (2008). Characterization of a tobacco TPK-type K^+ channel as a novel tonoplast K^+ channel using yeast tonoplasts. J. Biol. Chem., 283, 1911–1920.

Hanin, M., Ebel, C., Ngom, M., Laplaze, L., Masmoudi, K. (2016). New insights on plant salt tolerance mechanisms and their potential use for breeding. Front. Plant. Sci., 7, 1787.

Hannon, M., Gimpel, J., Tran, M., Rasala, B., Mayfield, S. (2010). Biofuels from algae: challenges and potential. Biofuels, 1, 763-784.

Hanson, P. J., Sucoff, E. I., and Markhart, A. H. (1985). Quantifying apoplastic flux through red pine root systems

using trisodium, 3-hydroxy-5,8,10- pyrenetrisulfonate. Plant Physiol., 77, 21–24.

Hardion, L., Verlaque, R., Baumel, A., Juin, M., Vila, B. (2012). Revised systematics of Mediterranean *Arundo* (Poaceae) based on AFLP fingerprints and morphology. Taxon, 61, 1217–26.

Hasegawa, P. M., Bressan, R. A., Zhu, J. -K., and Bohnert, H. J. (2000). Plant cellular and molecular responses to high salinity. Annual Review of Plant Biology, 51, 463–499.

He, T. and Cramer, G. R. (1996). Abscisic acid concentrations are correlated with leaf area reductions in two salt-stressed rapid cycling Brassica species. Plant and Soil, 179(1), 25–33.

He, X. J., Chen, T. and Zhu, J. K. (2011). Regulation and function of DNA methylation in plants and animals. Cell Res., 21, 442–465.

Heaton, E. A., Dohleman, F. G., Long, S. P. (2008). Meeting US biofuel goals with less land: the potential of Miscanthus. GCB Bioenergy, 14, 2000–2014.

Henderson, I. R., Dean, C. (2004). Control of *Arabidopsis* flowering: the chill before the bloom. Development, 131, 3829–3838.

Hernandez, J. A., Ferrer, M. A., Jimenez, A., Barcelo, A. R., and Sevilla, F. (2001). Antioxidant systems and O_2^{-}/H_2O_2 production in the apoplast of pea leaves. Its relation with salt-induced necrotic lesions in minor veins. Plant Physiol., 127, 817–831.

Herrera, A. M., Dudley, T. (2003). Reduction of riparian arthropods abundance and diversity as a consequence

of giant reed (*Arundo donax*) invasion. Biol. Invasions, 5, 167–77.

Hill, J., Nelson, E., Tilman, D., Polasky, S., Tiffany, D. (2006). Environmental, economic, and energetic costs and benefits of biodiesel and ethanol biofuels. Proc. Natl. Acad. Sci. Usa, 103, 11206-10.

Ho, D. P., Ngo, H. H., Guo, W. (2014a). A mini review on renewable sources for biofuel. Biores. Technol., 169, 742-749.

Höfler, S., Lorenz, C., Busch, T., Brinkkötter, M., Tohge, T., Fernie, A. R., Braun, H. P., Hildebrandt, T. M. (2016). Dealing with the sulfur part of cysteine: four enzymatic steps degrade l-cysteine to pyruvate and thiosulfate in *Arabidopsis* mitochondria. Physiol Plant., 157, 352–366.

Hoogwijk, M., Faaij, A., Eickhout, B., de Vries, B., Turkenburg, W. (2005). Potential of biomass energy out to 2100, for four IPCC SRES land-use scenarios. Biomass Bioenergy, 29, 225–257.

Hoogwijk, M., Faaij, A., van den Broek, R., Berndes, G., Gielen, D., Turkenburg, W. (2003). Exploration of the ranges of the global potential of biomass for energy. Biomass Bioenergy, 25, 119–133.

Hoque, M. A., Banu, M. N. A., Nakamura, Y., Shimoishi, Y., Murata, Y. (2008). Proline and glycinebetaine enhance antioxidant defense and methylglyoxal detoxification systems and reduce NaCl-induced damage in cultured tobacco cells. J Plant Physiol., 165, 813–824.

Hoque, M. A., Banu, M. N. A., Okuma, E. et al. (2007). Exogenous proline and glycinebetaine increase NaCl-

induced ascorbate-glutathione cycle enzyme activities, and proline improves salt tolerance more than glycinebetaine in tobacco Bright Yellow-2 suspension-cultured cells. Journal of Plant Physiology, 164(11), 1457–1468.

Horie, T., Costa, A., Kim, T. H., Han, M. J., Horie, R., Leung, H. -Y., et al. (2007). Rice OsHKT2;1 transporter mediates large Na^+ influx component into K^+-starved roots for growth. EMBO J., 26, 3003–3014.

Hossain, K. K., Itoh, R. D., Yoshimura, G. et al. (2010). Effects of nitric oxide scavengers on thermoinhibition of seed germination in *Arabidopsis thaliana*. Russian Journal of Plant Physiology, 57(2), 222–232.

Hossain, M. A., Munemasa, S., Uraji, M., Nakamura, Y., Mori, I. C., and Murata, Y. (2011). Involvement of endogenous abscisic acid in methyl jasmonate-induced stomatal closure in *Arabidopsis*. Plant Physiology, 156(1), 430–438.

Hu, Y., Chen, L., Wang, H., Zhang, L., Wang, F. and Yu, D. (2013). *Arabidopsis* transcription factor WRKY8 functions antagonistically with its interacting partner VQ9 to modulate salinity stress tolerance. The Plant Journal, 74, 730–745.

Huang, G., Ma, S., Bai, L., Zhang, L., Ma, H., Jia, P., Liu, J., Zhong, M., Guo, Z. (2011). Signal transduction during cold, salt, and drought stresses in plants. Mol. Biol. Rep., 39, 969–987.

Huettel, B., Kanno, T., Daxinger, L., Aufsatz, W., Matzke, A. J., Matzke, M. (2006). Endogenous targets of RNA-directed DNA methylation and Pol IV in *Arabidopsis*. EMBO J., 25, 2828–2836.

Hunter, A. W. S. (1934). A karyosystematic investigation in Gramineae. Can. J. Res., 11,213–41.

IEA, International Energy Agency (2017). Technology Roadmap. Delivering Sustainable Bioenergy. OECD/IEA, Paris.

Irizarry, R. A., Ladd-Acosta, C., Carvalho, B., Wu, H., Brandenburg, S. A., Jeddeloh, J. A., Wen, B., Feinberg, A. P. (2008). Comprehensive high-throughput arrays for relative methylation (CHARM). Genome Res., 18, 780-790.

Isayenkov, S. V. (2012). Physiological and molecular aspects of salt stress in plants. Cytol. Genet., 46, 302–318.

Isayenkov, S. V. and Maathuis, F. J. M. (2019). Plant salinity stress: many unanswered questions remain. Frontiers in Plant Science, 10, Article 80.

Ishitani, M., Liu, J., Halfter, U., Kim, C. S., Shi, W., Zhu, J. K. (2000). SOS3 function in plant salt tolerance requires N-myristoylation and calcium-binding. Plant Cell, 12, 1667-1677.

Isner, J. C., and Maathuis, F. J. M. (2016). cGMP signalling in plants: from enigma to mainstream. Functional Plant Biol., 45, 93–101.

Ito, Y., Katsura, K., Maruyama, K. et al. (2006). Functional analysis of rice DREB1/CBF-type transcription factors involved in cold responsive gene expression in transgenic rice. Plant and Cell Physiology, 47(1), 141–153.

James, R. A., Blake, C., Byrt, C. S. and Munns, R. (2011). Major genes for Na^+ exclusion, Nax1 and Nax2 (wheat HKT1;4 and HKT1;5), decrease Na^+ accumulation in bread wheat leaves under saline and waterlogged conditions. Journal of Experimental Botany, 62(8), 2939–2947.

Jayakannan, M., Bose, J., Babourina, O., Rengel, Z., and Shabala, S. (2013). Salicylic acid improves salinity tolerance in *Arabidopsis* by restoring membrane potential and preventing salt-induced K^+ loss via a GORK channel. J Exp. Bot., 64, 2255–2268.

Jeschke, W. D., Peuke, A. D., Pate, J. S. and Hartung, W. (1997). Transport, synthesis and catabolism of abscisic acid (ABA) in intact plants of castor bean (*Ricinus communis* L.) under phosphate deficiency and moderate salinity. Journal of Experimental Botany, 48(314), 1737–1747.

Jiang, W. Z., Henry, I. M., Lynagh. P. G., Comai, L., Cahoon, E. B., Weeks, D. P. (2016). Significant enhancement of fatty acid composition in seed of the allohexaploid, *Camelina sativa*, using CRISPR/Cas9 gene editing. Plant Biotechnol. J., 15(5), 648-657.

Jin, E., Sutherland, J. W. (2018). An integrated sustainability model for a bioenergy system: forest residues for electricity generation. Biomass Bioenergy, 119, 10-21.

Johnson, R. R., Wagner, R. L., Verhey, S. D. and WalkerSimmons, M. K. (2002). The abscisic acid-responsive kinase PKABA1 interacts with a seed-specific abscisic acid response element-binding factor, TaABF, and phosphorylates TaABF peptide sequences. Plant Physiology, 130(2), 837–846.

Jones, H. G., Jones, M. B. (1989). Introduction: some terminology and common mechanisms, in: Jones, H. G., Flowers, T. J., Jones, M. B. (Eds.), Plants Under Stress, Cambridge university Press, Cambridge, pp. 1–10.

Kachmar, J. F., and Boyer, P. D. (1953). The potassium activation and calcium inhibition of pyruvic phosphoferase. J. Biol. Chem., 200, 669–682.

Kagale, S., Koh, C., Nixon, J., Bollina, V., Clarke, W. E., Tuteja, R., Spillane, C., Robinson, S. J., Links, M. G., Clarke, C., Higgins, E. E., Huebert, T., Sharpe, A. G., Parkin, I. A. P. (2014). The emerging biofuel crop Camelina sativa retains a highly undifferentiated hexaploidy genome structure. Nat. Comm., 5, 3706.

Kang, D. -J., Seo, Y. -J., Lee, J. -D. et al. (2005). Jasmonic acid differentially affects growth, ion uptake and abscisic acid concentration in salt-tolerant and salt-sensitive rice cultivars. Journal of Agronomy and Crop Science, 191(4), 273–282.

Kankel, M. W., Ramsey, D. E., Stokes, T. L., Flowers, S. K., Haag, J. R., Jeddeloh, J. A., Riddle, N. C., Verbsky, M. L., Richards, E.J. (2003). *Arabidopsis* MET1 cytosine methyltransferase mutants. Genetics, 163, 1109–1122.

Kaur, G., Asthir, B. (2015). Proline: a key player in plant abiotic stress tolerance. Biol Plant., 59(4), 609-619.

Kendall, A., Yuan, J. (2013). Comparing life cycle assessment of different biofuel options. Curr. Opi. Chem. Biol., 17, 439-443.

Kerepesi, I. and Galiba, G. (2000). Osmotic and salt stress-induced alteration in soluble carbohydrate content in wheat seedlings. Crop Science, 40(2), 482–487.

Keskin, B. C., Sarikaya, A. T., Yuksel, B. and Memon, A. R. (2010). Abscisic acid regulated gene expression in bread wheat (*Triticum aestivum* L.). Australian Journal of Crop Science, 4(8), 617–625.

Khan, M. A., Ungar, I. A. and Showalter, A. M. (2000). Effects of sodium chloride treatments on growth and ion accumulation of the halophyte haloxylon recurvum.

Communications in Soil Science and Plant Analysis, 31(17-18), 2763–2774.

Khan, S., Stone, J. M. (2007). *Arabidopsis thaliana* GH3.9 influences primary root growth. Planta, 226, 21–34.

Khudamrongsawat, J., Tayyar, R., Holt, J. S. (2004). Genetic diversity of giant reed (*Arundo donax*) in the Santa Ana River, California. Weed Sci., 52, 395–405.

Kiegle, E., Moore, C. A., Haseloff, J., Tester, M. A., and Knight, M. R. (2000). Cell-type-specific calcium responses to drought, salt and cold in the *Arabidopsis* root. Plant J., 23, 267–278.

King, G. (2015). Crop epigenetics and the molecular hardware of genotype x environment interactions. Front. Plant Sci., 6, 968.

Knight, H., Trewavas, A. J., and Knight, M. R. (1997). Calcium signaling in *Arabidpsis thaliana* responding to drought and salinity. Plant J., 12, 1067–1078.

Kopetz, H. (2013). Renewable resources: build a biomass energy market. Nature, 494, 29-31.

Krishnamurthy, P., Ranathunge, K., Franke, R., Prakash, H., Schreiber, L., and Mathew, M. (2009). The role of root apoplastic transport barriers in salt tolerance of rice (*Oryza sativa* L.). Planta, 230, 119–134.

Krüßel, L., Junemann, J., Wirtz, M., Birke, H., Thornton, J. D., Browning, L. W., Poschet, G., Hell, R., Balk, J., Braun, H., Hildebrandt, T. M. (2014). The mitochondrial sulfur dioxygenase ETHYLMALONIC ENCEPHALOPATHY PROTEIN1 is required for amino acid catabolism during carbohydrate starvation and embryo development in *Arabidopsis*. Plant Physiol., 165, 92–104.

Kukurba, K.R. and Montgomery, S.B. (2015). RNA Sequencing and Analysis. Cold Spring Harb. Protoc.; doi:10.1101/pdb.top084970.

Kumar, S., Beena, A. S., Awana, M. and Singh, A. (2017). Salt-induced tissue-specific cytosine methylation downregulates expression of HKT genes in contrasting wheat (*Triticum aestivum* L.) genotypes. DNA and cell biology, 36(4), 283–294.

Kuromori, T., Seo, M., Shinozaki, K. (2018). ABA transport and plant water stress responses. Trends Plant Sci., 23(6), 513-522.

Ladanai, S., Vinterbäck, J. (2009). Global Potential of Sustainable Biomass for Energy. SLU report 013, ISSN 1654-9406, Department of Energy and Technology, Uppsala.

Lam, M. K., Lee, K. T. (2012). Microalgae biofuels: a critical review of issues, problems and the way forward. Biotech. Adv., 30, 673-690.

Lamattina, L., Garcìa-Mata, C., Graziano, M. and Pagnussat, G. (2003). Nitric oxide: the versatility of an extensive signal molecule. Annual Review of Plant Biology, 54, 109–136.

Lang, Z., Wang, Y., Tang, K., Tang, D., Datsenka, T., Cheng, J., Zhang, Y., Handa, A. K., Jian-Kang Zhu, J. K. (2017). Critical roles of DNA demethylation in the activation of ripening-induced genes and inhibition of ripening-repressed genes in tomato fruit. Proc. Natl Acad. Sci. USA. 114, E4511–E4519.

Lange, J. P. (2007). Lignocellulose conversion: an introduction to chemistry, process and economics. Biofuels, Bioprod. Biorefin., 1, 39–48.

Laohavisit, A., Richards, S. L., Shabala, L., Colaço, R. D. D. R., Swarbreck, S. M., et al. (2013). Salinity-induced calcium signaling and root adaptation in *Arabidopsis* require the calcium regulatory protein annexin1. Plant Physiol. 163, 253–262.

Latz, A., Mehlmer, N., Zapf, S., Mueller, T. D., Wurzinger, B., Pfister, B., Csaszar, E., Hedrich, R., Teige, M., Becker, D. (2013). Salt stress triggers phosphorylation of the arabidopsis vacuolar K^+ channel TPK1 by cal. Molecular Plant, 6 (4), 1274-1289.

Legué, V., Blancaflor, E., Wymer, C., Perbal, G., Fantin, D., and Gilroy, S. (1997). Cytoplasmic free Ca^{2+} in *Arabidopsis* roots changes in response to touch but not gravity. Plant Physiol., 114, 789–800.

Leng, Q., Mercier, R. W., Hua, B. G., Fromm, H., and Berkowitz, G. A. (2002). Electrophysiological analysis of cloned cyclic nucleotide-gated ion channels. Plant Physiol., 128, 400–410.

Lewandowski, I., Scurlock, J. M., Lindvall, E., Christou, M. (2003). The development and current status of perennial rhizomatous grasses as energy crops in the US and Europe. Biomass Bioenergy, 25, 335–61.

Li, X., et al. (2008). Major energy plants and their potential for bioenergy development in China. Environ. Manage., 46, 579–589.

Li, B., Carey, M. and Workman, J. L. (2007). The role of chromatin during transcription. Cell., 128, 707–719.

Li, J. J., Jiang, C. R., Brown, J. B., Huang, H., Bickel, P. J. (2011). Sparse linear modeling of next-generation mRNA sequencing (RNA-Seq) data for isoform discovery

and abundance estimation. Proc. Natl. Acad. Sci., 108, 19867–19872.

Li, W., Ma, M., Feng, Y., Li, H., Wang, Y., Ma, Y., Li, M., An, F. Y., Guo, H. W. (2015). EIN2-Directed translational regulation of ethylene signaling in *Arabidopsis*. Cell., 163, 670-683.

Li, Y. C., Korol, A. B., Fahima, T., Nevo, E. (2004). Microsatellites within genes: structure, function, and evolution. Mol. Biol. Evol., 21, 991–1007.

Light, K. M., Wisniewski, J. A., Vinyard, W. A., Kieber-Emmons, M. T. (2016). Perception of the plant hormone ethylene: known-knowns and known-unknowns. J Biol Inorg Chem., 21, 715–728.

Lindroth, A. M., Cao, X., Jackson, J. P., Zilberman, D., McCallum, C. M., Henikoff, S., Jacobsen, S. E. (2001). Requirement of CHROMOMETHYLASE3 for maintenance of CpXpG methylation. Science, 292, 2077–2080.

Liu, J., Ishitani, M., Halfter, U., Kim, C. S., Zhu, J. K. (2000). The *Arabidopsis thaliana* SOS2 gene encodes a protein kinase that is required for salt tolerance. Proc. Natl. Acad. Sci. USA, 97, 3730– 3734.

Liu, J. and Zhu, J. K. (1998). A calcium sensor homolog required for plant salt tolerance. Science, 280, 1943–1945.

Liu, Z. W., Shao, C. R., Zhang, C. J., Zhou, J. X., Zhang, S. W., Li, L., Chen, S., Huang, H. W., Cai, T., He, X. J. (2014). The SET domain proteins SUVH2 and SUVH9 are required for Pol V occupancy at RNA-directed DNA methylation loci. PLoS Genet., DOI: 10.1371/journal.pgen.1003948.

Lo Cicero, L., Madesis, P., Tsaftaris, A., Lo Piero, A. R. (2015). Tobacco plants over-expressing the sweet orange tau glutathione transferases (CsGSTUs) acquire tolerance to the diphenyl ether herbicide fluorodifen and to salt and drought stresses. Phytochemistry, 116(1), 69-77.

Lord, R. (2015). Reed canarygrass (*Phalaris arundinacea*) outperforms Miscanthus or willow on marginal soils, brownfield and non-agricultural sites for local, sustainable energy crop production. Biomass Bioenergy, 78, 110–125.

Lorenzi, G., Baptista, P. (2018). Promotion of renewable energy sources in Portuguese transport sector: a scenario analysis. J. Clean. Prod. 186, 918-932.

Lowe, S., Browne, M., Boudjelas, S., De Poorter, M. (2000). 100 of the world's worst invasive alien species: a selection from the global invasive species database. Proceedings of World Conservation Union (IUCN), Auckland.

Lu, C. and Kang, J. (2008). Generation of transgenic plants of a potential oilseed crop *Camelina sativa* by *Agrobacterium*-mediated transformation. Plant Cell Rep., 27, 273-278.

Lukens, L. N., Zhan, S. (2007). The plant genome's methylation status and response to stress: implications for plant improvement. Curr Opin Plant Biol., 10(3):317–322.

Maathuis, F. J. M. (2006). The role of monovalent cation transporters in plant responses to salinity. J. Exp. Bot., 57, 1137–1147.

Maathuis, F. J. M. (2009). Physiological functions of mineral macronutrients. Curr. Opin. Plant. Biol., 12, 250–258.

Maathuis, F. J. M. (2014). Sodium in plants: perception, signalling, and regulation of sodium fluxes. J. Exp. Bot., 65, 849–858.

Maathuis, F. J. M., Ahmad, I., and Patishtan, J. (2014). Regulation of Na^+ fluxes in plants. Front. Plant Sci., 5:467.

Maathuis, F. J. M., and Amtmann, A. (1999). K^+ nutrition and Na^+ toxicity: the basis of cellular K^+/Na^+ ratios. Ann. Bot., 84, 123–133.

Maathuis, F. J. M., and Sanders, D. (2001). Sodium uptake in *Arabidopsis* roots is regulated by cyclic nucleotides. Plant Physiol., 127, 1617–1625.

Mack, R. N. (2008). Evaluating the credits and the debits of a proposed biofuel species: giant reed (*Arundo donax*). Weed Sci., 56, 883–8.

Mahajan, S., Pandey, G. K., and Tuteja, N. (2008). Calcium- and salt-stress signaling in plants: shedding light on SOS pathway. Arch. Biochem. Biophys., 471, 146–158.

Mahajan, S., Tuteja, N. (2005). Cold, salinity and drought stresses: an overview. Archives of Biochemistry and Biophysics, 444, 139–158.

Makela, P., Karkkainen, J. and Somersalo, S. (2000). Effect of glycinebetaine on chloroplast ultrastructure, chlorophyll and protein content, and RuBPCO activities in tomato grown under drought or salinity. Biologia Plantarum, 43(3), 471– 475.

Mandi, L., Abissy, M. (2000). Utilization of *Arundo donax* and *Typha latifolia* for heavy metal removal from urban wastewater. Reuse of treated wastewater for alfalfa irrigation. Proceedings of world water congress, Paris.

Mantineo, M., D'Agosta, G. M., Copani, V., Patanè, C., Cosentino, S. L. (2009). Biomass yield and energy balance of three perennial crops for energy use in the semi-arid Mediterranean environment. Field Crop Res., 114, 204–213.

Mariani, C., Cabrini, R., Danin, A., Piffanelli, P., Fricano, A., Gomarasca, S. et al. (2010). Origin, diffusion and reproduction of the giant reed (*Arundo donax* L.): a promising weedy energy crop. Ann. Appl. Biol., 157, 191–202.

Marques, A. C., Fuinhas, J. A., Pereira, D. A. (2018). Have fossil fuels been substitute by renewable? An empirical assessment for 10 European countries. Energy Policy, 116, 257-265.

MartìnezAtienza, J., Jiang, X., Garciadeblas, B., Mendoza, I., Zhu, J., Pardo, J. M., Quintero, F. J. (2007). Conservation of the salt overly sensitive pathway in rice. Plant Physiol., 143, 1001–1012.

Mata, T. M., Martins, A. A., Caetano, N. (2010). Microalgae for biodiesel production and other applications: a review. Renew. Sust. Energy Rev., 14, 217-232.

Mathioudakis, V., Gerbens-Leenes, P. W., Van der Meer, T. H., Hoekstra, A. Y. (2017). The water footprint of second-generation bioenergy: a comparison of biomass feedstock and conversion techniques. J. Clean. Prod., 148, 571-582.

Matysik, J., Alia, A., Bhalu, B. and Mohanty, P. (2002). Molecular mechanisms of quenching of reactive oxygen

species by proline under stress in plants. Current Science, 82(5), 525–532.

McBride, A. C., Dale, V. H., Baskaran, L. M., Downing, M. E., Eaton, L. M., Efroymson, R. A., et al. (2011). Indicators to support environmental sustainability of bioenergy systems. Ecol. Indicat., 11, 1277-1289.

Mehmood, M. A., Ibrahimb, M., Rashid, U., Alib, M. N. S., Hussain, A., Gull, E. (2017). Biomass production for bioenergy using marginal lands. Sustainable Prod Consumption, 9, 3-2.

Metzger, J. O., Huttermann, A. (2009). Sustainable global energy supply based on lignocellulosic biomass from afforestation of degraded areas. Naturwissenschaften, 96, 279–288.

Metzker, M. L. (2010). Sequencing technologies—The next generation. Nat. Rev. Genet., 11, 31–46.

Mezlini, A. M., Smith, E. J. M., Fiume, M., Buske, O., Savich, G. L., Shah, S., Aparicio, S., Chiang, D. Y., Goldenberg, A., Brudno, M. (2013). iReckon: Simultaneous isoform discovery and abundance estimation from RNA-seq data. Genome Res., 23, 519–529.

Mian, A., Oomen, R. J., Isayenkov, S., Sentenac, H., Maathuis, F. J. M., and Véry, A. A. (2011). Over-expression of an Na^+-and K^+-permeable HKT transporter in barley improves salt tolerance. Plant J., 68, 468–79.

Miller, G., Suzuki, N., Ciftci-Yilmaz, S., and Mittler, R. (2010). Reactive oxygen species homeostasis and signalling during drought and salinity stresses. Plant Cell Environ., 33, 453–67.

Mizoi, J., Shinozaki, K. and Yamaguchi-Shinozaki, K. (2012). AP2/ERF family transcription factors in plant abiotic stress responses. Biochimica et Biophysica Acta—Gene Regulatory Mechanisms, 1819(2), 86–96.

Monti, A., Cosentino, S. L. (2015). Conclusive results of the European project OPTIMA: Optimization of perennial grasses for biomass production in the mediterranean area. BioEnergy Res., 8, 1459–1460.

Monti, A., Fazio, S., Venturi, G. (2009). Cradle-to-farm gate life cycle assessment in perennial energy crops. Eur. J. Agron 31, 77–84.

Moon, G. J., Clough, B. F., Peterson, C. A., and Allaway, W. G. (1986). Apoplastic and symplastic pathways in *Avicennia marina* (Forsk.) Vierh. roots revealed by fluorescent tracer dyes. Aust. J. Plant Physiol., 13, 637–648.

Msanne, J., Lin, J., Stone, J. M., Awada, T. (2011). Characterization of abiotic stress-responsive *Arabidopsis* thaliana RD29A and RD29B genes and evaluation of transgenes. Planta, 234(1), 97–107.

Muench, S., Guenther, E. (2013). A systematic review of bioenergy life cycle assessments. Appl. Energy, 112, 257-273.

Munns, R., and Passioura, J. B. (1984). Hydraulic resistance of plants. Effects of NaCl in barley and lupin. Aust. J. Plant Physiol., 11, 351–359.

Munns, R., and Termaat, A. (1986). Whole-plant responses to salinity. Aust. J. Plant Physiol., 13, 143–160.

Munns, R. and Tester, M. (2008). Mechanisms of salinity tolerance. Annual Review of Plant Biology, 59, 651–681.

Nackley, L. L. and Kim, S. H. (2015). A salt on the bioenergy and biological invasions debate: salinity tolerance of the invasive biomass feedstock *Arundo donax*. GCB Bioenergy, 7, 752–762.

Nakashima, K., Tran, L. -S. P., Van Nguyen, D. et al. (2007). Functional analysis of a NAC-type transcription factor OsNAC6 involved in abiotic and biotic stress-responsive gene expression in rice. Plant Journal, 51(4), 617–630.

Nassi o Di Nasso, N., Roncucci, N., Bonari, E. (2013). Seasonal dynamics of aboveground and belowground biomass and nutrient accumulation and remobilization in giant reed (*Arundo donax* L.): a three-year study on marginal land. Bioenergy Res., 6, 725–36.

Negrão, S., Courtois, B., Ahmadi, N., Abreu, I., Saibo, N., and Oliveira, M. (2011). Recent updates on salinity stress in rice: from physiological to molecular responses. Crit. Rev. Plant Sci., 30, 329–377.

Nguyen, H. T., Silva, J. E., Podicheti, R., Macrander, J., Yang, W., Nazarenus, T. J., Nam, J. W., Jaworski, J. G., Lu, C., Scheffler, B. E., Mockaitis, K., Cahoon, E. B. (2013). Camelina seed transcriptome: a tool for meal and oil improvement and translational research. Plant Biotech. J., 11, 759-769.

Nixon, D., Stephens, W., Tyrrel, S., Brierley, E. (2001). The potential for short rotation energy forestry on restored landfill caps. Bioresour. Technol., 77, 237–245.

Nounjan, N., Nghia, P. T. and Theerakulpisut, P. (2012). Exogenous proline and trehalose promote recovery of rice seedlings from salt-stress and differentially modulate

antioxidant enzymes and expression of related genes. Journal of Plant Physiology, 169(6), 596–604.

Oakes, C. C., La Salle, S., Robaire, B., and Trasler, J. M. (2006). Evaluation of a quantitative DNA methylation analysis technique using methylation-sensitive/ dependent restriction enzymes and real-time PCR. Epigenetics, 1(3), 146-152.

Offermann, R., Seidenberger, T., Thrän, D., Kaltschmitt, M., Zinoviev, S., Miertus, S. (2011). Assessment of global bioenergy potentials. Mitig. Adapt. Strateg. Glob. Change, 16, 103-115.

Ohlrogge, J., Allen, D., Berguson, B., DellaPenna, D., Shachar-Hill, Y., Stymne, S. (2009). Driving on biomass. Science, 324, 1019–1020.

Ortega-Galisteo, A. P., Morales-Ruiz, T., Ariza, R. R. & Roldan-Arjona, T. (2008). *Arabidopsis* DEMETER-LIKE proteins DML2 and DML3 are required for appropriate distribution of DNA methylation marks. Plant Mol. Biol., 67, 671–681.

Oshlack, A., Wakefield, M. J. (2009). Transcript length bias in RNA-seq data confounds systems biology. Biol. Direct., 4, 14.

Pan, Y. B., Scheffler, B. S., Richard, E. P. Jr. (2007). High throughput molecular genotyping of commercial sugarcane clones with microsatellite (SSR) DNA markers. Sugar Tech., 9, 176–181.

Panta, S., Flowers, T. J., Lane, P., Doyle, R., Haros, G., Shabala, S. (2014). Halophyte agriculture: success stories. Environ Exp Bot., 107, 71–83.

Papazoglou, E. G., Karantounias, G. A., Vemmos, S. N., Bouranis, D. L. (2005). Photosynthesis and growth responses of giant reed (*Arundo donax* L.) to the heavy metals Cd and Ni. Environ. Int., 31, 243–9.

Papazoglou, E. G., Serelis, K. G., Bouranis, D. L. (2007). Impact of high cadmium and nickel soil concentration on selected physiological parameters of *Arundo donax* L. Eur. J. Soil. Biol., 43, 207–15.

Parida, A. K., Das, A. B. and Mohanty, P. (2004). Investigations on the antioxidative defence responses to NaCl stress in a mangrove, *Bruguiera parviflora*: differential regulations of isoforms of some antioxidative enzymes. Plant Growth Regulation, 42(3), 213–226.

Patishtan, J., Hartley, T. N., Fonseca de Carvalho, R., and Maathuis, F. J. M. (2018). Genome wide association studies to identify rice salt-tolerance markers. Plant Cell Environ., 41, 970–982.

Pauwels, L., Morreel, K., De Witte, E., Lammertyn, F., Van Montagu, M., Boerjan, W., Inze, D., Goossens, A. (2008). Mapping methyl jasmonate-mediated transcriptional reprogramming of metabolism and cell cycle progression in cultured Arabidopsis cells. Proc Natl Acad Sci USA, 105, 1380–1385.

Peck, G. (1998). Hydroponic growth characteristics of *Arundo donax* L. under salt stress. Proceedings of the *Arundo* and saltcedar management workshop, Ontario.

Pedroli, B., Elbersen, B., Frederiksen, P., Grandin, U., Heikkilä, R., Krogh, P. H. et al. (2013). Is energy cropping in Europe compatible with biodiversity? – Opportunities and threats to biodiversity from land-based production of biomass for bioenergy purposes. Biomass & Bioenergy, 55, 73–86.

Perdue, R. E. (1958). *Arundo donax* — source of musical reeds and industrial cellulose. Econ. Bot., 12, 368–404.

Peterson, G., Galbraith, J. K. (1932). The concept of marginal land. J. Farm. Econ., 14, 295–310.

Pikaard, C. S. and Mittelsten Scheid, O. (2014). Epigenetic regulation in plants. Cold Spring Harb. Perspect. Biol., DOI: 10.1101/cshperspect.a019315.

Pilu, R., Cassani, E., Landoni, M., Cerino Badone, F., Passera, A., Cantaluppi, E., et al. (2014). Genetic characterization of Italian giant reed (*Arundo donax* L.) clones collection: exploiting clonal selection. Euphytica, 196, 169–81.

Pitman, M. G. (1982). Transport across plant roots. Q. Rev. Biophys., 15, 481–554.

Pizzolongo, P. (1962). Osservazioni cariologiche su *Arundo donax* e *Arundo plinii*. Annu. Bot., 27, 173–87.

Pompeiano, A., Vita, F., Miele, S., Guglielmetti, L. (2013). Freeze tolerance and physiological changes during cold acclimation of giant reed [*Arundo donax* (L.)]. Grass Forage Sci. http://dx.doi.org/10.1111/gfs.12097.

Poli, M., Salvi, S., Li, M., Varotto, C. (2017). Selection of reference genes suitable for normalization of qPCR data under abiotic stresses in bioenergy crop Arundo donax L. Sci. Rep., 7, 10719.

Polunin, O. and Huxley, A. (1987). Flowers of the Mediterranean. London: Hogarth Press.

Popova, L. P., Stoinova, Z. G. and Maslenkova, L. T. (1995). Involvement of abscisic acid in photosynthetic

process in *Hordeum vulgare* L. during salinity stress. Journal of Plant Growth Regulation, 14(4), 211–218.

Powell, W., Machray, G. C., Provan, J. (1996). Polymorphism revealed by simple sequence repeats. Trends Plant Sci., 1, 215–222.

Priya, P., Jain, M. (2013). Rice SRTFDB: a database of rice transcription factors containing comprehensive expression, cis-regulatory element and mutant information to facilitate gene function analysis. Database (Oxford), 2013, 027.

Puglisi, I., Lo Cicero, L., Lo Piero, A. R. (2013). The glutathione S-transferase gene superfamily: an in silico approach to study the post translational regulation. Biodegradation, 24(4), 471-485.

Qin, Z., Zhuang, Q., Zhu, X., Cai, X., Zhang, X. (2011). Carbon consequences and agricultural implications of growing biofuel crops on marginal agricultural lands in China. Environ. Sci. Technol., 45, 10765–10772.

Qiu, Q. S., Guo, Y., Dietrich, M. A., Schumaker, K. S., Zhu, J. K. (2002). Regulation of SOS1, a plasma membrane Na^+/H^+ exchanger in *Arabidopsis thaliana*, by SOS2 and SOS3. Proc. Natl. Acad. Sci. USA, 99, 8436–8441.

Quinn, L. D., Rauterkus, M. A., Holt, J. S. (2007). Effects of nitrogen enrichment and competition on growth and spread of giant reed (*Arundo donax*). Weed Sci., 55, 319–26.

Quintero, F. J., Ohta, M., Shi, H., Zhu, J. K., Pardo, J. M. (2002). Reconstitution in yeast of the *Arabidopsis* SOS signaling pathway for Na^+ homeostasis. Proc. Natl. Acad. Sci. USA, 99, 9061–9066.

Ragauskas, A. J. (2016). Challenging/interesting lignin times. Biofuels Bioprod Biorefining Biofpr., 10, 489–491.

Rajendran, K., Tester, M., and Roy, S. J. (2009). Quantifying the three main components of salinity tolerance in cereals. Plant Cell Environ., 32, 237–249.

REN21. (2016), Renewables 2016 Global Status Report, (Paris: REN21 Secretariat).

REN21. (2018), Renewables 2018 Global Status Report, (Paris: REN21 Secretariat).

Reyes, J. C. (2006). Chromatin modifiers that control plant development. Curr. Opin. Plant Biol., 9, 21–27.

Reyna-Lopez, G. E., Simpson, J., Ruiz-Herrera, J. (1997). Differences in DNA methylation patterns are detectable during the dimorphic transition of fungi by amplification of restriction polymorphisms. Mol. Gen. Genet., 253 (6), 703-710.

Richards, E. J. (1997). DNA methylation and plant development. Trends Genet., 13(8):319–323.

Riffaldi, R., Saviozzi, A., Cardelli, R., Bulleri, F., Angelini, L. (2012). Comparison of soil organic matter characteristics under the energy crop giant reed, cropping sequence and natural grass. Commun. Soil. Sci. Plant., 41, 173–80.

Roberts, A., Pimentel, H., Trapnell, C., Pachter, L. (2011a). Identification of novel transcripts in annotated genomes using RNA-Seq. Bioinformatics, 27, 2325–2329.

Roberts, A., Trapnell, C., Donaghey, J., Rinn, J. L., Pachter, L. (2011b). Improving RNA-Seq expression

estimates by correcting for fragment bias. Genome Biol., 12, R22.

Robertson, G. P., et al. (2008). Agriculture sustainable biofuels redux. Science, 322, 49.

Robertson, G., Schein, J., Chiu, R., Corbett, R., Field, M., Jackman, S. D., Mungall, K., Lee, S., Okada, H. M., Qian, J. Q., et al. (2010). De novo assembly and analysis of RNA-seq data. Nat. Methods., 7, 909–912.

Rocha, P. S., Sheikh, M., Melchiorre, R., Fagard, M., Boutet, S., Loach, R., Moffatt, B., Wagner, C., Vaucheret, H., Furner, I. (2005). The *Arabidopsis* HOMOLOGY DEPENDENT GENE SILENCING1 gene codes for an S-adenosyl-L-homocysteine hydrolase required for DNA methylation-dependent gene silencing. Plant Cell., 17, 404–417.

Röder, M., Thornley, P. (2018). Waste wood as bioenergy feedstock. Climate change impacts and related emission uncertainties from waste wood based energy systems in UK. Waste Manag., 74, 241-252.

Rodrigues, J., Zilberman, D. (2015). Evolution and function of genomic imprinting in plants. Genes Dev., 29, 2517–31.

Roos, A., Ahlgren, S. (2018). Consequential life cycle assessment of bioenergy systems. A literature review. J. Clean Prod., 189, 358-373.

Rossa, B,, Tuffers, A. V., Naidoo, G., von Willert, D. J. (1998). *Arundo donax* L. (Poaceae) - a C3 species with unusually high photosynthetic capacity. Bot. Acta., 111, 216–21.

Roy, S. J., Negrão, S., and Tester, M. (2014). Salt resistant crop plants. Curr. Opin. Biotechnol., 26, 115–124.

RoyChoudhury, A., Gupta, B. and Sengupta, D. N. (2008). Trans-acting factor designated OSBZ8 interacts with both typical abscisic acid responsive elements as well as abscisic acid responsive element-like sequences in the vegetative tissues of indica rice cultivars. Plant Cell Reports, 27(4), 779–794.

Rubio, F., Flores, P., Navarro, J. M., and Martınez, V. (2003). Effects of Ca^{2+}, K^{+} and cGMP on Na^{+} uptake in pepper plants. Plant Sci., 165, 1043–1049.

Rus, A., Yokoi, S., Sharkhuu, A., Reddy, M., Lee, B. H., Matsumoto, T. K., et al. (2001). AtHKT1 is a salt tolerance determinant that controls Na entry into plant roots. Proc. Natl. Acad. Sci. USA, 98, 14150–14155.

Sablok, G., Fu, Y., Bobbio, V., Laura, M., Rotino, G. L., Bagnaresi, P., Allavena, A., Velikova, V., Viola, R., Loreto, F., Li, M., Varotto, C. (2014). Fuelling genetic and metabolic exploration of C3 bioenergy crops through the first reference transcriptome of *Arundo donax* L. Plant Biotechnol. J., 12, 554–567.

Saha, M., Eckelman, M. J. (2018). Geospatial assessment of regional scale bioenergy production potential on marginal and degraded land. Resour. Conserv. Recycl., 128, 90-97.

Sairam, R. K. and Tyagi, A. (2004). Physiology and molecular biology of salinity stress tolerance in plants. Current Science, 86(3), 407–421.

Saito, S., Hirai, N., Matsumoto, C., Ohigashi, H., Ohta, D., Sakata, K., Mizutani, M. (2004). *Arabidopsis* CYP707As

encode (+)-abscisic acid 8′-hydroxylase, a key enzyme in the oxidative catabolism of abscisic acid. Plant Physiol., 134, 1439–1449.

Sánchez, E., Scordia, D., Lino, G., Arias, C., Cosentino, S. L., Nogués, S. (2015). Salinity and water stress effects on biomass production in different *Arundo donax* L. clones. BioEnergy Research, 8(4), 1461–1479.

Sanders, D. (2000). Plant biology: the salty tale of *Arabidopsis*. Current Biology, 10(13), R486–R488.

Sanderson, J. (1983). Water uptake by different regions of the barley root. Pathways of radial flow in relation to development of the endodermis. J. Exp. Bot., 34, 240–253.

Sang, T., Zhu, W. (2011). China's bioenergy potential. GCB Bioenergy, 3, 79–90.

Sarsekeyeva, F., Zayadan, B. K., Usserbaeva, A., Bedbenov, V. S., Sinetova, M. A., Los, D. A. (2015). Cyanofuels: Biofuels from cyanobacteria. Reality and perspectives. Photosynthesis Research, 125 (1-2), 329-340.

Sawada, H., Shim, I. -S. and Usui, K. (2006). Induction of benzoic acid 2-hydroxylase and salicylic acid biosynthesis-modulation by salt stress in rice seedlings. Plant Science, 171(2), 263–270.

Saxena, S. C., Kaur, H., Verma, P. et al. (2013). Osmoprotectants: potential for crop improvement under adverse conditions. In Plant Acclimation to Environmental Stress, 197–232, Springer, New York, NY, USA.

Scandalios, J. G. (2005). Oxidative stress: molecular perception and transduction of signals triggering antioxidant gene defenses. Braz J Med Biol Res., 38, 995-1014.

Scarlat, N., Dallemand, J. F., Banja, M. (2013). Possible impact of 2020 bioenergy targets on European Union land use. A scenario-based assessment from national renewable energy action plans proposals. Renew. Sust. Energy Rev., 18, 595–606.

Scarlat, N., Dallemand, J. F., Monforti-Ferrario, F., Nita, V. (2015). The role of biomass and bioenergy in a future bioeconomy: policies and fact. Env. Develop, 15, 3-34.

Schena, M., Shalon, D., Davis, R. W., Brown, P. O. (1995). Quantitative monitoring of gene expression patterns with a complementary DNA microarray. Science, 270, 467–470.

Schmidt, R., Mieulet, D., Hubberten, H. M., Obata, T., Hoefgen, R., Fernie, A. R., et al. (2013). Salt-responsive ERF1 regulates reactive oxygen species dependent signaling during the initial response to salt stress in rice. Plant Cell, 25, 2115–2131.

Schnable, P. S., Springer, N. M. (2013). Progress toward understanding heterosis in crop plants. Annu. Rev. Plant Biol., 64, 71–88.

Schulz, M. H., Zerbino, D. R., Vingron, M., Birney, E. (2012). Oases: Robust de novo RNA-seq assembly across the dynamic range of expression levels. Bioinformatics, 28, 1086–1092.

Scott, S. A., Davey, M. P., Dennis, J. S., Horst, I., Howe, C. J., Lea-Smith, D. J., Smith, A. G. (2010). Biodiesel from algae: challenges and prospects. Curr. Opi. Biotech., 21, 277-286.

Selkoe, K. A., Toonen, R. J. (2006). Microsatellites for ecologists: a practical guide to using and evaluating microsatellite markers. Ecol. Lett., 9, 615–629.

Serba, D. D., Uppalapati, S. R., Krom, N., Mukherjee, S., Tang, Y., Mysore, K., Saha, M. C. (2016). Transcriptome analysis in switchgrass discloses ecotype difference in photosynthetic efficiency. BMC Genom., 17, 1040.

Seymour, G., Poole, M., Manning, K., King, G. J. (2008). Genetics and epigenetics of fruit development and ripening. Curr. Opin. Plant. Biol., 11, 58–63.

Shabala, S. (2009). Salinity and programmed cell death: unravelling mechanisms for ion specific signalling. J. Exp. Bot., 60, 709–712.

Shabala, S. (2017). Signalling by potassium: another second messenger to add to the list? J. Exp. Bot., 68, 4003–4007.

Shabala, S., and Cuin, T. A. (2008). Potassium transport and plant salt tolerance. Physiol. Plant. 133, 651–669.

Shabala, S., and Pottosin, I. (2014). Regulation of potassium transport in plants under hostile conditions: implications for abiotic and biotic stress tolerance. Physiol. Plant. 151, 257–279.

Shavrukov, Y. (2012). Salt stress or salt shock: which genes are we studying? J. Exp. Bot., 63, 695–709.

Shendure, J. (2008). The beginning of the end for microarrays? Nat Methods, 5, 585–587.

Shi, H., Ishitani, M., Kim, C. S., Zhu, J. K. (2000). The *Arabidopsis thaliana* salt tolerance gene SOS1 encodes a

putative Na^+/H^+ antiporter. Proc. Natl. Acad. Sci. USA, 97, 6896–6901.

Shi, H., Lee, B. H., Wu, S. J., and Zhu, J. K. (2003). Overexpression of a plasmamembrane Na^+/H^+ antiporter gene improves salt tolerance in *Arabidopsis thaliana*. Nat. Biotechnol., 21, 81–85.

Shi, H., Quintero, F. J., Pardo, J. M., and Zhu, J. -K. (2002). The putative plasma membrane Na^+/H^+ antiporter SOS1 controls long distance Na^+ transport in plants. Plant Cell, 14(2), 465–477.

Skevas, T., Swinton, S. M., Hayden, N. J. (2014). What type of landowner would supply marginal land for energy crops? Biomass Bioenergy, 67, 252–259.

Slade, R., Bauen, A. (2013). Micro-algae cultivation for biofuels: cost, energy balance, environmental impacts and future prospect. Biomass. Bioen., 53, 29:38.

Slavov, G. T., Nipper, R., Robson, P., Farrar, K., Allison, G. G., Bosh, M., Clifton-Brown, J. C., Donnison, I., Jensen, E. (2014). Genome-wide association studies and prediction of 17 traits related to phenology, biomass and cell wall composition in the energy grass *Miscanthus sinensis*. New Phytol., 201, 1227-1239.

Smeets, E. M., Faaij, A. P., Lewandowski, I. M., Turkenburg, W. C. (2007). A bottom-up assessment and review of global bio-energy potentials to 2050. Prog. Energy Combust. Sci., 33, 56–106.

Smith, S. L., Thelen, K. D., MacDonald, S. J. (2013). Yield and qu ality analyses of bioenergy crops grown on a regulatory brownfield. Biomass Bioenergy, 49, 123–130.

Soldatos, P. (2015). Economic aspects of bioenergy production from perennial grasses in marginal lands of South Europe. BioEnergy Res., 8, 1562–1573.

Song, S. -Y., Chen, Y., Chen, J., Dai, X. -Y. and Zhang, W. -H. (2011). Physiological mechanisms underlying OsNAC5-dependent tolerance of rice plants to abiotic stress. Planta, 234(2), 331–345.

Spencer, D. F., Ksander, G. G., Whitehand, L. C. (2005). Spatial and temporal variation in RGR and leaf quality of a clonal plant: *Arundo donax*. Aquat. Bot., 81, 27–36.

Steward, N., Ito, M., Yamaguchi, Y., Koizumi, N., Sano, H. (2002). Periodic DNA methylation in maize nucleosomes and demethylation by environmental stress. J. Biol. Chem., 277, 37741–37746.

Steward, N., Kusano, T., Sano, H. (2000). Expression of ZmMET1, a gene encoding a DNA methyltransferase from maize, is associated not only with DNA replication in actively proliferating cells, but also with altered DNA methylation status in cold-stressed quiescent cells. Nucleic Acids Res., 28, 3250–3259.

Stewart, F. J., Panne, D., Bickle, T. A., Raleigh, E. A. (2000). Methyl-specific DNA binding by McrBC, a modification-dependent restriction enzyme. J. Mol. Biol., 298, 611-22.

Stewart, J., Toma, Y., Fernandez, F. G., Nishiwaki, A., Yamada, T., Bollero, G. (2009). The ecology and agronomy of Miscanthus sinensis, a species important to bioenergy crop development, in its native range in Japan: a review. GCB Bioenergy, 1, 126–153.

Stroud, H., Do, T., Du, J., Zhong, X., Feng, S., Johnson, L., Patel, D. J., Jacobsen, S. E. (2014). Non-CG methylation patterns shape the epigenetic landscape in *Arabidopsis*. Nat. Struct. Mol. Biol., 21, 64–72.

Sudha, S., Vasudeva, N. (2009). Constructed wetland for treating wastewater from crocodile farm. J. Ecotoxicol. Environ. Monit., 19, 277–84.

Sunarpi, Horie, T., Motoda, J., Kubo, M., Yang, H., Yoda, K., et al. (2005). Enhanced salt tolerance mediated by AtHKT1 transporter-induced Na unloading from xylem vessels to xylem parenchyma cells. Plant J., 44, 928–938.

Sung, C. H. and Hong, J. K. (2010). Sodium nitroprusside mediates seedling development and attenuation of oxidative stresses in Chinese cabbage. Plant Biotechnology Reports, 4(4), 243–251.

Szabados, L., Savoure, A. (2010). Proline: a multifunctional amino acid. Trends Plant Sci., 15, 89-97.

Taha, M., Foda, M., Shahsavari, E., Aburto-Medina, A., Adetutu, E., Ball, A. (2016). Commercial faesibility of lignocellulose biodegradation: possibilities and challenges. Curr. Opi. Biotech., 38, 190-197.

Tahir, M. A., Aziz, T., Farooq, M. and Sarwar, G. (2012).m Silicon-induced changes in growth, ionic composition, water relations, chlorophyll contents and membrane permeability in two salt-stressed wheat genotypes. Archives of Agronomy and Soil Science, 58(3), 247–256.

Takahashi, W., Takamizo, T., Kobayashi, M., Ebina, M. (2010). Plant regeneration from calli in giant reed (*Arundo donax* L.). Grassl. Sci., 4, 56224–9.

Tang, Y., Xie, J. S., Geng, S. (2010). Marginal land-based biomass energy production in China. J Integr Plant Biol, 52, 112–121.

Thomas, J. C., Sepahi, M., Arendall, B. and Bohnert, H. J. (1995). Enhancement of seed germination in high salinity by engineering mannitol expression in *Arabidopsis thaliana*. Plant, Cell and Environment, 18(7), 801–806.

Tilman, D., Hill, J., Lehman, C. (2006). Carbon-negative biofuels from low-input high-diversity grassland biomass. Science, 314, 1598-600.

Tollefsbol, T. O. (2004). Methods of epigenetic analysis. Methods Mol. Biol., 287, 1-8.

Tracy, J. L., DeLoach, C. J. (1998). Suitability of classical biological control for giant reed (*Arundo donax*) in the United States. Proceedings of the Arundo and saltcedar management workshop, Ontario.

Trapnell, C., Williams, Ba., Pertea, G., Mortazavi, A., Kwan, G., van Baren, M. J., Salzberg, S. L., Wold, B. J., Pachter, L. (2010). Transcript assembly and quantification by RNA-Seq reveals unannotated transcripts and isoform switching during cell differentiation. Nat. Biotechnol., 28, 511–515.

Tsugane, K., Kobayashi, K., Niwa, Y., Ohba, Y., Wada, K., and Kobayashi, H. (1999). A recessive *Arabidopsis* mutant that grows photoautotrophically under salt stress shows enhanced active oxygen detoxification. Plant Cell, 11, 1195–1206.

Valenzuela, C. E., Acevedo-Acevedo, O., Miranda, G. S., Vergara-Barros, P., Holuigue, L., Figueroa, C. R., Figueroa, P. M. (2016). Salt stress response triggers

activation of the jasmonate signaling pathway leading to inhibition of cell elongation in *Arabidopsis* primary root. J Exp Bot., 67, 4209–4220.

Vermaak, D., Ahmad, K. and Henikoff, S. (2003). Maintenance of chromatin states: an open-and-shut case. Curr. Opin. Cell Biol., 15, 266–274.

Virtue, J. G., Reynolds, T., Malone J, Preston C, Williams C. (2010). Managing the weed risk of cultivated *Arundo donax* L. Proceedings of 17th Australasian weeds conference, Christchurch.

Wada, Y., Miyamoto, K., Kusano, T., Sano, H. (2004). Association between up-regulation of stress-responsive genes and hypomethylation of genomic DNA in tobacco plants. Mol. Genet. Genom. 271, 658–666.

Wang, W. S., Pan, Y. J., Zhao, X. Q. (2011). Drought-induced site-specific DNA methylation and its association with drought tolerance in rice (*Oryza sativa* L.). J. Exp. Bot., 62, 1951–1960.

Wang, Y. and Nii, N. (2000). Changes in chlorophyll, ribulose bisphosphate carboxylase-oxygenase, glycine betaine content, photosynthesis and transpiration in *Amaranthus tricolor* leaves during salt stress. Journal of Horticultural Science and Biotechnology, 75(6), 623–627.

Wang, Z., Gerstein, M., Snyder, M. (2009). RNA-Seq: A revolutionary tool for transcriptomics. Nat. Rev. Genet., 10, 57–63.

Watts, D. A. (2009). Dynamics of water use and responses to herbivory in the invasive reed, *Arundo donax* (L.). Texas A&M University; [Master Thesis].

Webster, R. J., Driever, S. M., Kromdijk, J., Mcgrath, J., Leakey, A. D. B., Siebke, K., Demetriades-Shah, T., Bonnage, S., Peloe, T., Lawson, T., Long, S. P. (2016). High C3 photosynthetic capacity and high intrinsic water use efficiency underlies the high productivity of the bioenergy grass *Arundo donax*. Sci. Rep., 6, 20964.

Weinl, S., and Kudla, J. (2008). The CBL-CIPK Ca^{2+}-decoding signaling network: function and perspectives. New Phytol., 179, 675–686.

Welfle, A., Gilbert, P., Thornley, P., Stephenson, A. (2017). Generating low-carbon heat from biomass: Life cycle assessment of bioenergy scenarios. J. Clean. Prod., 149, 448-460.

Weng, H., Yoo, C. Y., Gosney, M. J., Hasegawa, P. M., Mickelbart, M. V. (2012). Poplar GTL1 is a Ca^{2+}/calmodulin-binding transcription factor that functions in plant water use efficiency and drought tolerance. PLoS ONE, 7(3), e32925.

Wijte, A. B., Mizutani, T., Motamed, E. R., Merryfield, M. L., Miller, D. E. (2005). Temperature and endogenous factors cause seasonal patterns in rooting by stem fragments of the invasive giant reed, *Arundo donax* (Poaceae). Int. J. Plant Sci., 166, 507–17.

Williams, C. M. J., Biswas, T. K., Schrale, G., Virtue, J. G., Heading, S. (2008). Use of saline land and wastewater for growing a potential biofuel crop (*Arundo donax* L.). Proceedings of irrigation Australia conference, Melbourne.

Woodward, A. W., Bartel, B. (2005). Auxin: regulation, action, and interaction. Ann Bot., 95, 707-35.

Wu, H., Shabala, L., Zhou, M., and Shabala, S. (2015b). Chloroplast generated ROS dominate NaCl-induced K^+

efflux in wheat leaf mesophyll. Plant Signal. Behav., 10:e1013793. doi: 10.1080/15592324.2015.1013793.

Wu, H., Zhang, X., Giraldo, J. P., and Shabala, S. (2018). It is not all about sodium: revealing tissue specificity and signalling roles of potassium in plant responses to salt stress. Plant Soil. 431, 1–17.

Xie, M., Zhang, J., Tschaplinski, T. J., Tuskan, G. A., Chen, J., Muchero, W. (2018). Regulation of lignin biosynthesis and its role in growth-defense tradeoffs. Front Plant Sci., 9, 1-9.

Xiong, J., Fu, G., Tao, L. and Zhu, C. (2010). Roles of nitric oxide in alleviating heavy metal toxicity in plants. Archives of Biochemistry and Biophysics, 497(1-2), 13–20.

Xiong, L., Ishitani, M., Lee, H., Zhu, J. K. (2001). The *Arabidopsis* LOS5/ABA3 locus encodes a molybdenum cofactor sulfurase and modulates cold stress- and osmotic stress-responsive gene expression, Plant Cell., 13, 2063–2083.

Yang, J., Zhang, J., Liu, K., Wang, Z., Liu, L. (2007). Involvement of polyamines in the drought resistance of rice. J Exp Bot., 58(6), 1545–1555.

Yeo, A., Yeo, M., and Flowers, T. (1987). The contribution of an apoplastic pathway to sodium uptake by rice roots in saline conditions. J. Exp. Bot., 38, 1141–1153.

Yoo, C. Y., Pence, H. E., Jin, J. B., Miura, K., Gosney, M. J., Hasegawa, P. M., Mickelbart, M. V. (2010). The *Arabidopsis* GTL1 transcription factor regulates water use efficiency and drought tolerance by modulating stomatal density via transrepression of SDD1. Plant Cell., 22, 4128-4141.

Yu, L., Nie, J., Cao, C., Jin, Y., Yan, M., Wang, F., et al. (2010). Phosphatidic acid mediates salt stress response by regulation of MPK6 in *Arabidopsis thaliana*. New Phytol., 188, 762–773.

Yue, D., You, F., Snyder, S. W. (2014). Biomass-to-bioenergy and biofuel supply chain optimization: overview, key issue and challenges. Comp. Chem. Engin., 66, 36-56.

Yusuf, N. N. A. N., Kamarudin, S. K., Yaakub, Z. (2011). Overview on the current trends in biodiesel production. Ener. Conv. Managm., 52, 2741-2751.

Zabaniotou, A. (2018). Redesigning a bioenergy sector in EU in the transition to circular waste-based Bioeconomy-A multidisciplinary review. Journal of Cleaner Production, 177, 197-206.

Zapata, P. J., Serrano, M., Pretel, M. T., Botella, M. A. (2008). Changes in free polyamine concentration induced by salt stress in seedlings of different species. Plant Growth Regul., 56, 167–177.

Zemach, A., Kim, M. Y., Hsieh, P. H., Coleman-Derr, D., Eshed-Williams L., Thao, K., Harmer, S. L., Zilberman, D. (2013). The *Arabidopsis* nucleosome remodeler DDM1 allows DNA methyltransferases to access H1-containing heterochromatin. Cell., 153, 193–205.

Zeven, A. C., de Wet, J. M. J. (1982). Dictionary of cultivated plants and their regions of diversity: excluding most ornamentals, forest trees and lower plants. 2nd rev ed. Wageningen: Centre Agricultural Pub & Document.

Zhang, D. W., Yuan, S., Xu, F., Zhu, F., Yuan, M., Ye, H. X., Guo, H. Q., Lv, X., Yin, Y., Lin, H. H. (2016). Light Intensity affects chlorophyll synthesis during greening

process by metabolite signal from mitochondrial alternative oxidase in *Arabidopsis*. Plant Cell Environ., 39, 12–25.

Zhang, H., Lang, Z. and Zhu, J. K. (2018). Dynamics and function of DNA methylation in plants. Nature Review. Molecular Cell Biology, 19, 489–506.

Zhang, J., Li Y, Zhang, C., Jing, Y. (2008). Adsorption of malachite green from aqueous solution onto carbon prepared from *Arundo donax* root. J Hazard Mater, 150, 774–82.

Zhang, J. J., Lu, Y. C., Zhang, S. H., Lu, F. F., Yang, H. (2016b). Identification of transcriptome involved in atrazine detoxification and degradation in alfalfa (Medicago sativa) exposed to realistic environmental contamination. Ecotoxicol. Environ. Saf., 130, 103–112.

Zhang, J. L., Flowers, T. J., and Wang, S. M. (2010). Mechanisms of sodium uptake by roots of higher plants. Plant Soil, 326, 45–60.

Zhang, X., Yazaki, J., Sundaresan, A., Cokus, S., Chan, S. W., Chen, H., Henderson, I. R., Shinn, P., Pellegrini, M., Jacobsen, S. E., Ecker, J. R. (2006). Genome-wide high-resolution mapping and functional analysis of DNA methylation in *Arabidopsis*. Cell, 126, 1189–1201.

Zhang, H., Zhu, J. K. (2012). Active DNA demethylation in plants and animals. Cold Spring Harb. Symp. Quant. Biol., 77, 161–173.

Zhao, M. -G., Chen, L., Zhang, L. -L. and Zhang, W. -H. (2009). Nitric reductase-dependent nitric oxide production is involved in cold acclimation and freezing tolerance in *Arabidopsis*. Plant Physiology, 151(2), 755–767.

Zhao, Y., Williams, R., Prakash, C. S., He, G. (2013). Identifcation and characterization of gene-based SSR markers in date palm (*Phoenix dactylifera* L.). BMC Plant Biol., 12, 237–44.

Zhou, J., Rocklin, A. M., Lipscomb, J. D., Que, L., Solomon, E. I. (2002). Spectroscopic studies of 1-aminocyclopropane-1-carboxylic acid oxidase: molecular mechanism and CO_2 activation in the biosynthesis of ethylene. J Am Chem Soc., 124(17), 4602–4609.

Zhu, J. K. (2002) Salt and drought stress signal transduction in plants. Annu. Rev. Plant Biol., 53, 247–273.

Zhu, H., Wang, G. H. & Qian, J. (2016). Transcription factors as readers and effectors of DNA methylation. Nat. Rev. Genet. 17, 551–565.

Zörb, C., Geilfus, C. M., Dietz, K. J. (2018). Salinity and crop yield. Plant Biol., 21, 31–38.